

Published online 2 June 2010 in Wiley InterScience  
(www.interscience.wiley.com) DOI: 10.1002/jlcr.1776

# 10th International Symposium on the Synthesis and Applications of Isotopes and Isotopically Labelled Compounds – Poster Presentations

Session 19, Sunday, June 14 to Thursday, June 18, 2009

**SESSION CHAIR: WILLIAM WHEELER**

IsotopicSolutions, LLC, USA

**Abstract:** The poster session is a series of papers dealing with a conglomeration of all of the previous sessions. Cristian Postolache, the fourth of the Wiley Young Scientist Award winners gave a Poster in this session.

**Keywords:** carbon-14; tritium; fluorine-18; In-111m; panabinostat; sulphur-35; coLogica Isotope synthesis database; QAB149; corn plant metabolism

## MICROWAVE-ASSISTED SYNTHESIS OF A CARBON-14 LABELED PYRROLOTRIAZINE PRECURSOR FOR CORE LABELED DRUG CANDIDATES

**ALBAN J. ALLENTOFF, MICHAEL W. LAGO, SHARON GONG, SCOTT BACH TRAN, MARC D. OGAN, AND SAMUEL J. BONACORSI JR.**

Department of Chemical Synthesis, Bristol-Myers Squibb Research and Development, One Squibb Drive, New Brunswick, NJ 08903, USA

**Summary:** The 5-methyl-pyrrolo[1,2-*f*][1,2,4]triazine system is a chemotype scaffold common to drug candidates within several therapeutic areas. Core carbon-14 labeled ethyl 5-methyl-4-oxo-2- $[^{14}\text{C}]$ -3,4-dihydropyrrolo[1,2-*f*][1,2,4]triazine-6-carboxylate was efficiently prepared via a microwave-assisted cyclization reaction of a known aminopyrrole with  $[^{14}\text{C}]$ triethylorthoformate.

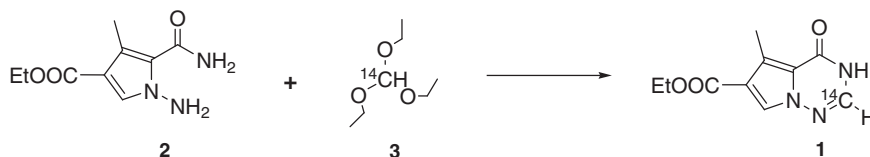
**Keywords:** microwave irradiation; pyrrolotriazine; core labeling; carbon-14; drug candidates; oncology; immunology

**Introduction:** The novel pyrrolotriazine **1** (Table 1, unlabeled) has been utilized by medicinal chemistry programs as a core chemotype for elaboration into drug candidates within the oncology and immunology therapeutic areas.<sup>1,2</sup> During the discovery and development of drug candidates, radiolabeled analogues are required for profiling their disposition in humans and animals, and for *in vitro* reaction phenotyping and transport studies. Therefore the preparation of **1** with carbon-14 ring labeling offered an opportunity to efficiently prepare core labeled drug candidates for diverse discovery and development activities via a single carbon-14 labeled precursor. In order to execute this approach, an efficient method for the preparation of substantial quantities of carbon-14 labeled **1** was required.

Previous work described by this group<sup>3</sup> and others<sup>4</sup> have shown the viability of utilizing carbon-14 labeled triethylorthoformate as a labeled formate equivalent in acid catalyzed cyclization reactions affording ring radiolabeled heterocycles. We now report on the cyclization of  $[^{14}\text{C}]$ triethylorthoformate **3** with the known N-aminopyrrole **2** to efficiently prepare labeled **1**.

**Results and Discussion:** Preparation of stable isotopically labeled **1** was previously described from the reaction of a stable-labeled analogue of aminopyrrole **2** with 7.5 equivalents of unlabeled triethylorthoformate and catalytic amounts of *p*-toluene sulfonic acid.<sup>5</sup> These conditions afforded almost quantitative yield of the stable-labeled analogue of pyrrolotriazine **1** (Table 1, Entry 1). In applying this reaction to carbon-14 incorporation, it was critical to lower the amounts of  $[^{14}\text{C}]$ triethylorthoformate to approximately one molar equivalent in comparison to **2** in order to obtain useful radiochemical yields. However, extensive heating at 120°C of **2** with 1.1 equivalents of  $[^{14}\text{C}]$ triethylorthoformate and *p*-toluenesulfonic acid (Table 1, Entry 2) gave crude product containing large amounts of unreacted starting aminopyrrole **2**. Purification via recrystallization and chromatography, afforded a 30% isolated radiochemical yield of **1**.

Initially, we explored the 250 W microwave irradiation of aminopyrrole **2** with 0.66 molar equivalents of  $[^{14}\text{C}]$ triethylorthoformate (Entry 3). These conditions allowed rapid reaction of **2** with  $[^{14}\text{C}]$ triethylorthoformate affording crude product **1** which after

**Table 1.** Effect of stoichiometry and reaction conditions on the yield of **1** from the cyclization of **2** and **3**

Entry	Molar equivalents		Reaction conditions (N,N-dimethylacetamide)	% yield <b>1</b> (isolated)
	2	3		
1	1	7.5	73°C, 40 min	99%*
2	1	1.1	70°C, (18 h) then 120°C (18 h)	30%**
3	1	0.66	Microwave (200 W) 15 min, Temperature Max = 150°C	73%**
4	1	1.3	Microwave (200 W) 20 min, Temperature Max = 150°C	53%**

\*Yield of **1** based on aminopyrrole **2**. This reaction was conducted using stable-labeled reactants [5].  
\*\*Radiochemical yield of **1** based on [<sup>14</sup>C]triethylorthoformate.

recrystallization followed by column chromatography yielded pure **1** in 73% radiochemical yield. In order to facilitate large scale preparations, the microwave-assisted cyclization reaction was also performed using 1.3 equivalents of [<sup>14</sup>C]triethylorthoformate (Entry 4) affording crude **1** with no observed aminopyrrole **2** remaining. Simple precipitation of the product by addition of water gave **1** in 53% radiochemical yield and radiochemical purity in excess of 97%.

**Conclusions:** We have developed a facile method for the preparation of a radiolabeled pyrrolo-triazine chemotype scaffold using a microwave-assisted cyclization reaction. This microwave-assisted process is readily scaled up and allowed the preparation of sufficient quantities of the precursor to support multiple labeling projects.

## References

- J. Hynes Jr., A. J. Dykeman, S. Lin, S. T. Wroblewski, H. Wu, K. M. Gillooly, S. B. Kanner, H. Lonial, D. Loo, K. W. McIntyre, S. Pitt, D. R. Shen, D. J. Shuster, X. Yang, R. Zhang, K. Behenia, H. Zhong, P. H. Marathe, A. M. Doweyko, J. S. Tokarski, J. S. Sack, M. Pokross, S. E. Kiefer, J. A. Newitt, J. C. Barrish, J. Dodd, G. L. Schieven, K. Leftheris, *J. Med. Chem.* **2008**, *51*, 4–16.
- R. M. Borzilleri, X. Zheng, L. Qian, C. Ellis, Z.-W. Cai, B. S. Wautlet, S. Mortillo, R. Jeyaseelan Sr., D. W. Kukral, A. Fura, A. Kamath, V. Vyas, J. S. Tokarski, J. C. Barrish, J. T. Hunt, L. J. Lombardo, J. Fargnoli, R. S. Bhide, *J. Med. Chem.* **2005**, *48*, 3991–4008.
- M. D. Ogan, D. J. Kucera, Y. R. Pendri, J. K. Rinehart, *J. Label. Compd. Radiopharm.* **2005**, *48*, 645–655.
- J. S. Valsborg, L. J. S. Knutsen, I. Lundt, C. Foged, *J. Label. Compd. Radiopharm.* **1995**, *36*, 457–464.
- M. D. Ogan, S. B. Tran, J. K. Rinehart, *J. Label. Compd. Radiopharm.* **2006**, *49*, 139–145.

## AN INNOVATIVE AND EFFICIENT SYNTHESIS OF STABLE ISOTOPE LABELLED N-METHYL PYRAZOLE

AUDREY ATHLAN, CALVIN MANNING, AND GEOFF BADMAN

Isotope Chemistry, GlaxoSmithKline Research and Development, Gunnels Wood Road, Stevenage SG1 2NY, UK

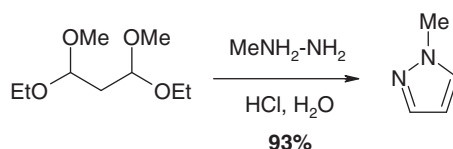
**Abstract:** Novel synthesis of stable isotopically labelled N-Methyl pyrazole in three steps from commercially available diethyl [<sup>13</sup>C<sub>3</sub>] malonate. The pyrazole ring is obtained by condensation between bisacetal derivative and hydrazine.

**Keywords:** pyrazole synthesis; reductive acetylation; hydrazine; malonate ester

**Introduction:** The synthesis of pyrazoles is of great interest due to the wide application of such heterocyclic motifs in the pharmaceutical industry eg COX-2 inhibitor celecoxib (Celebrex<sup>®</sup>),<sup>1</sup> CB1 antagonist acomplia (Rimonabant<sup>®</sup>)<sup>2</sup> and sildenafil (Viagra<sup>®</sup>).<sup>3</sup> In support of metabolism studies, a stable isotope labelled (SIL) synthesis of an M+6 N-methyl pyrazole building block was required.

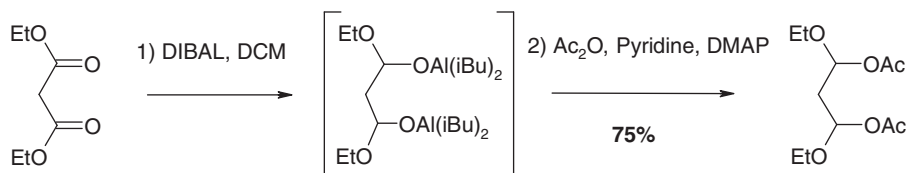
Synthesis of 1,2-pyrazole moiety is classically achieved by either a 1,3-dipolar cycloaddition of diazo compounds and alkynes or by condensation of hydrazine with 1,3 difunctionalised molecules, generally diketones. Such syntheses of a SIL version of N-methylpyrazole appeared quite challenging, since the number of isotopically labelled starting materials for either route is quite limited and we had therefore to design an alternative strategy towards this molecule.

**Results and discussion:** A literature review<sup>4</sup> showed a recent patent describing the synthesis of N-methylpyrazole from 1,3-bis(ethoxy)-1,3-bis(methoxy)propane and methylhydrazine (Scheme 1).



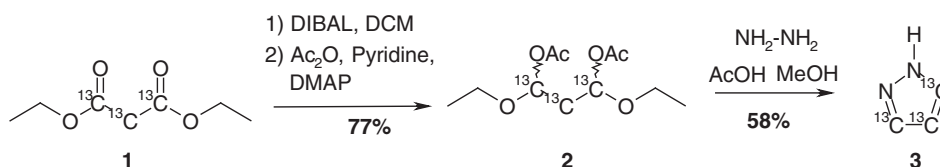
Scheme 1.

Furthermore, Kopecky and Rychnovsky<sup>5</sup> reported the synthesis of bisacetals by reductive acetylation of acyclic ester such as malonate esters. This reaction proceeds via an aluminium acetal intermediate, which subsequently undergoes an *in situ* acetylation (Scheme 2).



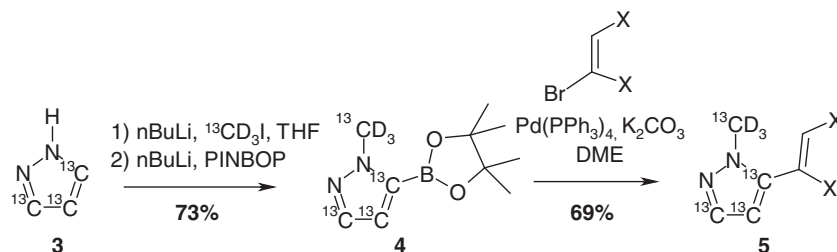
Scheme 2.

Encouraged by these results, we investigated the possibility of a Knorr condensation between hydrazine and bisacetal synthesised from readily available diethyl [ $^{13}\text{C}_3$ ] malonate (Scheme 3).



Scheme 3.

M+6 labelled pyrazole moieties were then obtained by N-methylation in presence of [ $^{13}\text{CD}_3$ ] iodomethane. Purification and isolation of this volatile material was problematic. We therefore designed a one-pot procedure, where the labelled pyrazole 3 undergoes N-methylation followed by an *in situ* boronylation. The labelled pyrazole molecule 4 was successfully used in a Suzuki reaction (Scheme 4).



Scheme 4.

**Conclusion:** We have developed an economical and efficient route towards labelled pyrazoles using SIL malonaldehyde equivalent. M+7 pyrazole 4 was thus synthesised in three steps from commercially available diethyl [ $^{13}\text{C}_3$ ] malonate with an overall yield of 33%.

This approach appears versatile and other alkyl pyrazoles could potentially be generated. [ $^{15}\text{N}_2$ ] hydrazine could also be used to prepare M+5 pyrazole.

We have also demonstrated that the labelled pyrazole boronylated species could successfully be used as a building block in cross-coupling reactions.

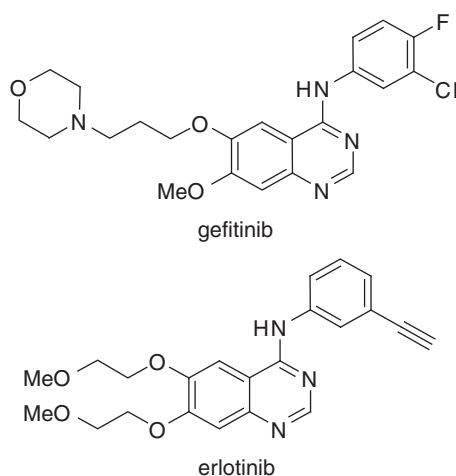
## References

- [1] T. D. Penning, J. J. Talley, S. R. Bertenshaw, J. S. Carte, *J. Med. Chem.* **1997**, *40*, 1347–1365.
- [2] S. R. Donohue, C. Halldin, V. W. Pike, *Tett. Lett.* **2008**, *49*, 2789–2791.
- [3] N. K. Terrett, A. S. Bell, D. Brown, P. Ellis, *Bioorg. Med. Chem. Lett.* **1996**, *6*, 1819–1824.
- [4] *Ger. Offen.* 10057194, **29 May 2002**.
- [5] D. J. Kopecky, S. D. Rychnovsky, *J. Org. Chem.* **2000**, *65*, 191–198.

## THE SYNTHESIS OF CARBON-14 LABELLED 3H-QUINAZOLIN-4-ONE BUILDING BLOCKS

RYAN A. BRAGG, NICK BUSHBY, JOHN R. HARDING, DAVID A. KILLICK AND ANGELA JORDAN

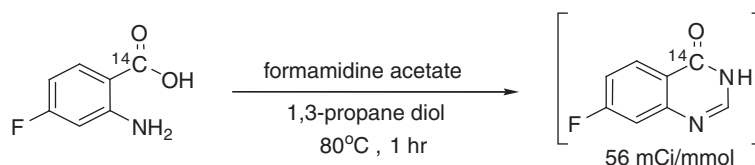
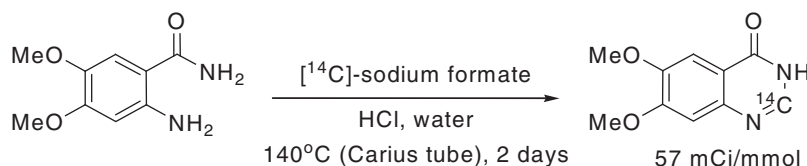
Isotope Chemistry, Clinical Pharmacology &amp; DMPK, AstraZeneca, Mereside, Alderley Park, Macclesfield, Cheshire, SK10 4TG, UK

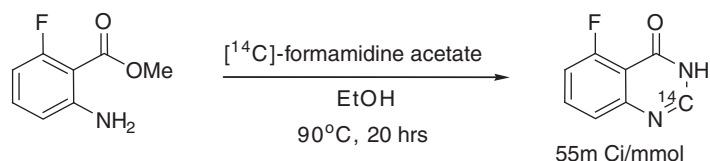
**Abstract:** The synthesis of carbon-14 labelled, 5-, 6-, 7- and 6,7- substituted, 3H-quinazolin-4-one building blocks are presented.**Keywords:** isotopic labelling; carbon-14; 3H-quinazolin-4-one**Introduction:** Over the past decade, 4-anilinoquinazolines have emerged as an important class of anticancer agent, as exemplified by gefitinib and erlotinib (Figure 1).<sup>1</sup> To support drug metabolism and distribution studies of this class of compound, a number of carbon-14 labelled materials were required. Early labelling work on these compounds focused upon labelling the side chains of 4-anilinoquinazolines, based on the assumption that labelling the quinazolinone core required a large excess of the labelled reagent.<sup>2</sup>**Figure 1.** Structures of gefitinib and erlotinib.

However, labelling the quinazolinone core of a molecule is often desirable as this provides material with the label in a metabolically stable position. We detail here the synthesis of carbon-14 labelled, 5-, 6-, 7- and 6,7- substituted, 3H-quinazolin-4-one building blocks, the precursors of substituted 4-anilinoquinazolines.

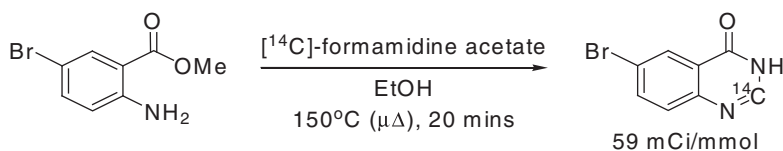
**Results and Discussion:** Our first approach to labelled quinazolinones is shown in Scheme 1. Reaction of 2-amino-4-fluoro-[1-<sup>14</sup>C]-benzoic acid with 2.0 equiv. of formamidine acetate at 80°C gave 7-fluoro-3H-[4-<sup>14</sup>C]-quinazolin-4-one in 76% yield. Whilst this approach was successful, the cost of carbon-14 labelled, tri-substituted, aromatic carboxylic acids is often high.

We therefore turned our attention to labelling the quinazolinone in the 2-position using commercially available [<sup>14</sup>C]-sodium formate.<sup>3</sup> As shown in Scheme 2, reaction of 2-amino-4,5-dimethoxybenzamide with 1.05 equiv. of [<sup>14</sup>C]-sodium formate gave 6,7-dimethoxy-3H-[2-<sup>14</sup>C]-quinazolin-4-one in 84% yield. However, it was necessary to heat this reaction to 140°C in a Carius tube for 2 days.

**Scheme 1.****Scheme 2.**



Scheme 3.



Scheme 4.

A more practical procedure was used for the synthesis of 5-fluoro-3H-[2- $^{14}\text{C}$ ]-quinazolin-4-one as shown in Scheme 3.<sup>4</sup> In this example, 2-amino-6-fluorobenzoic acid methyl ester was treated with 1.25 equiv. of [ $^{14}\text{C}$ ]-formamidinium acetate to give the desired product in 71% yield after heating in ethanol for 20 hours.

A further refinement of this approach was used for the synthesis of 6-bromo-3H-[2- $^{14}\text{C}$ ]-quinazolin-4-one (Scheme 4). Heating 2-amino-5-bromobenzoic acid methyl ester and [ $^{14}\text{C}$ ]-formamidinium acetate at 150°C in a microwave for 20 minutes gave the desired compound in 83% yield. The equivalent thermal reaction required 20 hours at reflux.

**Conclusions:** In conclusion, we have demonstrated that carbon-14 labelled, 5-, 6-, 7- and 6,7- substituted 3H-quinazolin-4-ones can be prepared by a number of different approaches. Furthermore, the use of labelled formamidinium acetate in conjunction with microwave heating has been shown to provide efficient access to these valuable building blocks.

**Acknowledgements:** The authors would like to acknowledge GE Healthcare for the synthesis of 6,7-dimethoxy-3H-[2- $^{14}\text{C}$ ]-quinazolin-4-one.

## References

- [1] G. Blackledge, S. Averbuch, *Br. J. Cancer* **2004**, *90*, 566–572.
- [2] J. A. Bergin, H. Booth, N. Bushby, J. R. Harding, D. Killick, C. D. King, D. J. Wilkinson, *J. Label. Compd. Radiopharm.* **2004**, *47*, 299–334.
- [3] E. J. Merrill, *J. Label. Compd. Radiopharm.* **1969**, *5*, 346–350.
- [4] Y. Zhang, Y. Huang, C. C. Huang, *J. Label. Compd. Radiopharm.* **2005**, *48*, 485–496.

## THE SYNTHESIS, CHARACTERIZATION AND CHEMISTRY OF [METHYL- $^{14}\text{C}$ ] METHYL NOSYLATE

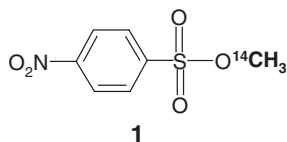
STEVEN A. CARR, LINDA P. LACY, SCOT POUNDS, AND CRIST N. FILER

PerkinElmer Health Sciences Inc., 940 Winter Street, Waltham, MA 02451, USA

**Abstract:** A method for the preparation of [methyl- $^{14}\text{C}$ ] methyl nosylate is described as well as representative examples of its use as a carbon-14 alkylating reagent.

**Keywords:** [ $^{14}\text{C}$ ] methyl iodide; [ $^{14}\text{C}$ ] methyl nosylate; methylation

**Introduction:** The use of substances labelled with carbon-14 has been extraordinarily valuable in many aspects of the life sciences for over half a century. One of the most versatile and simple ways to install carbon-14 in many compounds of interest is by methylating available heteroatoms like nitrogen, oxygen and sulfur to afford corresponding methyl- $^{14}\text{C}$  analogues. Over the years, [ $^{14}\text{C}$ ] methyl iodide has been a convenient electrophilic reagent of choice to employ in this regard. However recently, safety regulations<sup>1</sup> have restricted the shipment of [ $^{14}\text{C}$ ] methyl iodide by air and its limited stability has made other forms of prolonged transportation impractical and inadvisable. For that reason we decided to explore the synthesis, characterization and chemistry of [methyl- $^{14}\text{C}$ ] methyl nosylate (**1**) as a useful alternative carbon-14 radiomethylating reagent.



**Results and Discussion:** The synthesis of **1** is analogous to that of the corresponding tritiated reagent first reported by Pounds<sup>2,3</sup> and is described in the experimental section. The methylation chemistry of **1** is similar to and equally straightforward as that of the tritiated analogue and is illustrated in Scheme 1. Using **1**, estrone (**2**) could easily be converted to methyl ether **3** in approximately 95% radiochemical yield, while [methyl-<sup>14</sup>C] caffeine (**5**) and [methyl-<sup>14</sup>C] yohimbine (**7**) were correspondingly prepared from their respective desmethyl analogues in about 50% radiochemical yield. Employing **1** also permitted its safe addition to reaction vessels without concern for volatile carbon-14 contamination as with [<sup>14</sup>C] methyl iodide. Also, subsequent portions of **1** could easily be added to drive a radiomethylation reaction to completion.

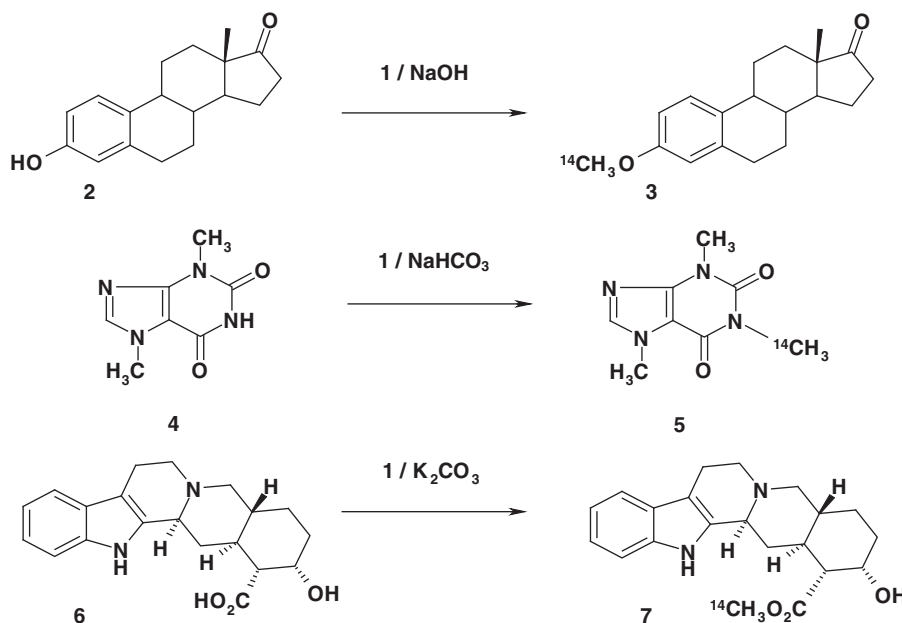
Besides solving a transportation and regulatory challenge, the availability of reagent **1** has also been accompanied by another valuable benefit; namely, significantly enhanced shelf life over that of [<sup>14</sup>C] methyl iodide. Preliminary studies have shown that the stability of **1** when stored in a solution of hexane:ethyl acetate (4:1) at -20°C is at least nine months before needing repurification. In contrast, [<sup>14</sup>C] methyl iodide is well known to be stable for only a few weeks at best.

**Experimental:** All reagents and solvents were purchased from Sigma-Aldrich Chemical Company. Proton NMR spectra were recorded on a Bruker 300 MHz spectrometer with internal TMS as reference standard.

[Methyl-<sup>14</sup>C] Methyl Nosylate (**1**)

Silver nosylate was freshly prepared in the following manner in the dark: Silver carbonate (2.08 g, 7.56 mmol) was placed in a round bottom flask and suspended in 10 mL of acetonitrile under nitrogen. To the flask was then added 3.6 g (15.1 mmol) of 4-nitrobenzenesulfonic acid (85% pure) in 40 mL of acetonitrile with stirring over the course of 20 min. After the addition, the dark green opaque solution was heated to 60°C for 1 h. The reaction was then cooled and filtered free of fine black solids. The filtrate was rotary evaporated and the resulting tan colored solid was crushed in a mortar and pestle in the dark. The silver nosylate was transferred to a breakseal flask fitted with a septum and vacuum attachment followed by the addition of 65 mL of dry acetonitrile. [<sup>14</sup>C] Methyl iodide (12.6 mmol at 51 mCi/mmol) was then added *via* syringe to the pre-evacuated reaction vessel and the syringe side arm was flame sealed. The reaction was heated to 80°C overnight and cooled to ambient temperature the next morning. The reaction vessel was then attached to a vacuum line and the acetonitrile was distilled away leaving a residue which was dissolved in a minimum amount of ethyl acetate. Silica gel flash chromatography purification using hexane:ethyl acetate (4:1) and pooling appropriate fractions afforded 501 mCi (a 78% radiochemical yield) of **1** that was homogeneous on silica gel TLC (hexane:ethyl acetate (10:3)) and provided a proton NMR (CDCl<sub>3</sub>) that was in concert with that of unlabelled methyl nosylate;  $\delta$  8.35 (d, 2), 8.05 (d, 2), 3.75 ppm (s, 3)

**General <sup>14</sup>C Methylation Procedure.** The compound to be methylated was dissolved in DMF at a concentration of 0.1–0.4 M. Excess appropriate base was added, followed by stirring at ambient temperature for an hour. After this time, an equivalent of **1** was added as a 0.02 M acetonitrile solution and stirring was continued at ambient temperature for several hours. The reaction could be monitored by TLC and excess **1** was added if starting material was still seen to be present. When the reaction had progressed to completeness, it was worked up by partitioning between an appropriate organic solvent and water followed by chromatographic purification.



Scheme 1. Methylation chemistry of **1**.

## References

- [1] US DOT Regulation 49CFR Part 172.
- [2] S. Pounds, Patent WO 2004/108636 A2, A3.
- [3] S. Pounds, *Synthesis and Applications of Isotopically Labelled Compounds*, Vol. 8 (Eds. D. C. Dean, C. N. Filer, K. E. McCarthy), **2004**, pp 469–472.

## THE AUTOSYNTHETIC AND SOLID EXTRACTION METHOD DEVELOPED ON [F-18]FLUMAZENIL RADIOSYNTHESIS

JENN-TZONG CHEN, KANG WEI CHANG, YEAN-HUNG TU, AND WUU-JYH LIN

Institute of Nuclear Energy Research, Taoyuan, Taiwan

**Abstract:** This study represents the newly developed autosynthetic and purification method for radiofluorinated flumazenil [<sup>18</sup>F]FMZ as the brain GABA/BZR receptor antagonist imaging agent. It represents a fast and convenient way to produce [<sup>18</sup>F]FMZ and is much easier to meet GMP compliance than preparative HPLC process. The process takes 45 minutes, decay corrected yield is 20–30%, and the radiochemical purity of the product is higher than 95%. The lipophilicity is a little higher partition coefficient with  $1.49 \pm 0.12$  which represents the high capability of penetrating the blood-brain barrier (BBB). An ex vivo study of this product bound to brain whole-hemisphere sections demonstrated complete inhibition of a BZR agonist which proved the capability of the newly developed solid extraction purification method can be applied in non-carrier added <sup>18</sup>F-flumazenil preparation for further animal and clinical studies.

**Keywords:** flumazenil; [<sup>18</sup>F]FMZ; GABA receptor antagonist

**Introduction:** Gama-aminobutyric acid (GABA) is one of the most important inhibitory neurotransmitters in epilepsy, anxiety and other psychiatric disorders. The GABA receptor is very sensitive to damaged and is abundant in the cortex of the brain. Part of the GABA receptor with chloride ion channel is the central benzodiazepine receptor. It can be traced by radioactive flumazenil derivatives and was found to be more sensitive and accurate than [<sup>18</sup>F]FDG image for focus localization in epilepsy foci<sup>1,2</sup>. <sup>11</sup>C-flunitrazepam, <sup>11</sup>C-flumazenil, <sup>3</sup>H-sarmazenil, <sup>18</sup>F-fluoroalkylflumazenil and <sup>18</sup>F-flumazenil ([<sup>18</sup>F]FMZ) have been studied for GABA/benzodiazepine receptor transmitting activity to determine their binding efficiency to the cortex<sup>3–7</sup>. Non-carrier added [<sup>18</sup>F]FMZ is the most potential radioligand for quantitative evaluation of the epileptogenic region, Alzheimer disease and for cortical damage after stroke in the brain. PET brain metabolic studies and blocking experiments of [<sup>18</sup>F]FMZ in cynomolgus monkey have shown it to be similar to <sup>11</sup>C-flumazenil<sup>3</sup>. However, a radio-HPLC unit is needed in the separation process and takes more than an hour to accomplish the radiosynthesis and purification. Therefore a faster and a more convenient automatic synthetic method is needed for better compliance with the GMP regulation. We investigated a solid phase extraction method based on a sequence controlled liquid target system and an automated radiosynthesizer to produce [<sup>18</sup>F]FMZ for application to the study of whole-hemisphere sections.

**Experimental:** No carrier added Fluorine-18 in this experiment is produced from a recently designed target system with a titanium or niobium target body and a programmable logical controlled target material delivering system with sixteen pneumatic valves. Oxygen-18 enriched water (Trace, 98%) was irradiated with 17 MeV protons (EBCO, TR30). Nitro-flumazenil precursor, Ro 15-2344, was purchased from SYNCOM (The Netherlands). Other chemicals and solvents were purchased from Fluka and Merck and all were of analytical grade. Thin layer chromatography silica gel plates (Si-60) were purchased from Merck. Radiofluorination synthesis reaction and solid extraction purifications were completed on a Nuclear Interface [<sup>18</sup>F]FDG synthesizer.

**Radiolabeling of nitro-flumazenil with F-18:** For all radiolabeling experiments, the nitro precursor was dissolved in DMSO with minimum of water content. [<sup>18</sup>F]fluoride from the pneumatic target water delivery system was delivered to the fluorine-18 separation unit to remove the cation impurities and oxygen-18 water by carbonated Bio-Rad AG1x8 resin. Tetra-butyl ammonia bicarbonate was used to elute the [<sup>18</sup>F] as TBA<sup>18</sup>F. Acetonitrile was used to remove water from TBA<sup>18</sup>F before the radiofluorination reaction. The nitro-flumazenil precursor was then delivered to the reactor to complete the fluorine-18 radiolabelling reaction at 160°C for 30 minutes (Figure 1).<sup>8</sup>

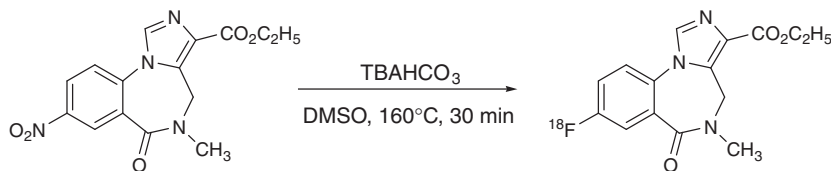


**Figure 1.** The non-carrier added [<sup>18</sup>F]FMZ radiofluorination reaction with tetra-butyl ammonia hydrogen carbonate phase catalyzed in DMSO nitro-flumazenil solution.

Solid phase extraction was completed by passing through a Waters Alumina-N cartridge. A Waters C-18 cartridge was used to remove organics generated during the reaction. The product was collected and its radiochemical purity was measured and then applied in brain tissue in ex vivo studies to check its inhibition with an agonist present.

**Results and discussion:** The radiochemical decay corrected yield was 15% to 20%. This yield is a little bit lower than the first studies of non-carrier added radiofluorinated flumazenil completed using radio-HPLC which takes 90 minutes for a single run. This is probably due to the pneumatic timer controlled valves in the system. This might cause some impurities during target water transportation. However, this is the first water target system designed and fabricated in Taiwan and then applied to [<sup>18</sup>F]FDG production for years. Radiochemical purity was determined by using Merck Si-60 silica gel plate and a radio-TLC imaging scanner (AR-2000, Bioscan). The mobile phase used for developing was a 90% acetonitrile solution. [<sup>18</sup>F]flumazenil had a R<sub>f</sub> = 0.4–0.5, while free [<sup>18</sup>F]-fluoride remained at the origin (R<sub>f</sub> = 0.0–0.1). The radiochemical purity was > 95% (Figure 2).

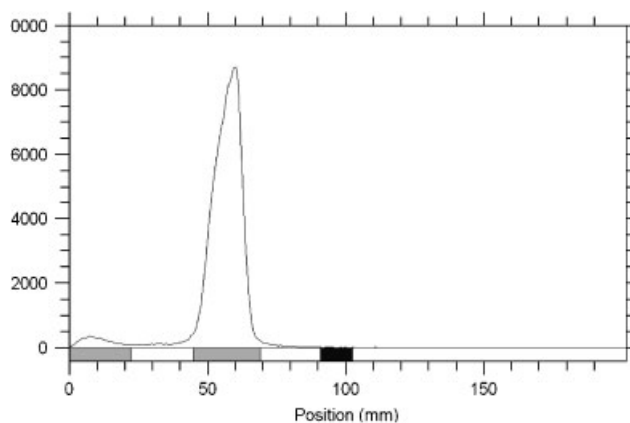


**Figure 2.** Radio-TLC analytical diagram of  $[^{18}\text{F}]\text{FMZ}$ .  $[^{18}\text{F}]\text{FMZ}$  is developed on Merck Si-60 plate with 90% acetonitrile solution.

Partition coefficients were measured by mixing  $[^{18}\text{F}]\text{FMZ}$  (3.7–5.0 KBq) with 3 mL each of 1-octanol and 0.1 M phosphate buffer saline, pH 7.4 in a test tube. The test tube was vortexed for 1 min at room temperature, followed by centrifugation (3000 g) for 3 min. Two samples (1 mL each) from the 1-octanol and buffer layers were assayed for radioactivity in a gamma scintillation counter. Samples from the 1-octanol layer were repartitioned until consistent partitions coefficient values were obtained.

Partition coefficient is an index of the lipophilicity of the probe in buffer.  $[^{18}\text{F}]\text{FMZ}$  had a little higher partition coefficient ( $1.49 \pm 0.12$ ), suggesting it was 30 fold more lipophilic and was capable of penetrating the blood-brain barrier (BBB).

A 14–16 month old *Sprague-Dawley*(SD) rat, anesthetized with ether, was injected with 37 MBq/200  $\mu\text{L}$  of  $[^{18}\text{F}]\text{FMZ}$  through the lateral tail vein. The rat was sacrificed by decapitation at 30 min postinjection. In a competition study, another rat was co-injected 200  $\mu\text{g}$  of diazepam (BZR agonist) with  $[^{18}\text{F}]\text{FMZ}$ . The brains were immediately removed and frozen in powdered dry ice. Sagittal sections of 1 mm were cut and exposed to Kodak XAR film for 72 h. *Ex vivo* film autoradiograms were obtained. Results from the rat brain study demonstrated the  $[^{18}\text{F}]\text{FMZ}$  can be clearly inhibited by the BZR agonist (Figure 3).

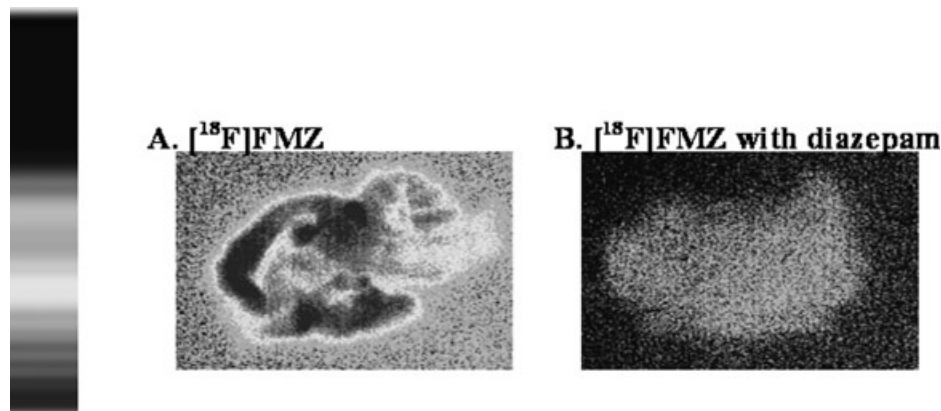


**Figure 3.**  $[^{18}\text{F}]\text{FMZ}$  rat autoradiography of whole-hemisphere sections in comparing with BZR agonist images.

The *ex vivo* autoradiography of rat whole-hemisphere sections demonstrated a high and similar uptake in areas known to contain a high density of BZR. The binding of  $[^{18}\text{F}]\text{flumazenil}$  demonstrated a high density of binding sites throughout the different cortical regions (cerebellum ratio was  $1.30 \pm 0.13$ ). Similar low binding ratios was observed between the cerebellum and hippocampus, thalamus and pons. (ratios were  $0.99 \pm 0.07$ ,  $0.98 \pm 0.10$  and  $0.91 \pm 0.08$ , respectively) The binding was completely inhibited by the addition of diazepam (BZR agonist) (Table 1).

PSL/mm <sup>2</sup>	Cortex	Hippocampus	Thalamus	Hypothalamus	Pons	Cerebellum
F-18-FMZ	$1698.67 \pm 158.68$	$1302.44 \pm 82.98$	$1289.16 \pm 122.85$	$1528.30 \pm 95.79$	$1197.23 \pm 107.30$	$1311.94 \pm 73.86$
F-18-FMZ with diazepam	$654.35 \pm 12.28$	$677.16 \pm 6.28$	$692.22 \pm 4.51$	$702.86 \pm 4.62$	$701.51 \pm 10.68$	$662.24 \pm 21.28$
F-18-FMZ compared with cerebellum	$1.30 \pm 0.13$	$0.99 \pm 0.07$	$0.98 \pm 0.10$	$1.17 \pm 0.09$	$0.91 \pm 0.08$	1



**Conclusion:** In conclusion, non-carrier added [ $^{18}\text{F}$ ]FMZ can be prepared in the simplified Nuclear Interface synthesizer such as using the [ $^{18}\text{F}$ ]FDG module. A solid extraction purification unit can be easily adapted on the synthesizer to remove the impurities generated in the reaction. This process is much easier to meet cGMP compliance in accordance with drug company standards. The purified product behaves as an ideal brain GABA/BZR receptor imaging agent.

## References

- [1] I. Savic, M. Ingvar, S. Stone-Elander, *J. Neurol. Neurosurg.* **1993**, *56*, 615–21.
- [2] B. Szelies, J. Sobesky, G. Pawlik, *Eur. J. Neurol.* **2002**, *9*, 137–42.
- [3] J. E. Litton, J. Neiman, S. Pauli, L. Farde, T. Hindmarsh, C. Halldin *et al.*, *Psychiatry Res.* **1993**, *50*, 1–13.
- [4] P. Leveque, S. Sanabria-Bohorquez, A. Bol, A. D. Volder, D. Labar, K. V. Rijckevorsel *et al.*, *Eur. J. Nucl. Med. Mol. Imaging.* **2003**, *30*, 1630–36.
- [5] Y. H. Yoon, J. M. Jeong, H. W. Kim, S. H. Hong, Y. S. Lee, H. S. Kil *et al.*, *Nucl. Med. Biol.* **2003**, *30*, 521–27.
- [6] A. D. Windhorse, R. P. Klok, C. L. Koolen, G. W. M. Visser, J. D. M. Herscheid, *J. Label. Compd. Radiopharm.* **2001**, *44*, S930.
- [7] A. D. Windhorse, M. P. J. Mooijer, R. P. Klok, G. W. M. Visser, J. D. M. Herscheid, *J. Label. Compd. Radiopharm.* **2003**, *46*, S148.
- [8] N. N. Ryzhikov, N. Seneca, R. N. Krasikova, N. A. Gomzina, E. Shchukin, O. S. Fedorova, D. A. Vassiliev, B. Gulyas, H. Hall, I. Savic, C. Halldin, *Nucl. Med. Biol.* **2005**, *32*, 109–16.

## AUTO-SYNTHESIS OF FLUORO-18-FDDNP ON ALZHEIMER'S RESEARCH

KANG-WEI CHANG,<sup>a,b</sup> SHIH-YING LEE,<sup>b</sup> WUU-JYH LIN,<sup>b</sup> CHIA-CHIEH CHEN,<sup>b</sup> JENN-TZONG CHEN<sup>b</sup>  
AND HSIN-ELL WANG<sup>a</sup>

<sup>a</sup>Department of Biomedical Imaging and Radiological Sciences, National Yang-Ming University, Taiwan

<sup>b</sup>Division of Isotope Application, Institute of Nuclear Energy Research, Atomic Energy Council, Taiwan

**Abstract:** Alzheimer's disease (AD) is an epidemic neurodegenerative disorder-affecting millions of elderly adults. Senile plaques (SPs) and neurofibrillary tangles (NFTs) are hallmarks in AD. [ $^{18}\text{F}$ ]FDDNP (2-(1-{ 6-[(2-fluoroethyl)(methyl)amino]-2-naphthyl} ethylidene)malononitrile) was superior binding with SPs and NFTs. High quality [ $^{18}\text{F}$ ]FDDNP was produced by an auto synthesizer. [ $^{18}\text{F}$ ]FDDNP has a partition coefficient of  $1.93 \pm 0.10$  mean was it shows hydrophobic ability to penetrate the blood brain barrier (BBB). *In vitro* autoradiography saturated with Tg2576, showed high retention ratio for A $\beta$  rich regions (for example in Tg2576, hippocampus and frontal cortex were  $2.10 \pm 0.34$  and  $1.90 \pm 0.17$ , respectively) and human brain section, postcentral gyrus, and occipital lobe showed significant different retention ratio ( $1.48 \pm 0.04$  and  $2.37 \pm 0.13$ , respectively). In *ex vivo* study, in hippocampus and frontal cortex region, Tg2576 had better retention than control mice. ( $2.40 \pm 0.33$  and  $2.19 \pm 0.22$ , respectively). In this paper, we show our modified protocol for the synthesis of [ $^{18}\text{F}$ ]FDDNP and report *in vitro*, *in vivo* and *ex vivo* results in transgenic mice as a model for applications in A $\beta$  radiopharmaceutical research.

**Keyword:** alzheimer's disease; FDDNP; auto-synthesizer

**Introduction:** Alzheimer's disease (AD) is predicted to become the most common form of dementia among the neurodegenerative diseases in the new millennium.<sup>1–3</sup> AD causes morbidity and mortality in about 40–60% of the population over 80 years of age.<sup>4</sup> Two hallmark lesions characterize this progressive neurodegenerative disease: (1) senile plaques (SPs) and (2) neurofibrillary tangles (NFTs).<sup>1,5</sup> AD involves deterioration in a broad spectrum of cognitive processes, including memory, language, knowledge, attention, and executive functions.<sup>7</sup> Conventional imaging techniques, such as computed tomography and magnetic resonance imaging, have limitations in diagnosis because they currently lack sensitivity and specificity.<sup>4,6,8</sup>

A strong association of amyloid plaques with an ideal biomarker could be used to improve diagnosis in the early stages of AD and evaluate the efficacy of therapeutic agents.<sup>3,9,10,11</sup> When labeled with appropriate isotopes, these biomarkers could develop into critical *in vivo* tools for monitoring the formation and aggregation of A $\beta$  plaques and assisting in the early diagnosis of patients with AD.<sup>2,8,12</sup> The solvent polarity- and viscosity-sensitive radioisotope probe, [ $^{18}\text{F}$ ]FDDNP (aminonaphthalene groups), can be used to label SPs and NFTs and shows excellent *in vitro* fluorescence visualization of these fibrillar aggregates.<sup>7,13</sup> When [ $^{18}\text{F}$ ]FDDNP combined with PET is used to quantify the A $\beta$  peptides load in the brains of patients with AD, it can lead to early diagnosis and could help elucidate the etiology of AD by correlating neuropathology with functional loss.<sup>7</sup>

Reported herein, we modified the auto-synthesis of [ $^{18}\text{F}$ ]FDG for the synthesis of [ $^{18}\text{F}$ ]FDDNP. We obtained encouraging results with this tracer in Tg2576 mice which overexpress a mutant form of the human amyloid precursor protein (APP) associated with an autosomal dominant form of AD suggesting that the development of imaging agents for mapping A $\beta$  plaques in the living human brain may be possible. We wish to present [ $^{18}\text{F}$ ]FDDNP in microPET imaging, to predict the pathogenic process and provide standard methods for AD.

### Materials and methods: Synthesis of [ $^{18}\text{F}$ ]FDDNP

[ $^{18}\text{F}$ ]FDDNP was synthesized by a modification of the procedure published in 2007 and for the preparation of FDG.<sup>6</sup> Nucleophilic substitution of the tosyl group with the no-carrier-added precursor [ $^{18}\text{F}$ ]KF/Kryptofix 222 in acetonitrile yielded FDDNP. The product was passed through an activated C-18 cartridge and then through the cartridge again to remove water and finally with 100% ethanol. The product was identified by high-performance liquid chromatography (Figure 1).

*Partition coefficient determination*

[<sup>18</sup>F]FDDNP combined with 1-octanol and 0.1 M phosphate-buffered saline, pH 7.4 in a test tube and vortexed the tube for 1 min at room temperature, followed by centrifugation (3000 × g) for 3 min. Two samples from the 1-octanol and buffer layers were assayed for radioactivity in a gamma scintillation counter.<sup>3</sup>

*In vitro autoradiography:* Frozen brain sections (20 μm thick) of Tg2576 and human brain tissue were incubated with [<sup>18</sup>F]FDDNP (10.25 μM cold FDDNP) at a concentration of 5 μCi/mL. The sections were rinsed with saturated Li<sub>2</sub>CO<sub>3</sub> in 40% EtOH, 40% EtOH and water. After drying, sections were exposed to Cronex MRF-34 film for 72 h.<sup>14</sup>

*Ex vivo plaque binding with [<sup>18</sup>F]FDDNP:* Tg2576 were anesthetized with ether, injected with 185 MBq of [<sup>18</sup>F]FDDNP through the lateral tail vein. Mice were sacrificed by decapitation at 5, 30, and 60 min after injection. The brains were cut as sagittal sections of 20 μm and exposed to Kodak XAR film for 72 h. Ex vivo film autoradiograms were obtained (Figure 2).<sup>15</sup>

**Result and discussion:** *Synthesis of [<sup>18</sup>F]FDDNP*

[<sup>18</sup>F]FDDNP was synthesized in high radiochemical yield (20–25%) and high radiochemical purity (> 90%).

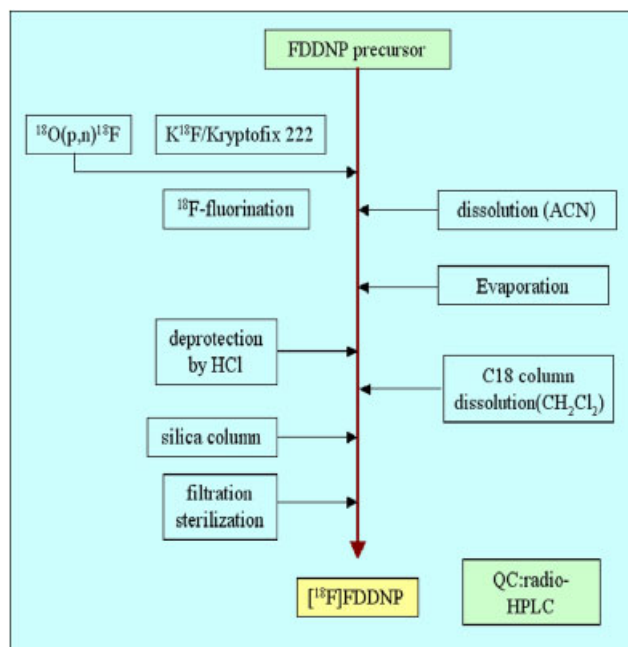


**Figure 1.** The synthesis protocol of [<sup>18</sup>F]FDDNP. Take the precursor of DMTEAN (lysis in acetonitrile) and complete the S<sub>N</sub>2 reaction at 95. Add 0.1N HCl for hydrolysis for 10 mins. Pass the reaction solution through an activated C18 cartridge. Wash with water, and finally elute with ethanol.

*Partition coefficient:* The partition coefficient of [<sup>18</sup>F]FDDNP was  $1.93 \pm 0.10$ , indicates it was suitable for penetration of the blood-brain barrier (BBB).

*In vitro autoradiography*

Tg2576 is a standard strain for AD research to develop AD pathology.<sup>16</sup> In this assay, strong binding of [<sup>18</sup>F]FDDNP in brain sections β-amyloid rich region was observed. And in competition assay added non-labeled FDDNP, the binding was significantly reduced Table 1.

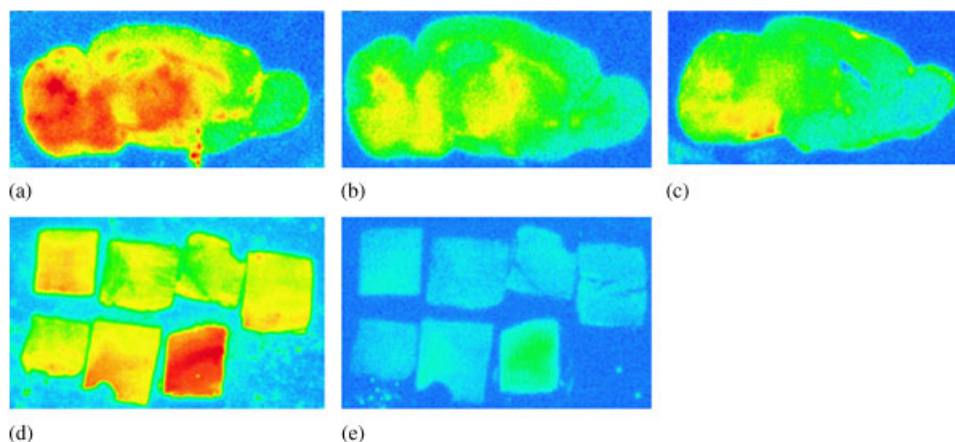


**Figure 2.** Film autoradiograms of the in vitro assay showing the binding of [<sup>18</sup>F]FDDNP in sagittal sections of the brains of mice from A to C (A and B were Tg2576, and C was control mice) and human brain section from D to E. B and E were the competition assay with non-labeled FDDNP (10.25 μM). It is evident that [<sup>18</sup>F]FDDNP labeled the Aβ plaques with high sensitivity and clarity, whereas binding was inhibited when non-labeled FDDNP was included.

**Table 1.** In vitro autoradiography results of [<sup>18</sup>F]FDDNP binding in the hippocampus and frontal cortex sections in Tg2576 mice and control normal mice. Competitive assay in Tg2576 mice brain sections involving co-incubation with cold FDDNP (10.25 μM). (N = 3, mean ± SD)

	Tg2576		Control mice	
	F-18-FDDNP	w/w 10.25 μM FDDNP	F-18-FDDNP	w/w 10.25 μM FDDNP
Cortex	109.41 ± 29.43	33.39 ± 16.90	7.19 ± 3.17	2.13 ± 1.44
Hippocampus	49.08 ± 17.24	23.52 ± 10.53	4.02 ± 0.75	2.13 ± 1.66
Thalamus	73.57 ± 29.63	17.75 ± 10.31	9.46 ± 4.68	10.61 ± 4.81
Hypothalamus	44.14 ± 28.48	19.46 ± 8.37	5.82 ± 2.97	4.06 ± 0.19
Midbrain	39.53 ± 16.68	20.96 ± 12.21	1.16 ± 3.57	2.35 ± 2.12
Pons	33.08 ± 10.53	20.89 ± 10.34	5.50 ± 3.63	3.34 ± 1.74
Medulla	38.19 ± 13.74	23.77 ± 9.24	9.84 ± 5.64	2.15 ± 2.09
Cerebellum	115.80 ± 50.36	48.012 ± 6.28	22.31 ± 14.23	21.73 ± 10.21

We noted two different in Tg2576 accumulated with [<sup>18</sup>F]FDDNP. One is in cerebellum, a different condition with AD patients. And the other is the ratio comparison with Tg2576 and control mice. Although that, it maybe be explained by the control mice having bred up to 15 months cause over-expression of APP protein and neurodegeneration. In addition, FDDNP not only binding with tangles and plaques in Alzheimer's disease also could associate with prion protein in neuro-disease (Table 2).<sup>8</sup>

**Table 2.** In vitro autoradiography results of [<sup>18</sup>F]FDDNP binding in the AD patient brain section. Competitive assay in Tg2576 mice brain sections involving co-incubation cold FDDNP (10.25 μM). (N = 3, mean ± SD)

	Frontal lobe	Temporal lobe	Hippocampus	Amygdala	Precentral gyrus	Postcentral gyrus	Occipital lobe
Comparison with control human brain	1.40 ± 0.16	1.08 ± 0.12	0.97 ± 0.06	1.15 ± 0.18	0.74 ± 0.10	1.48 ± 0.06	2.37 ± 0.13
Comparison with nonlabeled FDDNP	14.16 ± 0.93	125.93 ± 4.98	10.45 ± 0.74	14.49 ± 0.96	14.67 ± 1.09	14.67 ± 1.36	13.45 ± 0.69

*Ex vivo plaque binding with [<sup>18</sup>F]FDDNP:* The distribution of [<sup>18</sup>F]FDDNP in the brain is determined by ex vivo autoradiography. [<sup>18</sup>F]FDDNP uptake in the whole brain of Tg2576 was higher than that in normal control mice (Table 3).

**Table 3.** Ex vivo autoradiography assay determined binding with [<sup>18</sup>F]FDDNP showing brain sections of Tg2576 and control mice over a time course of 30 min. (N = 3, mean ± SD)

	Tg2576	Control mice
Cortex	48.24 ± 28.40	10.97 ± 8.54
Hippocampus	45.58 ± 25.13	14.75 ± 10.88
Thalamus	51.55 ± 29.16	12.55 ± 8.12
Hypothalamus	41.37 ± 20.47	10.71 ± 5.69
Midbrain	54.79 ± 28.76	16.13 ± 8.36
Pons	61.90 ± 34.96	15.08 ± 8.20
Medulla	73.54 ± 37.45	13.24 ± 9.70
Cerebellum	54.53 ± 26.50	14.24 ± 11.86

The ratio between the two animal models were about 3 to 4 fold at 30 min postinjection. The results were consistent with biodistribution studies (data not shown).

**Conclusion:** In this article, we show the successful synthesis of [<sup>18</sup>F]FDDNP by an automatic synthesizer. It could be provide the benefits to reduces the operator radiation dose for faster diagnosis. Encouraging results in Tg2576 and human brain section, suggest that develop imaging Aβ plaques in the living human brain may be possible. The present agent may prove a useful PET probe for imaging Aβ plaques in the living human brain.

## References

- [1] R. P. Brendza, B. J. Bacskai, J. R. Cirrito, K. A. Simmons, J. M. Skoch, W. E. Klunk, C. A. Mathis, K. R. Bales, S. M. Paul, B. T. Hyman, D. M. Holtzman, *J. Clin. Invest.* **2005**, *115*, 2.
- [2] M. P. Kung, C. Hou, Z. P. Zhuang, A. J. Cross, D. L. Maier, H. F. Kung, *Eur. J. Nucl. Med. Mol. Imaging.* **2004**, *31*, 8.
- [3] C. W. Lee, M. P. Kung, C. Hou, H. F. Kung, *Nucl. Med. Biol.* **2003**, *30*, 6.

- [4] P. V. Kulkarni, V. Arora, A. C. Roney, C. White III, M. Bennett, P. P. Antich, F. J. Bonte, *Nuclear Instruments and Methods in Physics Research B*. **2005**, 241.
- [5] L. Giovannelli, F. Casamenti, C. Scali, L. Bartolini, G. Pepeu, *Neuroscience*. **1995**, 66, 4.
- [6] J. Liu, V. Kepe, A. Zabjek, A. Petric, H. C. Padgett, N. Satyamurthy, J. R. Barrio, *Mol Imaging Biol*. **2007**, 9, 1.
- [7] E. D. Agdeppa, V. Kepe, A. Petri, N. Satyamurthy, J. Liu, S. C. Huang, G. W. Small, G. M. Cole, J. R. Barrio, *Neuroscience*. **2003**, 117, 3.
- [8] E. D. Agdeppa, V. Kepe, J. Liu, S. Flores-Torres, N. Satyamurthy, A. Petric, G. M. Cole, G. W. Small, S. C. Huang, J. R. Barrio, *J. Neurosci*. **2001**, 21, 24.
- [9] W. E. Klunk, Y. Wang, G. F. Huang, M. L. Debnath, D. P. Holt, C. A. Mathis, *Life Sci*. **2001**, 69, 13.
- [10] W. Zhang, M. P. Kung, S. Oya, C. Hou, H. F. Kung, *Nucl. Med. Biol*. **2007**, 34, 1.
- [11] A. B. Newberg, N. A. Wintering, K. Plössl, J. Hochold, M. G. Stabin, M. Watson, D. Skovronsky, C. M. Clark, M. P. Kung, H. F. Kung, *J. Nucl. Med*. **2006**, 47, 5.
- [12] M. P. Kung, C. Hou, Z. P. Zhuang, B. Zhang, D. Skovronsky, J. Q. Trojanowski, V. M. Lee, H. F. Kung, *Brain Res*. **2002**, 956, 2.
- [13] L. Ye, J. L. Morgenstern, J. R. Lamb, A. Lockhart, *Biochem. Biophys. Res. Commun*. **2006**, 347, 3.
- [14] Z. P. Zhuang, M. P. Kung, C. Hou, K. Plössl, D. Skovronsky, T. L. Gur, J. Q. Trojanowski, V. M. Lee, H. F. Kung, *Nucl. Med. Biol*. **2001**, 28, 8.
- [15] J. R. Barrios, V. Kepe, N. Satyamurthy, S. C. Huang, W. Gary, *Small International Congress Series*. **2006**, 1290.
- [16] S. Oddo, A. Caccamo, J. D. Shepherd, M. P. Murphy, T. E. Golde, R. Kaye, R. Metherate, M. P. Mattson, Y. Akbari, F. M. LaFerla, *Neuron*. **2003**, 39, 3.

## LABELLING OF PEPTIDE DERIVATIVE WITH IN-111 FOR RECEPTOR IMAGING

HUNG-MAN YU, MEI-HUI WANG, JENN-TZONG CHEN, AND WUU-JYH LIN

Institute of Nuclear Energy Research, Taoyuan, Taiwan

**Abstract:** DTPA-conjugated peptides can be labelled with radionuclides such as  $^{111}\text{In}$  and  $^{177}\text{Lu}$ . These radiolabelled peptides used for peptide receptor imaging (PRI) and radionuclide therapy (PRRT) require high specific activities. In this study, parameters influencing the kinetics of labelling of DTPA-peptides, including ligand concentration, type and pH of buffer, reaction temperature and time, were investigated and conditions were optimised to obtain the highest achievable specific activity. The labelling yield of DTPA-peptides was decreased with ligand concentration and was optimal at pH 2; pH  $\geq 4$  strongly decreased the labelling yield. Labelling with  $^{111}\text{In}$  in sodium citrate buffer was completed after 30 min at 60°C. The results in this study were helpful in optimising the specific activity of  $^{111}\text{In}$  labelled DTPA-peptide derivatives, and in increasing their effectiveness in PRI and PRRT.

**Keyword:** peptide; DTPA; indium-111; radiolabelling; specific activity

**Introduction:** Cells express on their cellular membranes a variety of receptor proteins with a high affinity for regulatory peptides. Alterations of receptor expression during disease, such as overexpression in many neoplasias, can be exploited by imaging techniques. Therefore, peptide receptor scintigraphy with the small radioactive peptide analogs appeared to be a sensitive and specific technique to show in vivo the presence of receptors on various tumors.<sup>1,2</sup>

Peptides can be easily chemically synthesized, modified and stabilized to obtain optimized pharmacokinetic parameters. Peptides are rapidly taken up and retained in target tissues, have fast plasma clearance due to the renal excretion, rapid tissue penetration and low antigenicity<sup>3</sup>. Since the late 1980s, peptide radiopharmaceuticals have become an important class of tracers for tumor detection and localization by peptide receptor imaging (PRI) and for therapy by peptide receptor radiotherapy (PRRT). The most frequently used isotopes for peptide labeling are radiometals, such as  $^{111}\text{In}$ ,  $^{99\text{m}}\text{Tc}$ ,  $^{68}\text{Ga}$ , or  $^{64}\text{Cu}$  for imaging purposes and  $^{90}\text{Y}$  and  $^{177}\text{Lu}$  for therapeutic approaches.<sup>4,5</sup>

DTPA-conjugated peptides can be readily labeled with radionuclides such as  $^{111}\text{In}$  and  $^{177}\text{Lu}$ . In order for these radiolabelled peptides to be successfully used in PRI or PRRT, high specific activities are required<sup>6</sup>. The aim of this study is to determine the optimal conditions for radiolabelling DTPA-peptides with the  $^{111}\text{In}$ . We investigated parameters that influence radiochemical yields and reaction kinetics in order to obtain maximal achievable specific activities.

### Experimental: Materials and methods

All chemicals used in the present work were of analytical grade. Sodium citrate, sodium acetate, citric acid and acetic acid were purchased from Sigma-Aldrich. Instant thin layer chromatography silica gel (ITLC-SG) plates were purchased from Pall Life Science.  $^{111}\text{InCl}_3$  was produced at our institute.

**Labeling of peptide with In-111:** For all radiolabeling experiments, the individual components were added in the following order: specific buffer solution (0.1 M, 20  $\mu\text{L}$ ), specific concentration of the ligand solution (0.26  $\mu\text{M}$  - 13  $\mu\text{M}$ , 5  $\mu\text{L}$ ), 1.1 MBq no-carrier-added  $^{111}\text{InCl}_3$  solution (0.55 GBq/1 mL, 2  $\mu\text{L}$ ) were added in the Eppendorf microcentrifuge tubes (0.5 mL). The reaction parameters that affect the radiochemical yield of  $^{111}\text{In}$ -DTPA-peptide like peptide concentration, reaction temperature (25°C, 60°C, 90°C), reaction time, type of buffer solution (sodium citrate, sodium acetate) and pH of buffer solution (2–6) were studied.

**Radiochemical yield:** The radiochemical yield was determined using ITLC-SG and radio-TLC imaging scanner (AR-2000, BIOSCAN). The mobile phase used for developing was 10 mM sodium citrate solution (pH 5). The labeled compound of peptide remained near the origin ( $R_f=0-0.1$ ), while free In-111 moved to the solvent front ( $R_f = 0.9-1$ ).

**Results and discussion:** Peptide concentration studies

The effect of peptide concentration on the radiochemical yield of  $^{111}\text{In}$ -DTPA-peptide was shown in Figure 1. The results indicate that the radiochemical yield of  $^{111}\text{In}$ -DTPA-peptide increased from 27% to >99% and 67% to >99% by increasing the amount of peptide for sodium citrate buffer and for sodium acetate buffer respectively. Under the same reaction conditions, 44 ng and 110 ng of ligand were needed to achieve >99% radiochemical yield for sodium citrate buffer and for sodium acetate buffer respectively.

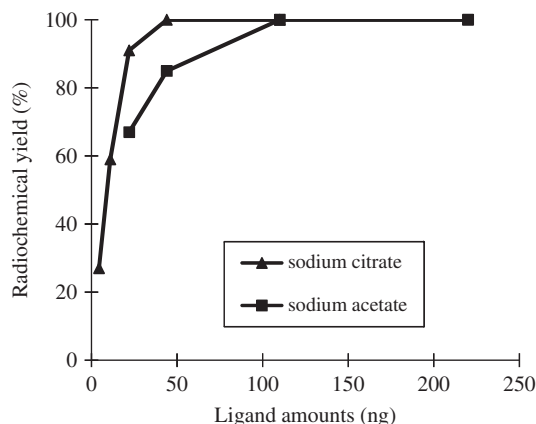


**Figure 1.** Influence of ligand amount on radiochemical yield in complexation of DTPA-peptide with In-111 at 25 (5  $\mu\text{L}$  ligand + 2  $\mu\text{L}$  1.1 MBq In-111 + 20  $\mu\text{L}$  buffer of pH 3).

**Reaction temperature studies:** The results in Figure 2 show that for both buffers and all ligand concentrations, by increasing the reaction temperature from 25°C to 60°C, the labeling yield was increased and the extent was greater for lower ligand concentration. By raising the reaction temperature to 90°C, the labeling yield was decreased (except labeling condition with 4.4 ng in sodium citrate buffer). The decreased yield of  $^{111}\text{In}$ -DTPA-peptide at 90°C may be attributed to the thermal decomposition of the labeled compound.

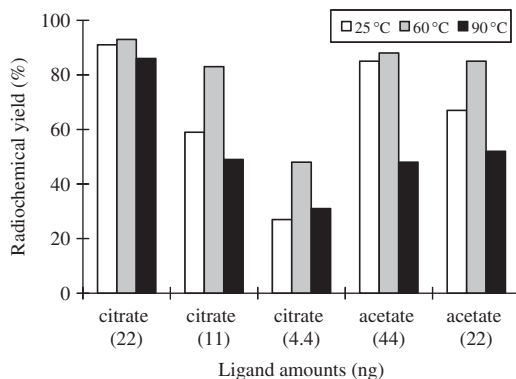


**Figure 2.** Influence of reaction temperature on radiochemical yield in complexation of DTPA-peptide with In-111 (5  $\mu\text{L}$  ligand + 2  $\mu\text{L}$  1.1 MBq In-111 + 20  $\mu\text{L}$  buffer of pH 3).

**Reaction time studies:** Figure 3 shows that the labeling yield increased with reaction time. At 25°C, the labeling yield for sodium citrate buffer and sodium acetate buffer increased gradually with reaction time. At 60°C, the labeling yield for sodium citrate buffer increased with time, but for sodium acetate buffer, the labeling yield reached maximum to 47% at 30 min and then decreased to 38% at 120 min. These results confirm that reaction time is more important at low reaction temperature for radiolabeling of  $^{111}\text{In}$ -DTPA-peptide in our study.

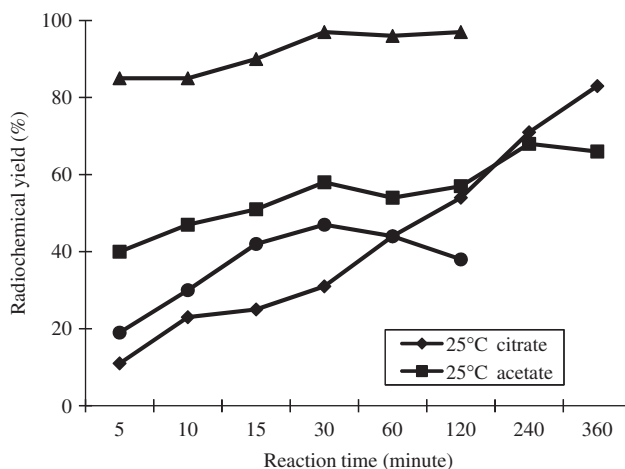


**Figure 3.** Influence of reaction time on radiochemical yield in complexation of DTPA-peptide with In-111 at 25 or 60 (5  $\mu\text{L}$  11ng ligand + 2  $\mu\text{L}$  1.1 MBq In-111 + 20  $\mu\text{L}$  buffer of pH 3).

**Buffer pH studies:** Figure 4 shows the variation of the radiochemical yield of  $^{111}\text{In}$ -DTPA-peptide as a function of pH in sodium citrate buffer solution. The maximum yield was obtained at pH 2. The yield had a steep decrease from pH 3 to pH 4. The results clarify that the pH is a significant factor that affects the labeling yield with  $^{111}\text{In}$ .

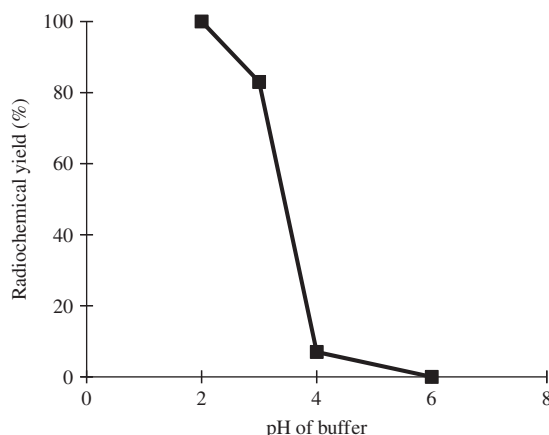


**Figure 4.** Influence of buffer pH on radiochemical yield in complexation of DTPA-peptide with In-111 at 25 (5  $\mu\text{L}$  11 ng ligand + 2  $\mu\text{L}$  1.1 MBq In-111 + 20  $\mu\text{L}$  sodium citrate buffer).

**Conclusion:** DTPA-peptides can be radiolabelled at high specific activity. Conditions were optimal at pH 2 and the reactions were complete after 30 min at 60°C. This study has shown that several parameters (ligand concentration, buffer solution, reaction temperature, reaction time and buffer pH) are important for radiolabelling of peptides with In-111 to obtain maximal achievable specific activities.

**Acknowledgement:** This research was supported by grant (98-2001-01-D-10) from National Science and Technology Program for Biotechnology and Pharmaceuticals (NSTPBP), National Science Council, Taiwan.

## References

- [1] D. J. Kwekkeboom, E. P. Krenning, M. de Jong, *J. Nucl. Med.* **2000**, *41*, 1704–1713.
- [2] W. A. Breeman, M. de Jong, D. J. Kwekkeboom, R. Valkema, W. H. Bakker, P. P. Kooij, T. J. Visser, E. P. Krenning, *Eur. J. Nucl. Med.* **2001**, *28*, 1421–1429.
- [3] M. de Jong, D. Kwekkeboom, R. Valkema, E. P. Krenning, *Eur. J. Nucl. Med.* **2003**, *30*, 463–469.
- [4] A. Signore, A. Annovazzi, M. Chianelli, F. Corsetti, C. Van de Wiele, R. N. Watherhouse, *Eur. J. Nucl. Med.* **2001**, *28*, 1555–1565.
- [5] H. J. Wester, M. Schottelius, T. Poethko, K. Bruus-Jensen, M. Schwaiger, *Cancer Biother. Radiopharm.* **2004**, *19*, 231–244.
- [6] W. A. Breeman, M. de Jong, T. J. Visser, J. L. Erion, E. P. Krenning, *Eur. J. Nucl. Med. Mol. Imaging* **2003**, *30*, 917–920.

## PHARMACOKINETIC EVALUATION OF RADIOLABELED HYALURONIC ACIDS: A POTENTIAL AGENT FOR THE EARLY OSTEOARTHRITIC THERAPY

HAO-WEN KAO,<sup>a</sup> CHI-JEN CHAN,<sup>a</sup> SUNG-CHING CHEN,<sup>b</sup> SHAIN-JY WANG,<sup>c</sup> MING-HSIEN LIN,<sup>a,d</sup> WUU-JYH LIN,<sup>e</sup> JENN-TZONG CHEN,<sup>e</sup> AND HSIN-ELL WANG<sup>a,\*</sup>

<sup>a</sup>Department of Biomedical Imaging and Radiological Sciences, National Yang-Ming University, Taipei, Taiwan

<sup>b</sup>Biomedical Engineering Research Laboratories, Industrial Technology Research Institute, Hsinchu, Taiwan

<sup>c</sup>Material and Chemical Research Laboratories, Industrial Technology Research Institute, Hsinchu, Taiwan

<sup>d</sup>Department of Nuclear Medicine, Zhongxiao Branch of Taipei City Hospital, Taipei, Taiwan

<sup>e</sup>Institute of Nuclear Energy Research, Department of isotope application, Taoyuan, Taiwan

\*Correspondence to: Hsin-Ell Wang, No. 155, Sec. 2, Linong st., Beitou District, Taipei 112, Taiwan

**Abstract:** Viscosupplementation treatment is a accepted therapeutic modality for osteoarthritis (OA). Intraarticular injection of hyaluronic acid (HA) provides pain relief by lessening the frictional resistance of the cartilage and improving joint function. This study evaluated the pharmacokinetics of  $^{131}\text{I}$ -labeled HAs in an osteoarthritis rabbit model. HA22/HA142 were conjugated with tyramine and labeled with I-131 to afford  $^{131}\text{I}$ -Tyr-HAs. Osteoarthritis in the left knee joint was surgically induced in New Zealand white rabbits. After intraarticular administration of  $^{131}\text{I}$ -Tyr-HAs into the OA and normal knee joints, the whole-body distribution of radioactivity was longitudinally monitored using scintigraphic imaging. Most of the radioactivity was found retained in the synovial joints. A small portion accumulated slowly in the liver and bladder, indicating that HA, after exiting synovial joints, was metabolized in the liver and excreted in urine. The pharmacokinetics was evaluated based on the counts of ROI derived from the scintigraphic images. The results revealed that HA of higher molecular weight ( $^{131}\text{I}$ -Tyr-HA142) enjoyed longer distribution half-life in normal and OA knee joints than that of lower molecular weight ( $^{131}\text{I}$ -Tyr-HA22). This study demonstrated that  $^{131}\text{I}$ -labeled tyramine-conjugated HA can be used as a scintigraphic probe that allows non-invasive long-term pharmacokinetic evaluation of HA in an OA rabbit model.

**Keywords:** viscosupplementation treatment; hyaluronic acid; scintigraphic imaging; pharmacokinetics

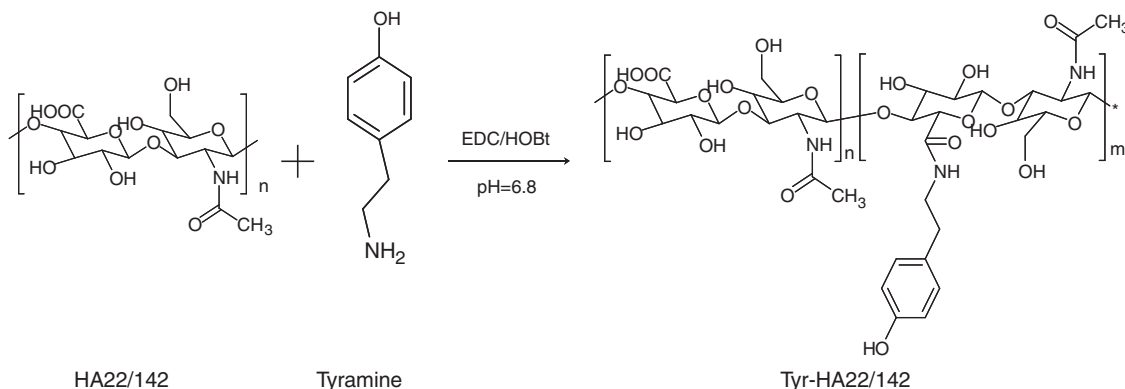
**Introduction:** Osteoarthritis (OA) is a common form of arthritis, characterized by the slow degeneration of cartilage, pain, and restriction of mobility.<sup>1</sup> Although increasing age and excessive articular surface contact stress increase the risk of degeneration in all joints, the pathophysiology of the joint degeneration that leads to clinical syndrome of OA remains poorly understood.<sup>2</sup> The treatment toward OA, including nonpharmacologic modalities, pharmacologic therapy and surgery, can help patients reduce pain, maintain or improve joint mobility, and limit functional impairment. The nonpharmacologic modalities contain weight loss, bracing, muscle-strengthening exercises and so on, while the prescription used in pharmacologic therapy includes oral analgesic agents, intraarticular (i.a.) relief supplements and topical treatment modalities.<sup>3,4</sup>

Hyaluronic acid (HA) is a high molecular weight unbranched polymer chain of repeating N-acetyl- D-glucosamine-D-glucuronic acid disaccharides.<sup>5</sup> HA, one of the components of trinary macromolecular complex in articular cartilage matrix, endowed articular cartilage with many specific mechanical properties, such as viscoelasticity. HA is also a major component of synovial fluid, which supplies nutrients to the articular cartilage and lubricates the joints, thereby minimizing friction on the surface of the articular cartilage. I.a. exogenous HA therapy, which has been approved by the US Food and Drug Administration since 1997, has recently become widely accepted for OA of the knee based on its anti-inflammatory effect and for reducing pain. The decrease of endogenous HA in the synovial fluid is believed to accelerate cartilage destruction in OA.<sup>5</sup> The effect of i.a. therapy with HA is to help replace synovial fluid that has lost its viscoelastic properties and provide improvement in pain, physical function, and quality of daily living. Studies on animals have shown that HA effectively reduces articular pain and slow down the degenerative process of OA.<sup>5-9</sup> Clinical trials and current studies have demonstrated that i.a. HA injection effectively relieves pain and improves motility function. However, the mechanism by which this occurs have not yet been elucidated.<sup>10</sup> The viscoelasticity of HA *in situ* depends on its molecular weight and local concentration. Although the effectiveness of the different molecular weight HAs are still debated, some previous studies revealed that the HA with higher molecular weight is more effective than that with lower molecular weight in inhibiting cartilage degeneration in early OA.<sup>5</sup>

Iodine-131, a radionuclide with a gamma emission of 364 keV and a physical half-life of 8.02 d, is suitable for longitudinal scintigraphic monitoring within one month post injection. Since HA does not contain any convenient group for radiolabeling, it is first conjugated with tyramine (Tyr) as a prosthetic group and then labeled with <sup>131</sup>I to afford <sup>131</sup>I-Tyr-HA. This study demonstrated the *in vivo* whole-body distribution and evaluated the pharmacokinetics in OA knees and normal knees of a rabbit model using non-invasive planar gamma imaging after i.a. administration with <sup>131</sup>I-Tyr-HAs of different molecular weights.

#### Results and discussion: Preparation and analysis of radiolabeled HA

Tyr-HA22/142 (molecular weight  $0.22/1.42 \times 10^6$  dalton) conjugates were synthesized by a carbodiimide/active ester-mediated coupling reaction in distilled water (Scheme 1).<sup>11</sup> Based on the <sup>1</sup>H NMR measurement, about one tyramine molecule was present per 3.0 repeat units of HA22, and 3.6 repeat units of HA142. After radioiodinated with chloramine-T and centrifugally purified with Microcon YM-30, <sup>131</sup>I-Tyr-HAs with different molecular weights were prepared with moderate radiochemical yield (about 30%) and high radiochemical purity (>95%). The radiochemical purity was determined using thin layer chromatography (TLC) performed with a reverse phase silica gel on aluminum sheets and methanol as developing agent.



**Scheme 1.** The synthesis of Tyr-HA22/HA142 conjugates.

***In vitro* stability studies:** The *in vitro* stability of <sup>131</sup>I-Tyr-HA22 and <sup>131</sup>I-Tyr-HA142 in PBS at 4°C was good; the radiochemical purities were >96% after 72 h incubation. The stability of the two tracers in rabbit plasma at 37°C was fair; the radiochemical purities declined to  $84.2 \pm 1.9\%$  for <sup>131</sup>I-Tyr-HA22 and  $84.1 \pm 0.5\%$  for <sup>131</sup>I-Tyr-HA142 (Figure 1) after 72 h incubation.

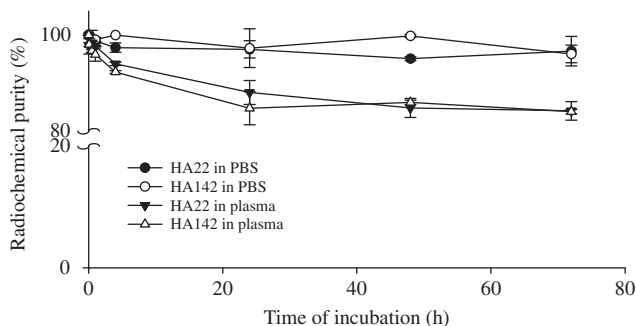


**Figure 1.** The stability of <sup>131</sup>I-Tyr-HA22 and <sup>131</sup>I-Tyr-HA142 in PBS at 4°C and in rabbit plasma at 37°C after incubation for 0.083, 0.5, 1, 2, 4, 8, 24, 48 and 72 h.

The planar gamma imaging studies New Zealand white rabbits (female, age  $14 \pm 1$  weeks, body weight  $2.5 \pm 0.2$  kg) were examined in this study. Experimental osteoarthritis in the left knee joint of the rabbit was surgically induced at six weeks after anterior cruciate ligaments transaction (ACLT) and posterior cruciate ligaments transaction (PCLT).<sup>7,9,12,13</sup> The planar gamma imaging was conducted to assess the whole-body distribution up to 3 weeks post i.a. injection of  $^{131}\text{I}$ -Tyr-HA22 and  $^{131}\text{I}$ -Tyr-HA142 in the normal and OA knees of the rabbits. The scintigrams showed that most of the radioactivity was retained in the knees for 504 h post injection (Figure 2). A slight accumulation of radioactivity in the liver and bladder was noticed, indicating that HA, after leaking from the synovial joint, might be degraded or metabolized in liver and excreted in the urine. Longitudinal monitoring the distribution of intravenously injected  $^{131}\text{I}$ -Tyr-HA142 in the same rabbit model using scintigraphic imaging was also performed to investigate the fate of  $^{131}\text{I}$ -labeled HA after leaving the synovial joints. The image showed significant accumulation in liver from 3 h post injection till 363 h (data not shown), indicating that the HA in systemic circulation was first trapped and metabolized in the liver and then excreted to urine.<sup>14,15</sup> In comparison with hepatic endothelial cells, normal synovial lining cells have limited capability for the metabolic degradation of HA.<sup>16</sup>

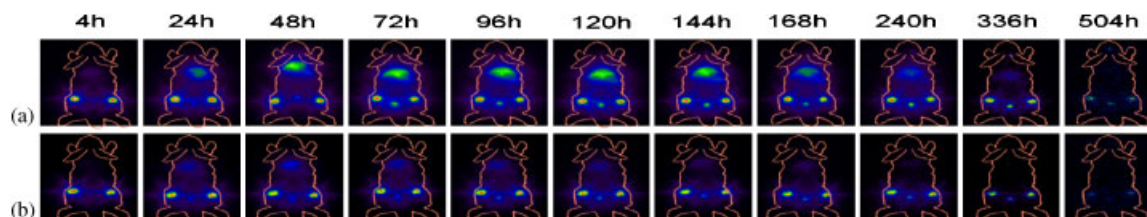


**Figure 2.** Scintigraphic images of New Zealand white rabbits with normal (right) and OA (left) knees at designated time points after intraarticular injection of (a)  $^{131}\text{I}$ -Tyr-HA22 (right,  $158 \mu\text{Ci}/0.5 \text{ mL}$ ; left,  $165 \mu\text{Ci}/0.5 \text{ mL}$ ) (b)  $^{131}\text{I}$ -Tyr-HA142 (right,  $62 \mu\text{Ci}/0.5 \text{ mL}$ ; left,  $49 \mu\text{Ci}/0.5 \text{ mL}$ ) in the knee joints. Imaging was performed under initial anesthesia with intravenous injection of propofol ( $10 \text{ mg/kg}$ ) and constant anesthesia with isoflurane using a vaporizer system during 20 min.

i.a. injection of  $^{131}\text{I}$ -tyramine was conducted to clarify whether the  $^{131}\text{I}$ -tyramine were degraded from  $^{131}\text{I}$ -Tyr-HAs in synovial joints. The results of scintigraphic imaging (data not shown) revealed that the  $^{131}\text{I}$ -tyramine injected in the knee joint eliminated rapidly from the synovial joint. Most of the radioactivity was excreted in the urine within 6 h. Hence the low but persistent radioactivity accumulation in liver after i.a. injection of  $^{131}\text{I}$ -Tyr-HAs was most probably attributed to the escaped  $^{131}\text{I}$ -Tyr-HAs, or the radioactive metabolites with smaller molecular weight, from the joints.

**Pharmacokinetics of  $^{131}\text{I}$ -Tyr-HA22/142:** The radioactivity-time curves of  $^{131}\text{I}$ -Tyr-HA22 and  $^{131}\text{I}$ -Tyr-HA142 in OA knee and normal knee derived from planar gamma images are shown in Figure 3a. The difference in the retention of radiolabeled HAs in normal knee and OA knee was not obvious ( $P=0.82$  and  $0.64$  for  $^{131}\text{I}$ -Tyr-HA22 and  $^{131}\text{I}$ -Tyr-HA142).

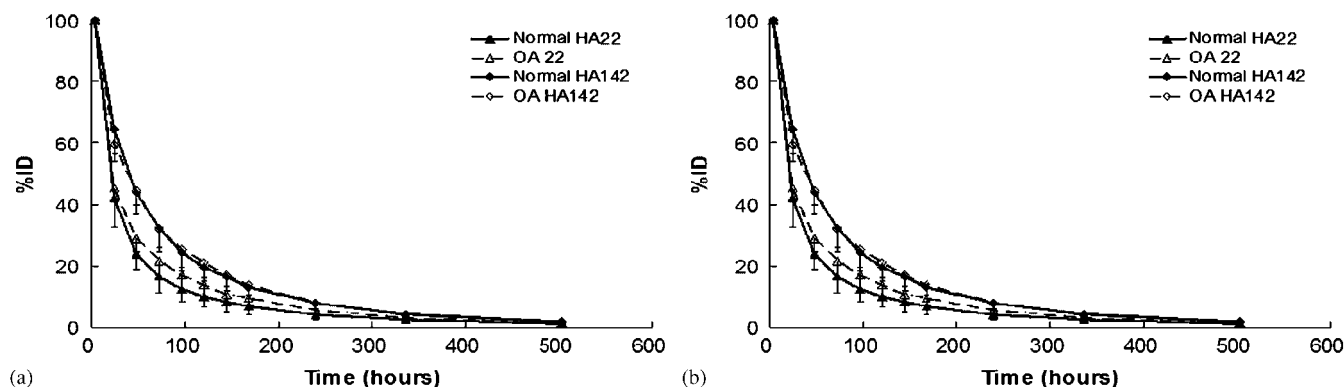


**Figure 3.** Radioactivity in ROI of (a) knee joints and (b) livers after intraarticular injection of  $^{131}\text{I}$ -Tyr-HA22 and  $^{131}\text{I}$ -Tyr-HA142 were derived from the scintigraphic images of rabbits at designated time points ( $n=3$ ). The radioactivity concentration were expressed as the percentage of injection dose (%ID) according to the following formula:  $\%ID = (A_t/A_0) \times 100\%$ , where  $A_t$  = decay-corrected radioactivity (counts) of ROI (knee joint and liver) is derived from the gamma images at designated time points. For the knee joint,  $A_0$  is the counts in the specific knee at 4 h post injection; for the liver,  $A_0$  is the total counts in the whole imaging field at 4 h post injection.

However, the differences in the retention of HA22 and HA142 in the joints of both normal and OA knees are significant ( $P < 0.05$ ). The pharmacokinetic parameters derived from the radioactivity-time curves of  $^{131}\text{I}$ -Tyr-HAs were summarized in Table 1. The half-life ( $T_{1/2}$ ) and  $\text{AUC}_{(0 \rightarrow \infty)}$  of radiolabeled HA142 in synovial joints of normal and OA knees after i.a. administration were significantly longer and higher than that of  $^{131}\text{I}$ -Tyr-HA22. The maximum radioactivity accumulation in liver after i.a. administration of  $^{131}\text{I}$ -Tyr-HA22 and  $^{131}\text{I}$ -Tyr-HA142 (Figure 3b) were 46.81 and 22.06 %ID at 24 h post injection, respectively. The higher the molecular weight of  $^{131}\text{I}$ -Tyr-HA administered, the lower the accumulation of radioactivity in liver was observed. These results indicate that HA with higher molecular weights escape the knee joints (both normal and OA) less readily.



**Table 1.** Pharmacokinetics parameters derived from the scintigraphic images of rabbits after intraarticular injection of  $^{131}\text{I}$ -Tyr-HA22 and  $^{131}\text{I}$ -Tyr-HA142 in normal and OA knees using Matlab 7.0 (The MathWorks, Natick, MA) with one-compartmental analysis model

	Normal knee		Osteoarthritis knee	
	Half-life (T1/2) (h)	AUC <sub>(0→∞)</sub> (h*%ID)	Half-life (T1/2) (h)	AUC <sub>(0→∞)</sub> (h*%ID)
HA22	19.29 ± 2.7	3107.27	22.02 ± 9.1	3383.67
HA142	45.84 ± 1.1	6778.87	48.13 ± 11.3	6834.37

Although the pathogenesis of OA is still unclear, many experimental methods have been used to induce OA in animals, including joint immobilization<sup>6,17</sup> and resection of cruciate ligaments.<sup>7,9,12,13</sup> ACLT has been used to induce knee OA in rabbit models in some previous studies. In our study, both ACLT and PCLT were carried out in the left knee to ensure OA would developed within six weeks.<sup>12</sup>

$^3\text{H}$ -labeled HAs with different molecular weights have been applied as radiotracers to study the pharmacokinetics of HA in normal rabbits.<sup>18</sup> The pharmacokinetic parameters were evaluated based on the metabolic  $^3\text{H}_2\text{O}$  formed in the plasma. The mean intrasynovial half-life of  $^3\text{H}$ -hyaluronic acid with high molecular weight ( $M_r > 6.0 \times 10^6$ , 13.2 h) was longer than that of low molecular weight ( $M_r > 0.09 \times 10^6$ , 10.2 h). In this study, HAs were conjugated with tyramine and labeled with iodine-131 to afford  $^{131}\text{I}$ -Tyr-HAs with high *in vitro* stability and medium *in vivo* stability.  $^{131}\text{I}$ -Tyr-HAs was employed and scintigraphic imaging was performed to monitor the distribution and to evaluate the pharmacokinetics of HA in normal and OA knees joints longitudinally after i.a. administration. Only a trace amount of radioactivity was noticed in rabbit thyroid revealed that free iodine-131 was not an immediate metabolite of  $^{131}\text{I}$ -Tyr-HAs even after the radiotracer has escaped the knee joints. Compared with  $^3\text{H}$ -hyaluronic acid,  $^{131}\text{I}$ -Tyr-HA might be a more pertinent radiotracer that would allow direct monitoring of the distribution and pharmacokinetics of HA in a rabbit OA models for up to 3 weeks.

**Conclusion:** This study demonstrated that the pharmacokinetics of  $^{131}\text{I}$ -Tyr-HAs (molecular weight ranged from 220 to 1420 kDa) in the OA knee joints was not significantly different from those in normal knee joints after intraarticular injection. HA with higher molecular weights was retained longer than that with lower molecular weights was in both normal and OA knee and may provide better therapeutic efficacy, at least in the lubrication, after single injection for treatment of OA knees.

**Acknowledgements:** This work was supported by grant (96002-62-074) from the Department of Health, Taipei City Government, Taiwan. HA22 and HA142 were kind gifts from the Industrial Technology Research Institute, Taiwan.

## References

- [1] N. Gerwin, C. Hops and A. Lucke, *Adv. Drug. Deliv. Rev.* **2006**, *58*, 226–242.
- [2] J. A. Buckwalter and J. A. Martin, *Adv. Drug. Deliv. Rev.* **2006**, *58*, 150–167.
- [3] *Arthritis Rheum* **2000**, *43*, 1905–1915.
- [4] M. C. Barron and B. R. Rubin, *J. Am. Osteopath. Assoc.* **2007**, *107*, ES21–27.
- [5] T. Kikuchi, H. Yamada and M. Shimmei, *Osteoarthritis Cartilage* **1996**, *4*, 99–110.
- [6] L. L. Fu, N. Maffulli and K. M. Chan, *Clin. Rheumatol.* **2001**, *20*, 98–103.
- [7] T. Kawano, H. Miura, T. Mawatari, T. Moro-Oka, Y. Nakanishi, H. Higaki and Y. Iwamoto, *Arthritis Rheum.* **2003**, *48*, 1923–1929.
- [8] L. W. Moreland, *Arthritis. Res. Ther.* **2003**, *5*, 54–67.
- [9] K. D. Brandt, G. N. Smith, Jr. and L. S. Simon, *Arthritis. Rheum.* **2000**, *43*, 1192–1203.
- [10] P. Juni, S. Reichenbach, S. Trelle, B. Tschannen, S. Wandel, B. Jordi, M. Zullig, R. Guetg, H. J. Hauselmann, H. Schwarz, R. Theiler, H. R. Ziswiler, P. A. Dieppe, P. M. Villiger and M. Egger, *Arthritis. Rheum.* **2007**, *56*, 3610–3619.
- [11] M. Kurisawa, J. E. Chung, Y. Y. Yang, S. J. Gao and H. Uyama, *Chem. Commun (Camb)* **2005**, 4312–4314.
- [12] H. Lorenz and W. Richter, *Prog. Histochem. Cytochem.* **2006**, *40*, 135–163.
- [13] Y. S. Park, S. W. Lim, I. H. Lee, T. J. Lee, J. S. Kim and J. S. Han, *Arthritis Res. Ther.* **2007**, *9*, R8.
- [14] U. B. Laurent, L. B. Dahl and R. K. Reed, *Exp. Physiol.* **1991**, *76*, 695–703.
- [15] T. C. Laurent, K. Lilja, L. Brunnberg, A. Engstrom-Laurent, U. B. Laurent, U. Lindqvist, K. Murata and D. Ytterberg, *Scand J. Clin. Lab. Invest.* **1987**, *47*, 793–799.
- [16] B. Smedsrod, H. Pertoft, S. Eriksson, J. R. Fraser and T. C. Laurent, *Biochem. J.* **1984**, *223*, 617–626.
- [17] A. Wigren, J. Falk and O. Wik, *Acta. Orthop. Scand.* **1978**, *49*, 121–133.
- [18] T. J. Brown, U. B. Laurent and J. R. Fraser, *Exp. Physiol.* **1991**, *76*, 125–134.

## COMBINING DOCKING, MOLECULAR DYNAMICS AND MM/PBSA METHODS TO IDENTIFY THE BINDING MODES OF CONGO RED TOWARDS AMYLOID PROTOFIBRILS

JIAN-HUA ZHAO,<sup>a</sup> HSUAN-LIANG LIU,<sup>a,b</sup> KUNG-TIEN LIU,<sup>c</sup> and JENN-TZONG CHEN<sup>d</sup>

<sup>a</sup>Department of Chemical Engineering and Biotechnology National Taipei University of Technology 1 Sec. 3 ZhongXiao E. Rd. Taipei, 10608, Taiwan

<sup>b</sup>Graduate Institute of Biotechnology National Taipei University of Technology 1 Sec. 3 ZhongXiao E. Rd. Taipei, 10608, Taiwan

<sup>c</sup>Chemical Analysis Division Institute of Nuclear Energy Research 1000, Wunhua Rd., Longtan Township Taoyuan County, 32546, Taiwan

<sup>d</sup>Isotope Application Division Institute of Nuclear Energy Research 1000, Wunhua Rd., Longtan Township Taoyuan County, 32546, Taiwan

**Abstract:** In this study, molecular docking, molecular dynamics (MD) simulations and binding free energy calculation were conducted to investigate the binding modes of Congo red toward the protofibril formed by an amyloidogenic fragment (GNNQQNY) from yeast prion protein Sup35. Four specific binding sites were indentified in our simulations. In the primary binding site, it shows that Congo red bound to a regular groove formed by the first three residues (G1-N2-N3) of the  $\beta$ -strands along the  $\beta$ -sheet extension direction with a strong binding free energy as estimated by the MM-PBSA method ( $-24.4$  kcal/mol), which is consistent with recent theoretical measurements using the MM-GBSA method ( $-22.8 \pm 1.6$  kcal/mol). Moreover, our simulations further indentified other binding sites: the long groove between two  $\beta$ -sheet layers, the aromatic pitch of Y7 and the top or bottom of the protofibril, implying that these binding sites could be bound by Congo red and other long flat molecules. These results not only yield valuable insight into the nature of the molecular form in which the amyloid dye binds the fibril and the binding locations on the fibril, but also provide a clue to design new compounds for clinical purposes.

**Keywords:** docking; molecular dynamics; binding modes; Congo red; GNNQQNY

**Introduction:** Congo red has been commonly used to identify amyloid fibrils in tissues for more than 80 years (Figure 1A). Derivatives, such as [<sup>11</sup>C]PIB, [<sup>11</sup>C]SB-13, [<sup>18</sup>F]FDDNP, have been developed as positron emission tomography (PET) tracers and helped to detect and visualize amyloid plaques and neurofibrillary tangles in living subjects.<sup>1,2</sup> However, the specificity and the stabilities of these binding modes and their roles in amyloid fibril detection remain elusive. It is clear that obtaining a molecular level of understanding of binding is essential in order to interpret binding experiments as well as for the design of better dyes for clinical purposes. In this study, molecular docking, molecular dynamics (MD) simulations and binding free energy calculation were used to explore the nature of the molecular form in which the amyloid dye binds the fibril and the binding locations on the fibril.

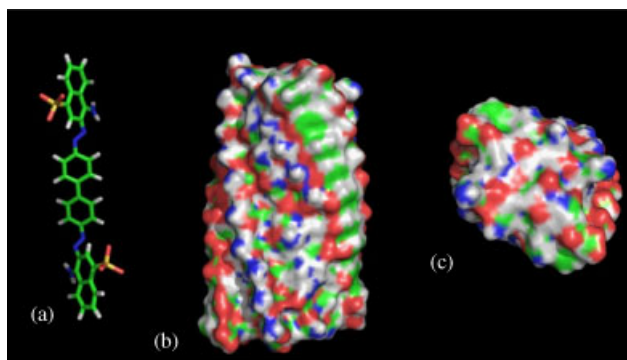


**Figure 1.** (a) Structures of Congo red molecule. (b) The top and (c) side view of protofibril structure formed by amyloidogenic fragment (GNNQQNY) from the yeast prion protein Sup35.

**Results and discussion:** We identified and characterized four specific binding modes of Congo red molecules (Figure 1A) to a protofibril formed by an amyloidogenic fragment (GNNQQNY) from the yeast prion protein Sup35 (Figure 1B and C)<sup>3</sup> as follows: groove between two  $\beta$ -sheet layers (Figure 2A), groove formed by the first three residues G1-N2-N3 (Figure 2B), the aromatic pitch of Y7 (Figure 2C) and the top or bottom of protofibril (Figure 2D). Our analysis, consistent with recent MD simulation results, suggest that Congo red primarily binds to a regular groove of the first three residues (G1-N2-N3) of the  $\beta$ -strands along the  $\beta$ -sheet extension direction (Figure 2B).<sup>4</sup> This primary binding mode exhibits a strong binding free energy of  $-24.4$  kcal/mol, is in qualitative agreement with the previous theoretical measurements ( $-22.8 \pm 1.6$  kcal/mol).<sup>4</sup> Moreover, our simulations also indicate that Congo red could stably bind to the other three binding sites during the 500-ps MD simulations (Figure 2A, C and D). These results led us to propose that these four binding interaction could be general recognition modes of amyloid fibrils by Congo red, Thioflavin T, and other long flat molecules. To examine the generality of the conclusions, we further explored the binding of Thioflavin T to a protofibrillar oligomer of  $A\beta(9-40)$  peptide,<sup>5</sup> and our preliminary results reveal multiple binding sites on  $A\beta(9-40)$  protofibril surface (data not shown), which are also consistent with the previous experimental observations.<sup>6-8</sup>

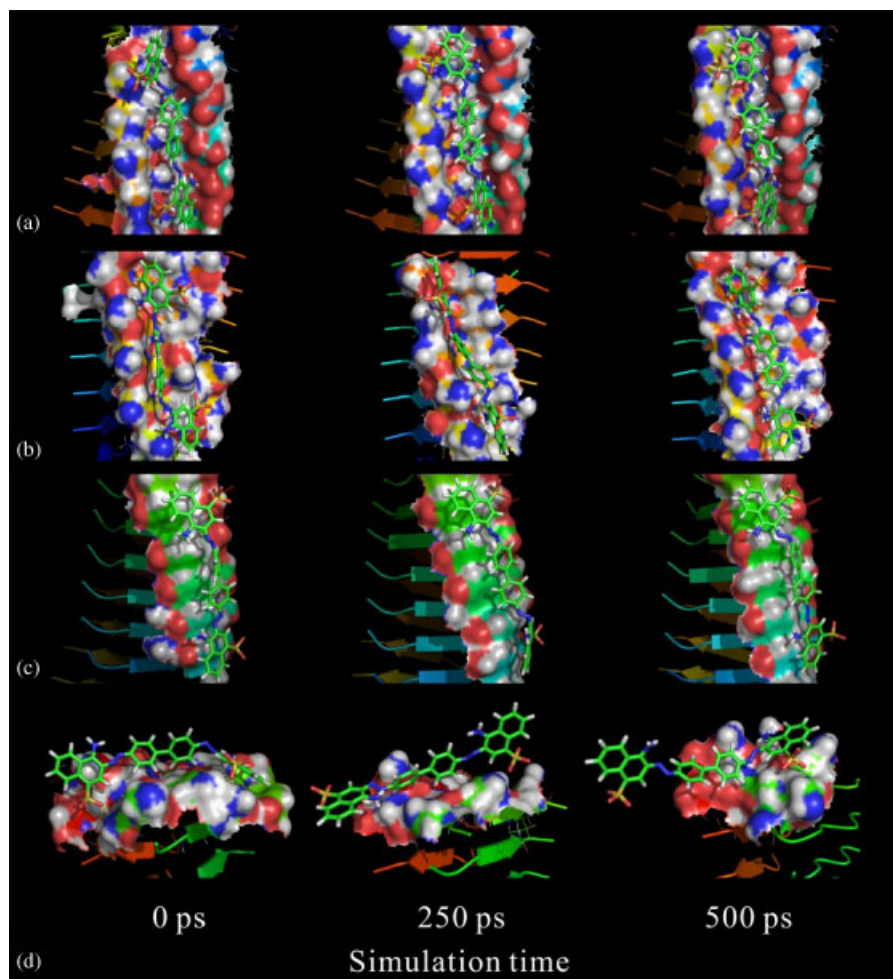


**Figure 2.** Snapshots of four binding modes of Congo red to GNNQQNY protofibril structure at 0, 250 and 500 ps. Four binding sites are as follows: (A) groove between two  $\beta$ -sheet layers, (B) groove formed by the first three residues G1-N2-N3, (C) the aromatic pitch of Y7 and (D) the top or bottom of protofibril.

## References

- [1] L. Cai, R. B. Innis, V. W. Pike. *Curr. Med. Chem.* **2007**, *14*, 19–52.
- [2] S. Furumotoa, N. Okamurab, R. Iwatac, K. Yanaib, H. Araid and Y. Kudo. *Curr. Top. Med. Chem.* **2007**, *7*, 1773–1789.
- [3] L. Esposito, C. Pedone, and L. Vitagliano. *Proc. Natl. Acad. Sci. USA.* **2006**, *103*, 11533–11538.
- [4] C. Wu, Z. Wang, H. Lei, W. Zhang, and Y. Duan. *J. Am. Chem. Soc.* **2007**, *129*, 1225–1232.
- [5] A. T. Petkova, W.-M. Yau, and R. Tycko. *Biochemistry.* **2006**, *45*, 498–512.
- [6] H. Levine 3rd. *Amyloid.* **2005** ; *12*, 5–14.
- [7] Lockhart, L. Ye, D. B. Judd, A. T. Merritt, P. N. Lowe, J. L. Morgenstern, G. Hong, A. D. Gee, and J. Brown. *J. Biol. Chem.* **2005**, *280*, 7677–7684.
- [8] L. Ye, J. L. Morgenstern, A. D. Gee, G. Hong, J. Brown, and A. Lockhart. *J. Biol. Chem.* **2005**. *280*, 23599–23604.

## SYNTHESIS OF RADIO- AND STABLE-LABELED LBH589 (PANABINOSTAT) TO SUPPORT ANIMAL AND HUMAN ADME STUDIES

GRAZYNA CISZEWSKA, BOHDAN MARKUS, LAWRENCE JONES, AMY WU, AND TAPAN RAY

Isotope Laboratories, Translational Sciences, Drug Metabolism and Pharmacokinetics, Novartis Institutes for Biomedical Research, East Hanover, NJ, USA

**Abstract:** Radiolabeled LBH589 was required to support animal and human ADME studies and also *in vitro* protein binding study. Stable labeled LBH589 (with an appropriately high number of labeled mass units) was also needed as an LC/MS internal standard for use in bioanalytical assays.

**Keywords:** radiolabeled; stable labeled; LBH589 (Panabinostat)

**Introduction:** Histone deacetylases (HDACs) act on chromatin and on transcription factors themselves, and modulate gene regulation including the function of tumor suppressor genes, p53 and Rb. Thus, HDACs are a compelling therapeutic target for cancer therapy. Histone deacetylase inhibitors (HDACi) have been shown to inhibit the growth of tumor cells *in vitro* and activate genes regulating cell cycle arrest, apoptosis and differentiation in a tumor cell specific manner. LBH589 (Panobinostat) was designed as a synthetic deacetylase inhibitor (DACi) belonging to a structurally novel cinnamic hydroxamic acid class of compounds.

[<sup>14</sup>C]LBH589 was labeled in two different positions: <sup>14</sup>C-methylene-phenyl position and with <sup>14</sup>C uniformly incorporated into the benzene ring of the indole moiety (Figure 1). Stable labeled LBH589 was prepared with six-<sup>13</sup>C situated in the phenyl ring of the indole part of molecule (Figure 2).

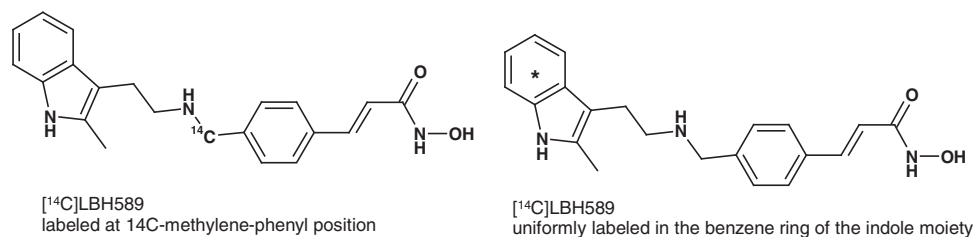


**Figure 1.** Structures of [<sup>14</sup>C]LBH589 isotopomers.

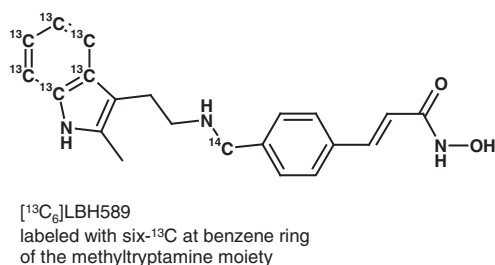
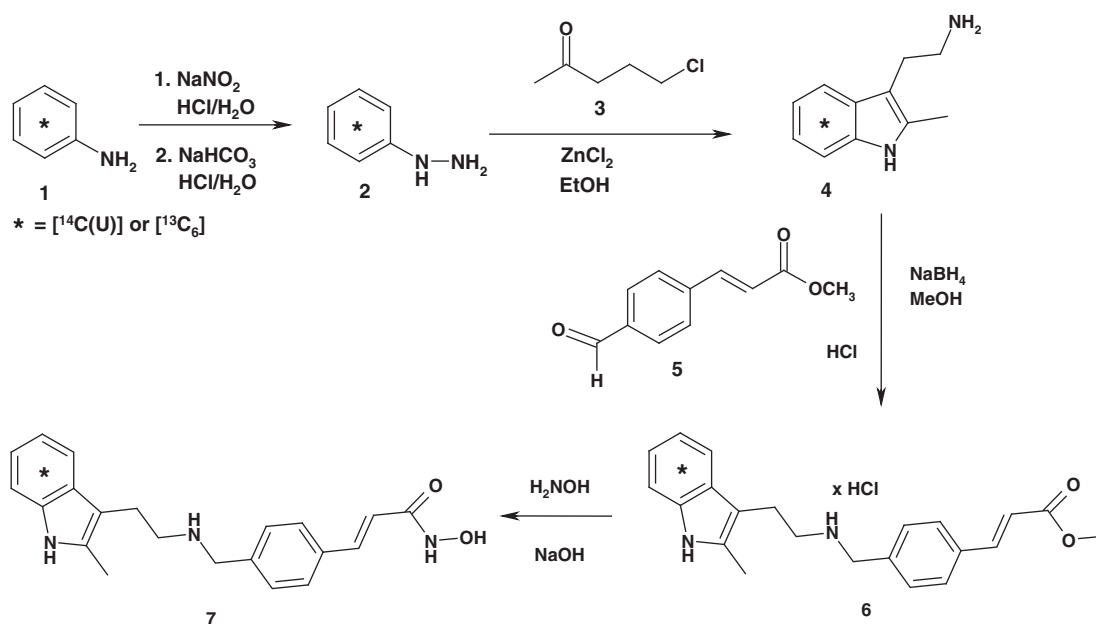


**Figure 2.** Structure of [<sup>13</sup>C<sub>6</sub>]LBH589.

**Results and Discussion:** The procedures used for the preparation of [<sup>14</sup>C] and [<sup>13</sup>C]LBH589 were a modification of the synthetic route developed by Novartis Chemical and Analytical Development. <sup>11</sup> <sup>13</sup>C<sub>6</sub>-Phenyl hydrazine was synthesized based on a literature procedure.<sup>2</sup>

**Syntheses of (2E)-N-hydroxy-3-[4-[[[2-(2-methyl-1H-indol-3-yl-benzene-<sup>14</sup>C)]ethyl]amino]methyl]phenyl]-2-propenamide and (2E)-N-hydroxy-3-[4-[[[2-(2-methyl-1H-indol-3-yl-benzene-<sup>13</sup>C<sub>6</sub>)]ethyl]amino]methyl]phenyl]-2-propenamide (Scheme 1).**

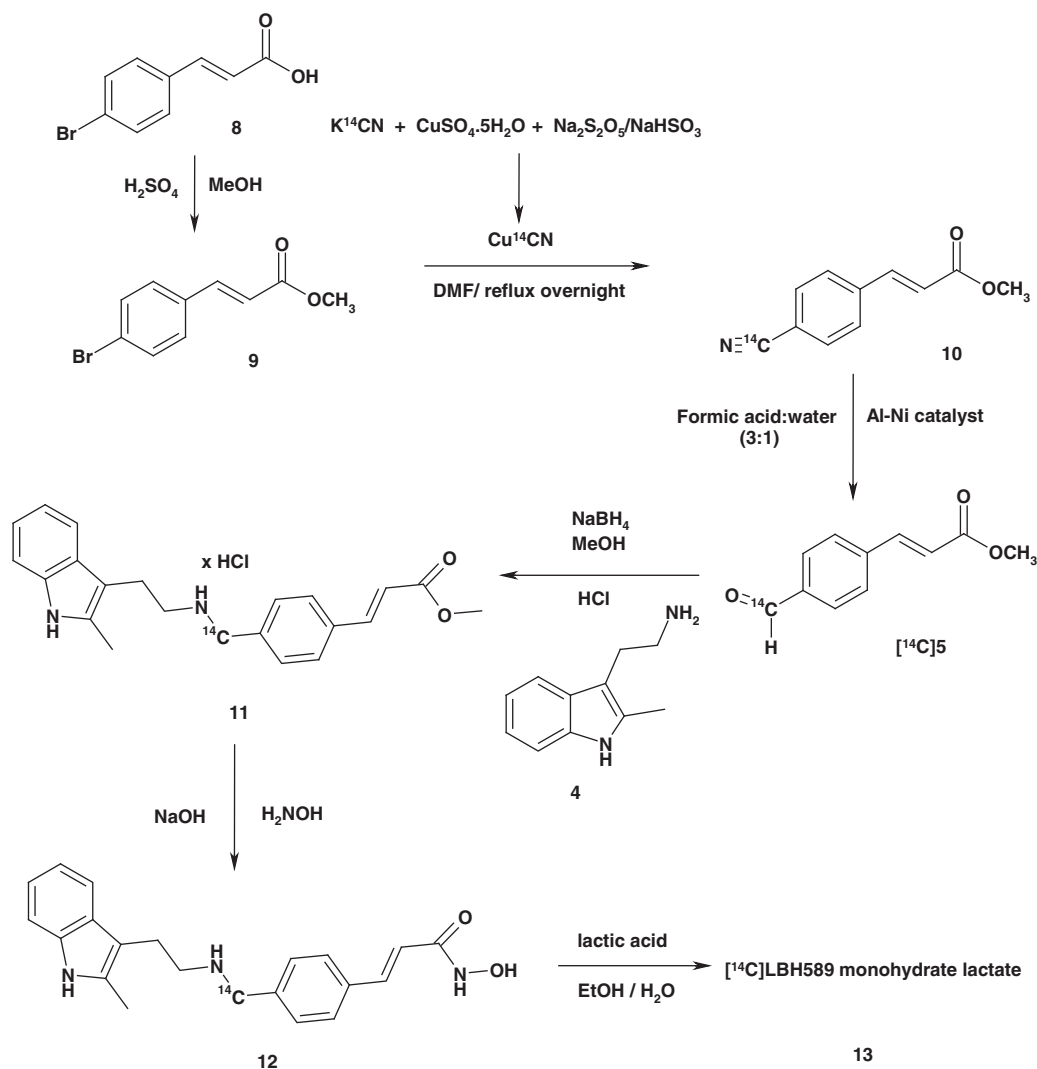
The syntheses were done in the same way using two different starting materials: <sup>14</sup>C-uniformly labeled aniline or [<sup>13</sup>C<sub>6</sub>]aniline. In both cases the following synthesis route was applied: Starting from labeled aniline **1**, the aryldiazonium-salt was formed, which was reduced to the appropriate phenylhydrazine **2**. The Fischer indole synthesis was applied to produce compound **4** from labeled phenylhydrazine **2** and ketone **3** under acidic conditions. Reductive amination of **4** with compound **5** afforded ester intermediate **6**, which reacted with hydroxylamine to provide labeled LBH589 (**7**).



**Scheme 1.**

**Synthesis of (2E)-N-hydroxy-3-[4-[[[2-(2-methyl-1H-indol-3-yl)ethyl]amino]methyl-<sup>14</sup>C]phenyl]-2-propenamide lactate (Scheme 2).**

The synthesis consisted of seven steps. (2E)-3-(4-bromophenyl)-2-propenoic acid (**8**) was converted to methyl ester **9**. Starting from compound **9**, by utilizing the Rosenmund-von Braun reaction **10** was formed. Compound [<sup>14</sup>C]**5** was obtained by hydrolysis of cyano-group to an aldehyde, which was achieved by treatment of **10** with the mixture of formic acid/water (3:1) in the presence of powdered Raney nickel alloy. Reductive amination of [<sup>14</sup>C]**5** with **4** in the presence of sodium borohydride in methanol provided **11**, which reacted with hydroxylamine to form the crude drug substance. HPLC purification of crude reaction mixture provided compound **12**. Treatment of **12** with lactic acid in ethanol/water afforded [<sup>14</sup>C]LBH589 as a monohydrate lactate salt (**13**).



Scheme 2.

**Analytical Data:** The radiochemical purity of the drug substance was determined by high performance liquid chromatography (HPLC) and thin layer chromatography (TLC). The chemical identity was confirmed by retention time comparison using HPLC and R<sub>f</sub> values for TLC. The chemical identity was further confirmed by Mass Spectroscopy (MS), Nuclear Magnetic Resonance (NMR) and Differential Scanning Calorimetry (DSC).

**Conclusion:** [<sup>14</sup>C]LBH589 is not radiochemically stable. Esters **6** and **11** were much more stable than the drug substance, so it was possible to store these intermediates and synthesize the drug substance when needed for the studies.

[<sup>13</sup>C<sub>6</sub>]LBH589 was labeled at benzene ring of the methyltryptamine moiety. For [M+6]LBH589, no parent peak was detected by mass spectrometry (MS).

**References**

- [1] J. Slade and coworkers: CHAD-US Laboratory Process Description.
- [2] M. Hunsberger, E. Shaw, J. Fugger, R. Ketcham and D. Lednicer, *J. Org. Chem.* **1956**, *21*, 394–396.

## EXPLORING A METHYLSULFINATION APPROACH TO HIGH SPECIFIC ACTIVITY ARYL METHYL [<sup>35</sup>S]SULFONES

RICHARD V. COELHO, JR., AND KLAAS SCHILDKNEGT

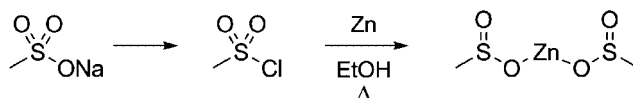
Pfizer Global Research & Development, Groton/New London Laboratories, Pfizer Inc, Groton, CT 06340, USA

**Abstract:** An experimentally straightforward procedure has been developed to prepare functionally diverse aryl methyl [<sup>35</sup>S]sulfones from sodium methane[<sup>35</sup>S]sulfonate. High specific activity methane[<sup>35</sup>S]sulfonyl chloride was prepared from sodium methane[<sup>35</sup>S]sulfonate and reduced with zinc metal to afford zinc methane[<sup>35</sup>S]sulfinate. This intermediate was immediately subjected to copper (I) catalyzed coupling with a variety of aryl iodides to afford aryl methyl [<sup>35</sup>S]sulfones.

**Keywords:** sulfur-35; methanesulfonyl chloride; sulfinate, sulfone

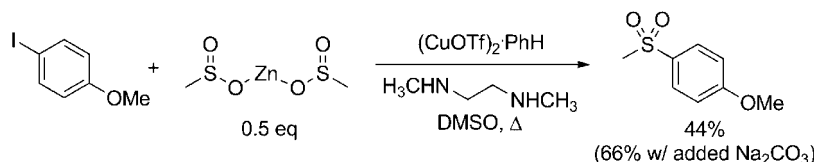
**Introduction:** Sulfur-35 enjoys wide use in the radiosynthesis of small molecules primarily because it's specific activity is comparable to that of iodine-125, and it is a pure  $\beta$ - emitter. However, within this ever-growing body of work the primary <sup>35</sup>S functional group form is a methyl sulfonamide – undoubtedly a result of the ready commercial availability of methane[<sup>35</sup>S]sulfonate. We sought to expand the use of this reagent toward the synthesis of aryl methyl [<sup>35</sup>S]sulfones, another commonly encountered high oxidation state sulfur functionality. Two endgame strategies appeared to be amendable to the use of methane[<sup>35</sup>S]sulfonate to access aryl methyl sulfones: Friedel-Crafts sulfonylation of arenes with methanesulfonyl chloride, and metal catalyzed methanesulfinic acid couplings to functionalized aromatics. Because the former strategy had been explored in sulfur-35 form<sup>1</sup> (and was shown to be non-regioselective), we chose to explore the latter approach.

**Results and Discussion:** Central to realizing a successful methane[<sup>35</sup>S]sulfinic acid approach to aryl methyl[<sup>35</sup>S]sulfones was demonstrating a straightforward partial reduction of methane[<sup>35</sup>S]sulfonate. The literature did not provide useful procedures for this exact transformation, but did showcase transition metal and hydride mediated methods for accessing methanesulfinic acid via reduction of methanesulfonyl chloride. After reviewing these methods for their probable ease of processing radioactivity, we focused our attention on a zinc metal reduction,<sup>2</sup> Scheme 1.



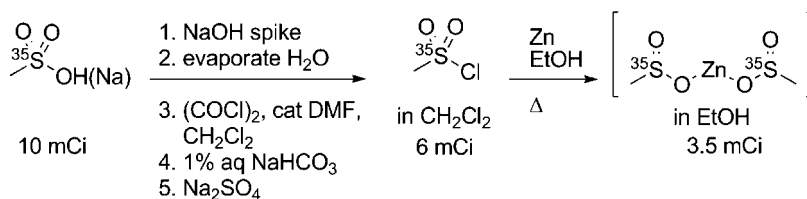
**Scheme 1.** Zinc Methanesulfinate Formation.

Initial experimentation was performed on gram scale using nonlabeled reagents. Methanesulfonyl chloride was added drop-wise to a refluxing suspension of zinc powder (1.1 eq) in ethanol. At the end of the addition the reaction was cooled and filtered to remove trace zinc solids. Water was added to the filtrate to precipitate zinc methanesulfinate as a white solid. We envisioned adapting a recently published copper catalyzed sulfinate based sulfone synthesis<sup>3</sup> to prepare sulfur-35 sulfones. Although this process utilized *sodium* methanesulfinate as the sulfur source, we demonstrated that our synthesized zinc reagent participated in the reaction as well. Experimentally, a suspension of zinc sulfinate, aryl iodide and *N,N'*-dimethylethylenediamine in DMSO was treated with catalytic copper (I) triflate and heated at 110°C for 20 hours. Reaction workup involved an ethyl acetate/brine partition, Scheme 2. Of note, adding excess Na<sub>2</sub>CO<sub>3</sub> to the reaction (for the purpose of *in situ* sodium methanesulfinate generation<sup>4</sup>) did increase reaction yield.



**Scheme 2.** Model Aryl Methyl Sulfone Synthesis.

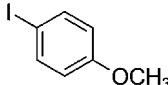
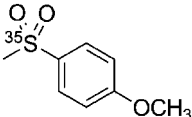
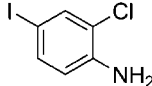
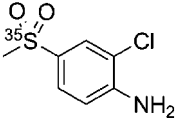
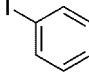
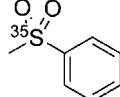
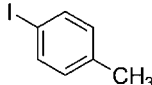
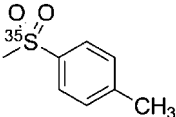
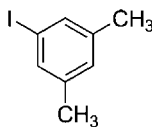
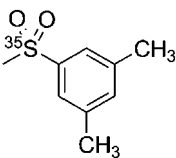
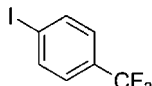
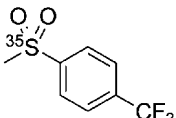
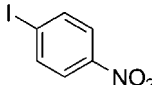
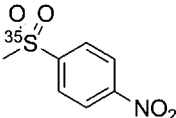
Several adaptations were necessary to efficiently process methane[<sup>35</sup>S]sulfonate through the demonstrated zinc metal reduction, Scheme 3. A 10 mCi portion of purchased methane[<sup>35</sup>S]sulfonate<sup>5</sup> (1400 Ci/mmol) in water was treated with 10 mL of 1N NaOH (to ensure reagent existed in non-volatile sodium methane[<sup>35</sup>S]sulfonate form) and the solution was evaporated to dryness with a stream of N<sub>2</sub> gas. The residue was treated with CH<sub>2</sub>Cl<sub>2</sub> solvent, excess (COCl)<sub>2</sub> and catalytic DMF. After 18 hours the reaction was washed with 1% aq NaHCO<sub>3</sub> and dried over Na<sub>2</sub>SO<sub>4</sub> to afford 6 mCi of methane[<sup>35</sup>S]sulfonyl chloride in CH<sub>2</sub>Cl<sub>2</sub> solvent. The high purity of methane[<sup>35</sup>S]sulfonyl chloride prepared in this way was separately confirmed by its efficient use in the formation of a known sulfonamide. The CH<sub>2</sub>Cl<sub>2</sub> solution was distilled to a minimum volume and this solution was added directly to refluxing EtOH containing excess zinc powder. After 30 minutes the EtOH solution was cooled and decanted from residual zinc – no water was added to the solution as previously described. The EtOH solution was assayed to contain 3.5 mCi of radioactivity, presumably in the form of zinc methane[<sup>35</sup>S]sulfinate.



**Scheme 3.** Zinc Methane<sup>[35S]</sup>sulfinate Formation.

Portions of the zinc methane<sup>[35S]</sup>sulfinate solution were transferred to reaction tubes, evaporated to residues with N<sub>2</sub> gas and reacted with a series of functionally diverse aryl iodides under the previously tested reaction conditions - with added Na<sub>2</sub>CO<sub>3</sub>, Table 1.

**Table 1.** Aryl Methyl <sup>[35S]</sup>Sulfone Examples

	$  \text{ArI} + \left[ \begin{array}{c} \text{O} \quad \text{O} \\ \parallel \quad \parallel \\ \text{ } ^{35}\text{S} \text{---} \text{O} \text{---} \text{Zn} \text{---} \text{O} \text{---} \text{ } ^{35}\text{S} \end{array} \right] \xrightarrow[\text{Na}_2\text{CO}_3, \text{DMSO}, \Delta]{\text{(CuOTf)}_2 \text{PhH}, \text{H}_3\text{CHN} \text{---} \text{NHCH}_3} \begin{array}{c} \text{O} \quad \text{O} \\ \parallel \quad \parallel \\ \text{ } ^{35}\text{S} \text{---} \text{Ar} \\ \text{mCi}^a \end{array} \text{ (radiochemical yield)}  $		
1		0.50	 0.15 (30)
2		0.50	 0.11 (22)
3		0.50	 0.24 (48)
4		0.50	 0.22 (44)
5		0.25	 0.08 (32)
6		0.50	 0.11 (22)
7		0.50	 0.06 (12)

a. Product activity corrected for radio-HPLC purity

As reported in the non-radioactive account of this reaction, both electron-rich and electron-poor aryl iodides delivered sulfone products. However, we did identify a trend favoring electron-rich aryl iodides (entries 1, 3, 4 and 5 vs. 6 and 7) which was not clearly evident within the unlabeled work. It is plausible that this reactivity difference is rooted in our introduction of a zinc counterion. Although clearly evident from reaction design, it is worth reinforcing that this process delivers single isomer products. Finally, the [ $^{35}\text{S}$ ]sulfone products were not isolated from these reactions, but rather identified and quantified by radio-HPLC and LSC.

## References

- [1] M. A. Wallace, C. Raab, D. Dean, D. Melillo, *J. Label. Compd. Radiopharm.* **2007**, *50*, 347–349.
- [2] N. Chumachenko, P. Sampson, *Tetrahedron*, **2006**, *62*, 4540–4548.
- [3] J. M. Baskin, Z. Wang, *Org. Lett.* **2002**, *4*, 4423–4425.
- [4] F. C. Whitmore, F. H. Hamilton, *Org. Synth.* **1941**, *Collect. Vol. I*, 492–494.
- [5] PerkinElmer Life and Analytical Sciences.

## EXPEDIENT DEUTEROLABELLING OF LIGNANS USING IONIC LIQUID–DCL/D<sub>2</sub>O UNDER MICROWAVE HEATING

MONIKA POHJOISPÄÄ, ULLASTIINA HAKALA, GUDRUN SILVENNOINEN, AND KRISTIINA WÄHÄLÄ

Laboratory of Organic Chemistry, Department of Chemistry, University of Helsinki, P.O. Box 55, 00014 University of Chemistry, Finland

**Abstract:** We have developed a fast and high-yielding deuteration method for lignans using 35% DCl/D<sub>2</sub>O and ionic liquids, namely 1-butyl-3-methylimidazolium chloride [bmim]Cl or 1-butyl-3-methylimidazolium bromide [bmim]Br, as co-solvents, under MW irradiation. This methodology is generally applicable and simple to carry out with reaction times shortened from several days or 15 hours to 20–40 minutes. The ionic solvent is easily recycled.

**Keywords:** deuterium labelling; lignan; ionic liquid; microwave; anhydrosecoisolariciresinol; matairesinol; enterolactone

**Introduction:** The lignans are a major group of compounds found in the plant kingdom from where they end up as mammalian metabolic products. They vary widely in structure, but most of the lignans appear as polyphenols. The growing interest in these compounds is due to their beneficial health effects.<sup>1</sup> The analytical techniques used for quantitation of lignans are based on HPLC-MS and ID-GC-MS.<sup>2</sup> In these methods stable isotope polylabelled compounds are needed as internal standards.

Dibenzylbutyrolactone type lignans are readily accessed by a tandem Michael addition-alkylation reaction.<sup>3</sup> Thus we have studied H/D exchange reactions within the lignan molecule framework. Synthetic labelling schemes often rely on laborious and expensive total synthesis using prelabelled starting materials.

All aromatic region lignan labelling methods have been based on H/D exchange reactions under acidic conditions. In our earlier work, enterolactone was refluxed with a mixture of PBr<sub>3</sub>/D<sub>2</sub>O to give [2,4,6,2',4',6'-D<sub>6</sub>]-enterolactone.<sup>4</sup> Later, we carried out deuterium labelling under strongly acidic conditions by deuterated phosphoric acid-boron trifluoride complex, prepared *in situ*.<sup>5</sup> The method was found to be expedient for various butyrolactone type lignans but required rather long reaction times.<sup>6</sup> We have now developed faster method to deuterate lignans and other polyphenolic compounds, using microwave irradiation and ionic liquids.

Ionic liquids have achieved wide recognition as green alternatives to conventional volatile organic compounds (VOCs) used as solvents in many chemical processes. Ionic liquids are defined as salts that are in a liquid form at or below 100°C. Their chemical and physical properties can be adjusted by varying the choice of cations, anions and substituents. Ionic liquids have essentially no vapor pressure under normal conditions and thus serve as potential replacements for VOCs in the chemical industry.<sup>7</sup>

Use of dielectric microwave (MW) heating has been increasingly exploited in organic synthesis,<sup>8</sup> including deuteration reactions.<sup>9</sup> Using dipolar or ionic solvents, MW energy can be transferred to the reaction media using two primary mechanisms — dipole rotation and ionic conduction. Utilizing ionic liquids as a primary or co-solvent, both mechanisms for energy transfer can operate, thus making ionic liquids a highly suitable medium for MW-assisted organic synthesis.<sup>10</sup>

**Experimental:** Microwave heating was provided in a CEM Discover<sup>®</sup> microwave reactor with single mode irradiation at 2.45 GHz. Reaction temperature and pressure were monitored using the built-in, on-line IR temperature sensor and pressure sensor. The reactions were carried out in sealed pressure-proof vials under argon with magnetic stirring. <sup>1</sup>H NMR spectra were recorded using a 300 MHz instrument. Mass spectra (ESI+ and ESI–) were measured on a ESI-TOF mass spectrum.

35% DCl/D<sub>2</sub>O was purchased from Aldrich and was used directly as received. Matairesinol,<sup>3</sup> enterolactone<sup>11</sup> and anhydrosecoisolariciresinol<sup>12</sup> were prepared in our laboratory as previously reported by us.

The predeuterated (evaporated from D<sub>2</sub>O/acetone) lignan compound (15–70 mg, 0.04–0.23 mmol) and [bmim]Cl or [bmim]Br (8 eqvs) were dried under high vacuum (1–0.5 mbar) after which they were placed in a dried 5 ml or 10 ml pressure-proof reaction vial. 35% DCl/D<sub>2</sub>O (0.2–1.0 ml) was added and the vial was sealed. The vial was irradiated for 20–40 min with 20 W microwave power (with continuous compressed air cooling, 2 bar) at 70°C. After completion of the reaction, 0.5–1 ml of D<sub>2</sub>O was added and the mixture was extracted with EtOAc. The organic layer was washed with water and brine, dried over MgSO<sub>4</sub>, concentrated in a rotary evaporator



and the product was dried under high vacuum. The deuterated lignan (87–95%) was obtained as white solid compound. If necessary, the deuteration was repeated until the isotopic purity was more than 90%.

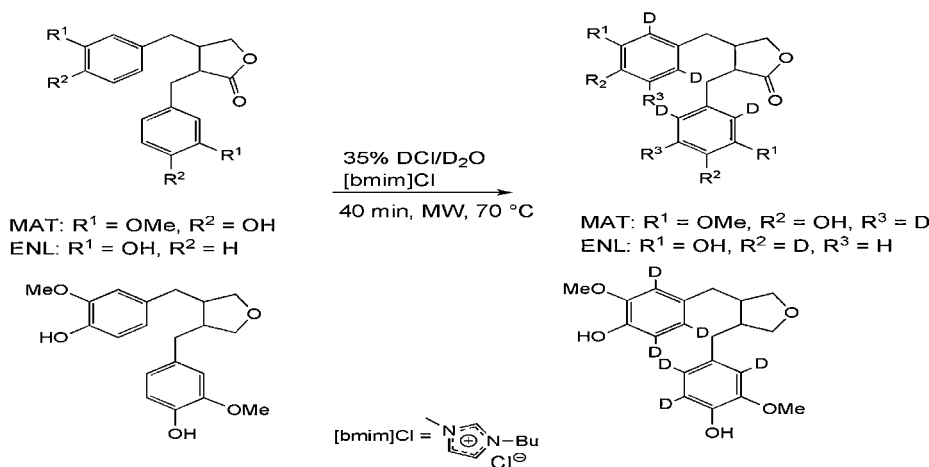
The  $^1\text{H}$  NMR spectra were found to be the same as for unlabeled compounds,<sup>3,11,12</sup> with the exception that deuterated aromatic protons were lacking and in  $\text{D}_6$ -labelled enterolactone the unlabelled 5- ja 5'-protons had undergone a change to singlets.

[2,5,6,2',5',6'- $\text{D}_6$ ]-**Matairesinol** [(2,5,6,2',5',6'- $\text{D}_6$ )-4,4'-dihydroxy-3,3'-dimethoxy lignano-9,9'-lactone].  $^1\text{H}$  NMR ( $\text{CDCl}_3$ ):  $\delta$  = 2.41–2.63 (4H, m, 7', 8, 8'), 2.89–2.95 (2H, m, 7), 3.81 (6H, s,  $2 \times \text{OCH}_3$ ), 3.85 (1H, m, 9'a), 4.14 (1H, m, 9'b), 5.52 (1H, s, OH), 5.53 (1H, s, OH).  $\text{C}_{20}\text{H}_{16}\text{D}_6\text{O}_6$   $m/z$  (ESI $^-$ ) 363.

[2,4,6,2',4',6'- $\text{D}_6$ ]-**Enterolactone** [(2,4,6,2',4',6'- $\text{D}_6$ )-3,3'-dihydroxy lignano-9,9'-lactone].  $^1\text{H}$  NMR ( $d_6$ -acetone):  $\delta$  = 2.47–2.58 (2H, m, 8, 8'), 2.64–2.73 (2H, m, 7'), 2.87–3.01 (2H, m, 7), 3.85–3.91 (1H, m, 9'a), 4.01–4.07 (1H, m, 9'b), 7.09, 7.13 (2H, s, 5, 5'), 8.21, 8.25 (2H, s,  $2 \times \text{OH}$ ).  $\text{C}_{18}\text{H}_{12}\text{D}_6\text{O}_4$   $m/z$  (ESI $^+$ ) 304.

[2,5,6,2',5',6'- $\text{D}_6$ ]-**Anhydrosecoisolariciresinol** [(2,5,6,2',5',6'- $\text{D}_6$ )-4,4'-dihydroxy-3,3'-dimethoxy lignano-9,9'-furan].  $^1\text{H}$  NMR ( $\text{CDCl}_3$ ):  $\delta$  = 2.15–2.21 (2H, m, 8, 8'), 2.48–2.62 (4H, m, 7, 7'), 3.50–3.55 (2H, m, 9a, 9'a), 3.82 (6H, s,  $2 \times \text{OCH}_3$ ), 3.89–3.94 (2H, m, 9b, 9'b), 5.47 (2H, s,  $2 \times \text{OH}$ ).  $\text{C}_{20}\text{H}_{18}\text{D}_6\text{O}_4$   $m/z$  (ESI $^+$ ) 350.

**Results and discussion:** We have developed aryl-ring-selective acid catalyzed deuteration method for representative polyphenols in ionic liquid, namely 1-butyl-3-methylimidazolium chloride [bmim]Cl or 1-butyl-3-methylimidazolium bromide [bmim]Br, using 35%  $\text{DCI}/\text{D}_2\text{O}$  as an inexpensive deuterium source under microwave irradiation.<sup>13</sup> Scheme 1. shows the reaction scheme for deuteration of matairesinol, enterolactone and anhydrosecoisolariciresinol. Our method is fast and simple to carry out as reaction times are shortened from several days or hours to 20–40 minutes. Other green chemistry considerations are also satisfied in our method: the deuterated products are easy to isolate, purification steps are minimized and the reaction solvent is recyclable.



**Scheme 1.** Deuteration of matairesinol (MAT), enterolactone (ENL) and anhydrosecoisolariciresinol under microwave conditions using  $\text{DCI}/\text{D}_2\text{O}$  – IL reaction media.

**Acknowledgements:** KW is grateful for the Finnish Academy (the grant number 126431) support.

## References

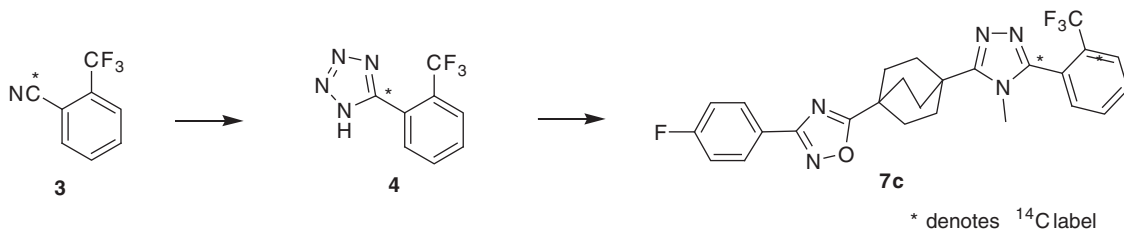
- [1] B. Raffaelli, A. Hoikkala, E. Leppälä, K. Wähälä, *J. Chromatogr. B.* **2002**, 777, 29–43.
- [2] A. Hoikkala, E. Schiavoni, K. Wähälä, *Br. J. Nutr.* **2003**, 89(suppl.1), 5–18.
- [3] B. Raffaelli, E. Leppälä, C. Chappuis, K. Wähälä, *Environ. Chem. Lett.* **2006**, 4, 1–9.
- [4] K. Wähälä, T. Mäkelä, R. Bäckström, G. Brunow, T. Hase, *J. Chem. Soc. Perkin Trans. I.* **1986**, 95–98.
- [5] E. Leppälä, K. Wähälä, *J. Label. Compd. Radiopharm.* **2004**, 47, 25–30.
- [6] E. Leppälä, M. Pohjoispää, J. Koskimies, K. Wähälä, *J. Label. Compd. Radiopharm.* **2008**; 51, 407–412.
- [7] P. Wasserscheid, T. Welton (eds.) *Ionic Liquids in Synthesis*. WILEY-VCH, Germany, **2003**.
- [8] (a) O. Kappe. *Angew. Chem., Int Ed.* **2004**; 43, 6250–6284; b) A. Loupy. *Chim.* **2004**, 7, 103–112; c) M. Larhed, A. Hallberg. *Drug Discovery Today*. **2004**, 6, 406–416.
- [9] J. R. Jones, S-Y. Lu in *Microwaves in Organic Synthesis* (Loupy ed.) Wiley-VCH, New York, USA, **2006**.
- [10] J. Hoffmann, M. Nuchter, B. Ondruschka, P. Wasserscheid. *Green Chem.* **2003**, 5, 296–299.
- [11] T. H. Mäkelä, K. T. Wähälä, T. A. Hase. *Steroids*. **2000**, 65, 437–441.
- [12] (a) W. Mazur, T. Fotsis, K. Wähälä, S. Ojala, A. Makkonen, H. Adlercreutz. *Anal. Biochem.* **1996**, 233, 169–180; b) S. Rasku, W. Mazur, H. Adlercreutz, K. Wähälä. *J. Med. Food.* **1999**, 2, 103–105.
- [13] U. Hakala, K. Wähälä. *J. Org. Chem.* **2007**, 72, 5817–5819.

## PREPARATION OF $^{14}\text{C}$ -LABELED 1,2,4-TRIAZOLES FROM $^{14}\text{C}$ -LABELED TETRAZOLES VIA DIELS-ALDER REACTION: SYNTHESIS OF $11\beta$ -HYDROXYSTEROID DEHYDROGENENASE TYPE 1 (HSD1) INHIBITORS

JONATHAN Z. HO AND MATTHEW P. BRAUN

Department of Process Research, Merck Research Laboratories, Merck & Co., Inc., RY800-B375, 126 East Lincoln Avenue, Rahway, New Jersey, USA

**Abstract:**  $^{14}\text{C}$ -labeled HSD1 inhibitors were synthesized for metabolic profiling and selection of drug candidates. A three-step reaction sequence was applied. 1-Iodo-2-trifluoromethylbenzene was labeled *via* a Pd-catalyzed cyanation with  $\text{Zn}(^{14}\text{C})_2$  to give [cyano- $^{14}\text{C}$ ]-2-trifluorobenzonitrile (**3**). The nitrile was then converted to  $^{14}\text{C}$ -labeled tetrazole (**4**). Diels-Alder reaction of **4** with the appropriate imidate yielded the desired  $^{14}\text{C}$ -labeled triazole tracers exemplified by **7c**.



**Keywords:**  $^{14}\text{C}$ -labeled triazole;  $^{14}\text{C}$ -labeled tetrazole;  $^{14}\text{C}$ -labeled synthesis

**Introduction:** The  $11\beta$ -hydroxysteroid dehydrogenase type 1 (HSD1) enzyme regulates intracellular concentrations of glucocorticoids by generating cortisol in humans whereas corticosterone in rodents from  $11$ -hydrocorticosterone.<sup>1</sup> Cortisol is a metabolically active hormone and cortisone is an inactive analogue.<sup>2</sup> Increased intracellular cortisol levels may induce metabolic syndrome which is a constellation of unhealthy factors such as low HDL levels,<sup>3</sup> elevated triglycerides,<sup>4</sup> hypertension,<sup>5</sup> elevated fasting glucose,<sup>6</sup> hypercholesterolemia,<sup>7</sup> diabetes<sup>8</sup> and increased waist circumference<sup>9</sup> with visceral adiposity.<sup>10</sup> When those multiple risk factors occur together, the likelihood of incidence of cardiovascular disease increases exponentially.<sup>11</sup> Since the cortisol hormone actions on tissues depend on both intracellular metabolism and circulating glucocorticoid levels,<sup>12</sup> the inhibition of HSD1 would lower intracellular cortisol concentration, and, therefore, it would serve as a treatment of metabolic syndrome.<sup>13</sup> Compound **1** was discovered by Merck medicinal chemists as the lead compound<sup>14</sup> for HSD1 (Figure 1). In order to conduct metabolic profiling, a  $^{14}\text{C}$ -labeled tracer was needed.

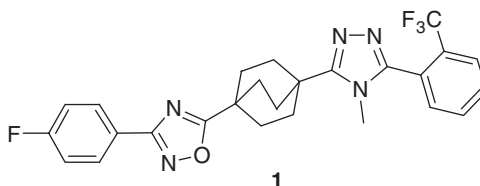


**Figure 1.** New HSD1 inhibitor **1**.

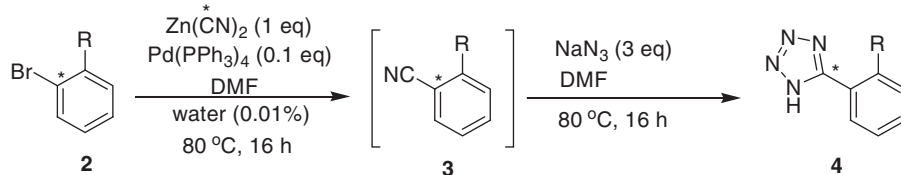
**Results and Discussion:** Previous studies from our laboratory demonstrated that cyanation of an aryl bromide with  $\text{Zn}(^{14}\text{C})_2$  is an important method for the introduction of a  $^{14}\text{C}$ -labeled CN group.<sup>15</sup> In this study, we examined aryl bromides with both electron-withdrawing and electron-donating groups. The desired cyanides were generated in the presence of  $\text{Pd}(\text{PPh})_4$  (10% loading). It is crucial that the reaction mixture be purged with nitrogen gas for several minutes before it was heated to the reaction temperature. After cyanation,  $\text{NaN}_3$  was added, affording the corresponding  $^{14}\text{C}$ -labeled tetrazoles in good yields (Table 1).

After obtaining  $^{14}\text{C}$ -labeled tetrazoles, compound **4a** was converted to several  $^{14}\text{C}$ -labeled triazoles and the results are listed in Table 2.

We envisioned that a tetrazole compound would react like a diene with a dienophile under Diels-Alder conditions to give a [2.2.1]bicyclo adduct. When  $^{14}\text{C}$ -labeled tetrazole **4a** reacted with chloroimidate **6**, freshly prepared from amide **5**,  $^{14}\text{C}$ -labeled triazoles **7** and **8** were formed, with **7** as the favored isomer in each case. Each of **7a-c** was isolated but the ratios of **7:8** were determined by analyzing the reaction mixtures. The results are located in Table 2. When R was an adamantyl group as in **6c**, the product ratio was > 99:1 (entry 3 in Table 2). However, when R was a phenyl group as in **6a**, the product ratio of **7a** to **8a** was 89:11 (entry 1 in Table 2), due to less steric interaction.

The stereoselectivity can be explained as follows (Scheme 1). When chloroimidate **6** reacts with tetrazole **4a**, intermediate **9** is favored over **10** due to less steric interactions in the transition state (TS). Upon release of nitrogen from **9** and **10**, tetrazoles **7** and **8** are obtained. When R was a bulky *tert*-butyl group as in **6b**, the product ratio of **7b** to **8b** increased to 96:4 (entry 2 in Table 2).

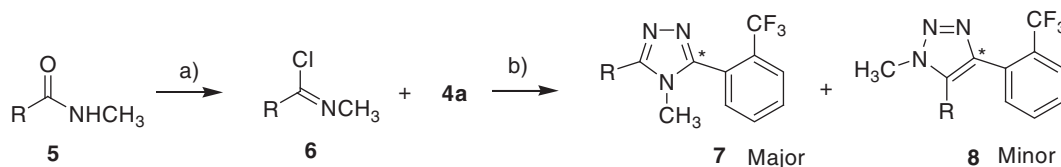
**Table 1.** Preparation of  $^{14}\text{C}$ -labeled tetrazoles



entry	SM	R	Product	yield of <b>4</b> (%)
1	<b>2a</b>	CF <sub>3</sub>	<b>4a</b>	84
2	<b>2b</b>	CH <sub>3</sub> O	<b>4b</b>	87
3	<b>2c</b>	CH <sub>3</sub>	<b>4c</b>	85
4	<b>2d</b>	H	<b>4d</b>	81
5	<b>2e</b>	NO <sub>2</sub>	<b>4e</b>	72

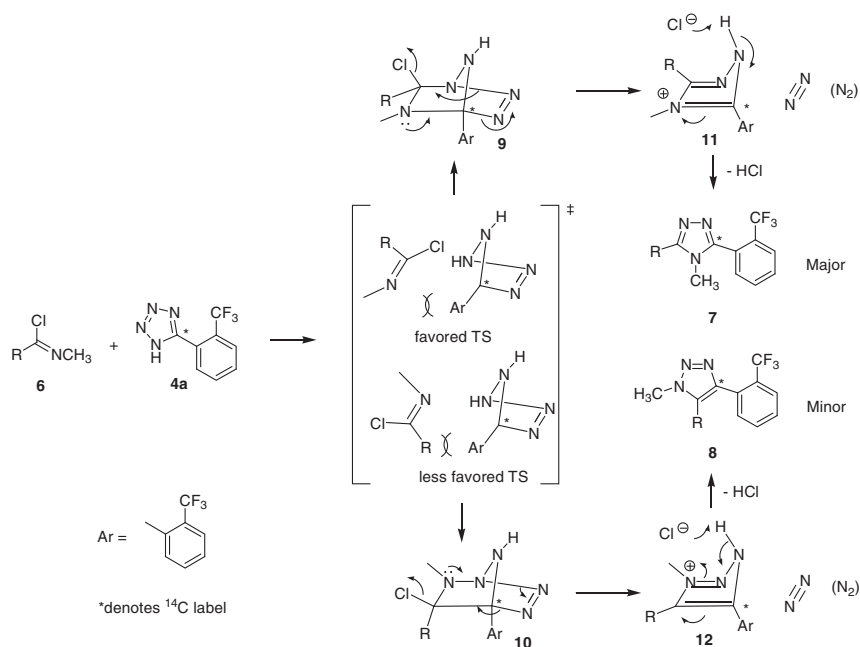
\* denotes a  $^{14}\text{C}$  label.

**Table 2.** Synthesis of  $^{14}\text{C}$ -labeled triazoles *via* Diels-Alder Reaction



entry	Amide	Substrate R =	imidate	% yield	ratio of 7:8
1	<b>5a</b>	Ph	<b>6a</b>	<b>7a</b> (62%)	89:11
2	<b>5b</b>	t-Bu	<b>6b</b>	<b>7b</b> (64%)	96:4
3	<b>5c</b>		<b>6c</b>	<b>7c</b> (65%)	>99:1

a) Oxalyl chloride, catalytic amount of DMF, CH<sub>2</sub>Cl<sub>2</sub>, 0°C, 1h; b) DMF, 100°C, 16h.



**Scheme 1.** Proposed mechanism for the synthesis of C-labeled triazoles **7** and **8**.

[<sup>14</sup>C]-labeled **7c** was a radio-tracer of the HSD1 inhibitor **1**, which later was identified as a very potent human HSD1 (*h*-HSD1) inhibitor with an excellent HSD1/HSD2 selectivity, outstanding PK profile, low clearance, long half life and very high oral bioavailability.<sup>14</sup> Details of those studies will be published in due course.

This methodology for preparation of <sup>14</sup>C-labeled triazoles is a general one. It is known<sup>17</sup> that a wide variety of pharmaceutical products have the triazole functionality and a great deal of molecules with a triazole display biological activity such as antibacterial,<sup>17a</sup> antitumor<sup>17b</sup> and antiviral agents.<sup>17c</sup> A good method for the preparation of <sup>14</sup>C-labeled triazoles could help to conduct much needed drug metabolism studies in a timely manner.

In conclusion, a novel and convenient synthesis of <sup>14</sup>C-labeled tetrazoles and triazoles has been developed. We utilized this method in the preparation of a <sup>14</sup>C-labeled HSD1 inhibitor tracer **7c**.

**Acknowledgements:** The authors wish to thank Mr. Steven J. Staskiewicz for analytical support. J.Z.H. gratefully acknowledges Dr. Lee J. Silverberg for help in the preparation of this manuscript.

## References

- [1] Recent reviews on HSD1 see: (a) M. Causevic, M. Mohaupt, *Molecular Aspects of Medicine* **2007**, 28(2), 220–6; (b) M. Wang, *Current Opinion in Investigational Drugs* **2006**, 7(4), 319–323; (c) M. C. Holmes, J. R. Seckl, *Molecular and Cellular endocrinology* **2006**, 248(1–2), 9–14.
- [2] (a) J. P. Monson, *Clinical Endocrinology (Oxford)* **1998**, 49(3), 281–282. (b) J. Tourniaire, M. G. Daumont, *Annales de l'Anesthesiologie Francaise* **1976**, 17(4), 406–10.
- [3] (a) P. H. J. van der Voort, R. T. Gerritsen, A. J. Bakker, E. C. Boerma, M. A. Kuiper, I. Heide, *Inten. Care Med.* **2003**, 29(12), 2199–203; (b) A. Hautanen, H. Adlercreutz, *J. Int. Med.* **1993**, 234(5), 461–9.
- [4] K. K. Mishra, H. P. Pandey, R. H. Singh, *Ind. J. Clin. Biochem.* **2007**, 22(2), 41–43.
- [5] J. P. F. Chin-Dusting, B. A. Ahlers, D. M. Kaye, J. J. Kelly, A. Whitworth, *Hypertension* **2003**, 41(6), 1336–1340.
- [6] P. J. Hornnes, C. Kuhl, *Diabete Metabol.* **1984**, 10(1), 1–6.
- [7] K. Yamaguchi, N. Nakamura, H. Uzawa *J. Clin. Endocrin. Metabol.* **1984**, 58(5), 786–9.
- [8] G. B. Phillips, C. H. Tuck, T. Y. Jing, B. Boden-Albala, I. F. Lin, N. Dahodwala, R. L. Sacco *Diabetes Care* **2000**, 23(1), 74–9.
- [9] R. Rosmond, G. Holm, P. Bjorntorp, *Int. J. Obes. Metabol. Disorders: J. Int. Ass. Study Obes.* **2000**, 24(4), 416–22.
- [10] G. Gueder, J. Bauersachs, S. Frantz, D. Weismann, B. Allolio, G. Ertl, C. E. Angermann, S. Stoerk, *Circulation* **2007**, 115(13), 1754–1761.
- [11] A. Steptoe, S. R. Kunz-Ebrecht, L. Brydon, J. Wardle, *Int. J. Obes.* **2004**, 28(9), 1168–1173.
- [12] D. A. Ehrmann, D. Breda, M. C. Corcoran, M. K. Cavaghan, J. Imperial, G. Toffolo, C. Cobelli, K. S. Polonsky, *Am. J. Physio. Endocrin. Metabol.* **2004**, 287(2), E241–6.
- [13] D. Sousa, R. A. Peixoto, S. Turban, J. H. Battle, K. E. Chapman, J. R. Seckl, N. M. Morton. *Endocrinology* **2008**, 149(4), 1861–1868.
- [14] (a) X. Gu, J. Dragovic, K. G. C. Jasminka, S. L. Koprak, C. LeGrand, S. S. Mundt, K. Shah, S. Kashmira, M. S. Springer, E. Y. Tan, R. Thieringer, A. Hermanowski-Vosatka, H. J. Zokian, J. M. Balkovec, S. T. Waddell, *Bioorg. Med. Chem. Lett.* **2005**, 15(23), 5266–5269; (b) J. M. Balkovec, R. Thieringer, S. S. Mundt, A. Hermanowski-Vosatka, G. F. Patel, S. D. Aster, S. T. Waddell, S. H. Olson, M. Maletic, *PCT Int. Appl. WO 2003065983 A2 20030814* **2003**; (c) N. J. Kevin, X. Gu, S. T. Waddell, *PCT Int. Appl. WO 2007087150 A2 20070802* **2007**; (d) S. T. Waddell, J. M. Balkovec, N. J. Kevin, X. Gu, *PCT Int. Appl. WO 2007047625 A2 20070426* **2007**; (e) L. J. Mitnaul, J. Tian, C. Burton, M. H. Lam, Y. Zhu, S. H. Olson, J. E. Schneeweis, P. Zuck, S. Pandit, M. Anderson, M. Maletic, S. T. Waddell, S. D. Wright, C. P. Sparrow, E. G. Lund. *J. Lipid Res.* **2007**, 48(2), 472–482.
- [15] C. S. Elmore, D. C. Dean, T. M. Marks, M. P. Braun, N. X. Yu, Y. Zhang, C. E. Raab, R. Singh, L. Jin, D. G. Melillo, C. J. Dinsmore, T. M. Williams, *Abs. Papers 224th ACS National Meeting, Boston, MA, USA, August 18–22, 2002*, MEDI-132.
- [16] T. Yoshioka, M. Kitagawa, M. Oki, S. Kubo, H. Tagawa, K. Ueno, W. Tsukada, M. Tsubokawa, A. Kasahara, *J. Med. Chem.* **1978**, 21(7), 633–9.
- [17] (a) P. D. Cook, G. Wang, T. W. Bruice, V. Rajappan, K. Sakthivel, K. D. Tucker, J. L. Brooks, J. M. Leeds, M. E. Ariza, P. C. Fagan, *PCT Int. Appl. WO 2003073989 A2 20030912* (2003); (b) R. S. Varma, *J. Ind. Chem. Soc.* **2004**, 81(8), 627–638; (c) S. M. Rida, S. A. M. El-Hawash, H. T. Y. Fahmy, A. A. Hazzaa, M. M. M. El-Meligy. *Arch. Pharm. Res.* **2006**, 29(10), 826–833.

## EFFORTS ON THE SYNTHESIS OF TRITIUM LABELED PEG-PEPTIDE TRACERS

JONATHAN Z. HO, ANDY S. ZHANG, YUI S. TANG, STEVEN J. STASKIEWICZ, AND MATTHEW P. BRAUN

Department of Process Research, Merck Research Laboratories, Merck & Co., Inc., RY800-B375, 126 East Lincoln Avenue, Rahway, New Jersey, USA

**Abstract:** PEG-peptides refer to polyethylene glycol (PEG) peptides. PEGylation is a commonly used strategy to improve the pharmacokinetics and metabolic stability of bioactive peptides intended for therapeutic use. The synthesis and purification of tritium labeled PEG-peptide tracers are discussed.

**Key words:** <sup>3</sup>H-labeled synthesis; <sup>3</sup>H-labeled PEG-peptide; Oxyntomodulin.

**Introduction:** It is of a great deal of interest in developing biomimetic polymers that control interactions of a biological system.<sup>1</sup> This issue is particularly important in designing polymers, such as polyethylene glycol peptides (PEG-peptides), for drug targeting or

tissue engineering.<sup>2</sup> PEG, dextran, poly(vinyl alcohol) and polyacrylamide are hydrophilic and nonionic polymers which are non conductive to protein and peptide adsorption.<sup>3</sup> Although these polymers are water-soluble, they are not unambiguously suited to tissue engineering because they can not form a stable three-dimensional constructs for cell attachment and proliferation.<sup>4</sup> However, when these materials are appropriately copolymerized with another polymer (e.g. peptide B), new peptides with a general structure illustrated in Figure 1 are formed.

To support metabolism and pharmacokinetic (PK) studies of PEG-peptide conjugates, both radioisotope and stable isotope labeled tracers are typically needed. Radiolabeling of select residues (e.g. Tyr) within the primary sequence affords tracers that are commonly used to determine the proteolytic fate of the peptide moiety. Incorporation of radiolabels into the PEG linker, however, while synthetically more challenging allows the disposition of PEGylated metabolites to be monitored independent of proteolytic events that could otherwise result in loss of the radiolabel. In this paper, the synthesis and purification of PEG-peptide tracers incorporating radiolabel within the PEG linker are discussed.

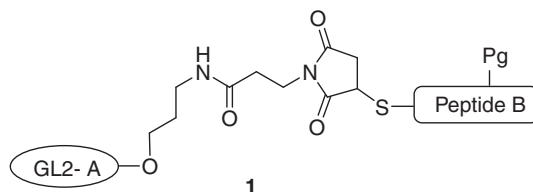
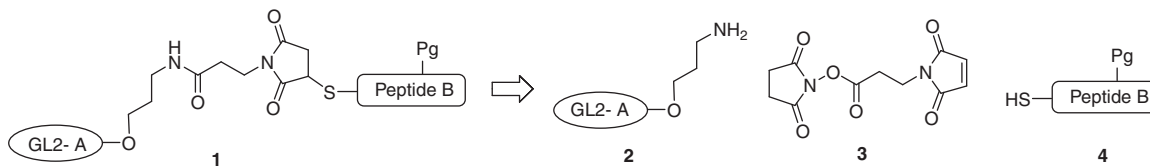


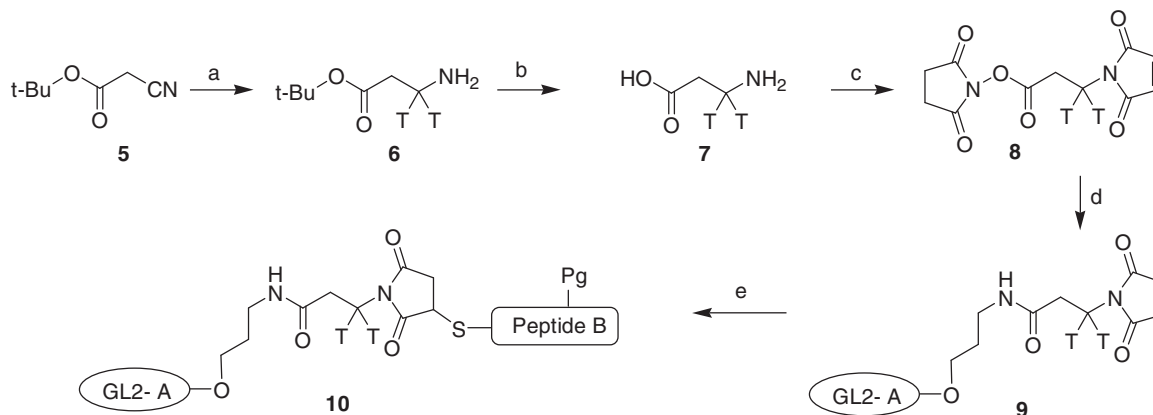
Figure 1. PEGylated co-polymers.

**Results and discussion:** The retro-synthetic analysis for the preparation of the tracer is outlined in Scheme 1. There are three building blocks, **2**, **3**, and **4**, on which tritium label could be placed. Succinimidyl maleimido propionate (SMP) **3** serves as a linker between the fragments **2** and **4**, therefore, putting a label on **3** would maximize the possibility of making a series of the tracers to support SAR effort for this program



Scheme 1. Oxyntomodulin analog **1** and the retro-synthetic strategy for making [<sup>3</sup>H] labeled tracers.

Raney-Ni catalyzed tritiation of **5** in IPA provided [<sup>3</sup>H]<sub>2</sub> labeled  $\beta$ -alanine *tert*-butyl ester **6**, with a specific activity of 35 mCi/mmol. It was crucial to conduct preparative HPLC purification and lyophilization of **6**, because using crude **6** resulted in low yield in the subsequent reaction. The Boc group was removed under acidic conditions to afford acid **7**. Many coupling conditions were investigated and dicyclohexylcarbodiimide (DCC) was the only reagent found to give the key intermediate **8**. It was noted that **8** was stable under mild acid conditions but rapidly decomposed when a base was present, and **8** can be stored in EtOH solution at  $-80^{\circ}\text{C}$  for 2 months. With different building blocks **2** and **3**, many targets **10** were obtained by using common peptide coupling techniques (Scheme 2). The major issue, however, is to purify the final compound with general structure **10**. The best purification condition found was follows. A TSKgel SP-5PW HPLC column eluted with 0.2% HCO<sub>2</sub>H and 1M NaCl aqueous solution, followed by a Jupiter-300 C18 column eluted with water and 0.2% HCO<sub>2</sub>H in MeCN provided the final tracers with radiochemical purity >97.6%. Final lyophilization of **10** resulted in very little changes in radiochemical purity. In this way, seven tracers of this kind have been prepared. This methodology is a general one in preparation of tritium labeled PEG-peptide tracers.



Scheme 2. (a) <sup>3</sup>H<sub>2</sub>, Raney-Ni, IPA, rt, 0.5 h, 62%; (b) TFA/DCM, 0<sup>o</sup>C, 2 h, 90%; (c) *N*-Hydroxysuccinimide, DCC, DMF, 55%; (d) **2**, TEA/DCM, reflux, 18 h, 32–66%; (e) **4**, buffer, 6 h, TSKgel SP-5PW HPLC column eluted with water with 0.2% HCO<sub>2</sub>H & 1 M NaCl, followed by HPLC column Jupiter-300 C18 column eluted with water and 0.2% HCO<sub>2</sub>H in MeCN.

**Acknowledgements:** The authors would like to thank Dr. Elisabetta Bianchi for providing reference samples and procedures for the PEGylation purification; Dr. George Doss, Dr. Vijay Reddy and Mr. Tom Bateman from Merck-DMPK Rahway for their help in analysis and characterization; Dr. Joseph Lynch, Dr. Ping Zhuang and Ms. Lisa Dimichele from Process Research for their help in providing **2** and sharing previous analytical experience on this program. J.Z.H. gratefully acknowledges Dr. Lee J. Silverberg for help in the preparation of this manuscript.

## References

- [1] B. Ahren, *Nature Reviews Drug Discovery* **2009**, 8(5), 369–385.
- [2] S. P. Baldwin, W. M. Saltzman, *Trends Polym. Sci.* **1996**, 4, 177–182.
- [3] M. Zhang, T. Desai, M. Ferrari, *Biomaterials* **1998**, 19, 953–960.
- [4] S. Zito, J. Shinde, I. C. S. Chen, T. Taldone, M. Barletta, *Cur. Bioact. Compd.* **2008**, 4(2), 68–85.

## REGIO-SELECTIVE IRIIDIUM-CATALYZED TRITIUM EXCHANGE LABELING OF NON-STEROIDAL ANTI-INFLAMMATORY DRUGS (NSAIDS) ZOMEPIRAC AND TOLMETIN USING BROMINE AS A PROTECTIVE GROUP

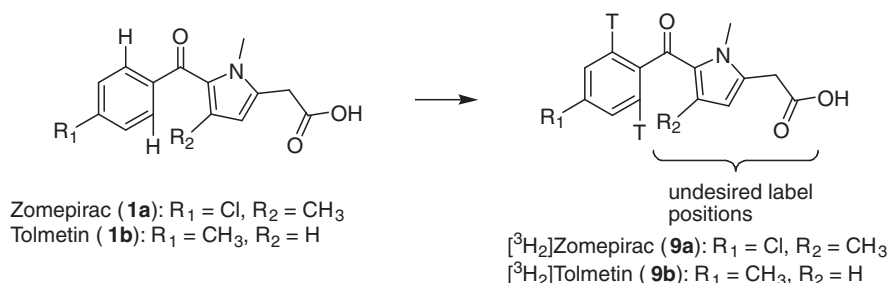
YUI S. TANG, WENSHENG LIU, MATTHEW P. BRAUN, AND JONATHAN Z. HO

Department of Process Research, Merck Research Laboratories, 126 E. Lincoln Avenue, PO Box 2000, RY800-B375, Rahway, New Jersey 07065, USA

**Abstract:** Regio-selective tritium labeled Zomepirac and Tolmetine were obtained with Ir-catalyzed tritium exchange in which the undesired labeling position was temporary protected by bromine.

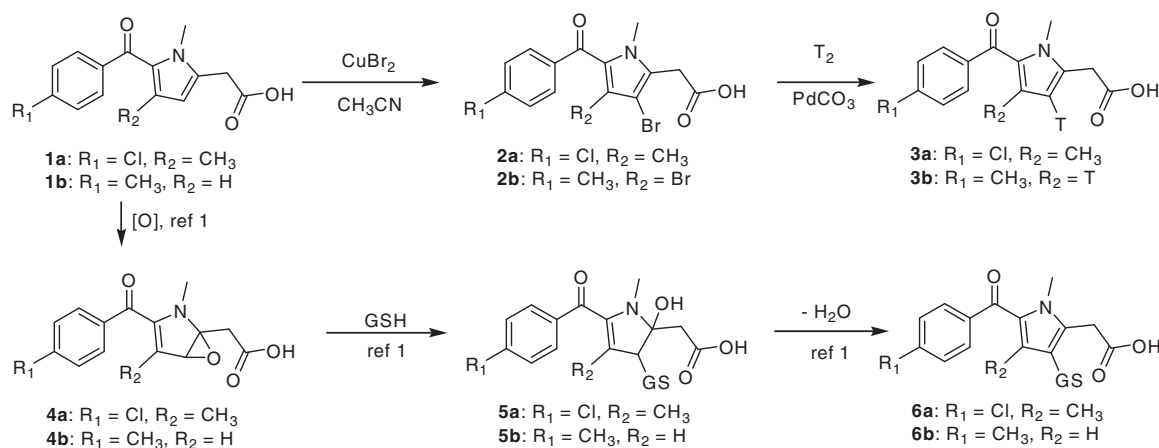
**Keywords:**  $^3\text{H}$ -label; Zomepirac and Tolmetine

**Introduction:** Zomepirac (**1a**) and Tolmetin (**1b**) are non-steroidal anti-inflammatory drugs (NSAIDs) used to treat a wide variety of inflammatory conditions such as osteo- and rheumatoid arthritis.<sup>1</sup> These two structurally similar drugs present an interesting case in the role of bioactivation in idiosyncratic adverse drug events (ADEs).<sup>2</sup> While Zomepirac was removed from the market due to a relatively high rate of anaphylactic liver toxicity, Tolmetin use has continued in Europe due to its relatively clean profile.<sup>3</sup> The cause of the different ADE profiles remains obscure and has drawn research interest in understanding the metabolic bioactivation mechanisms.<sup>4</sup> Radiolabeled Zomepirac (**1a**) and Tolmetin (**1b**) are important tools in this endeavor provided the label is placed in a position that is not involved in the metabolic activation process.<sup>5</sup> We describe herein a selective catalytic tritium isotope exchange approach to its tritium labeled tracers, [ $^3\text{H}$ ]-**1a** and [ $^3\text{H}$ ]-**1b**, through temporary blocking of the pyrrole functionality with bromine.



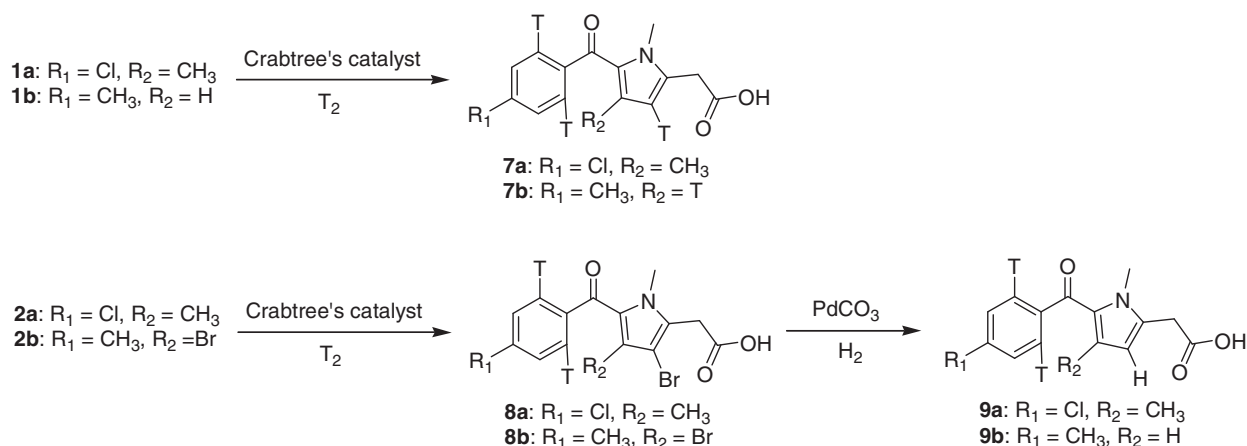
**Results and Discussion:** The study of drug metabolism and the identification of metabolic pathways is greatly aided by using radiolabeled tracers, which allow researchers to track what the drug does through the complex biological matrix and to detect a low abundance of bio-adducts.<sup>6</sup> For this purpose, it is ideal that the label is located at those positions which will not be cleaved through metabolism. The mechanism of catalytic tritiation to reduce a carbon-halide bond to a carbon-tritium bond is different than that of the catalytic exchange of a hydrogen atom with a tritium.<sup>7</sup> Application of these two techniques in a controlled way could achieve radiolabeled tracers in a highly regio-selective manner.

As shown in Scheme 1, Zomepirac (**1a**) and Tolmetin (**1b**) were converted to their bromide intermediates (**2a** and **2b**), and subsequent tritiation gave both tracers, **3a** and **3b**.<sup>6</sup> However, this strategy only put tritium label in the pyrrole ring. A preliminary metabolism study showed that the glutathione-bearing pyrrole adducts (**6a** and **6b**) were obtained from biooxidation (**4a** and **4b**), glutathione addition (**5a** and **5b**) and dehydration.<sup>1</sup> Based on this study, the tracers with tritium labels on the pyrrole were deemed to be unacceptable, and new tracers with tritium labels at the phenyl ring were desired.



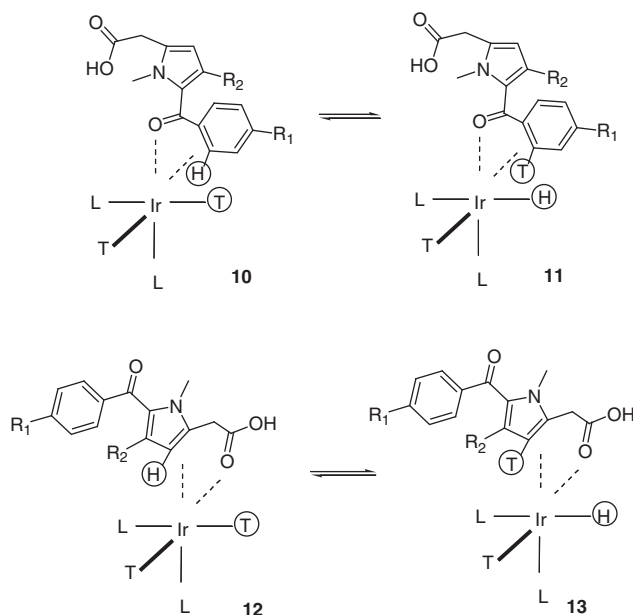
Scheme 1.

Crabtree's catalyst,  $[\text{Ir}(\text{COD})\text{PCy}_3(\text{py})]\text{PF}_6$ , and other Iridium based catalysts<sup>7</sup> have been used in tritium exchange condition, Zomepirac (**1a**) and Tolmetin (**1b**) were converted to tracers **7a** and **7b**, respectively (Scheme 2). The only problem is that in this method the tritium labels were placed not only in the desired phenyl ring but also in the undesired pyrrole functionality. To attempt to avoid putting labels at pyrrole of either **1a** or **1b**, bromination intermediates **2a** and **2b** were subjected to Ir-catalyzed tritium/hydrogen exchange. As shown in Scheme 2, both **2a** and **2b** were transformed to tracers **8a** and **8b**. Catalytic hydrogenation of **8a** and **8b** provided desired final tracers **9a** and **9b**. Since they were easily resolvable under preparative HPLC conditions,<sup>9</sup> both tracers, **9a** and **9b**, were prepared in a one-pot fashion.



Scheme 2.

The mechanism for tritiation from **1a** and **1b** to **7a** and **7b** can be explained as the following. The ketone carbonyl serves as a directing group. When it is coordinated to the Ir-catalyst to form intermediate **10** (Scheme 3), the protons at ortho-position in the phenyl group are accessible for exchange with tritium bonded to the catalyst to provide **11**. The acid carbonyl group serves as a directing group, too. When it is coordinated to the Ir-catalyst, the intermediate **12** is formed. In this situation, the acid carbonyl group is responsible for directing the H atom at 3-pyrrole to exchange with the tritium atom on the catalyst to afford **13**. When **2a** and **2b** are the substrates, there is a Br atom at 3-pyrrole. Therefore, Ir-mediated tritium/proton exchange tritiation of **2a** and **2b** can only lead to the products **8a** and **8b**. Subsequent Pd-catalyzed hydrogenation gave the desired tracer **9a** and **9b** where all tritium labels were located on the phenyl ring.



Scheme 3.

In summary, we have prepared zomepirac tracer (**9a**) and tolmetin tracer (**9b**) in which the tritium labels are on the phenyl ring. This was achieved by application of hydrogen/tritium isotopic exchange technique with bromine as a blocking group on the pyrrole. This temporary halogen-blocking strategy should serve as a viable approach for other regio-specifically labeled tritium tracers.

**Acknowledgements:** We would like to thank Ms Rosemary Marques and Mr. Steven J. Staskiewicz for analytical support. J.Z.H. gratefully acknowledges Dr. Lee J. Silverberg for help in the preparation of this manuscript.

## References

- [1] Q. Chen, G. A. Doss, E. C. Tung, W. Liu, Y. S. Tang, M. P. Braun, V. Didolkar, J. Strauss, R. W. Wang, R. A. Stearns, D. C. Evans, T. A. Baillie, W. Tang, *Drug Metab. Dispos.* **2006**, *34*, 145–151.
- [2] H. Takakusa, H. Masumoto, H. Yukinaga, C. Makino, S. Nakayama, O. Okazaki, K. Sudo, *Drug Metab. Dispos.* **2008**, *36*, 1770–1779.
- [3] B. W. Gutting, L. W. Updyke, D. E. Amacher, *J. Appl. Tox.* **2002**, *22*, 177–83.
- [4] P. Wellendorph, S. Hoeg, C. Skonberg, H. Brauner-Osborne, *Fund. Clin. Pharm.* **2009**, *23*, 207–213.
- [5] H. Takakusa, H. Masumoto, C. Makino, O. Okazaki, K. Sudo, *Drug Metab. Pharmacokinetics* **2009**, *24*(1), 100–107.
- [6] S. K. Johansen, L. Sorenson, L. Martiny, *J. Label Compd. Radiopharm.* **2005**, *48*, 569–576.
- [7] For review see: R. Crabtree, *Acc. Chem. Res.* **1979**, *12*, 331–337.
- [8] A. Y. L. Shu, D. Saunders, S. Levinson, S. W. Landvatter, A. Mahoney, S. G. Senderoff, J. F. Mack, J. R. Heys, *J. Label Compd. Radiopharm.* **1999**, *42*, 797–807.
- [9] Prep. HPLC conditions: ACE or Phenomenex C18 column (30 × 250 mm) with an eluant of 27% of MeCN in water (containing 0.1% HCO<sub>2</sub>NH<sub>4</sub>).

## REDUCTION OF UNSATURATED CARBON-CARBON BONDS WITH SODIUM BOROTRITIDE/NICKEL CHLORIDE

YUI S. TANG AND JONATHAN Z. HO

Department of Process Research, Merck Research Laboratories, Merck & Co., Inc., RY800-B375, 126 East Lincoln Avenue, Rahway, New Jersey, USA

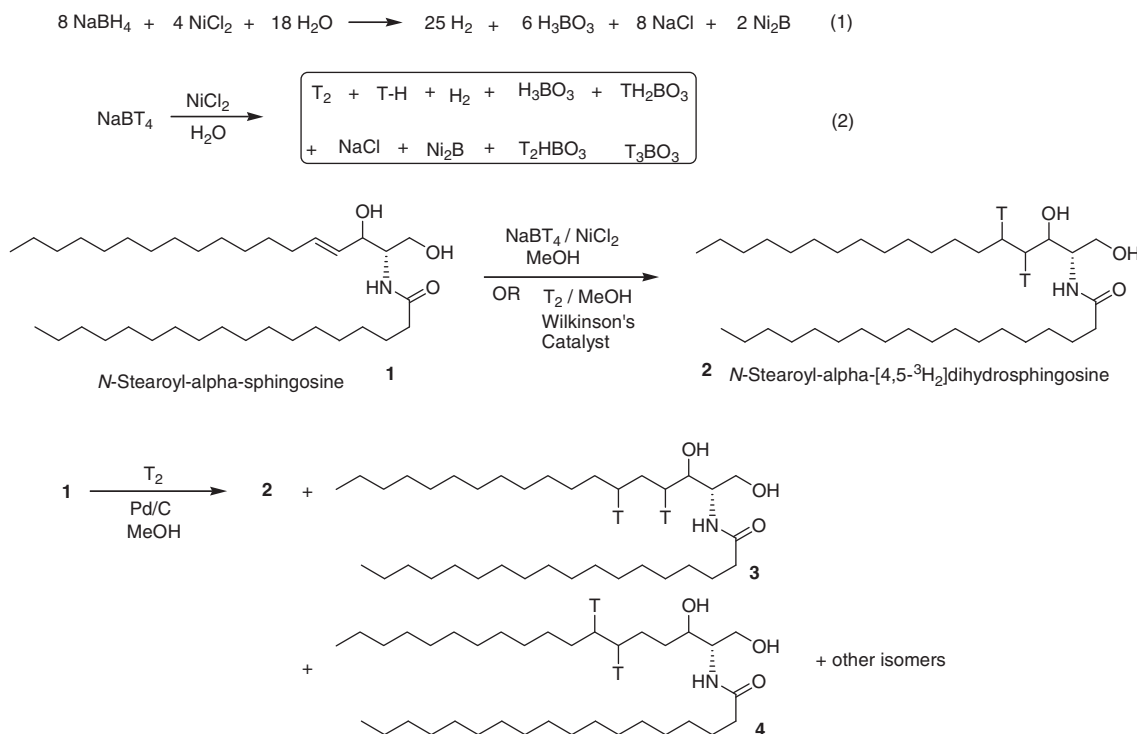
**Abstract:** Tritiation of olefins with sodium borotritide in the presence of nickel chloride proceeds to afford tritium tracers with no tritium-label scrambling. This method is effective for reductive tritium labeling of carbon-carbon double and triple bonds but inert toward bromides, thus providing a powerful chemo-selective labeling option for tritium chemists.

**Keywords:** sodium borotritide; nickel chloride; reduction; specific activity; regio-selectivity



**Introduction:** Tritiation of olefins is a straightforward method for the synthesis of tritium labeled tracers.<sup>1</sup> To date, this simple and convenient one step reaction was still being employed for easy access to many [<sup>3</sup>H]-labeled tracers.<sup>2</sup> Since virtually all Pd-based catalysts can mediate hydrogenation of unsaturated double bonds, tritiation with tritium gas instead of hydrogen gas would provide tritium tracers with high specific activity.<sup>3</sup> However, with palladium catalysts, double-bond migration can take place in competition with reduction<sup>4</sup> thus resulting in label-scrambling during tritiation, although it is not an issue for hydrogenation.<sup>2</sup> To minimize this double bond isomerization process, certain soluble transition metal complexes are chosen for labeling, and the most commonly used one is tris(triphenylphosphine)chlororhodium, known as Wilkinson's catalyst.<sup>5</sup> It was found in our lab that no label-scrambling tracer was detected when an olefin was reacted with T<sub>2</sub> in the presence of Wilkinson's catalyst. However, this method required excess amount of T<sub>2</sub>, which was expensive. In order to cut down the reaction cost and reduce the radiochemical waste stream, a solid tritium source is needed. Abe and co-workers<sup>6</sup> reported that five-membered  $\alpha,\beta$ -unsaturated lactones were reduced to the corresponding saturated lactones with NaBH<sub>4</sub> in the presence of transition metal salts. In light of this result, a novel tritiation technique with NaBT<sub>4</sub> in the presence of transition metal salts was investigated in our lab. To extend this reductive method from lactone to olefins, many transition metal salts were screened. In this paper, a general [<sup>3</sup>H]-labeling method by tritiation of olefins with sodium borotritide in the presence of nickel chloride hydrate is reported.

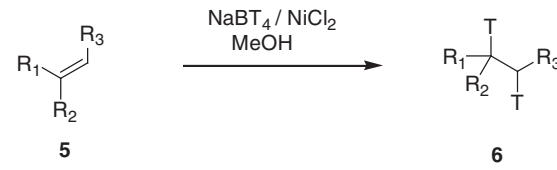
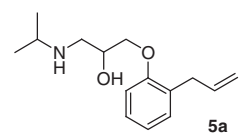
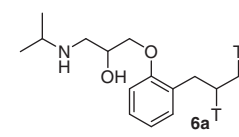
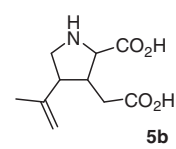
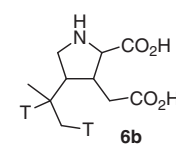
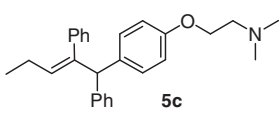
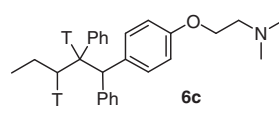
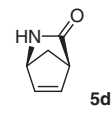
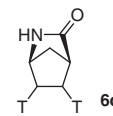
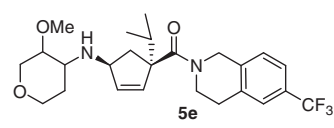
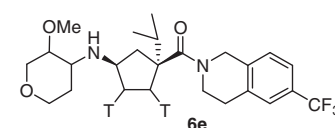
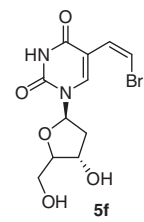
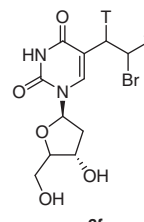
**Results and Discussion:** Upon the treatment of sodium borohydride with nickel chloride hydrate, a small amount of hydrogen gas is formed (Eq. 1). By substitution of sodium borohydride with sodium borotritide, tritium gas was generated (Eq. 2). It is this tritium gas that reduces olefins to corresponding [<sup>3</sup>H]-labeled tracers. It was found that tritium tracers can be prepared by using NaBT<sub>4</sub>/NiCl<sub>2</sub> as a labeling agent, and one example is shown in Scheme 1. *N*-Stearoyl- $\alpha$ -sphingosine (**1**) was converted to its [<sup>3</sup>H]-labeled tracer *N*-stearoyl- $\alpha$ -[4,5-<sup>3</sup>H]dihydrosphingosine (**2**) with specific activity (SA) of 38 Ci/mmol, as the only product. The [<sup>3</sup>H]-labels were regiospecifically placed at the predicted positions.<sup>7</sup> The same result was obtained by using T<sub>2</sub>/Wilkinson's catalyst, and the SA of **2** was 32 Ci/mmol. For comparison, alkene **1** was also reduced to **2** with tritium gas in the presence of Pd/C as a catalyst.<sup>8</sup> Under these conditions, a mixture of products (SA 48 Ci/mmol) was formed based on analyses with a <sup>3</sup>H NMR spectroscopy.<sup>9</sup> In addition to the desired tracer **2**, there were other [<sup>3</sup>H]-labeled tracers such as **3** and **4**, the [<sup>3</sup>H]-label scrambling products.



**Scheme 1.** Reductive tritiation of *N*-stearoyl- $\alpha$ -sphingosine.

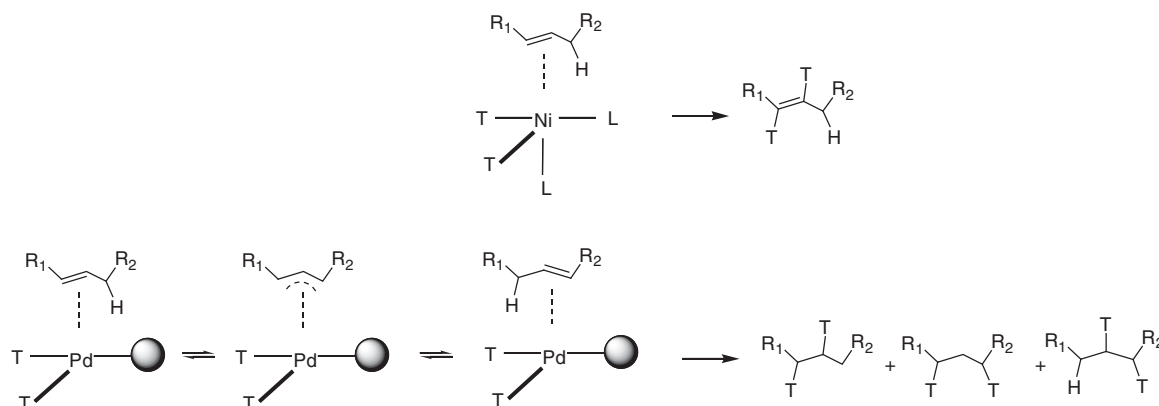
Encouraged by this positive result, a series of alkenes (**5a-f**) with various substitution patterns were submitted to NaBT<sub>4</sub>/NiCl<sub>2</sub> to give desired tracers **6a-f**, and the results are listed in Table 1. No [<sup>3</sup>H]-label scrambling products were detected for all cases. Kainic acid **5b** (a glutamine uptake inhibitor) and alprenolol **5a** (a  $\beta$ -3 adrenergic antagonist) were regio-specifically transformed to their tracers **6a** and **6b**, respectively (entries 1 and 2 in Table 1). Compound **5a** was chosen because it has both allylic and benzylic protons. Tamoxifen (**5c**) was converted to **6c** (entry 3 in Table 1), which indicated that this method can be applied to tri-substituted olefins. Due to slow conversion, moderate yields for tracers **6d** and **6e** were achieved from their precursors cyclopentenes **5d** and

**Table 1.** Reductive tritiation with NaBT<sub>4</sub>/NiCl<sub>2</sub>

Entry	Olefin	product	yield (%)
	 <p style="text-align: center;">5 <span style="margin-left: 150px;"></span> 6</p>		
1	 <p style="text-align: center;">5a</p>	 <p style="text-align: center;">6a</p>	74
2	 <p style="text-align: center;">5b</p>	 <p style="text-align: center;">6b</p>	62
3	 <p style="text-align: center;">5c</p>	 <p style="text-align: center;">6c</p>	37
4	 <p style="text-align: center;">5d</p>	 <p style="text-align: center;">6d</p>	58
5	 <p style="text-align: center;">5e</p>	 <p style="text-align: center;">6e</p>	51
6	 <p style="text-align: center;">5f</p>	 <p style="text-align: center;">6f</p>	49

**5e**, respectively (entry 4 and 5 in Table 1). This is because cyclopentenes are usually difficult to reduce under low hydrogenation pressure. High conversion could be achieved at higher pressure (> 15 psi). The tritiation condition in this method was under ambient pressure. Unlike tritiation with T<sub>2</sub>, only a stoichiometric amount of reagent, NaBT<sub>4</sub>, was used for the reduction of alkenes. Such a condition is an important factor in the reduction of **5f** to **6f** (entry 6 in Table 1), in which only the vinyl group was reduced and the bromide was retained.

The [<sup>3</sup>H]-labeling with NaBT<sub>4</sub>/NiCl<sub>2</sub> can be explained by the formation of a π-complex with Ni metal (Scheme 2). Transfer of tritium from nickel to carbon provides the [<sup>3</sup>H]-labeled tracers. When Pd-based catalysts were used, the double bond could be migrated via a π-allyl intermediate to give a mixture of olefins. Under hydrogenation conditions, this mixture of olefins would give the same saturated product. However, under tritiation conditions, the same mixture leads to a mixture of tracers. It is noted that NiCl<sub>2</sub> is a key ingredient. A control experiment showed that in the absence of NiCl<sub>2</sub> there was no desired tritiation product detected in the reaction mixture.



Scheme 2.

In conclusion, a novel method for introducing tritium across unsaturated carbon-carbon bonds with sodium borotritide and nickel chloride has been developed. This reaction can reduce mono-, di- and tri-substituted olefins, and it had excellent selectivity in the reduction of a carbon-carbon double bond over a carbon-bromide bond.

**Acknowledgments:** The authors would like to acknowledge the contributions of the following Merck co-workers: Dr. George Doss for his interpretation of NMR spectra, the staff of the Medicinal Chemistry Department for providing materials and procedures, Drs. Dennis Dean and Matt Braun for helpful discussion, and Dr. Allen Jones' analytical group of the Department of Drug Metabolism for the analytical support. J.Z.H. gratefully acknowledges Dr. Lee J. Silverberg for help in the preparation of this manuscript.

## References

- [1] E. A. Evans, *'Tritium and Its Compounds'* Butterworths, London (1974).
- [2] E. A. Evans, D. C. Warrell, J. A. Elvidge, J. R. Jones (Eds.), *'Handbook of Tritium NMR Spectroscopy and Applications'* Wiley, Chichester (1985).
- [3] P. G. Williams, Y. S. Tang, H. Morimoto, *Chem. Ind Aust.* **1988**, 55(3), 75–77.
- [4] H. C. Brown, C. A. Brown, *J. Amer. Chem. Soc.* **1963**, 85, 1003–1005.
- [5] B. R. Jones, *Homogeneous Hydrogenation* Wiley, New York, 1973.
- [6] N. Abe, F. Fujisaki, K. Sumoto, S. Miyano, *Chem. Pharm. Bull.* **1991**, 39(5), 1167–1170.
- [7] General procedure for reduction of alkenes using sodium borotritide/nickel chloride: A solution of alkene (0.05 mmol in 0.300 mL of THF) was injected into a septum micro-flask containing a solution of NaBT<sub>4</sub> (0.05 mmol, 85 Ci/mmol in 0.025 mL of THF) and nickel chloride (0.005 mmol) at room temperature. After 30 minutes of stirring, the sample was quenched with methanolic HCl (1 mL of 1 M), and the excess gas and solvent were removed by evacuation. The product was purified by reverse phase HPLC using a semi-preparative HPLC column (Phenomenex Phenyl Hexyl, 10 × 250 mm, MeCN/water/TFA from 20/80/0.1 to 50/50/0.1 in 45 min, flow rate = 10 mL/min), and the radiochemical yield was determined by liquid scintillation counting.
- [8] A mixture of substrate (0.5 mmol), catalyst (10 mg), and anhydrous solvent (1–2 mL) was degassed and stirred at room temperature. Carrier-free tritium gas stored as uranium tritritide (<sup>235</sup>U<sup>3</sup>H<sub>3</sub>) was liberated at approximately 1 atmospheric pressure and reacted for 1 hour. Excess tritium gas was returned to the uranium trap and the catalyst was filtered through an autovial syringeless device (Whatman 0.45 μm PVDF membrane) and the excess tritium gas was removed, and reaction mixture was evaporated. Ethanol (10 mL) was used to wash the residue then pumped down to dryness. This process was repeated three times before the reaction mixture was taken up by acetonile/water (5/1, 0.5 mL). The product was purified by reverse phase HPLC using a semi-preparative HPLC column (Phenomenex Phenyl Hexyl, 10 × 250 mm, MeCN/water/TFA from 20/80/0.1 to 50/50/0.1 in 45 min, flow rate = 10 mL/min), and the radiochemical yield was determined by liquid scintillation counting.
- [9] <sup>1</sup>H NMR and <sup>3</sup>H NMR spectra were measured at 400 MHz on a Varian Unity-400 spectrometer. Chemical shifts were reported in ppm (δ) and were referenced to the residual solvent peak (chloroform at 7.26 ppm). Radioactivity measurements were carried out using a Packard 1200 liquid scintillation counter with a Packard Ultima Gold TM scintillant. Analytical HPLC measurements were performed on a system consisting of Shimadzu LC-10ADVP pumps, SPD-10AVP UV detector, CTO-10ASVP column oven, SIL-10ADVP auto-injector, SCL-10AVP system controller and Packard Radiomatic™ 150TR flow monitor controlled by a Compaq computer running Shimadzu Class-VP software. Preparative and semi-preparative HPLCs were performed on a system comprised of a Thermo-separation pump and Krutas UV detector. Mass spectra were recorded on an HP1100 LCMSD instrument in API-ES positive ionization mode.

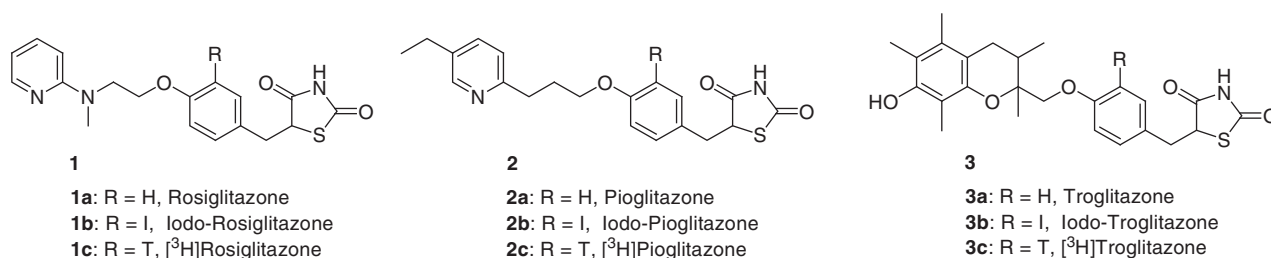
## A PRACTICAL PROCEDURE OF SYNTHESIS OF TRITIUM LABELED TROGLITAZONE

YUI S. TANG, WENSHENG LIU, MATTHEW P BRAUN, AND JONATHAN Z. HO

Department of Process Research, Merck Research Laboratories, Merck &amp; Co., Inc., RY800-B375, 126 East Lincoln Avenue, Rahway, New Jersey, USA

**Abstract:** Tritium labeled Troglitazone (**3c**) has been prepared *via* an iodination-tritiation sequence.**Keywords:** tritium labeling; iodination; Troglitazone

**Introduction:** [<sup>3</sup>H]-Labeling is an invaluable technique for probing structure and functional properties of drug or drug candidates in metabolic processes.<sup>1</sup> The ideal way to make a tritium tracer is to convert a target to its tracer in one step.<sup>2</sup> While Rh-catalyzed tritium-hydrogen exchange is one way to achieve this for some compounds,<sup>3</sup> direct iodination followed by catalytic reduction with T<sub>2</sub> is another way for many others.<sup>4</sup> To that end, *N*-Iodosuccinimide (NIS) is a common reagent used in the key iodination step.<sup>5</sup> One problem with this method is that preparation of iodo-intermediates can be tricky and often inconsistent yields are obtained for those with the same pharmacophore. For example, Jordan and co-workers reported iodination of Rosiglitazone (**1a**) and Pioglitazone (**2a**) were successful while iodination of Troglitazone (**3a**) was fruitless, even though these three compounds are of the same skeleton (Figure 1).<sup>6</sup> Consequently, tritium labeled Rosiglitazone and Pioglitazone, but not Troglitazone, were prepared *via* an iodination-tritiation sequence.

**Figure 1.** Structures of three TZDs and their iodinated analogs and tritium-labeled isotopomers.

Troglitazone is a member of the thiazolidindione class of insulin sensitizer (TZDs) which are used for the treatment of type 2 diabetes mellitus (T2DM).<sup>7</sup> Troglitazone was removed from the market shortly after approval due to hepatic toxicity. Rosiglitazone and Pioglitazone are members of the same class of drug but remain on the market with relatively clean hepatic toxicity profiles.<sup>8</sup> In order to better understand the metabolic pathways that may influence the hepatotoxicity profile of these TZDs there has been interest in preparing radiolabeled forms.

While it was initially difficult to apply the strategy of iodination-tritiation sequence toward tritium labeled troglitazone preparation, a practical procedure was developed in our lab to make iodo-Troglitazone (**3b**) which was subsequently converted to the desired tritium labeled Troglitazone (**3c**)

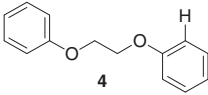
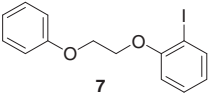
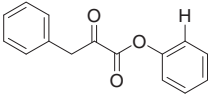
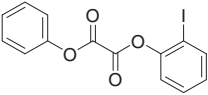
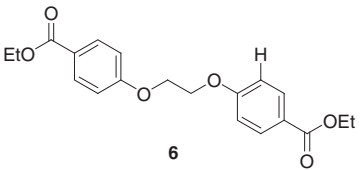
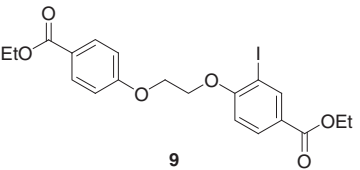
**Results and discussion:** From arenes to iodo-arenes is an important transformation, and the related methods are periodically reviewed.<sup>9</sup> From the tritium-label angle, iodo-arenes always provide tracers with the highest specific activity compared to those from their chloro- or bromo- counterparts. NIS iodination of arenes with the phenol ether moiety in presence of triflic acid would proceed but the yield is substrate-dependent. The most critical factor, however, was found to be the reaction temperature. Extremely low temperature (−78°C) made the iodination rate too slow to be useful, while elevated temperature (> 0°C) resulted the desired product decomposing. A good temperature range for this reaction is between −30 to −10°C. Several arenes were converted to their iodo-analogues with NIS and a catalytic amount of triflic acid at −20°C for 20 min, and the results are list in Table 1.<sup>10</sup> The radical nature<sup>11</sup> of NIS reactions often gives many iodinated by-products. Those impurities could compete with desired intermediate to consume T<sub>2</sub> gas during the subsequent tritiation reaction. Thus, a purification step was needed. Model compounds, **4**, **5**, and **6**, were converted to desired products, **7**, **8**, and **9**, respectively, in moderate yields. Rosiglitazone (**1a**), Pioglitazone (**2a**) and Troglitazone (**3a**) were converted to **1b**, **2b**, and **3b**, respectively. Tritiation with T<sub>2</sub> provided the final tracers **1c**,<sup>6</sup> **2c**,<sup>6</sup> and **3c**,<sup>12</sup> respectively.

All iodination reactions performed in Table 1 gave a cleaner reaction profile at low conversion than that at high conversion, which made the subsequent purification easier. The low yields were acceptable because the short reaction-time made it possible to carry out multiple runs so that sufficient tracers can be prepared quickly.

In summary, a tritium labeled Troglitazone (**3c**) has been prepared *via* an iodination-tritiation sequence.

**Acknowledgments:** The authors would like to acknowledge Rosemary Marques for analytical support. J.Z.H. thanks Dr. Lee J. Silverberg for help in the preparation of this manuscript.

**Table 1.** Low temperature iodination with NIS in the present of acetic acid.

Entry	Ar-H	Ar-I	conversion (%)	yield (%)
1			72	62
2			78	62
3			74	61
4	<b>1a</b>	<b>1b</b>	49	38
5	<b>2a</b>	<b>2b</b>	36	21
6	<b>3a</b>	<b>3b</b>	20	11

## References

- [1] R. E. Gibson, H. D. Burns, T. G. Hamill, W. Eng, B. E. Francis, C. Ryan, *Cur. Pharma. Design.* **2000**, *6*, 973–981.
- [2] M. Sljoughian, P. G. Williams, *Cur. Pharma. Design.* **2000**, *6*, 1057–1059.
- [3] For review see: R. Crabtree, *Acc. Chem. Res.* **1979**, *12*, 331–337.
- [4] E. A. Evans, *'Tritium and Its Compounds'* Butterworths, London (1974).
- [5] G. A. Olah, Q. Wang, G. Sandford, G. K. S. Prakash, *J. Org. Chem.* **1993**, *58*, 3194–3195.
- [6] N. Bushby, J. R. Harding, A. Jordan, G. N. Nilsson, R. Simonsson, K. Wiklund, *J. Label. Compd. Radiopharm.* **2007**, *50*, 410–411.
- [7] S. H. Choi, Z. S. Zhao, Y. J. Lee, D. J. Kim, C. W. Ahn, S. K. Lim, H. C. Lee, B. S. Cha, *Diabetes/Metabolism Res. Rev.* **2007**, *23*(5), 411–416.
- [8] C. V. Rizos, M. Elisaf, D. P. Mikhailidis, E. N. Liberopoulos, *Expert Opin. Drug Safety* **2009**, *8*(1), 15–24.
- [9] D. M. Golden, S. W. Benson, *Chem. Rev.* **1969**, *69*(1), 125–134.
- [10] Iodination: A suspension of substrate (0.011 mmol) mixed with NIS (2 mg) at  $-20^{\circ}\text{C}$  was added to a solution of NIS (1 mg) in triflic acid (1 mL). The mixture was stirred at  $-20^{\circ}\text{C}$  for 20 minutes. A solution of 1 M (0.5 mL) aqueous solution of sodium metabisulfite ( $\text{Na}_2\text{S}_2\text{O}_5$ ) was added, and the brown suspension was filtered through a syringe-less filtering device to remove solid. MeOH (1 mL) was used to rinse the solid and combined filtrate was concentrated under vacuum to give an oil which was purified by Reverse Phase HPLC (Luna C8 column,  $22.5 \times 250$  mm) with an isocratic eluent of MeCN:water:TFA = 30:70:0.1 at a flow rate of 10 mL/min.
- [11] P. S. Skell, J. C. Day, *J. Am. Chem. Soc.* **1978**, *100*(6), 1951–1953.
- [12] Tritiation: A suspension of **3b** (2 mg, 0.0035 mmol) and 10% Pd/ $\text{CaCO}_3$  (5 mg) in anhydrous DMF (0.8 mL) was degassed and stirred at  $0^{\circ}\text{C}$  for 5 min. A carrier-free tritium gas (1.2 Ci) was introduced under vacuum of 240 mm Hg, and the resulting mixture was stirred at  $0^{\circ}\text{C}$  for 2 h. Excess tritium gas was removed, and the mixture was filtered through a syringe-less filter device (0.45  $\mu\text{m}$ , polytetrafluoroethylene; autovial; Whatman, Clifton, NJ). The filtrate was concentrated under vacuum to give an oil. EtOH (2 mL) was added to make a solution which was purified by HPLC (Phenomenex Luna Phenyl-Hexyl column,  $9.4 \text{ mm} \times 250 \text{ mm}$ , Torrance, CA) with a gradient eluent of MeCN:water:TFA from 25:75:0.1 to 30:70:0.1 in 50 min at a flow rate of 10 mL/min. The product **3c** was collected at the retention time of 28 min (25 mCi; 23 Ci/mmol, radiochemical purity > 99%). The identity was confirmed by LC/MS analysis and HPLC co-elution with unlabeled reference sample.

## ISOTOPE EFFECTS IN OXIDATIVE DEAMINATION OF L-PHENYLALANINE

MARIANNA KANSKA AND KATARZYNA SKOWERA

Department of Chemistry, University of Warsaw, Pasteur Str. 1, 02-093 Warsaw, Poland

**Abstract:** The mechanism of reversible oxidative deamination of L-phenylalanine into phenylpyruvic acid catalyzed by enzyme L-Phenylalanine Dehydrogenase (EC 1.4.1.20) using kinetic and solvent isotope effects was studied.

**Keywords:** deuterium; isotope effects; L-phenylalanine; phenylpyruvic acid; tritium

**Introduction:** Phenylketonuria (PKU), a human genetic disease, is accompanied by elevated levels of L-phenylalanine (L-Phe) and its metabolites such as phenylacetate, phenyllactate, and phenylpyruvate in body fluids. The knowledge about the mechanism of enzymatic conversion of L-Phe into phenylpyruvic acid (PPA) is essential for proper therapy of PKU patients. One of metabolic pathway of conversion of L-Phe into PPA is reversible, oxidative deamination<sup>1</sup> catalyzed by enzyme L-Phenylalanine Dehydrogenase (EC 1.4.1.20), PheDH, Figure 1.

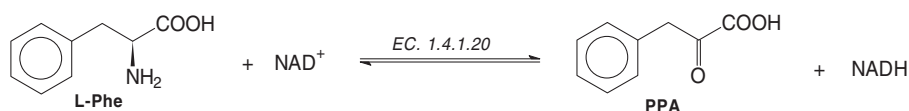


**Figure 1.** Enzymatic conversion of L-Phe into PPA.

For the above reaction, we studied the deuterium and tritium kinetic and solvent isotope effects using non competitive and competitive (combined with internal <sup>14</sup>C- radioactive standard) methods. For purposes of this study we synthesized the isotopomers of L-Phe labeled with deuterium, tritium and <sup>14</sup>C, i. e., [(3S)-<sup>2</sup>H]-, **1**, [(3R)-<sup>2</sup>H]-, **2**, [2-<sup>2</sup>H]-, **3**, [2-<sup>3</sup>H]-, **4**, and [1-<sup>14</sup>C]-L-Phe.

**Results and Discussion:** 1. Synthesis of isotopomers of L-Phe and PPA. The deuterium labeled isotopologues **1** and **2** were obtained by addition of ammonia to (*E*)-cinnamic (using fully deuteriated incubation medium) or (*E*)-[3-<sup>2</sup>H]-cinnamic acid, respectively, catalyzed by the enzyme Phenylalanine Ammonia Lyase (ec 4.1.3.5).<sup>2</sup> Isotopomers **3** and **4** were afforded by reductive amination of PPA catalyzed by the enzyme PheDH carried out in a fully deuteriated or tritiated medium, respectively. <sup>14</sup>C-labeled **5**, needed as radioactive internal standard, was obtained by addition of ammonia to [1-<sup>14</sup>C]-cinnamic acid.<sup>3</sup>

**2. Deuterium isotope effects:** a) *Solvent isotope effects, SIE.* The values of solvent isotope effects (SIE on  $V_{\max} = 1.66 \pm 0.11$  and SIE on  $V_{\max}/K_m = 1.90 \pm 0.13$ ) in the reaction of oxidative deamination of L-Phe to PPA, Figure 1, catalyzed by the enzyme PheDH, were determined by a non competitive spectrophotometric method. The maximum reaction rate ( $V_{\max}$ ) and Michaelis constant ( $K_m$ ) are the parameters in Michaelis-Menten's equation (1).

$$K_m = S \left[ \frac{V_{\max}}{v} - 1 \right] \quad (1)$$

Where:  $k_m$  is Michaelis constant,  $S$  is concentration of substrate ( $S \gg$  concentration of enzyme),  $v$  is reaction rate at concentration  $S$  and  $V_{\max}$  is maximum reaction rate.

The progress of reaction was monitored indirectly by measuring the absorbance of the NADH at 340 nm. The reaction was carried out in glycine buffer (pH 10.7) with different concentrations of substrate and enzyme.

b) *Kinetic isotope effects, KIE.* The primary deuterium kinetic isotope effect (KIE on  $V_{\max} = 1.11 \pm 0.10$  and KIE on  $V_{\max}/K_m = 1.06 \pm 0.08$ ) in the above mentioned reaction were also measured spectrophotometrically using deuterium labeled isotopomer **3**.

The secondary deuterium KIE's were determined the same way applying stereospecifically labeled isotopologues **1** and **2** and are given in Table 1.

Table 1. Secondary deuterium kie's for oxidative deamination of L-Phe		
Isotopologue	Kind of KIE	
	KIE on $V_{\max}$	KIE on $V_{\max}/K_m$
[(3S)- <sup>2</sup> H]-L-Phe, <b>1</b>	<b>1.16 ± 0.12</b>	<b>1.01 ± 0.09</b>
[(3R)- <sup>2</sup> H]-L-Phe, <b>2</b>	<b>1.13 ± 0.13</b>	<b>1.03 ± 0.11</b>

**3. Tritium kinetic isotope effect.** The kinetic assays of the reaction (Figure 1) were carried out using a competitive internal standard method which measures <sup>3</sup>H/<sup>14</sup>C ratio instead of the specific activity of <sup>3</sup>H-labeled L-Phe. Therefore, the determination of KIE is much more precise. The assayed mixture was composed of [2-<sup>3</sup>H]-L-Phe, **3**, and [1-<sup>14</sup>C]-L-Phe, **5**, (internal standard) isotopomers, and cofactor NADH dissolved in 10ml of 0.1M glycine buffer (pH 10.7). The reaction was started by adding the enzyme

Phe dehydrogenase (0.2 U) to the incubation medium. During the course of the kinetic run, 1 ml samples were taken at preset times and the reaction was quenched by freezing with liquid nitrogen. The unreacted substrate and product were separated chromatographically and their  $^3\text{H}/^{14}\text{C}$  ratios were measured by liquid scintillation counting. The degree of conversion was determined using  $^{14}\text{C}$ -radioactivities of the substrate (L-Phe) and product (PPA). Bigeleisen-Wolfsberg's equation was used to calculate KIE.<sup>4</sup>

$$\alpha = \frac{\ln \left[ 1 - f \frac{(1-f)R_0}{R_f} \right]}{\ln(1-f)} \quad (2)$$

where:

- $\alpha$  -  $^1\text{H}/^3\text{H}$  kinetic isotope effect,
- $R_0$  -  $^3\text{H}/^{14}\text{C}$  radioactivity ratio in L-Phe at the start of reaction,
- $R_f$  -  $^3\text{H}/^{14}\text{C}$  radioactivity ratio in L-Phe after  $f$  degree of conversion,
- $f$  - degree of conversion.

The average value of tritium KIE derived from the five different levels of conversion of L-Phe into PPA was equal  $1.09 \pm 0.19$ . The experimental errors were calculated using Student's equation with 0.95 confidence level.

Small deuterium SIE and KIE's, as well as, no tritium KIE observed in the oxidative deamination of L-Phe to PPA strongly suggest that an abstraction of proton from the  $\alpha$ -position of L-Phe is not the rate determining step of its conversion to PPA.

## References

- [1] M. Norbert, W. Brunhuber, J. B. Thoden, J. S. Blanchard, J. L. Vanhooke, *Biochemistry* **2000**, *39*, 9174–9187.
- [2] K. Skowera, M. Kanska, *J. Label. Compd. Radiopharm.* **2008**, *51*, 321–324.
- [3] W. Augustyniak, J. Bukowski, J. Jemielity, R. Kanski, M. Kanska, *J. Radioanal. Nucl. Chem.* **2001**, *247*, 371–374.
- [4] J. Biegeleisen, *J. Chem. Phys.* **1947**, *17*, 675–678.

## ISOTOPE EFFECTS IN THE ENZYMATIC HYDROXYLATION OF TYRAMINE

MARIANNA KAŃSKA AND EDYTA PANUFNIK

Department of Chemistry, University of Warsaw, Pasteur Str. 1, 02–093 Warsaw, Poland

**Summary:** We studied the mechanism of hydroxylation of tyramine to dopamine catalyzed by enzyme monophenol oxidase (EC 1.14.18.1) using kinetic and solvent isotope effects methods.

**Keywords:** enzyme; dopamine; hydroxylation; isotope effects; tyramine

**Introduction:** Tyramine, TA, plays an important role in many metabolic processes occurring in mammalian and plants cells. In adrenal gland L-tyrosine, L-Tyr, is transformed into dopamine, DA, a precursor of adrenaline - an important neurotransmitter, Figure 1.

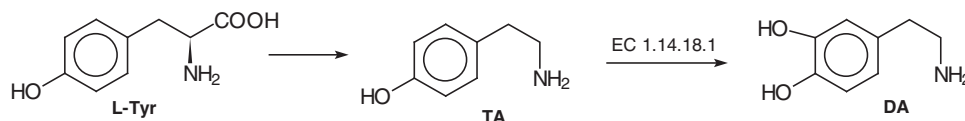


Figure 1. Biotransformation of L-tyrosine into dopamine.

In this report we investigated the mechanism of hydroxylation of TA to DA, one step of above metabolic path, catalyzed by enzyme monophenol oxidase<sup>1</sup> (tyrosinase, EC 1.14.18.1) using Kinetic Isotope Effect (KIE) and Solvent Isotope Effect (SIE) methods.

**Results and discussion:** *Synthesis of isotopomers of tyramine (TA).* The rings labeled with deuterium and tritium isotopomers of TA, needed for kinetic studies, were synthesized *via* two different routes. In the first,<sup>2</sup> under acid catalyzed conditions the deuterium and tritium label was introduced into the 3'- and 5'-positions of TA yielding  $[3',5'\text{-}^2\text{H}_2]$ -, **1**,  $[3',5'\text{-}^3\text{H}_2]$ -, **2**, and  $[3',5'\text{-}^2\text{H}/^3\text{H}]$ -TA, **3**, respectively, dependent upon type of exchanging medium used ( $\text{D}_2\text{O}$ , HTO or DTO), Figure 2. In the second, the isotopomer  $[2',6'\text{-}^2\text{H}_2]$ -TA, **4**, was afforded by enzymatic decarboxylation<sup>2</sup> of commercial  $[2',6'\text{-}^2\text{H}_2]$ -L-Tyr.

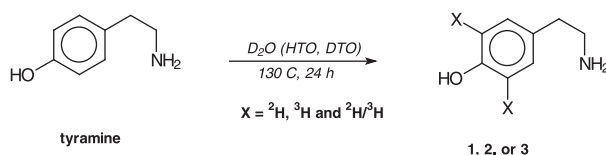
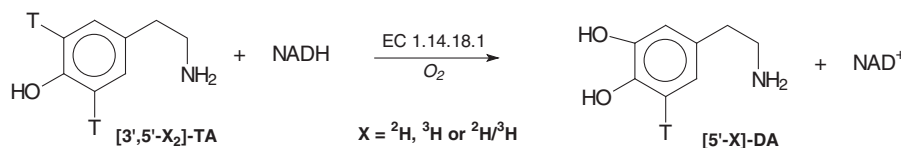


Figure 2. Biotransformation of L-tyrosine into dopamine.

*KIE assays.* Numerical values for  $^1\text{H}/^3\text{H} = 2.06 \pm 0.16$  and  $^2\text{H}/^3\text{H} = 1.77 \pm 0.04$  of KIE's for the 3'-position were determined in the reaction of hydroxylation (Figure 3) of TA (**2** or **3**) catalyzed by the enzyme monophenol oxidase (EC 1.14.18.1) using the competitive method, with commercial [ $1\text{-}^{14}\text{C}$ ]-TA as internal radioactive standard and Yankwich-Tong's equations<sup>3</sup> to calculate KIE.



**Figure 3.** Biotransformation of L-tyrosine into dopamine.

Table 1 shows the results of kinetic studies on enzymatic hydroxylation of TA (**1** and **4**) in water and heavy water, using a non competitive spectrophotometric method.

*SIE assays.* The kinetic data needed for calculation of the numerical values of deuterium SIE's for **1** and **4** were determined spectrophotometrically and are given in Table 2.

Substrate and incubation medium	Type of SIE	
	SIE on $V_{\max}$	SIE on $V_{\max}/K_m$
TA in $\text{H}_2\text{O}$ /TA in $\text{D}_2\text{O}$	$3.34 \pm 0.14$	$3.48 \pm 0.21$
<b>1</b> in $\text{H}_2\text{O}$ / <b>1</b> in $\text{D}_2\text{O}$	$2.57 \pm 0.14$	$3.05 \pm 0.24$
<b>4</b> in $\text{H}_2\text{O}$ / <b>4</b> in $\text{D}_4\text{O}$	$1.82 \pm 0.02$	$1.13 \pm 0.05$

The magnitude of the H/T and D/T KIE's for the hydrogen atom in the 3'-position of TA (2.06 and 1.77, respectively), as well as, the size of deuterium KIE on  $V_{\max}$  (3.43 and 2.45) and  $V_{\max}/K_m$  (1.63 and 1.31) indicates its significant role in the conversion of complex 'enzyme-substrate' into complex 'enzyme-product'. The magnitude of SIE also indicates that 3'-hydrogen and solvent' protons are involved in the formation of the reaction transition state. The size of deuterium isotope effects for the hydrogen atoms in the 2' and 6'-positions of TA are typical for secondary isotope effect is implying that these atoms are not directly involved in the course of reaction. The comparison of H/T and D/T KIE's by means of the Swain-Schaad criterion<sup>4</sup> shows that proton tunneling is not occurring in enzymatic hydroxylation of TA to DA catalyzed by monophenol oxidase.

**Experimental:** *Synthesis of [ $3',5'\text{-}^2\text{H}_2$ ]-TA, 1.* This deuterated isotopomer of TA was obtained by isotopic H/D exchange between  $\text{D}_2\text{O}$  and authentic TA catalyzed by DCI according to the procedure described by us earlier.<sup>2</sup> The  $^1\text{H}$  NMR spectrum shows near 100% deuterium incorporation into the 3' and 5' positions of **1**.

*Synthesis of [ $3',5'\text{-}^3\text{H}_2$ ]-TA, 2.* Tritiated isotopomer **2** was obtained by acid catalyzed H/T exchange between tritiated water and tyramine as described earlier.<sup>2</sup> As a result 125 mg (0.92 mmol) sample of **2** with total radioactivity 64 MBq was obtained (sp. activity 69 MBq/mmol).

*Synthesis of [ $3',5\pm\text{-}^2\text{H}/^3\text{H}$ ]-TA, 3.* Doubly labeled **3** was synthesized in a similar manner<sup>2</sup> to that used for **2**. For reaction 200 mg (1.15 mmol) of tyramine hydrochloride, 0.9 mL of  $\text{D}_2\text{O}$ , 0.2 mL of conc. DCI/ $\text{D}_2\text{O}$ , and 0.1 mL of tritiated water with total radioactivity 11.1 GBq were reacted. As a result 113 mg (0.83 mmol) of **3** was obtained (yield 72%) with total radioactivity 61 MBq (sp. activity 73.5 MBq/mmol).

*Kinetic assays: Tritium KIE for the 3 ring positions of TA (radiometric competitive method).* KIE's were determined at room temperature for low conversion of substrate. Typical assayed medium was composed of 6 mL of 0.1 phosphate buffer (pH 5.5), c.a. 1 mg of **2** or **3**, and water solution of [ $1\text{-}^{14}\text{C}$ ]-TA. Isotopic ratio  $^3\text{H}/^{14}\text{C}$  for each sample ( $R_0$  parameter) was measured using a liquid scintillation counter and a dual label program. The reaction was started by adding 300  $\mu\text{L}$  (0.4 U) solution of enzyme tyrosinase. At preset time 1 mL sample was taken and reaction was quenched by adding 1 mL of 1 M HCl. Next, the substrate (TA) and product (dopamine) were eluted (silica gel column) with solution of  $\text{CH}_3\text{OH}:25\%\text{NH}_3 = 20:1$ . The  $^3\text{H}/^{14}\text{C}$  ratios ( $R_s$  for tyramine and  $R_p$  for dopamine) were measured and degree of conversion ( $f$ ) was determined using radioactivity of  $^{14}\text{C}$ . Average value of each KIE was calculated from 5 independent kinetic runs using all<sup>4</sup> Yankwich-Tong's equations.<sup>3</sup>

*Deuterium KIE and SIE (non competitive spectrophotometric method).* The assayed medium (1.5 mL) composed of 0.1 M phosphate buffer, the enzyme tyrosinase (0.4 U) and solutions of 0.4 mM NADH and appropriate isotopomer of TA (**1** or **4** with conc. between  $-0.06$  to 1.3 mM) was placed in the quartz spectroscopic cuvette. The progress of reaction was determined indirectly by measuring the decreasing of absorbancy of NADH at  $\lambda = 340$  nm. The average  $V_{\max}$  and  $V_{\max}/K_m$  parameters (Michaelis-Menten equation) were calculated using Enzfitter 1.05 and processing data from 30 independent kinetic runs.

## References

- [1] K. Lerch, *Meth. Enzymol.* **1987**, *142*, 165–169.
- [2] E. Panufnik, M. Kanska, *J. Label. Compd. Radiopharm.* **2007**, *50*, 85–89.
- [3] J. T. Tong, P. E. Yankwich, *J. Phys. Chem.* **1957**, *61*, 540–543.
- [4] G. Swain, E. C. Stivers, J. F. Reuwer, L. J. Schaad, *J. Am. Chem. Soc.* **1958**, *80*, 5885–5893.



SYNTHESIS OF [ $^{14}\text{C}$ ]- AND [ $^{13}\text{C}_6$ ]-LABELED POTENT HIV NON-NUCLEOSIDE REVERSE TRANSCRIPTASE INHIBITOR<sup>1</sup>

BACHIR LATLI, MATT HRAPCHAK, CARL A. BUSACCA, DHILEEPKUMAR KRISHNAMURTHY, AND CHRIS H. SENANAYAKE

Department of Chemical Development, Boehringer Ingelheim Pharmaceuticals, Research and Development Center, 900 Ridgebury Road, P.O. Box 368, Ridgefield, Connecticut 06877-0368, USA

**Abstract:** Compound **1** (Figure 1), labeled with carbon-14 in the quinoline-benzene ring, in one of the pyridine rings of the dipyridodiazepinone tricyclic moiety, and in the side chain, was prepared in three different syntheses with specific activities ranging from 44 to 47 mCi/mmol (1.63 to 1.75 GBq/mmol). In the first synthesis, **2** was coupled to 4-hydroxyquinoline, [benzene- $^{14}\text{C}$ (U)]- under Mitsunobu conditions, followed by oxidation of the quinoline nitrogen with *m*-CPBA to give [ $^{14}\text{C}$ ]-(**1a**) in 43% radiochemical yield. Secondly, 3-Amino-2-chloropyridine, [2,6- $^{14}\text{C}$ ]- was used to prepare **8**, which was converted to **10**. Mitsunobu etherification and oxidation as seen before, gave [ $^{14}\text{C}$ ]-(**1b**) in eight steps and in 11% radiochemical overall yield. Finally, carbon-14 potassium cyanide was used to prepare isopropyl cyanoacetate (**12**), which was used to transform bromide **8** to aryl acetic acid **13** under palladium catalysis. Alcohol **14**, obtained from the reduction of acid **13**, was used as described above to prepare [ $^{14}\text{C}$ ]-(**1c**) in 4.3% radiochemical yield. To prepare [ $^{13}\text{C}_6$ ]-(**1**), [ $^{13}\text{C}_6$ ]-4-hydroxyquinoline was prepared from [ $^{13}\text{C}_6$ ]-aniline and then coupled to **2** and oxidized as seen before.

**Keywords:** NNRT inhibitor; HIV; radiosynthesis; carbon-14; carbon-13

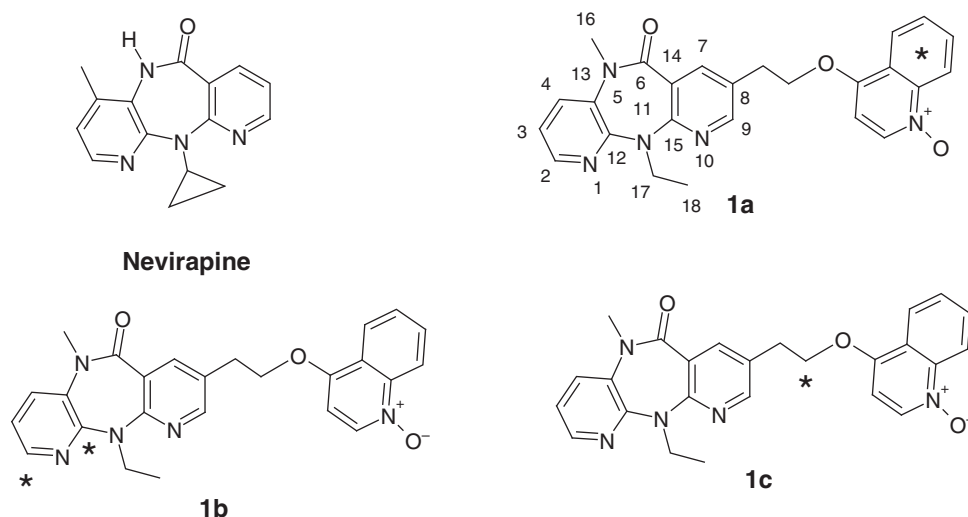
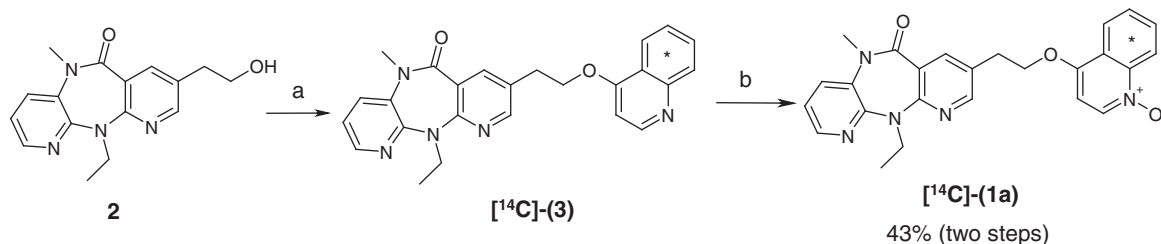


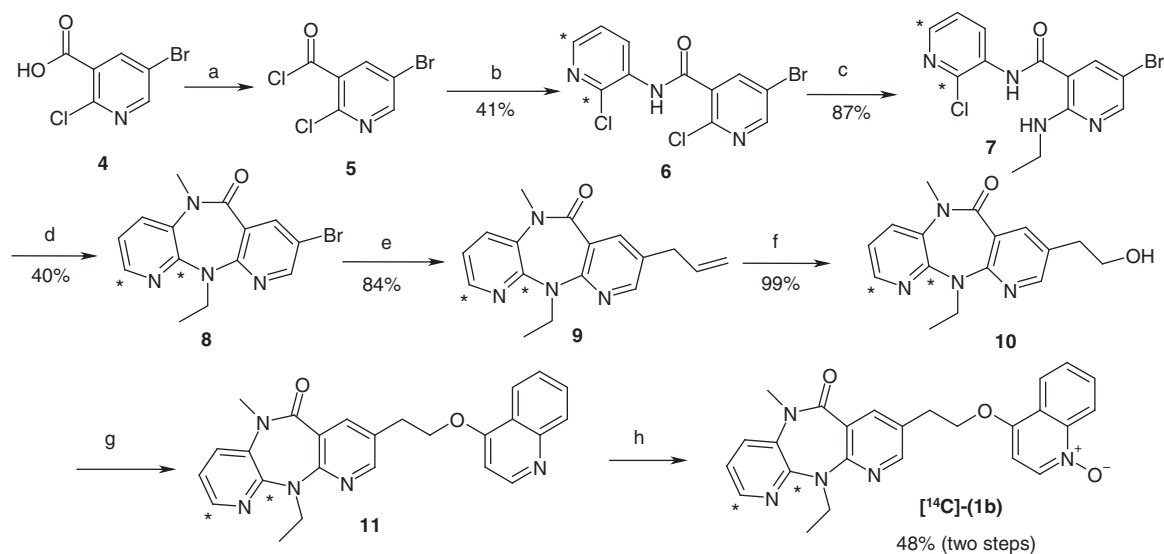
**Figure 1.** Nevirapine (viramune<sup>®</sup>) and its analogue **1**, asterisks indicate position of carbon-14 atom(s).

**Results and Discussion:** The preparation of [ $^{14}\text{C}$ ]-(**1a**) (Scheme 1), was accomplished in two steps by coupling [ $^{14}\text{C}$ ]-labeled 4-hydroxyquinoline (Moravek Biochemicals) to **2** via a Mitsunobu reaction and then oxidizing the quinoline nitrogen with *m*-CPBA.



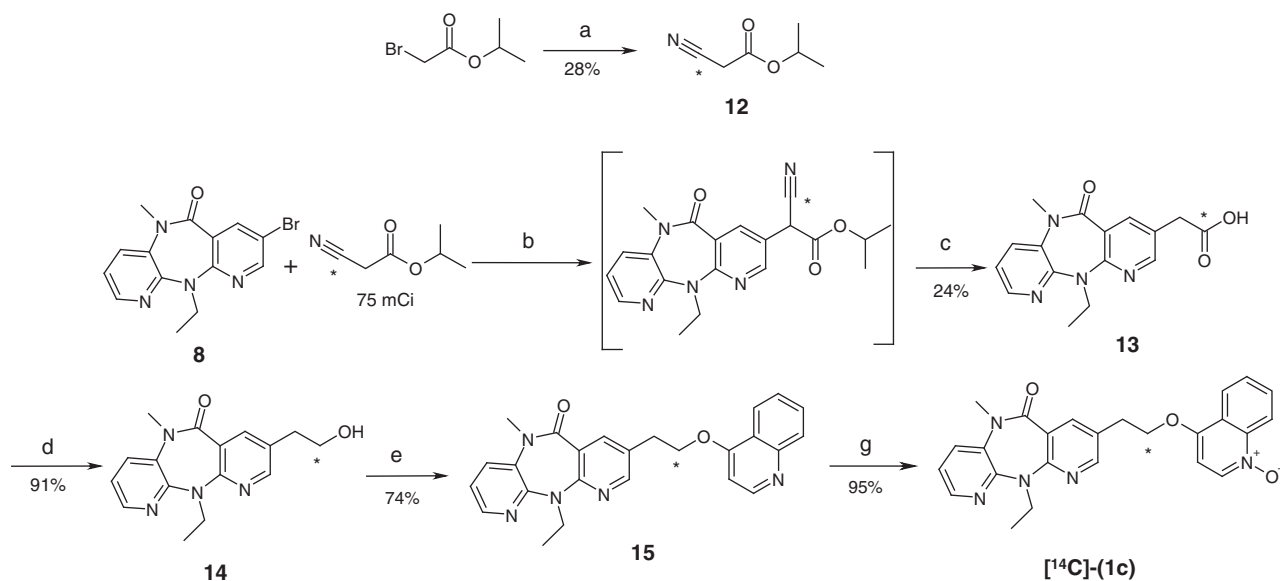
**Scheme 1.** (a) DEAD,  $\text{Ph}_3\text{P}$ , 4-hydroxyquinoline, [benzene- $^{14}\text{C}$ (U)], THF; (b) *m*-CPBA,  $\text{CH}_2\text{Cl}_2$ .

[ $^{14}\text{C}$ ]-(**1b**) was prepared in 11% yield over eight steps and with a specific activity of 44 mCi/mmol (1.63 GBq/mmol); see Scheme 2; using commercially available 3-amino-2-chloropyridine, [2,6- $^{14}\text{C}$ ]-, (GE HealthCare).



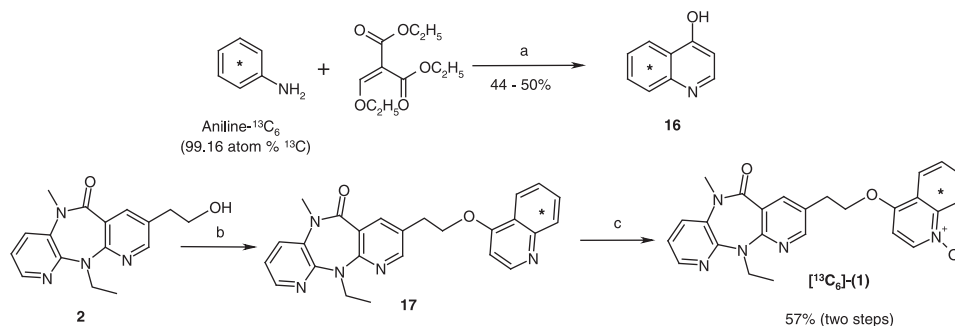
**Scheme 2.** (a)  $\text{SOCl}_2$ ; (b) 3-Amino-2-chloropyridine,  $[2,6\text{-}^{14}\text{C}]$ -,  $\text{NaHCO}_3$ , MeCN; (c)  $\text{EtNH}_2$ , THF; (d)  $\text{NaHMDS}$ , pyridine, MeI, THF; (e) Allyl(tributyl)tin,  $(\text{Ph}_3\text{P})_4\text{Pd}$ , DMF; (f)  $\text{O}_3$ , 10%  $\text{MeOH}/\text{CH}_2\text{Cl}_2$ ,  $\text{NaBH}_4$ ; (g) 4-Hydroxyquinoline, DEAD,  $\text{Ph}_3\text{P}$ , THF; (h) *m*-CPBA,  $\text{CH}_2\text{Cl}_2$ .

To prepare  $[^{14}\text{C}]$ -(1c), carbon-14 isopropyl cyanoacetate was prepared from the reaction of isopropyl bromoacetate and potassium  $[^{14}\text{C}]$ cyanide (American Radiolabeled Compounds). Then, arylation by bromide **8** under palladium catalysis using triphenylphosphine as a ligand, followed by hydrolysis/ decarboxylation gave the carboxylic acid **13** in one pot. Reduction of acid **13** to alcohol **14** followed by Mitsunobu's etherification with 4-hydroxyquinoline derivative gave **15** in 74% yield. Oxidation with *m*-CPBA in methylene chloride as used before, gave  $[^{14}\text{C}]$ -(1c) in 95% yield (Scheme 3).



**Scheme 3.** (a)  $\text{KCN}$ ,  $[^{14}\text{C}]$ -, 25%  $\text{MeOH}/\text{H}_2\text{O}$ ; (b)  $\text{Pd}(\text{OAc})_2$ ,  $\text{Ph}_3\text{P}$ ,  $\text{NaH}$ ,  $\text{PhCH}_3$ ; (c)  $\text{NaOH}$ ,  $80^\circ\text{C}$ ; (d)  $\text{BH}_3\text{-THF}$ ; (e) 4-Hydroxyquinoline, DIAD,  $\text{Ph}_3\text{P}$ , THF; (f) *m*-CPBA,  $\text{CH}_2\text{Cl}_2$ .

To prepare  $[^{13}\text{C}_6]$ -(1), commercially available  $[^{13}\text{C}_6]$ -aniline (*Isotec*) was condensed with diethyl ethoxymethylene malonate first at  $110^\circ\text{C}$  neat and then in phenyl ether at  $260^\circ\text{C}$ . Saponification, followed by decarboxylation gave  $[^{13}\text{C}_6]$ 4-hydroxyquinoline in 44% overall yield. Mitsunobu's reaction with **2** and oxidation with *m*-CPBA as described before gave  $[^{13}\text{C}_6]$ -(1) in 57% over two steps. The product was more than 99 atom %  $^{13}\text{C}$  (Scheme 4).



**Scheme 4.** (a)  $\text{Ph}_2\text{O}$ ,  $\text{NaOH}$ , heat; (b) DIAD,  $\text{Ph}_3\text{P}$ , THF, (**16**); (c) *m*-CPBA,  $\text{CH}_2\text{Cl}_2$ .

## Reference

- [1] B. Latli, M. Hrapchak, C. A. Busacca, D. Krishnamurthy, C. H. Senanayake, *J. Label. Compd. Radiopharm.* **2009**, *52*, 84–90.

## SYNTHESIS OF TWO ISOTOPICALLY LABELED VERSIONS OF AURORA A KINASE INHIBITOR

YUEXIAN LI AND SHIMOGA R. PRAKASH

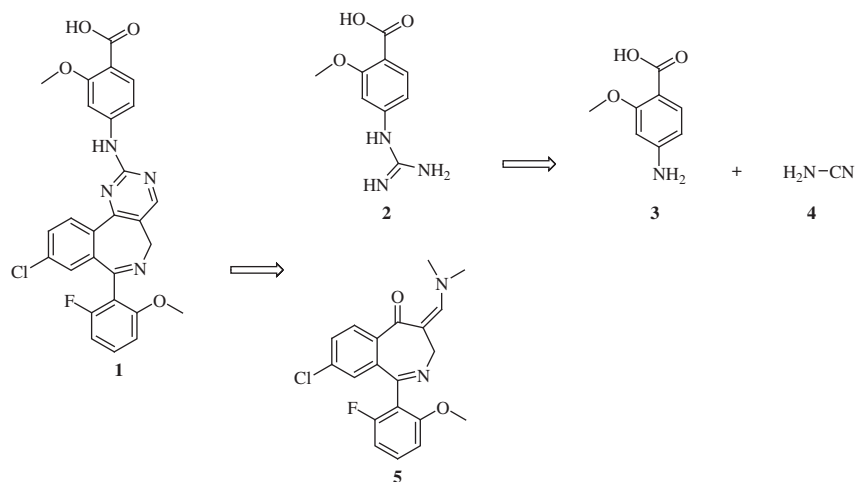
Department of Drug Metabolism and Pharmacokinetics, Isotope Chemistry Group, Millennium Pharmaceuticals, Inc., The Takeda Oncology Company, 35 Landsdowne Street, Cambridge, MA 02139, USA

**Abstract:** [ $^{14}\text{C}$ ]-sodium 4-[[9-chloro-7-(2-fluoro-6-methoxyphenyl)-5H-pyrimido[5,4-d][2]benzazepin-2-yl]amino]-2-methoxy benzoate was synthesized from [ $^{14}\text{C}$ ]- $\text{CO}_2$  in a yield of 5%. [ $^{13}\text{CD}_3$ ,  $^{15}\text{N}_2$ ]-sodium 4-[[9-chloro-7-(2-fluoro-6-methoxyphenyl)-5H-pyrimido[5,4-d][2]benzazepin-2-yl] amino]-2-methoxy benzoate was prepared from [ $^{13}\text{CD}_3$ ]-iodomethane and [ $^{15}\text{N}_2$ ]-cyanamide in an overall yield of 22%.

**Keywords:** [ $^{14}\text{C}$ ]-sodium 4-[[9-chloro-7-(2-fluoro-6-methoxyphenyl)-5H-pyrimido[5,4-d][2]benzazepin-2-yl]amino]-2-methoxy benzoate; [ $^{13}\text{CD}_3$ ,  $^{15}\text{N}_2$ ]-sodium 4-[[9-chloro-7-(2-fluoro-6-methoxyphenyl)-5H-pyrimido[5,4-d][2]benzazepin-2-yl]amino]-2-methoxy benzoate

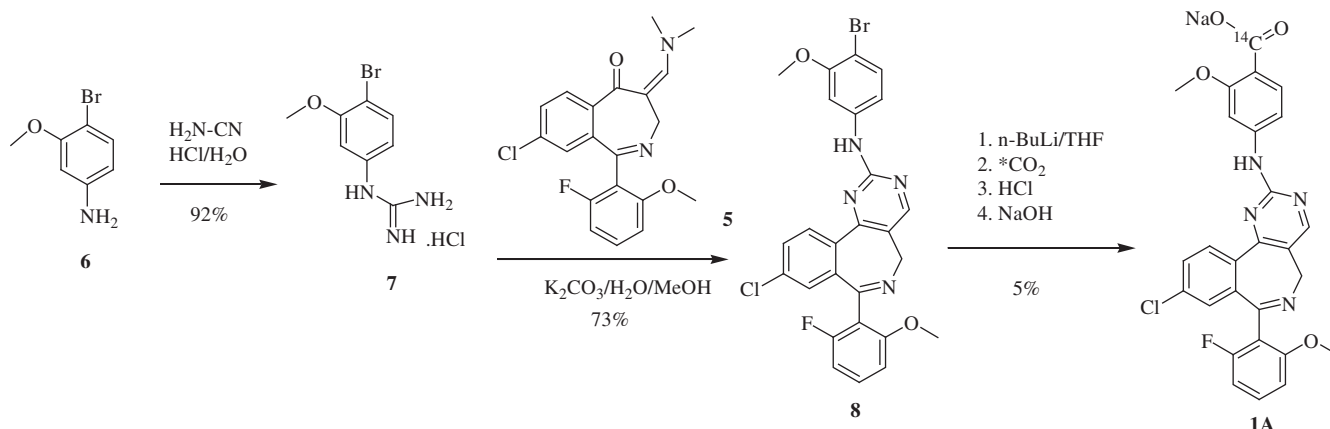
**Introduction:** Aurora A kinase plays an essential role in the proper assembly and function of the mitotic spindle.<sup>1,2</sup> Inhibition of Aurora A kinase represents an attractive modality for therapeutic intervention of human cancers.<sup>3</sup> The biological activity of the recently discovered Aurora A kinase inhibitor, sodium 4-[[9-chloro-7-(2-fluoro-6-methoxyphenyl)-5H-pyrimido[5,4-d][2]benzazepin-2-yl]amino]-2-methoxy benzoate (MLN8237),<sup>1–4</sup> led to detailed investigations on its disposition characteristics. The radiolabeled version was required to assist such investigations, especially in metabolite profiling and whole-body autoradiography studies in experimental animals. The stable isotope labeled version was also required as an internal standard for mass spectrometry based bio-analytical assays.

**Results and Discussion:** The structure of 4-[[9-chloro-7-(2-fluoro-6-methoxyphenyl)-5H-pyrimido[5,4-d][2]benzazepin-2-yl]amino]-2-methoxy benzoic acid (**1**) provides two potential sites for labeling, either on the top pyrimidinimine benzoic acid portion or the bottom benzazepine portion of the molecule (Scheme 1).<sup>4</sup> Preclinical metabolism results indicated that radiolabeling either portion of the molecule would be adequate for the intended ADME studies in animals. For expedient synthesis, we chose labeling guanidinobenzoic acid **2** instead of benzoazepine **5** for both stable isotope and radiolabeled versions (Scheme 1).



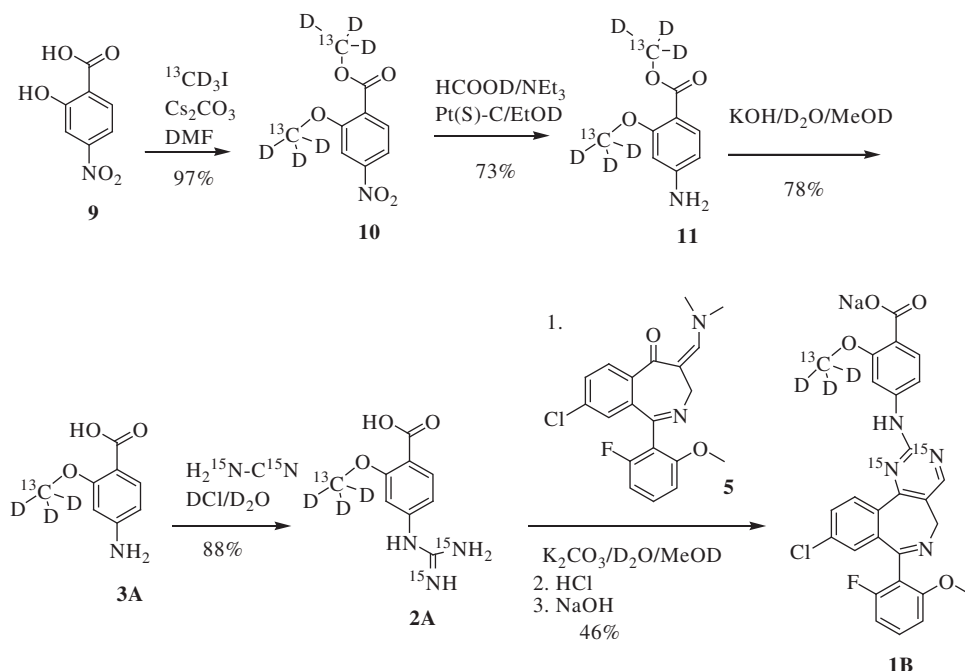
**Scheme 1.** Retro-synthesis of MLN8237.

There are two possible approaches to the C-14 labeled compound **1**, either on the guanidine portion to prepare the ring-labeled **1** or on carboxylic group to the carboxyl labeled **1** (Scheme 1). We chose to synthesize the carboxyl labeled compound **1** either from [ $^{14}\text{C}$ ]-4-amino-2-methoxybenzoic acid or lithiation of bromo derivative **8** followed by carbonation with [ $^{14}\text{C}$ ]-CO $_2$ . To reduce radiosynthetic steps and cost, we chose [ $^{14}\text{C}$ ]-CO $_2$  as the radiolabeled precursor (Scheme 2). Reaction of **6** with cyanamide provided guanidine **7** in a yield of 92%.<sup>5</sup> The key intermediate **8** was prepared by K $_2$ CO $_3$ -mediated coupling of **7** with **5** in methanol (73%).<sup>4</sup> [ $^{14}\text{C}$ ]-sodium 4-[[9-chloro-7-(2-fluoro-6-methoxyphenyl)-5H-pyrimido[5,4-d][2]benzazepin-2-yl]amino]-2-methoxy benzoate (**1A**) was synthesized by lithiating **8** followed by carbonation with [ $^{14}\text{C}$ ]-CO $_2$  (5%).<sup>6</sup> The low yield could be due to formation of multiply lithiated species.



Scheme 2. Synthesis of [ $^{14}\text{C}$ ]-MLN8237.

Because MLN8237 contains a chlorine atom, a labeled version that is at least 5 amu higher than the unlabeled version is required to ensure complete separation of labeled and unlabeled molecular ion clusters during mass spectrometric assays of MLN8237. To increase the molecular weight, labeling of the pyrimidinimine benzoic acid portion of the molecule or benzazepine portion was required. Labeling the 2-methoxy-4-guanidinobenzoic acid **2A** with carbon-13, deuterium, and nitrogen-15 was chosen.



Scheme 3. Synthesis of [ $^{13}\text{C}$ , D $_3$ ,  $^{15}\text{N}_2$ ]-MLN8237.

To prepare **1B**, commercially available [ $^{13}\text{C}$ ]-iodomethane and [ $^{15}\text{N}_2$ ]-cyanamide were used as the labeled precursors (Scheme 3). Treatment of **9** with [ $^{13}\text{C}$ ]-iodomethane and Cs $_2$ CO $_3$  in DMF provided nitro ester **10**.<sup>7</sup> Reduction of this nitro ester by transfer

hydrogenation (NEt<sub>3</sub> and HCOOH) followed by hydrolysis of the resulting compound yielded 4-amino-2-methoxybenzoic acid **3A**.<sup>8,9</sup> Reaction of **3A** with [<sup>15</sup>N<sub>2</sub>]-cyanamide provided the labeled guanidine **2A**.<sup>5</sup> [<sup>13</sup>C, D<sub>3</sub>, <sup>15</sup>N<sub>2</sub>]-sodium 4-[[9-chloro-7-(2-fluoro-6-methoxyphenyl)-5H-pyrimido[5,4-d][2] benzazepin-2-yl]amino]-2-methoxy benzoate (**1B**) was prepared by K<sub>2</sub>CO<sub>3</sub>-mediated coupling **2A** with **5** in MeOD.<sup>4</sup>

**Conclusions:** In summary, practical methods for the preparation of carbon-14 and stable isotope labeled Aurora A kinase inhibitor, 4-[[9-chloro-7-(2-fluoro-6-methoxyphenyl)-5H-pyrimido[5,4-d][2]benzazepin-2-yl]amino]-2-methoxy benzoic acid, were developed. The key intermediate product for C-14 synthesis, bromo derivative **8**, was synthesized from 4-bromo-3-methoxy benzenamine in two steps. The key intermediate product for stable isotope labeled synthesis, guanidine **2A**, was prepared from 2-hydroxy-4-nitro-benzoic acid in four steps. [<sup>14</sup>C]-sodium 4-[[9-chloro-7-(2-fluoro-6-methoxyphenyl)-5H-pyrimido[5,4-d][2]benzazepin-2-yl]amino]-2-methoxy benzoate was synthesized from [<sup>14</sup>C]-CO<sub>2</sub> in a yield of 5%. [<sup>13</sup>CD<sub>3</sub>, <sup>15</sup>N<sub>2</sub>]-sodium 4-[[9-chloro-7-(2-fluoro-6-methoxyphenyl)-5H-pyrimido[5,4-d][2]benzazepin-2-yl]amino]-2-methoxy benzoate was prepared from [<sup>13</sup>CD<sub>3</sub>]-iodomethane and [<sup>15</sup>N<sub>2</sub>]-cyanamide in an overall yield of 22%.

## References

- [1] K. Hoar, A. Chakravarty, C. Rabino, D. Wysong, D. Bowman, N. Roy, J. A. Ecsedy. *Mol. Cell. Biol.* **2007**, *27*, 4513–4525.
- [2] P. J. LeRoy, J. J. Hunter, K. M. Hoar, K. E. Burke, V. Shinde, J. Ruan, D. Bowman, K. Galvin, J. A. Ecsedy. *Cancer Res* **2007**, *67*, 5362–5370.
- [3] M. G. Manfredi, J. A. Ecsedy, K. A. Meetze, S. K. Balani, O. Burenkova, E. Chen, K. M. Galvin, K. M. Hoar, J. J. Huck, P. J. LeRoy, E. T. Ray, T. B. Sells, B. Stringer, S. G. Stroud, T. J. Vos, G. S. Weatherhead, D. R. Wysong, M. Z. Zhang, J. B. Bolen, C. F. Claiborne. *PNAS* **2007**, *104*, 4106–4111.
- [4] C. F. Claiborne, T. B. Sells, S. G. Stroud. *US Pat Appl Publ* **2008**, US 063525.
- [5] A. H. Binham, R. J. Davenport, L. Gowers, R. L. Knight, C. Lowe, D. A. Owen, D. M. Parry, W. R. Pitt. *Bioorg. Med. Chem. Lett.* **2004**, *14*, 409–412.
- [6] Y. Li, M. Plesescu, S. R. Prakash. *J. Label Compd. Radiopharm.* **2006**, *49*: 789–799.
- [7] D. D. Dischino, V. K. Gribkoff, P. Hewawasam, G. M. Luke, J. K. Rinehart, Y. L. Spears, J. E. Starrett. *J. Label Compd. Radiopharm.* **2003**, *46*: 139–149.
- [8] Y. Li, S. R. Prakash. *J. Label Compd. Radiopharm* **2005**, *48*, 323–330.
- [9] C. C. M. Janssen, H. H. C. Lenoir, J. J. A. Thijssen, A. A. Knaeps, J. J. P. Heykants. *J. Label Compd. Radiopharm.* **1987**, *24*, 1493–1501.

## USING THE COLOGICA ISOTOPIC SYNTHESIS DATABASE: A COMPLEMENTARY APPROACH TO SYNTHESIS SEARCHING VIA THE MAJOR SEARCH ENGINES

WILLIAM J. S. LOCKLEY

CoLogica Scientific, 92, Loughborough Rd, West Bridgford, Nottingham, NG2 7JH, UK

**Abstract:** The CoLogica database is a structure-searchable synthesis database of compounds labelled with isotopes of hydrogen and carbon. It is extensive but not comprehensive, comprising of abstracts from both the early and the recent isotopic synthesis literature. Examples are provided of the use of the database in searching for reagents and conditions, for reaction feasibility assessment, in reconstructing literature syntheses and in *de novo* synthesis planning.

**Keywords:** labelled-compound; isotopic-synthesis; database; CoLogica; <sup>2</sup>H; <sup>3</sup>H; <sup>14</sup>C

**Introduction:** The CoLogica database is an isotopic synthesis database covering compounds labelled with the isotopes <sup>2</sup>H, <sup>3</sup>H, <sup>11</sup>C, <sup>13</sup>C & <sup>14</sup>C. It contains the main fields of interest to chemists involved in isotopic synthesis and is extensive but not comprehensive, currently containing ca. 20,000 records. It is comprised of abstracts from both the early and the recent isotopic synthesis literature, particularly concentrating on literature which is not easily retrieved by search engines. Included, for example, are many records from sources such as local and international IIS symposium proceedings and from the classic text books on isotopic synthesis, many of which are now out of print. The accent of the database is on molecules likely to be of use as synthetic intermediates. As such, it is a more rapid, but complementary, adjunct to researching isotopic synthesis pathways via the major search engines. The database utilises the Symyx MDL IsisBase<sup>®</sup> platform running on a stand alone or networked PC system under Windows 2000, XP or Vista. A typical record from the database is shown below (Figure 1).

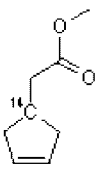
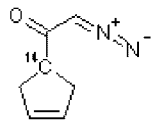
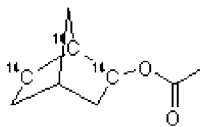
			<p>Other Reagent(s)</p> <p>Ag<sub>2</sub>O MeOH</p>
<p>Name</p> <p>Methyl 2-([4-<sup>14</sup>C]Cyclopenten-4-yl)-acetate, methyl ([1-<sup>14</sup>C]cyclopent-3-en-1-yl)acetate.</p>	<p>Abundance</p>	<p>Yield</p> <p>Used directly</p>	
<p>Reaction Conditions</p> <p>The rearrangement is typically carried out on the diazoketone (often from the acid chloride via CH<sub>2</sub>N<sub>2</sub>) with freshly prepared Ag<sub>2</sub>O. For related chemistry see K. Murdock, B. Angier, J. Org. Chem. 37, 2825 (1972).</p>	<p>Other Data</p> <p>Wolff variant of the Arndt-Eistert rearrangement. The intermediate is probably the ketene.</p>	<p>ID</p> <p>13278</p>	<p>Donor</p> <p><sup>14</sup>CCH(CO<sub>2</sub>R)<sub>2</sub></p>
<p>Reference</p> <p>C. J. Collins, C. E. Harding, Ann. Chem., 745, 124 (1971). Also reported in "Organic Synthesis with Carbon-14", R. R. Muccino, Wiley Interscience, John Wiley and Sons, New York, p.461, 1983. [ISBN 0-471-05165-9]</p>	<p>Code</p> <p>14CRM</p>		

Figure 1. A typical synthesis record from the CoLogica database.

**Results & Discussion:** The simplest use of the database is in the search for references to the synthesis of a particular labelled compound. This is facilitated by three database options; structure, substructure and name searching. Such searching, especially via substructure, is the basis of the following more complex, but typical, applications.

**Example 1: Searching for reagents and conditions.** Consider the commonly used reaction below (Figure 2).



Figure 2. Nucleophilic displacement of halide by labelled cyanide.

Here the database returned 201 records, of which 128 used alkali metal cyanides, 50 used cuprous cyanide, 3 used zinc cyanide, 2 hydrogen cyanide and 1 silver cyanide. Fifteen of the records described Pd-catalysis and 3 the use of microwaves. A total of 76 records gave some practical details whilst in 25 cases the experimental detail was extensive.

**Example 2: Searching for feasible reactions.** Here the database was interrogated for approaches to the *ortho*-labelling of nitroaromatics with tritium (Figure 3):

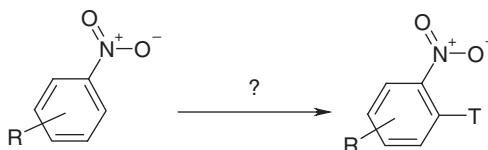


Figure 3. *Ortho*-labelling of nitroaromatics with tritium.

This yielded 20 hits, including five exchange approaches; two iridium-catalysed, one acid-catalysed, one base-catalysed and one metal-catalysed. In addition an interesting selective tritioderhalogenation<sup>1</sup> was identified.

**Example 3: Reconstructing literature synthesis schemes.** The database is structured so that reaction schemes can be rapidly extracted. By searching from each labelled compound hit *via* the database's 'precursor' field the complete scheme can be constructed, including data on the yields, conditions, etc. The example below shows the results of an initial search for specific <sup>14</sup>C-labelled phenanthrene syntheses which yielded, amongst other routes, the complete synthesis scheme<sup>2</sup> as shown (Figure 4).

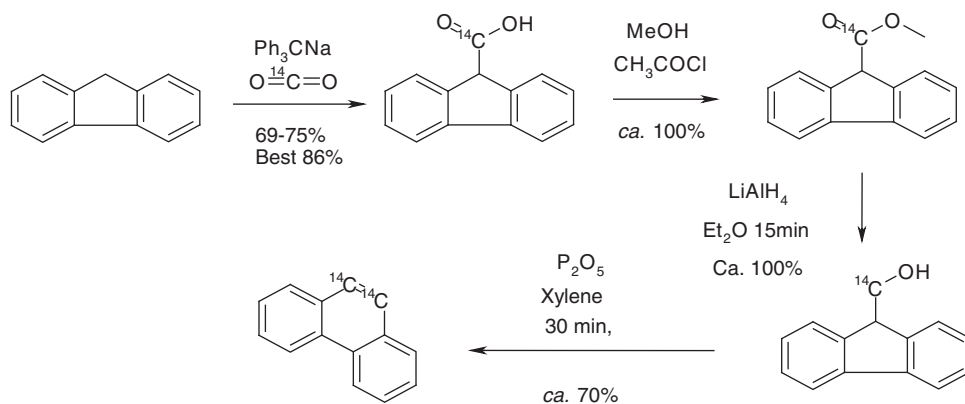


Figure 4. Synthesis scheme for ring B  $^{14}\text{C}$ -labelled phenanthrene.

**Example 4: De novo synthesis planning.** Consider the tumour growth inhibitor below. Ring A is metabolically stable and a labelled compound is needed for metabolic studies and cell uptake work. Hence  $^3\text{H}$ -labelling in ring A is appropriate. This could have been approached from a labelled nitrobenzene (54 hits), an aniline (44 hits) or a nitroaniline (4 hits). The database also returned the possible option of a one-step selective Ir-catalysed exchange tritiation at high specific activity<sup>3</sup> directed by a  $\text{NO}_2$  group. In addition, the database shows the synthesis below which was carried out in 1975 before the advent of Ir catalysis, via the nitroaniline route shown (Figure 5).<sup>4</sup>

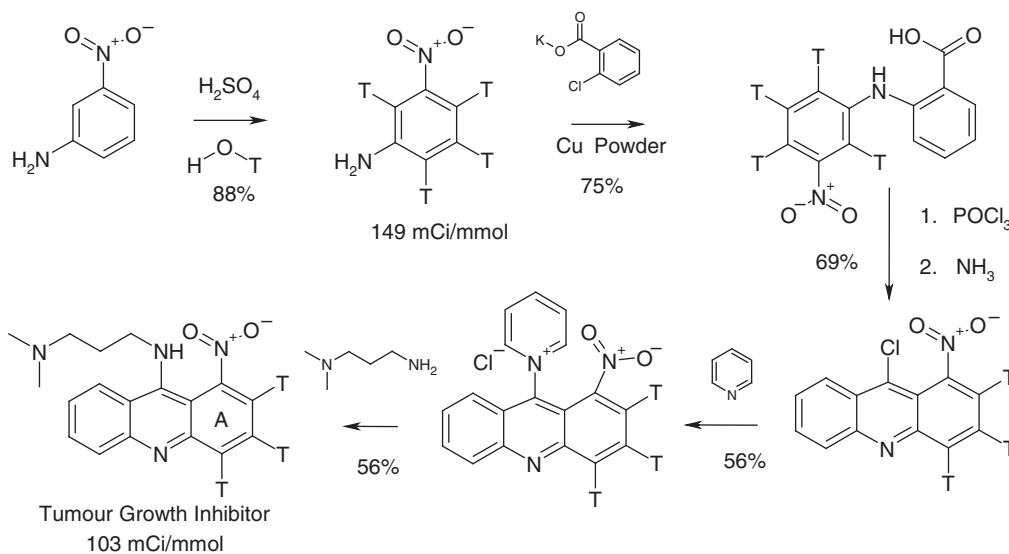


Figure 5. One route to a  $^3\text{H}$ -labelled tumour growth inhibitor.

Since the database is based exclusively on isotopic synthesis, even the most complex multiple searches for the above examples required less than 10 minutes search time.

**Conclusion:** The database is highly focussed on isotopic synthesis and hence offers a quick and complimentary approach to the use of the major search engines. It facilitates rapid synthesis screening, planning and evaluation whilst providing rapid access to common isotopic synthesis intermediates and labelling procedures.

## References

- [1] W. T. Stolle, J. A. Easter, Z. Jian, V. K. Mahindroo, B. D. Maxwell, M. B. Skaddan, *Synth Appl Isotop Labelled Compds, Vol 8, Proc 8th Int Sym 2003* (Eds: D. C. Dean, C. N. Filer, K. McCarthy), John Wiley and Sons Ltd, **2004**, 447–450.
- [2] C. J. Collins, *J. Amer. Chem. Soc.*, **1948**, *70*, 2418.
- [3] M. J. Hickey, L. P. Kingston, W. J. S. Lockley, P. Allen, A. N. Mather, D. J. Wilkinson in *Synth Appl Isotop Labelled Compds, Proc 9th Int Symp, Edinburgh 2006* (Eds: C. L. Willis, W. J. S. Lockley), *J. Label. Compd. Radiopharm.* **2007**, *50*, 286–289.
- [4] A. Kolodziejczyk, A. Arendt, *J. Label. Compd*, **1975**, *11*, 385–394.

ELECTRONIC EFFECTS IN THE *ORTHO*-<sup>2</sup>H-LABELLED ANILIDE SYSTEM

OLIVER R. STEWARD AND WILLIAM J. S. LOCKLEY

Division of Chemistry, Faculty of Health and Medical Sciences, University of Surrey, Guildford, GU2 7XH, UK

**Abstract:** 2-Deuterated anilides demonstrate a significant upfield shift of the remaining 6-proton in their <sup>1</sup>H-NMR spectra. This is occasioned by a preference for the conformation in which the deuterium is adjacent to the anilide carbonyl group. The electronic effects in this system have been investigated by the preparation of a range of structural variants. The results are consistent with a hydrogen-bonding hypothesis but further work is required to investigate alternative explanations.

**Keywords:** [2-<sup>2</sup>H]anilide; conformation; <sup>1</sup>H-NMR; *ortho*-deuterium; isotope-effect

**Introduction:** Deuterium isotope effects on conformation are of interest since they produce unexpected differences in spectroscopic properties between the labelled and unlabelled compound. Conformational changes occasioned by *ortho*-substitution with deuterium or tritium are particularly interesting since the resulting labelled compounds are the products of catalytic *ortho*-directed isotope exchange, a widely-utilised approach for the isotopic labelling of aromatic systems.

A striking conformational effect resulting from a single *ortho*-substitution by deuterium is shown by 2'-deuterated anilides. These compounds show an unusually large shift<sup>1</sup> of the remaining *ortho*-proton (the 6'-proton) in the <sup>1</sup>H-NMR (Figure 1).

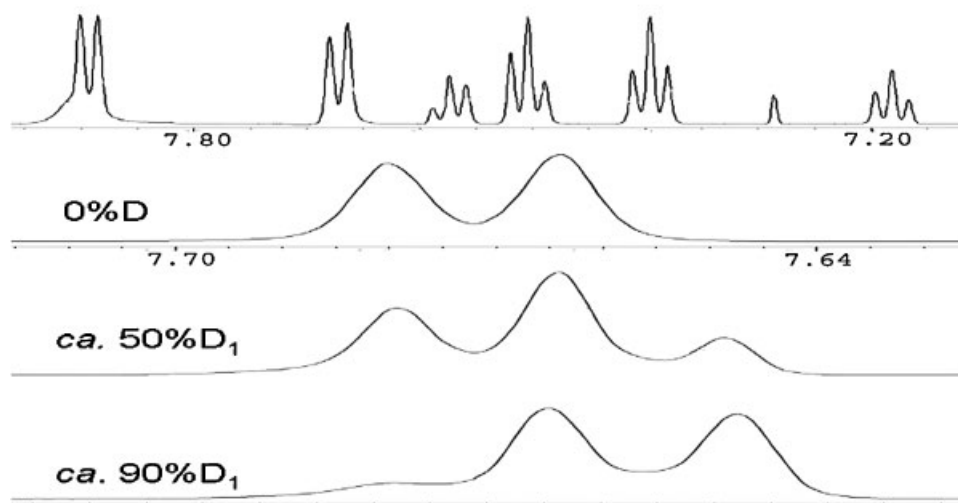


**Figure 1.** <sup>1</sup>H-NMR of benzanilide and of the anilide 6'-proton of benzanilide at various degrees of 2'-deuteration.

It has long been recognised that the deshielding effect of the carbonyl group on the *ortho*-proton affords a sensitive probe into the conformation of 2-substituted anilides about the N-Ar bond.<sup>2,3,4,5</sup> Since conformer **3** (Figure 2) is already known to be strongly preferred over conformer **4**, for R = CH<sub>3</sub> and bulkier substituents, we assume that the above large isotope shift in the NMR of 2-deuterated anilides arises from a slight preference for conformer **1** over conformer **2**.

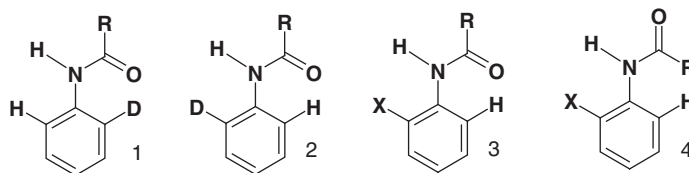


**Figure 2.** Anilide conformers.

Previous NMR results<sup>6</sup> with 2'-deuteroanilides have shown a decrease in  $\Delta H$  between the two conformations with increasing solvent polarity, which argues strongly that electronic factors are important. This brings into question explanations based solely upon reduced steric repulsion between the carbonyl group and the shorter C-D bond. (Figure 3, **5c**).

To explore the issue further we have undertaken an examination of substituent effects in the system by preparation of a range of 2-deuterated anilides in which both the aromatic and the carbonyl substituents possess varying electronic properties.

The *ortho*-deuterium substituents were introduced either by RhCl<sub>3</sub>·3H<sub>2</sub>O catalysed isotope exchange<sup>7</sup> or via deuterodebromination of 2-bromoaniline followed by subsequent *N*-acylation. NMR spectra were then recorded on mixtures of the unlabelled and labelled compounds, enabling measurement of the isotopic shift.

**Results and Discussion:** Variation of the 4-substituent in the aromatic ring shows that distant electron-withdrawing substituents lead to an increase in the isotopic shift (CHO > NO<sub>2</sub> > H > Me > OH > OMe). Conversely, variation of the carbonyl substituent shows that



electron-withdrawing substituents lead to an increase in the shift ( $\text{Me}_2\text{CH} > \text{Et} > \text{tBu} > \text{Me} > \text{CH}_2\text{Cl} > \text{CF}_3 > \text{Cl}_2\text{CH} > \text{CH}_3\text{COCH}_2$ ). However changes in this latter part of the molecule are problematic due to the known intramolecular H-bonding between electronegative substituents and the N-H.<sup>8</sup> Hence, this data in particular needs to be interpreted with care and further studies are indicated.

Previous studies<sup>2,3,4</sup> have ascribed the deshielding of the H6' proton in anilides to hydrogen bonding between the N-H and the 2'-substituent (Figure 3, **5a**). In this case, the interatomic distances and bond angles would seem to render weak H-bonding,<sup>9</sup> interaction unlikely. Nevertheless, the results are consistent with this explanation (acidification of the N-H donor by R' vs competitive H-bonding by electronegative R'' substituents<sup>8</sup>).

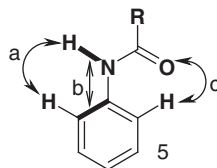


Figure 3. Potential *ortho*-interactions in anilides.

Another explanation involves an anomeric-like interaction (Figure 3, **5b**) between the N-H sigma bond and the antibonding orbital of the adjacent ring C1-C2 bond.<sup>5</sup> Such behaviour has been advanced to account for conformational preferences in anisoles and enol ether methoxy groups. Analysis of the system by a suitable computational chemistry approach will be needed to investigate if the more electronegative 2'-<sup>2</sup>H-substituent would render the N-H/C1-C6 interaction preferable to the alternative N-H/C1-C2 interaction.

It is also clear that the *ortho* D/H atoms are in close proximity<sup>10,12,13</sup> to the carbonyl oxygen (Figure 3, **5c**). If the origin of the effect is indeed electronic rather than steric we might simply ascribe the data from the aromatic substituents to increasing coplanarity<sup>11,12</sup> of the system leading to a greater C=O anisotropic effect on the *ortho* position. However, models suggest that increasing the sp<sup>3</sup> character of the nitrogen results in closer approach of the carbonyl oxygen to the *ortho* proton. Hence carbonyl substituents which stabilise the ketoamine canonical of the amide should increase the effect, as observed, provided the carbonyl/ring coplanarity is unchanged.

## References

- [1] W. J. S. Lockley, R. J. Lewis, D. J. Wilkinson, J. R. Jones, *J. Label. Compd. Radiopharm.* **2005**, *48*, 536–537.
- [2] A. Ribera, M. Rico, *Tetrahedron Lett.* **1968**, 535
- [3] B. D. Andrews, I. D. Rae, B. E. Reichert, *Tetrahedron Lett.* **1969**, 1859–1862.
- [4] G. W. Gribble, P. F. Bousquet, *Tetrahedron*, **1971**; *27*, 3786.
- [5] P. Camilleri, A. J. Kirby, R. J. Lewis, *Chem. Commun.*, **1988**, 1537–1538.
- [6] W. J. S. Lockley, R. J. Lewis, D. J. Wilkinson, J. R. Jones, in *Synth Appl Isotop Labelled Compds, Proc 9th Int Symp, Edinburgh, 2006* (Eds: C. L. Willis, W. J. S. Lockley), *J. Label. Compd. Radiopharm.* **2007**, *50*, 535–536.
- [7] W. J. S. Lockley, *J. Label. Compd. Radiopharm.* **1985**, *22*, 623–630.
- [8] G. Venkateshwarlu, R. P. Padmavathi, B. Subrahmanyam, *Proc. Indian Acad. Sci. Chem. Sci.* **1989**, *101*, 75–82.
- [9] T. Steiner, G. R. Desiraju, *Chem. Commun.*, **1998**, 891–892.
- [10] J. F. Olsen, S. Kang, *Theoret. Chim. Acta (Berl.)*, **1970**, *17*, 329–333.
- [11] R. F. C. Brown, L. Radom, S. Sternhell, I. D. Rae, *Can. J. Chem.*, **1968**, 2577–2587 & D. L. Bate, I. D. Rae, *Aus. J. Chem.* **1974**, *27*, 2611–16.
- [12] S. Ilieva, B. Hadjjeva, B. Galabov, *J. Mol. Struct.* **1999**, *508*, 73–80 & *J. Org. Chem.* **2002**, *67*, 6210–6215.
- [13] W. Caminati, A. Maris, A. Millimaggi, *New Chem. J.*, **2000**, *24*, 821.

## LABELLED QAB149\_ SUPPORTING NEW DRUG DEVELOPMENT

BOHDAN MARKUS, AMY WU, TAPAN RAY, GRAZYNA CISZEWSKA, AND LAWRENCE JONES

DMPK-DMBA-IL - Novartis Biomedical Research Institute, One Health Plaza, East Hanover, NJ 07936, USA

**Abstract:** QAB149 which is indicated for asthma and chronic obstructive pulmonary disease (COPD) was synthesized labeled with tritium (<sup>3</sup>H), carbon-14, and deuterium/carbon 13. These compounds were used for ADME and HADME studies.

**Keywords:** Indacaterol (QAB149); asthma and COPD; tritium (<sup>3</sup>H); stable label [M+4] and carbon-14 label QAB149; ADME and HADME studies

**Introduction:** Indacaterol (QAB149) is a beta -agonist that is indicated for asthma and chronic obstructive pulmonary disease (COPD). Its development started in Novartis in the late 1990s.<sup>1,2,3</sup> The Isotope Lab (IL) contributed to this effort by the synthesis of labeled compounds [<sup>14</sup>C]QAB149, [<sup>3</sup>H] QAB149 and [M+4]QAB149 that were used in preclinical and Human ADME studies (HADME).

**[<sup>3</sup>H]QAB149 synthesis to support early ADME studies (Figure 1)** The quick synthesis and purification of [<sup>3</sup>H]QAB149 that was metabolically stable allowed our ADME colleagues to conduct their studies at an early stage. Also, due to the low dose, <sup>3</sup>H labeled material provided enough sensitivity for sample analysis.

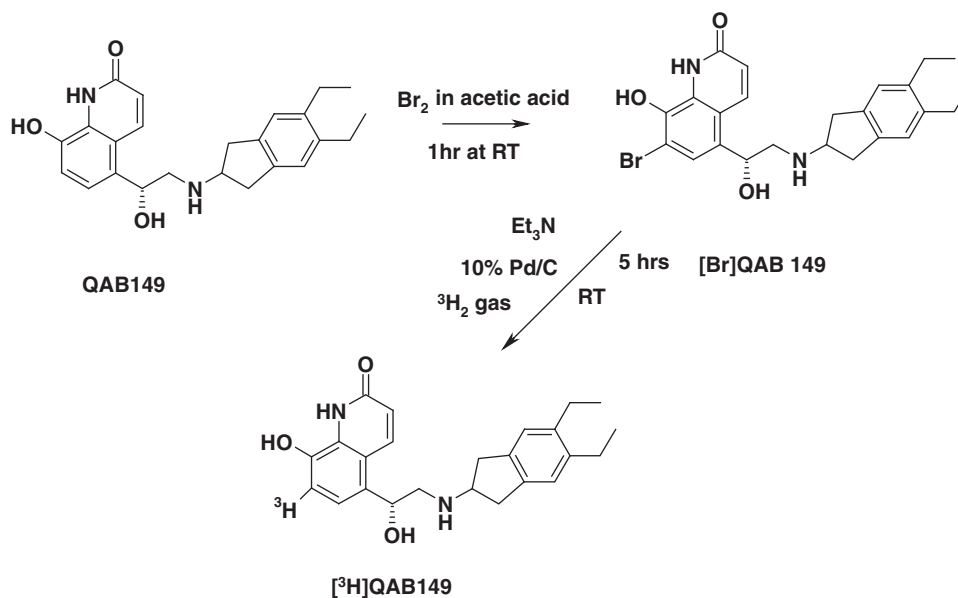
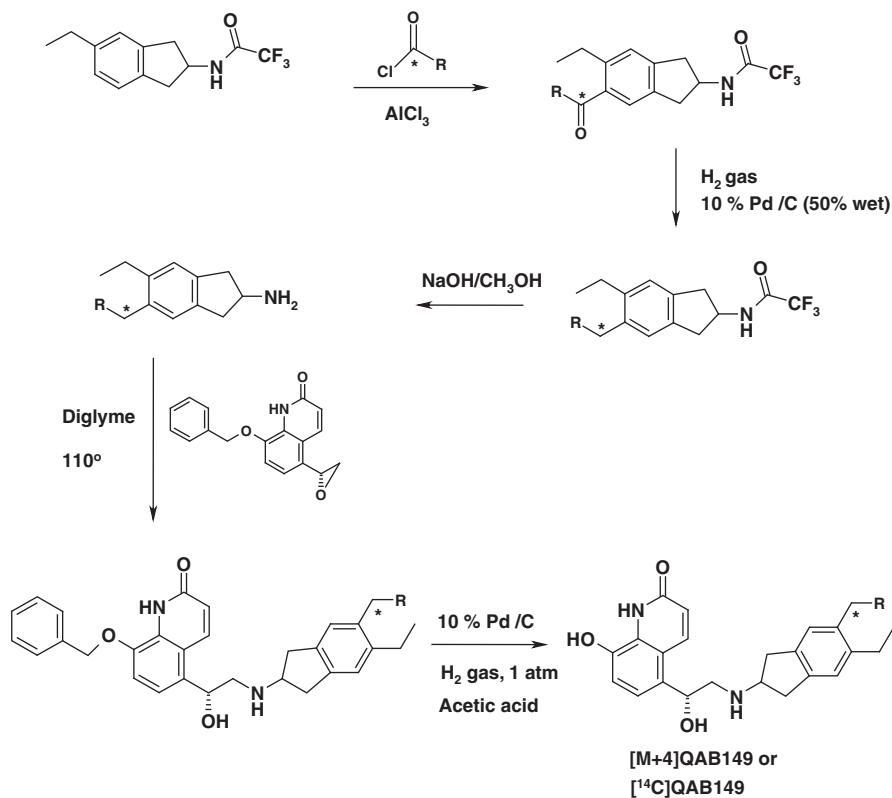


Figure 1. Synthesis of tritiated QAB149.

**[<sup>14</sup>C]QAB149 and [M + 4]QAB149 synthesis to support Human ADME studies and Bioanalytical studies respectively (Figure 2):** As the project moved forward, there was a need to prepare [<sup>14</sup>C]QAB149 to conduct Human ADME study. The original synthetic design involved a 9 step synthesis with low yield that was not sufficient to conduct studies. Subsequently, a new shorter 5 step synthetic route with a higher yield of the carbon-14 labeled product was developed. This same synthetic route was used to synthesize stable labeled product, [M + 4]QAB149.



If R = CD<sub>3</sub> then \* is <sup>13</sup>C in [M + 4]QAB149

If R = CH<sub>3</sub> then \* is <sup>14</sup>C in [<sup>14</sup>C]QAB149

Figure 2. Synthesis of C-14 and stable labeled QAB149.

**Conclusion:** For a low dose compound like QAB149, synthesis with  $^3\text{H}$  label is a good first choice for initial ADME studies because of low cost, fast turn around time and high sensitivity. For advanced ADME/HADME/ Bioanalytical studies various synthetic carbon-14 and stable label labeling techniques were developed, and optimized.

## References

- [1] M. Prashad, B. Hu, D. Har, O. Repic, and T. J. Blacklock. Process R&D, Chemical and Analytical Development, Novartis Pharmaceuticals Corporation, One Health Plaza, East Hanover, New Jersey 07936, U.S.A. Olivier Lohse Process R&D, Chemical and Analytical Development, Novartis Pharma AG, CH-4002 Basel, Switzerland. *Org. Process Res. Dev.*, **2006**, *10*(1), pp 135–141
- [2] B. Cuenoud, I. Bruce, R. Fairhurst, D. Beattie. WO 00/75114, December 14, 2000.
- [3] O. Lohse, C. Vogel. (Novartis AG; Novartis Pharma GmbH). *Process for preparing 5-[(R)-2-(5,6-diethyl-indian-2-ylamino)-1-hydroxyethyl]-8-hydroxy-(1H)-quinolin-2-one salt, useful as an adrenoceptor agonist*. PCT Int. Appl. (2004), WO 2004076422.

## FIRST SYNTHESIS OF [1,3,5- $^{13}\text{C}_3$ ]GALLIC ACID

LAURA J. MARSHALL,<sup>a</sup> KARL M. CABLE,<sup>b</sup> AND NIGEL P. BOTTING<sup>a</sup>

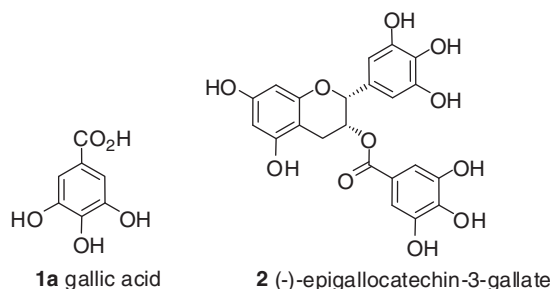
<sup>a</sup>School of Chemistry, University of St Andrews, North Haugh, St Andrews, Fife, KY16 9ST, UK

<sup>b</sup>GSK Medicines Research Centre, Gunnels Wood Road, Stevenage, SG1 2NY, UK

**Summary:** Gallic acid is a phenolic plant metabolite which is normally encountered in plant tissues in ester form. These esters include a group of catechins with antioxidant properties which are found in green tea. Epigallocatechin-3-gallate is the most abundant catechin in green tea and has been shown to inhibit carcinogenesis.<sup>1,2</sup> An efficient and high-yielding synthesis for [1,3,5- $^{13}\text{C}_3$ ]gallic acid from non-aromatic precursors is presented. This will allow compounds such as gallic acid and its derivatives to be used as internal standards for analysis by LC-MS or GC-MS techniques.

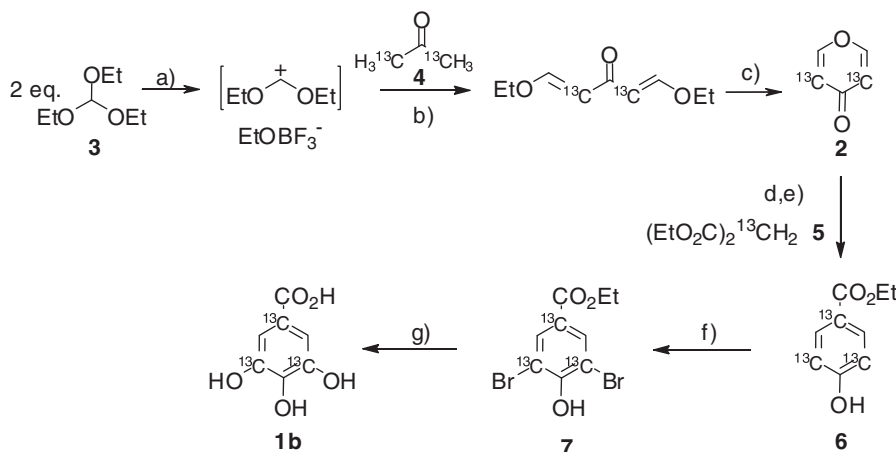
**Keywords:** polyphenol; gallic acid; pyranone; antioxidants

**Introduction:** There is currently a high level of interest in dietary compounds which can have beneficial effects on human health. However, more studies into the biological characteristics and effects of tea catechins must be carried out. These studies require accurate quantification of the compounds in plasma samples which is commonly done by LC-MS and GC-MS analysis due to their ability to separate and quantify subnanomolar quantities of an analyte in complex matrices. However, the sensitivity of the mass spectrometer is not constant and therefore calibration is required using an internal standard. The ideal internal standard would be a stable isotope labelled analogue of the analyte as it will have similar chemical and physical properties to the analyte. New synthetic routes to isotopically labelled catechins are therefore required.



Our aim was to prepare a stable isotope labelled version of gallic acid **1a** for incorporation into tea catechins such as **2**. Previous syntheses include the preparation of deuterium labelled [2,6- $^2\text{H}_2$ ]gallic acid by Tuck *et al.*,<sup>3</sup> and the synthesis of [carboxy- $^{14}\text{C}$ ]gallic acid by Zeng *et al.*<sup>4</sup> and Schildkecht *et al.*,<sup>5</sup> but no ring-labelled  $^{13}\text{C}$  versions had been reported until the work of our group.

**Results and Discussion:** In the context of GC-MS and LC-MS analysis, deuterated phenolic standards are often not suitable, as the deuterium atoms can exchange out of the compound during sample preparation and analysis giving broad MS envelopes.<sup>6,7</sup> In order to avoid these problems, we chose to prepare ring-labelled versions of gallic acid containing multiple  $^{13}\text{C}$ -atoms. The labels are therefore incorporated directly into the backbone of the structure and will not exchange out during preparation or analysis. Our strategy was to construct the aromatic ring using a pyranone intermediate which could be prepared from simple acyclic precursors, consequently removing the need for the use of expensive uniformly labelled aromatic compounds. Our approach allows regioselective placement of  $^{13}\text{C}$ -atoms into the aromatic rings, giving the possibility to prepare a number of isotopomers of gallic acid.



**Scheme 1.** Synthesis of [1,3,5- $^{13}\text{C}_3$ ]gallic acid. Reagents and conditions: (a)  $\text{BF}_3 \cdot \text{OEt}_2$  (6 eq.), DCM; (b)  $i\text{Pr}_2\text{NEt}$  (6 eq.) quant.; (c) EtOH, HCl,  $\text{H}_2\text{O}$ , quant.; (d)  $^t\text{BuOH}$ ,  $\text{KO}^t\text{Bu}$  (1.1 eq.); (e) HCl,  $\text{H}_2\text{O}$ , 74% (f) AcOH, NaOAc,  $\text{Br}_2$  (4.2 eq.) 99% (g) NaOH,  $\text{H}_2\text{O}$ ,  $\text{CuSO}_4 \cdot 5\text{H}_2\text{O}$  (0.6 eq.), 48%.

An efficient and high-yielding synthesis of [1,3,5- $^{13}\text{C}_3$ ]gallic acid **1b** from non-aromatic precursors was developed (**Scheme 1**).<sup>8</sup> [3,5- $^{13}\text{C}_2$ ]4H-Pyran-4-one **2** was first prepared from the reaction between triethyl orthoformate **3** and [1,3- $^{13}\text{C}_2$ ]acetone **4**.<sup>9</sup> The third  $^{13}\text{C}$ -atom was introduced into the ring by reaction of the pyranone **2** with diethyl [2- $^{13}\text{C}$ ]malonate **5**.<sup>10,11</sup> The resulting ethyl 4-hydroxy-[1,3,5- $^{13}\text{C}_3$ ]benzoate **6** was brominated in the 3- and 5-positions to give ethyl 3,5-dibromo-4-hydroxy-[1,3,5- $^{13}\text{C}_3$ ]benzoate **7**. Subsequent hydrolysis of the ester and substitution of the bromine atoms with hydroxyl groups was achieved under basic conditions in a single step to yield the desired [1,3,5- $^{13}\text{C}_3$ ]gallic acid **1b**. Purification was only required at the final stage of the synthesis, thus reducing the amount of losses of labelled material. The synthesis of [2,6- $^{13}\text{C}_2$ ]4H-pyran-4-one was also carried out using triethyl [ $^{13}\text{C}$ ]orthoformate and unlabelled acetone to demonstrate the potential of the methodology for the regioselective placement of  $^{13}\text{C}$ -atoms into the ring.

**Conclusion:** A fast, efficient and high yielding route to [1,3,5- $^{13}\text{C}_3$ ]gallic acid has been developed starting from commercially available  $^{13}\text{C}$ -labelled acyclic building blocks. The route allows the regioselective placement of  $^{13}\text{C}$ -atoms within the aromatic ring.

**Acknowledgements:** Financial support from the BBSRC and GlaxoSmithKline is gratefully acknowledged.

## References

- [1] J. A. Joule, G. F. Smith, *Heterocyclic Chemistry*; 2<sup>nd</sup> Edition ed.; Van Nostrand Reinhold (UK): Wokingham, 1987.
- [2] L. Li, T. H. Chan, *Org. Lett.* **2001**, *3*, 739–741.
- [3] K. L. Tuck, H. W. Tan, P. J. Hayball, *J. Labelled Compd. Radiopharm.* **2000**, *43*, 817–823.
- [4] W. Zeng, Y. H. Heur, T. H. Kinstle, G. D. Stoner, *J. Labelled Compd. Radiopharm.* **1992**, *29*, 657–666.
- [5] H. Schildknecht, R. Milde, *Carbohydr. Res.* **1987**, *164*, 23–31.
- [6] D. B. Clarke, A. S. Lloyd, M. F. Oldfield, N. P. Botting, P. W. Needs, H. Wiseman, *Anal. Chem.* **2002**, *309*, 158–172.
- [7] K. Wähälä, S. Rasku, K. J. Parikka, *J. Chromatogr. B.* **2002**, *777*, 111–122.
- [8] L. J. Marshall, K. M. Cable, N. P. Botting, *Org. Biomol. Chem.* **2009**, *7*, 785–788.
- [9] D. Hobuss, S. Laschat, A. Baro, *Synlett.* **2005**, 123–124.
- [10] J. Beyer, S. Lang-Fugmann, W. Steglich, *Synthesis* **1998**, 1046–1051.
- [11] M. Lang, S. Lang-Fugmann, W. Steglich, *Org. Synth.* **2002**, *78*, 113–122.

## A GENERAL METHODOLOGY FOR THE SYNTHESIS OF SUBSTITUTED PHENOLS FROM PYRANONE PRECURSORS

LAURA J. MARSHALL,<sup>a</sup> KARL M. CABLE,<sup>b</sup> AND NIGEL P. BOTTING<sup>a</sup>

<sup>a</sup>School of Chemistry, University of St Andrews, North Haugh, St Andrews, Fife, KY16 9ST, UK

<sup>b</sup>GSK Medicines Research Centre, Gunnels Wood Road, Stevenage, SG1 2NY, UK

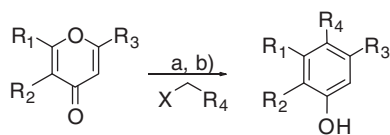
**Summary:** Phenols are an important group of organic compounds,<sup>1</sup> with many natural products such as polyketides, coumarins and flavonoids containing mono- or poly-phenolic moieties. The synthesis of substituted phenols from pyranone precursors is presented. A variety of pronucleophiles were used in combination with *tert*-butanol as solvent and potassium *tert*-butoxide as base, using both conventional heating methods and microwave conditions.

**Keywords:** phenol; pyranone; maltol; chelidonic acid; pronucleophile

**Introduction:** Commonly employed methods for phenol synthesis include the displacement of aromatic halides, Bayer-Villiger oxidation, the hydrolysis of diazonium salts, and, more recently the catalytic C-H activation/borylation/oxidation.<sup>2,3</sup> An alternative strategy involves the construction of the aromatic ring from acyclic precursors with the substituents already in place, therefore overcoming problems such as the formation of isomeric mixtures through direct introduction of ring substituents.<sup>4</sup> This type of methodology is important in the potential application for the preparation of isotopically labelled compounds. The number of commercially available [<sup>13</sup>C]-labelled benzene derivatives is relatively small. They are often only available in uniformly ring-labelled form and tend to be expensive. New methods for construction of benzene derivatives from non-aromatic precursors with regioselective placement of isotopes within the ring are therefore potentially useful.

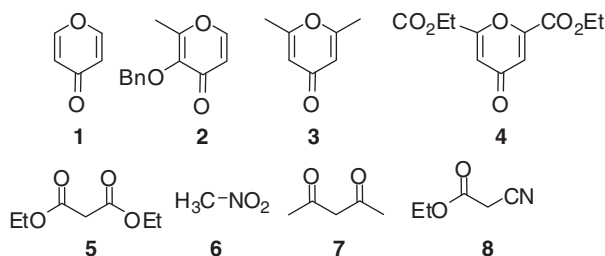
Another strategy is the synthesis of aromatic compounds from heterocycles which undergo either an extrusion process or a rearrangement. In this approach the substituents present in the heterocycle are incorporated into the aromatic product in a regioselective manner. Heterocyclic systems such as pyranones are an excellent source of phenols, as they are susceptible to nucleophilic attack followed by hydrolysis to yield aromatic compounds. Our aim was therefore to utilise various substituted pyranones and pronucleophiles in the synthesis of substituted phenols.

**Results and Discussion:** The syntheses of various substituted phenols from pyranone precursors, namely 4*H*-pyran-4-one **1**, 3-(benzyloxy)-2-methyl-4*H*-pyran-4-one (*O*-benzyl maltol) **2**, 2,6-dimethyl-4*H*-pyran-4-one **3** and diethyl 4-oxo-4*H*-pyran-2,6-dicarboxylate (diethyl chelidonate) **4** have been examined (**Schemes 1** and **2**). These syntheses employ the use of our developed methodology, reacting the pyranone with a variety of pronucleophiles in the presence of potassium *tert*-butoxide as base and *tert*-butanol as solvent, using conventional heating methods.<sup>5,6,7</sup> The pronucleophiles used were diethyl malonate **5**, nitromethane **6**, acetylacetone **7** and ethyl cyanoacetate **8** (**Scheme 2**). During the second stage of the reaction (reflux in aqueous acid), one portion of the pronucleophile is lost. This is followed by aromatisation to give the *para*-substituted phenol. In the case of unsymmetrical pronucleophiles **6** and **8**, the methylene and ester group respectively are lost during this stage to give the nitro and nitrile products.



X = leaving group  
a: <sup>t</sup>BuOH, KO<sup>t</sup>Bu, reflux  
b: 2M HCl, reflux 1h

**Scheme 1.** General reaction scheme.



**Scheme 2.** Pyranones and pronucleophiles used in the reactions.

Under conventional heating methods a range of reaction conditions were studied for each pyranone-pronucleophile combination. Reaction times, equivalents of base and equivalents of pronucleophile were varied during the study. The most successful conditions are outlined in Table 1 below. A range of yields from 2 to 95% were observed, with the substituted pyranones giving the poorest yields – most likely due to deprotonation of the methyl groups<sup>8,9</sup> on compounds **2** and **3** consuming the base and causing side-reactions to occur. All reactions with the unsubstituted pyranone **1** gave excellent yields.

The use of microwave irradiation was found to be beneficial to many of these reactions. Once again, a range of conditions were studied, and the most successful outlined in Table 1. Higher yields were observed in the majority of cases – most importantly in those reactions which proved to be the most problematic under conventional heating. This may be due to the shorter reaction times preventing side-reactions taking place.

**Conclusion:** We have explored the scope of the base-catalysed reaction of pyran-4-ones with a range of carbon nucleophiles for the synthesis of phenols. Under conventional heating methods, the most successful results were obtained with 4*H*-pyran-4-one **1** and *O*-benzyl maltol **2**. Limited success was achieved with 2,6-dimethyl-4*H*-pyran-4-one **3** and diethyl chelidonate **4**. The use of microwave irradiation accelerated the reactions, and in the majority of cases substantial improvements in yield were observed.

**Acknowledgements:** Financial support from the BBSRC and GlaxoSmithKline is gratefully acknowledged.

**Table 1.** Reaction conditions and results for microwave-assisted reactions, including comparison with yields obtained using conventional heating methods

Pyranone	Pronucleophile	Conventional Heating				Microwave-Assisted				
		Eq. base	Eq. proN	Time (h)	Yield (%)	Eq. base	Eq. proN	Time (min)	Temp (°C)	Yield (%)
1	5	1.3	1.0	3	94	1.1	1.1	30	120	67
	6	1.1	1.1	5	80	1.1	1.1	15	120	80
	7	2.0	2.0	20	95	2.0	1.1	30	150	57
	8	3.0	1.6	27	78	3.0	1.6	30	150	86
2	5	3.0	1.6	47	73	2.3	1.6	30	120	99
	6	2.3	1.6	44	20	3.0	1.6	30	120	53
	7	2.3	1.6	42	10	2.3	1.6	30	150	86
	8	3.0	1.6	47	93	2.3	1.6	30	120	99
3	5	3.0	1.6	44	18	2.0	1.6	30	150	81
	8	3.0	1.6	47	57	2.0	1.6	30	120	47
4	6	3.0	1.1	24	46	2.3	1.6	30	120	48
	7	3.0	1.1	24	2	2.3	1.6	30	120	35

## References

- [1] J. H. P. Tyman, *Synthetic and Natural Phenols*; Elsevier: New York, 1996.
- [2] C. A. Fyfe, In *The Chemistry of the Hydroxyl Group*; Patai S Ed; Wiley Interscience: New York, 1971, **Vol 1**, 83–127.
- [3] R. E. Maleczka, F. Shi, D. Holmes, M. R. Smith, *J. Am. Chem. Soc.* **2003**, *125*, 7792–7793.
- [4] F. Bamfield, F. Gordon, *Chem. Soc. Rev.* **1984**, *13*, 441–448.
- [5] L. J. Marshall, K. M. Cable, N. P. Botting, *Org. Biomol. Chem.* **2009**, *7*, 785–788.
- [6] J. Beyer, S. Lang-Fugmann, A. Muhlbauer, W. Steglich, *Synthesis* **1998**, 1046–1051.
- [7] M. Lang, S. Lang-Fugmann, W. Steglich, *Org. Synth.* **2002**, *78*, 113–122.
- [8] F. G. West, P. V. Fisher, C. A. Willoughby, *J. Org. Chem.* **1990**, *55*, 5936–5938.
- [9] F. G. West, C. M. Amann, P. V. Fisher, *Tetrahedron. Lett.* **1994**, *35*: 9653–9656.

## SYNTHESIS OF N-PHENYLSUCCINIMIDE-T<sub>2</sub>, 1,4-DIPHENYLBUTANE-T<sub>8</sub> AND 1,4-DIPHENYL-2-BUTENE-T<sub>6</sub>

### C. POSTOLACHE AND LIDIA MATEI

National Institute of Research and Development for Physics and Nuclear Engineering 'Horia Hulubei', Street Atomistilor 407, Magurele, Bucharest, Romania

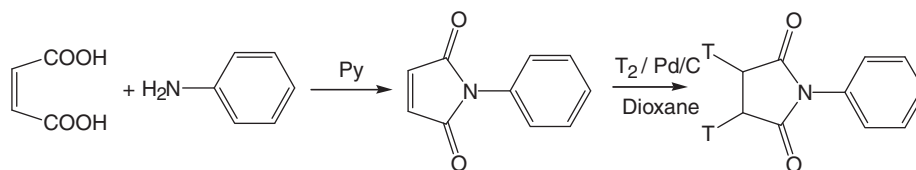
**Abstract:** N-phenylsuccinimide, 1,4-diphenylbutane and 1,4-diphenyl-2-butene labeled with tritium have been obtained by catalytic hydrogenation with T<sub>2</sub>(g) of unsaturated derivatives (N-phenyl maleimide, 1,4-diphenylbutan-1,3-diyne). The stability of labeled compounds has been analyzed by determination of radioactive emission and by quantum-chemical studies. Tritium labeled compounds were used in producing of surface and radioluminescent sources

**Keywords:** tritium; labeled compounds; self radiolysis; quantum-chemical simulations

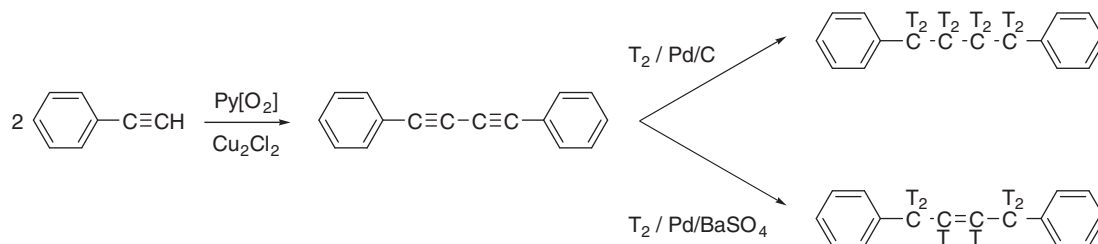
**Introduction:** Polymers labeled with tritium are used in production of radioluminescent and surface sources. The synthesis of labeled polymers is difficult and occurs with low reaction yield. The paper describes the experimental results obtained in the synthesis of tritium labeled compounds with low molecular weights and high specific activities. The synthesized products are stable and have been used in obtaining of radioluminescent<sup>1</sup> and surface sources.

**Material and Methods: Synthesis of the Labeled Compound.** The N-phenylsuccinimide (NPSI) labeled with tritium has been obtained by catalytic hydrogenation of N-phenylmaleimide (NPMI) using T<sub>2</sub> and Pd/C as catalyst (Scheme 1). The labeled compound was purified by TLC using Silica GF<sub>254</sub> and a mixture of benzene: acetone 4:1 v/v. NPMI was synthesized by condensing maleic anhydride with aniline in pyridine. The crude product was purified by double crystallization from cyclohexane.

Labeled 1,4-diphenyl butane (DPB) and 1,4-diphenyl, 2-butene (DPBE) were obtained by hydrogenation using 1,4-diphenylbutane-1,3-diyne (DPBDI) as a substrate and T<sub>2</sub> (g). The reaction was conducted using Pd/C and Pd/BaSO<sub>4</sub> as catalytic support and cyclohexane as solvent (Scheme 2).



**Scheme 1.** Reaction path for synthesis of tritiated NPSI.



**Scheme 2.** Reaction path for the synthesis of DPB and DPBE.

DPBDI was obtained by oxidative condensation of phenyl acetylene in pyridine in presence of  $O_2$  using  $Cu_2Cl_2$  as a catalyst. The crude product was purified by double crystallization from methanol and ether. The purified product was characterized by the determination of the melting point, FTIR and TLC analysis. The raw labeled products were purified by preparative TLC using RP-18  $F_{254}$  plates and cyclohexane: methanol: benzene (12:1:1 v/v/v). The products were characterized by determination of radioactive and chemical amounts, radiochemical purity and specific activities. The stability of the labeled compounds was evaluated by the analysis of radioactivity decay and by quantum-chemical studies.

**The Study of Radioactivity in the Composite Materials.** Each solution of 250 mL NPSI- $T_2$ , 225 mL DPB- $T_8$ , and 245 mL DPBE- $T_6$  were mixed with 1 mL solution of 1% polystyrene in benzene. The specific activities obtained were about 9250 GBq/g. The final solutions were used for obtaining of radioluminescent composite material with a specific activity of 74 GBq/g. Samples of 100 mg from each composite material were introduced into sealed glass vials and stored for 1 year. After the storage period, the vials were combusted and the tritiated water collected<sup>2</sup>. The tritiated water retained in the traps was diluted with distilled water. The radioactivity was measured by Liquid Scintillation Counting using a TRICARB TR 2800 counter. Radioactive emissions in composite materials were analyzed also by quantum chemical simulation<sup>3</sup>.

**Results: Synthesis of N-phenylmaleimide.** 7.24 g of NPMI (m. p. 85–90°C) was prepared in 82% yield. After purification 5.51 g of product (m. p. 90°C) was recovered.

**Synthesis of DPBDI, DPB and DPBE.** By oxidative condensation of phenylacetylene 9.03 g of crude DPBDI (m.p 86–88°C) was obtained. The product was purified by double crystallization producing 5.6 g of purified product ( $R_f = 0.82$ , m.p. = 88°C).

1.1 g of unlabeled DPB was obtained by hydrogenation of 1.05 g DPBDI. After purification by double crystallization from chloroform producing 0.85 g of pure product ( $R_f = 0.92$ , m.p. 52°C). Unlabeled DPBE was obtained by controlled hydrogenation of 2.5 g DPBDI. After purification by column chromatography 1.9 g of pure product ( $R_f = 0.85$ , m.p 145°C) was obtained.

**Synthesis of NPSI- $T_2$ , DPB- $T_8$  and DPBE- $T_6$ .** The radioactive concentration, chemical concentration and radiochemical purity were determined for labeled NFSI, DPB and DPBD after TLC purification. The obtained results are presented in Table 1

**Study of Radioactive Emissions in Composite Materials.** The results are in concordance with radiochemical yields (G) obtained by simulation using quantum-chemical methods as shown in Table 2.

	NPSI	DPB	DPBE
Radioactivity of purified product [GBq]	11.688	86.950	68.820
Radiochemical purity of purified product [%]	98	97	97
Radioactive concentration [MBq/mL]	37	41	38
Specific activity [MBq/mg]	11935	41000	38000
Specific activity [GBq/mmol]	2089	8610	7904

Compound	$\Lambda_{\text{sample}}$ [MBq]	$\Lambda_{\text{sp}}$ Polymer:Labeled compound [GBq/g]	$\Lambda_{\text{sp}}$ RL pigment [GBq/g]	$\Delta\Delta/\Lambda_{\text{sample}}$ [%]	G
PS : NPSI- $T_2$	4037	9250	74	4.24	0.011
PS : DPB- $T_8$	4314	9250	74	5.93	0.017
PS : DPBE- $T_6$	4492	9250	74	4.90	0.017
Polystyrene- $\alpha,\beta$ - $T_2$	–	6700–7400	37	4–4.5[4]	0.009

The relative percentage of decreasing activities is between 4.2 and 6%, relatively similar with percentage obtained for tritiated polystyrene (4–4.5 %).<sup>4</sup> The decreased stability comparing with tritiated polystyrene is compensated by higher specific activities of the mixture of labeled compounds in polystyrene.

**Conclusions:** N-phenylsuccinimide, 1,4-diphenylbutane and 1,4-diphenyl-2-butene labeled with tritium have been synthesized by catalytic hydrogenation of N-phenylmaleimide and 1,4-diphenylbutan-1,3-diyne respectively. The stability of the labeled compounds was analyzed by the determination of the emissions of tritium from composites of polystyrene with the labeled compound. The results obtained by simulation of fundamental radiolytical processes have been correlated with experimental values.

N-phenylsuccinimide is the most stable compound. The relative activity loss was 4.25%. Experiments have been correlated with data obtained by simulation. In the case of 1,4-diphenyl-2-butene-T<sub>6</sub> the simulation revealed the stability to be similar with 1,4-diphenylbutane-T<sub>8</sub>. The experimental values suggest a high stability of 1,4-diphenyl-2-butene-T<sub>6</sub> in relationship with 1,4-diphenylbutane-T<sub>8</sub>. Only external radiolytical effects have been analyzed by simulation. The high specific activity of tritiated compounds and their high stability toward self radiolysis allowed them to be used as an active component in radioluminescent and standard surface sources. N-phenylsuccinimide-T<sub>2</sub> is recommended for use because it is obtained in high yields and is stable towards radiolysis.

## References

- [1] US Department of Energy. 'Radioluminescent Lighting Technology'. Proceeding of Technology Transfer Conference (U.S.), 1990, Annapolis, Md., Publ. The Office; Springfield. VA. Washington. DC.
- [2] C. Postolache, L. Matei, R. Georgescu *J. of Radioanal. and Nuclear Chemistry*, **2009**, 280, 2, 251–258.
- [3] C Postolache, L. Matei, *Radiation Physics and Chemistry*, **2007**, 76, 1267–1271.
- [4] K. Krejci and A. Zeller Jr, *Tritium pollution in the Swiss luminous compound industry in Proceedings of the International Symposium on the Behaviour of Tritium in the Environment. Vienna, IAEA, 1979*, SM 232, 65–78.

## SYNTHESIS OF E27-5 CLASS NUCLEOSIDE ANALOGUE BY ISOTOPE EXCHANGE TECHNIQUE

C. POSTOLACHE,<sup>a</sup> C. TANASE,<sup>b</sup> LIDIA MATEI,<sup>a</sup> AND G BUBUEANU<sup>a</sup>

<sup>a</sup>Horia Hulubei' National Institute for Physics and Nuclear Engineering 407 Atomistilor st., Magurele, ILFOV 007125, ROMANIA

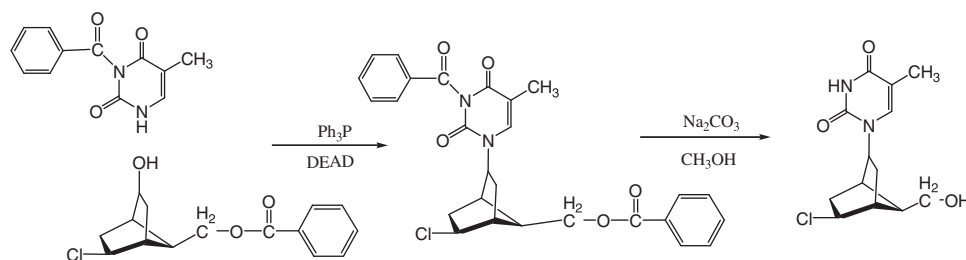
<sup>b</sup>National Institute of Chemical and Pharmaceutical Researches Calea Vitan 112, sector 3, Bucharest, ROMANIA

**Abstract:** The development of new drugs with antitumor and antiviral activity that exhibit greater efficacy, more favorable toxicity profiles less-susceptible to cross-resistance requires the synthesis of new biologically active nucleoside analogues, modified at the base or more frequently at the sugar moiety. E27-5-T and E27-5-FU derivatives have been obtained using the Vorbruggen method. The new nucleoside showed good biological activity.

The labelling was completed by isotopic exchange with Pd/C (10%) as the catalyst and dioxane in the presence of phosphate buffer. The labeled compounds were purified by TLC chromatography.

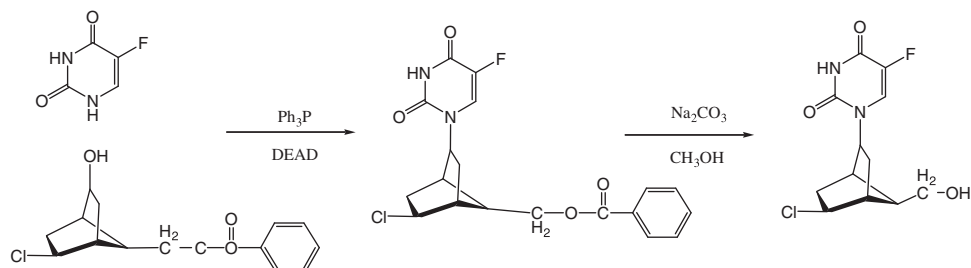
**Keywords:** Tritium; labelled compounds; nucleoside analogues; antitumor; antiviral

**Introduction:** In the present paper we explored the synthesis of new biologically active nucleoside analogues, modified at the sugar moiety. An important number of new nucleoside analogues in which the glycoside radical was replaced by a structural fragment bicyclo [2.2.1] heptane (E275 class)<sup>1</sup> were synthesized. The bicyclo [2.2.1] heptane fragment was coupled to the nucleoside group using the Mitsunobu<sup>2,3</sup> respectively Vorbruggen<sup>4,5</sup> method. The antitumor activity of the new nucleoside analogues was tested. Two compounds with potentially antitumor activity were selected: 11-(5-Chloro-7-hydroxymethyl-bicyclo[2.2.1]hept-2-yl)-5-methyl-1H-pyrimidine-2,4-dione (E27-5-T) (Scheme 1) and 1-(5-Chloro-7-hydroxymethyl-bicyclo[2.2.1]hept-2-yl)-5-fluoro-1H-pyrimidine-2,4-dione (E27-5-FU) (Scheme 2).



**Scheme 1.** Reaction path for the synthesis of E27-5-T.





**Scheme 2.** Reaction path for the synthesis of E27-5-FU.

### Experimental: The synthesis of E-27-5-T and E27-5-FU

Both E27-5 nucleosides were synthesized using a Mitsunobu reaction of bicyclo [2.2.1] heptane alcohol with N-benzoylthymine or 5-F-Uracyl with diethylazodicarboxylate and triphenylphosphine (Schemes 1 and 2).

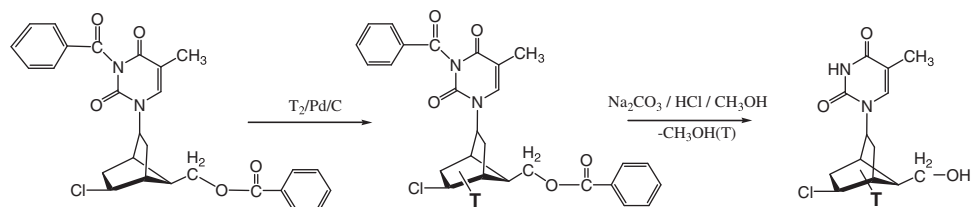
The synthesized compounds were characterized by TLC, FTIR –ATR (FTIR ATR spectrometer Bruker type TENSOR 27) and by  $^1\text{H-NMR}$ , and  $^{13}\text{C NMR}$  (Varian Gemini 300 BB (300 MHz for  $^1\text{H}$ , 75 MHz for  $^{13}\text{C}$  and UNITY 400 PLUS (400 MHz for  $^1\text{H}$ , 100 MHz for  $^{13}\text{C}$ ).

### The synthesis of E27-5-T-T(G) and E27-5-FU-T(G).

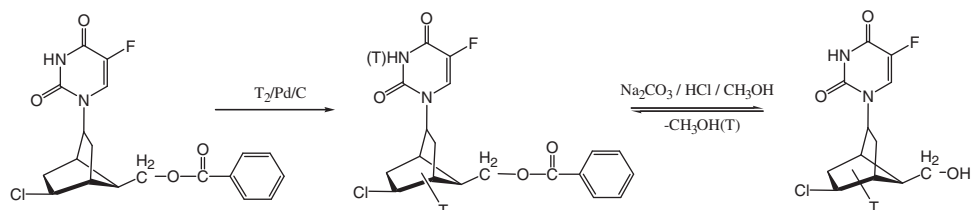
Synthesis of E27-5-T-T(G) and E27-5-FU-T(G) was completed by isotopic exchange with heterogenous catalysis. Two labelling systems were used:

(a) Pd/BaSO<sub>4</sub> (10%) as catalyst, dioxane: ethanol: phosphate buffer (10:5:1 v/v/v) as solvent mixture and T<sub>2</sub> obtained by desorbition from U-bed. The reaction time was 20 hrs.

(b) Pd/C (10%) as catalyst, dioxane: ethanol: acetic acid (10:10:0.1 v/v/v) as solvent mixture and a mixture of T<sub>2</sub>:<sup>3</sup>He obtained from of expired radioluminescent sources<sup>6</sup>. The reaction time was 42 hrs. Benzoate group protected substrates were used (Schemes 3 and 4).



**Scheme 3.** Reaction path for synthesis of tritiated E27-5-T.



**Scheme 4.** Reaction path for synthesis of tritiated E27-5-FU.

Labile tritium was removed by rotary evaporation using methanol as a solvent.

The benzoate groups were removed by hydrolysis on a methanolic K<sub>2</sub>CO<sub>3</sub>. Progress of the reaction was followed by TLC (Silica GF<sub>254</sub> and a mixture hexane: ethyl acetate: acetic acid 5:2:0.1 as mobile phase) R<sub>f</sub> = 0.41 (benzoate E27-5-FU) and 0.58 (E27-5-FU) R<sub>f</sub> = 0.38 (benzoate E-27-5-T) and 0.52 (E27-5-T). The labelled compounds were purified by TLC chromatography using the chromatographic system presented above. The purified labelled compounds were characterized by LSC (Liquid Scintillation Counter TRICARB 2800TR PE), UV (UV VIS SPECTROCORD 210 ANALYTIC JENA) and TLC/Rad (Scanner LB 2723 Berthold).

**The synthesis of E-27-5-T and E-27-5-FU:** After purification by flash chromatography 630 mg (E27-5-FU) (yield 26.42%, m.p. 101.2–102.8°C) and 360 mg E275-T (yield 31,54% and m.p. = 97.4–105.8°C) were obtained.

**E-27-5-FU:**  $^1\text{H-NMR}$ -(400 MHz, DMSO-d<sub>6</sub>,  $\delta$  ppm, J Hz): **8.33** (d, 1H, H-6', 2.7); **8.30**(s, 1H); **4.83** (d, 0.5H, H-5, 4.8); **4.60** (d, 0.5H, H-5, 4.6); **4.52** (broad s, OH); **4.07** (m, 1H, H-5); **3.73** (dd, 1H, H-8, 4.3, 11.2); **3.66** (dd, 1H, H-8, 6.0, 11.2); **2.56** (d, 1H, H-4, 4.3); **2.36** (dd, 1H, H-1, 4.5; 10.9) [or 2.38(d, 0.5H, 4.5); 2.35 (d, 0.5H, 4.7)]; **2.22-2.16** (m, 1H, H-7, 6.0, 4.3); **2.15-2.06** (m, 1H, H-3, 14.2); **2.03-1.87** (m, 2H, H-3-6); **1.58** (m, 1H, H-6, 14.1).  $^{13}\text{C-NMR}$ -100MHz (DMSO,  $\delta$  ppm): **158.81** (C4'); **158.24**; **158.12** (C-, J = 11.4); **140.03**; **143.83** (C-); **143.72**; **141.23** (d, J = 249, C-); **78.64**; **78.46** (C-5), **60.14**; **59.90**(CH-Cl); **58.42**; **58.31** (C-8), **50.29**; **50.17** (CH, C-7), **45.87**; **45.80** (CH, C-1); **43.35** (CH, C-4), **38.33** (CH<sub>2</sub>, C-6), **35.57**; **35.35** (CH<sub>2</sub>, C-3).

**E-27-5-T:**  $^1\text{H-NMR}$  (400 MHz,  $\text{DMSO-d}_6$ ,  $\delta$  ppm, J Hz): **8.08**(s, 1H, H-6'); **4.80**(dd, 0.5H, H-5, 2.5, 7.0); **4.64**(dd, 0.5H, H-5, 2.5, 6.8); **4.05**(q, 1H, H-2, 7.0); **3.73**(dt, 1H, AB syst., H-8, 9.1, 10.7); **3.66**(dd, 1H, H-8, 5.5, 10.7), **2.38**(dd, 1H, H-4, 4.8, 11.3) [2d :2.39(d, 0.5H, 4.8); 2.36(d, 0.5H, 4.6)]; **2.25-2.19**(m, 1H, H-1 or H-7, 4.7); **2.14**(dt, 1H, H-3, 8.0, 14.9); **2.04-1.98**(m large, 1H, H-7 or 1, 4.5, 8.1); **1.985**(2s,  $\text{CH}_3$ ); **1.91**(ddd, 1H, H-3, 7.2, 10.2, 13.8); **1.56**(broad t, 1H, H-6, 13.3), **1.19**(t, 1H, H-6, 7.1).  $^{13}\text{C-NMR}$ -(100MHz,  $\text{CDCl}_3$ ,  $\delta$  ppm); **167.87**(C4'); **162.48**(CO-2') **157.60**(CH, C-6'); **110.53**(CH, C-5'); **77.54; 77.11**(C-5); **60.48; 60.19**(CH-Cl); **58.47; 58.36**(C-8), **50.16**(CH, C-7), **45.90; 45.74**(CH, C-1); **43.38**(CH, C-4), **38.43**( $\text{CH}_2$ , C-6), **35.67; 35.51**( $\text{CH}_2$ , C-3); 14.52; 11.39( $\text{CH}_3$ ).

**The synthesis of E27-5-T-T(G) and E27-5-FU-T(G):** Solutions from labelling reactions were diluted to a volume of 30 ml and the total activities were measured by LSC. The values of initial activities (Table 1) indicate a low grade of isotopic exchange in the case of use of the (b) labelling system. After purification the labelled compounds were characterized for radioactive concentration, chemical concentration and radiochemical purity and are shown in Table 1.

	E27-5-T-T(G)		E27-5-FU-T(G)	
	$T_2$	Mixture $T_2 : ^3\text{He}$	$T_2$	Mixture $T_2 : ^3\text{He}$
Radioactivity of mixture reaction [TBq]	116.55	36.26	105.08	30.34
Radioactivity of purified product [MBq]	1610	120	1340	86
Radiochemical purity of purified product [%]	98	~95	97	~95
Radioactive concentration [MBq/ml]	34	14	34	11
Chemical concentration [mg/ml]	0.029	0.162	0.038	0.183
Specific activity [GBq/mmol]	334	25	258	17

**Conclusions:** In case of isotopic exchange labelling technique the radioactivity of crude product is over 10 times lower than in case of using the recovered tritium as labelling agent. Also, the mass and specific activities are more than 10 times lower. The obtained results reveal the inhibitory effect of  $^3\text{He}$  over the catalytic system. For this reason, the use of tritium recovered from the process of treatment of radio luminescent sources without previous removal of  $^3\text{He}$  from the system, is not recommendable in synthesis of labelled compounds by catalyzed isotopic exchange technique. In case of labelling reaction by chemical synthesis, the inhibitory effect did not affect the mass and specific activities of labelled compounds<sup>6</sup>.

**Acknowledgments:** Authors express their personal gratitude to John Wiley & Sons, Ltd. for awarding of present work at the 10<sup>th</sup> International Symposium on the Synthesis and Applications of Isotopes and Isotopically Labelled Compounds held in June 14-18<sup>th</sup>, 2009 in Chicago, Illinois, USA

## References

- [1] C. Tanase, G. Manda, F. G. Cocu, M. T. Caproiu, C. Draghici, M. Neagu, C. Constantin, I. Neagoe and R. Haita, *BIT's 6<sup>th</sup> Annual Congress of International Drug Discovery Science and Technology*, 18–22-Oct. **2008**, Beijing, China, 473.
- [2] O Mitsunobu, *Synthesis*, **1981**, 1981:pp 1–28 DOI: 10.1055/s-1981-29317.
- [3] D. L Huges, *Org. Prep. Proced. Int.* **1996**, 28, 127–164.
- [4] H. Vorbruggen, K. Krolkiewicz, B. Bennua, *Chemische. Berichte.* **1981**, 114, 1234–1255.
- [5] C. Postolache, C. Tanase, L. Matei, V. Serban, *J. of Label. Compd and Radiopharm.* **2007**, 50, 5–6, 442–443.
- [6] L. Matei, C. Postolache, G Bubueanu, *Fus. Sci. and Technol.*, **2008**, 54, 2, 643–646.

## BIOAFFINITY OF RADIOLABELLED NEUROTENSIN AGONIST AND ANTAGONIST TO NEUROTENSIN RECEPTORS

**DIANA CHIPER, VALERIA LUNGU, CATALINA BARNA, LIDIA MATEI, MIHAI RADU, GEORGE BUBUEANU, AND CRISTIAN POSTOLACHE**

'Horia Hulbei' National Institute for Physics and Nuclear Engineering, 407 Atomistilor Street, Magurele, Romania

**Abstract:** The aim of our studies was to evaluate the emergent paradigm which measures the preference expressed of radiolabelled neurotensin agonist and antagonist to neurotensin receptors. Receptor binding  $^{177}\text{Lu-DOTA-Neurotensin}$  ( $^{177}\text{Lu-DOTA-NT}$ ) and  $^{177}\text{Lu-DOTA-SR48692}$  ( $^{177}\text{Lu-DOTA-SR}$ ) was examined on rat brain cortex membrane. By Scatchard analysis of experimental results regarding the bioaffinity ( $\text{IC}_{50}$ ) and specific binding ( $K_d$ ) of both mentioned radiobiocomplexes we obtained the following values:  $\text{IC}_{50} = 0.40267$  nM and  $K_d = 1.15637$  nM for  $^{177}\text{Lu-DOTA-NT}$  and  $\text{IC}_{50} = 0.55929$  nM and  $K_d = 0.04046$  pM for  $^{177}\text{Lu-DOTA-SR}$ .

**Keywords:** bioaffinity; cortex membrane; neurotensin; agonist; antagonist;  $^{177}\text{Lu}$

**Introduction:** Cancer is now explained as a series of somatic mutations leading from a normal cell to a cancer cell. The information is transmitted from the cell surface to the nucleus. Targeting the cell's surface by receptor binding radionuclide therapy ligands or by radioimmunotherapy is an essential mode of treatment of cancer either alone or in conjunction with other modalities like surgery and chemotherapy<sup>1,2</sup>. Targeted therapy has several potential advantages over external beam therapy including the possibility of delivering doses more selectively to the tumor, does not depend on expensive and sophisticated machines and is well tolerated by patients.

The paradigmatic peptide neurotensin and its receptors are extensively reviewed in the light of *in vivo* targeting of neuroendocrine tumors. The role of the more recently described targeting peptides is discussed. Both central and peripheral actions of neurotensin are initiated by association of the peptide to specific receptors located on the plasma membrane of target cells. The aim of our studies was to evaluate the emergent paradigm which measures the preference expressed of radiolabelled neurotensin agonist and antagonist to neurotensin receptors.

**Results and Discussion:** In the present study, we have compared the bioaffinity of a <sup>177</sup>Lu-DOTA-Neurotesin analogue agonist and <sup>177</sup>Lu-DOTA-SR48692 nonpeptide neurotensin antagonist by competitive binding methods to their neurotensin receptors, using an ascending dose paradigm. The binding affinity were determined by evaluation of receptor binding affinity of the cold and radiolabelled conjugates by a competitive and direct binding assay. Competition binding was performed using rat brain cortex membrane. 35,000–40,000 cpm of radiolabelled conjugate was added in each test tube in the presence of increasing concentration of neurotensin agonist and antagonist cold conjugates. After incubation, the samples were processed and measured on a NaI (TI) Gamma counter. We analyzed the experimental results on PRISM 4, fitting the total binding data to determine the values of IC<sub>50</sub> and K<sub>d</sub> (Figures 1–4).

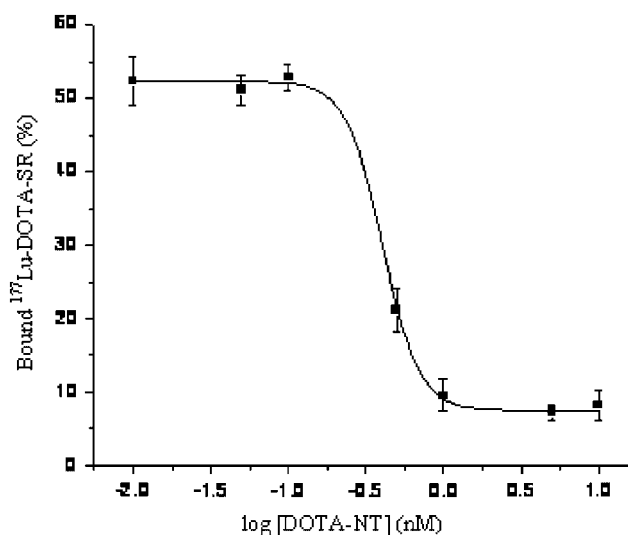


**Figure 1.** Competitive inhibition of <sup>177</sup>Lu-DOTA-SR binding by DOTA-NT (IC<sub>50</sub> = 0.40267 ± 0.0365 nM).

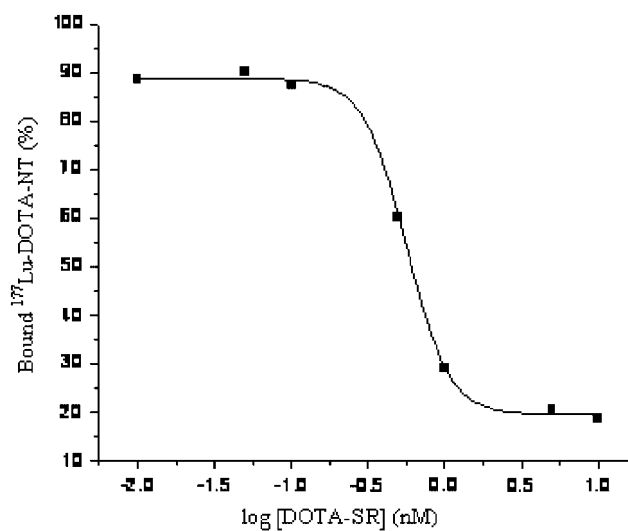


**Figure 2.** Competitive inhibition of <sup>177</sup>Lu-DOTA-NT binding by DOTA-SR (IC<sub>50</sub> = 0.55691 ± 0.02589 nM).

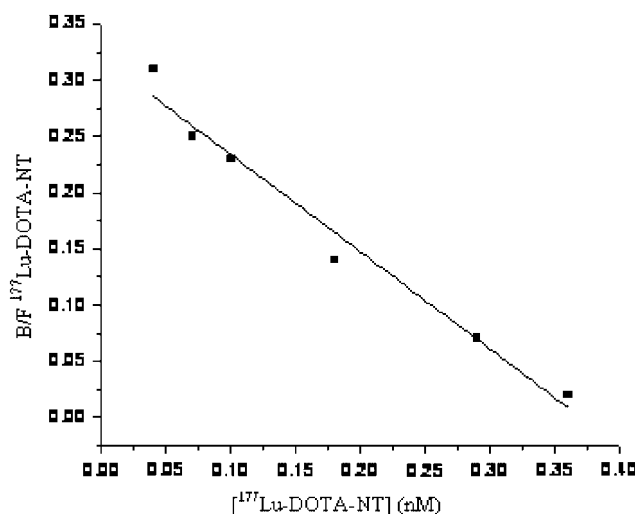


**Figure 3.** Scatchard analysis of <sup>177</sup>Lu-DOTA-NT specific binding to brain cortex membrane ( $K_d=1.15637$  nM).

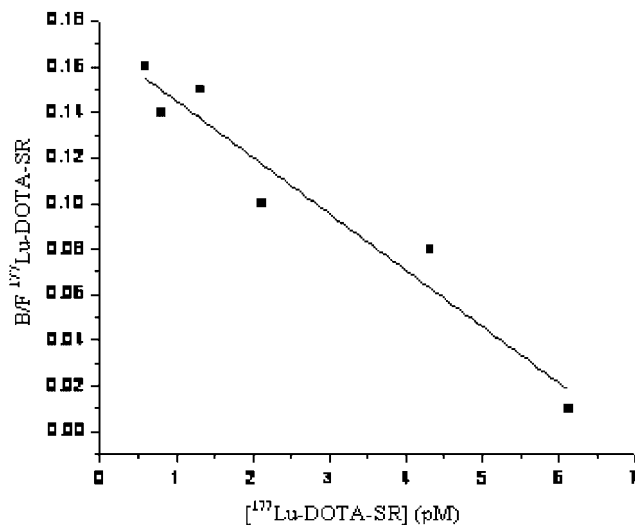


**Figure 4.** Scatchard analysis of <sup>177</sup>Lu-DOTA-SR specific binding to brain cortex membrane ( $K_d=0.04046$  nM).

The results for  $IC_{50}$  show a comparable high affinity ( $IC_{50}=0.40267 \pm 0.0365$  nM and  $IC_{50}=0.55691 \pm 0.02589$  nM) of both radiolabelled neurotensin agonist and antagonist to neurotensin receptors. The dissociation constant ( $K_d$ ) suggest that specific binding of <sup>177</sup>Lu DOTA-NT ( $K_d=1.15637$  nM) is higher than specific binding of <sup>177</sup>Lu-DOTA-SR ( $K_d=0.044046$  pM) to neurotensin receptors.

**Conclusions:** The results in this work constitute a database for the *in vivo* research regarding the pharmacokinetic and efficiency of treatment using <sup>177</sup>Lu-DOTA-Neurotensin in the presence of neurotensin antagonist (SR48692) on pathological animal models, in the hypothesis that targeting neuromodulatory systems, may offer new strategies in the targeted radionuclide therapy of cancer. The use of *in vitro* assays is an important approach to minimize the need of animal experimentation.

**Acknowledgements:** The authors would like to acknowledge: Ministry of Education and Research for scientific advises and for financial support from Project PNCDI 41-080/2007 from the national budget funds, to SanofiAventis for supplying SR48692, the research workgroup of the National Institute of Oncology (Prof. Dr. Rodica Anghel, Prof. Dr. Iuliana Gruia, Dr. Valentina Negoita, Daniela Glavan, Mirela Dumitru, Cristina Dorobantu, Monica Vasilescu, Cristina Dancus), to collaborators from the BM0607 ESF-COST Project. 'Targeted Radionuclide Therapy'.

## References

- [1] E. G. Garayoa, P. Blauenstein, M. Bruehlmeier, A. Blanc, K. Iterbeke, P. Conrath, D. Tourwe, P. A. Schubiger, *J. Nucl. Med.* **2002**, *43*, 374–383.
- [2] M. D. Visser, P. J. Janssen, A. Srinivasan, J. C. Reubi, B. Waser, J. L. Erion, M. A. Schmidt, E. P. Krenning, M. D. Jong, *European Journal of Nuclear Medicine and Molecular Imaging*, **2003**, *30*, 1134–1139.

RADIOLABELLING OF NEUROTENSIN AGONIST AND ANTAGONIST WITH  $^{177}\text{Lu}$ VALERIA LUNGU, DIANA CHIPER, LIDIA MATEI, CATALINA BARN, IULIANA GRUIA<sup>a</sup>, CATALIN TUTA, CRISTIAN POSTOLACHE, AND CATALINA CIMPEANU<sup>1</sup>Horia Hulubei' National Institute for Physics and Nuclear Engineering, 407 Atomistilor Street, Magurele, Romania<sup>a</sup>'Alexandru Trestioreanu' Institute of Oncology, Bucharest, Romania

**Abstract:** The representative biomolecules chosen as tumor targeting agents for radiolabelling with  $^{177}\text{Lu}$  are neurotensin agonist and antagonist, early documented as potent tumor-avid substrates. As direct incorporation of the  $^{177}\text{Lu}$  in either molecule is not feasible, indirect incorporation of  $^{177}\text{Lu}$  through a suitable bifunctional chelating agent is envisaged. For the present study, DOTA-Neurotensin agonist (DOTA-NT) was purchased and DOTA-Neurotensin antagonist (DOTA-SR48692) was synthesized in our laboratory. The bioconjugates DOTA-NT and DOTA-SR48692 were radiolabelled with  $^{177}\text{Lu}$  taking into account the specific variables of both radionuclide and bioligands. The IR and UV spectroscopy methods were used for the analysis of DOTA-SR48692.

The radiochemical purity of  $^{177}\text{Lu}$ -DOTA-NT and  $^{177}\text{Lu}$ -DOTA-SR48692 was determined by PC and TLC technique. The results show a good stability and radiochemical purity of the obtained radioconjugates.

**Keywords:**  $^{177}\text{Lu}$ ; DOTA; SR48692; radiolabelling; neurotensin; agonist; antagonist

**Introduction:** Neurotensin (NT) is a tri-decapeptide with dual function of both neurotransmitter/neuromodulator in the nervous system and a local hormone in the periphery through interaction with receptors. This peptide is specific to the human body, with a very short biologic half live that causes lack of balance at specific receptors saturation level which can cause diseases. Therefore, NT analogues were synthesized and coupled with different heterocycle chelators.

Neurotensin acts through high affinity receptors (NTR). NTRs as NTR1 ( $K_d = 0.1\text{--}0.3\text{ nM}$ ), NTR2 ( $K_d = 3\text{--}10\text{ nM}$ ), NTR3 ( $K_d = 0.1\text{--}0.3\text{ nM}$ ) have been found to be expressed in a majority of pancreatic tumors <sup>1-3</sup>.

The binding effects of NT to the NTR can be blocked by selective nonpeptide ligands known as NTR antagonists. SR48692 and SR142948A block the effects of NT at cancer cell level and Levocabastine, with antagonistic effects to NT bioaffinity.

$^{177}\text{Lu}$  is medical nuclide with the following nuclear characteristics: half-life = 6.7 days, tissue mean range = 670 ( $\mu\text{m}$ ),  $E_\gamma = 140\text{ KeV}$ ,  $E_\beta = 500\text{ KeV}$ . These nuclear characteristics confer the therapeutical effects in treatment of small tumor and micrometastasis by deliver radioactive doses to the specific target.

**Materials:** The following materials were used :  $^{177}\text{LuCl}_3$  (specific activity 45 Ci/mg, in 0.05 N HCl solution) from IDB Netherlands, DOTA (2,2',2'',2'''-(1,4,7,10-tetraazacyclododecane-1,4,7,10-tetrayl) tetraacetamide), from CheMatech, DOTA-Neurotensin (DOTA-NT) from piCHEM Austria and SR48692 NT antagonist, from SanofiAventis.

**Experimental:** Synthesis of DOTA-SR48692

A mixture of SR48692/DMSO and DOTA/0.1M  $\text{NaHCO}_3$  pH = 8.8, in 1:1.5 molar ratio, was reacted at 25°C for 6h. The DOTA-SR48692 was purified by Sephadex-25 gel chromatography and lyophilized.

Radiolabelling of DOTA-NT and DOTA-SR48692 with  $^{177}\text{Lu}$

Taking into account the multitude of variables that must be considered, some relating to the radioisotope, and others to the biological carrier, we selected the indirect radiolabelling method of the DOTA-Neurotensin (DOTA-NT) and DOTA-SR48692.

In this study, we developed a simple and efficient procedure for labelling of the bioconjugates with  $^{177}\text{Lu}$ . The samples consisting of 10–100  $\mu\text{g}$  bioconjugates in 50–500  $\mu\text{L}$  of 0.4 M acetate buffer pH 4.5 were labelled with 10–100 mCi of  $^{177}\text{LuCl}_3$  in 0.05 N HCl. The optimal values for obtaining the maximum complexation yield are: 3.7 DOTA-NT/ $^{177}\text{Lu}$ , 5.8 DOTA-SR48692/ $^{177}\text{Lu}$  molar ratios, 90 min. incubation time at 90°C in 0.4 M acetate buffer pH 4.5. After incubation of the samples at the specific conditions of temperature and cooling, were added different concentrations of HABA (3-hydroxy-4 aminobenzoic acid) or GA (gentisic acid) as radiolitic stabilizers. The identification and characterization of DOTA-NT and DOTA-SR48692 bioconjugates were completed by IR spectroscopy. The TLC and HPLC methods were used to determine the radiochemical purity of  $^{177}\text{Lu}$ -DOTA-NT and  $^{177}\text{Lu}$ -DOTA-SR48692 selected radiobioconjugates.

**Analytical methods:** The labelling yield and radiochemical purity for  $^{177}\text{Lu}$ -DOTA-NT were checked by Whatman 1 PC and Silicagel TLC using different solvents: 0.1 M Na-citrate pH = 5 with  $R_f = 0.62\text{--}0.70$  for  $^{177}\text{Lu}$ -DOTA-NT and  $R_f = 1.0$  for  $^{177}\text{LuCl}_3$ . In Butanol:acetic acid:water (5:2:1) the radiopeptide had an  $R_f = 0.60\text{--}0.70$  and free  $^{177}\text{Lu}$  to  $R_f = 0.08\text{--}0.25$ . Other solvents used for TLC were 10%  $\text{NH}_4$  acetate: Methanol (30:70) and  $R_f = 0.76\text{--}0.85$  for  $^{177}\text{Lu}$ -DOTA-NT and  $R_f = 0.00\text{--}0.16$  for free  $^{177}\text{Lu}$ . Radiochemical purity of  $^{177}\text{Lu}$ -DOTA-NT was > 95%.

**Results and Discussion:** The obtained results regarding analysis of radiobioconjugates show radiochemical purity higher than 95% for  $^{177}\text{Lu}$ -DOTA-NT and higher than 94.2% for  $^{177}\text{Lu}$ -DOTA-SR48692 and good stability in 0.9% NaCl up to 24 hours at room temperature (Figures 1–3).

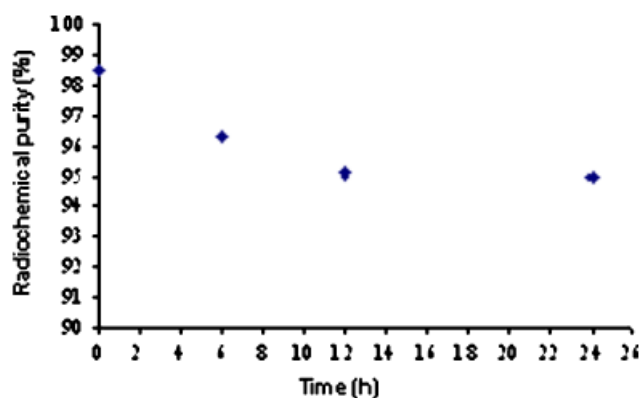


Figure 1. The stability of  $^{177}\text{Lu}$ -DOTA-NT in 0.9% NaCl solution.

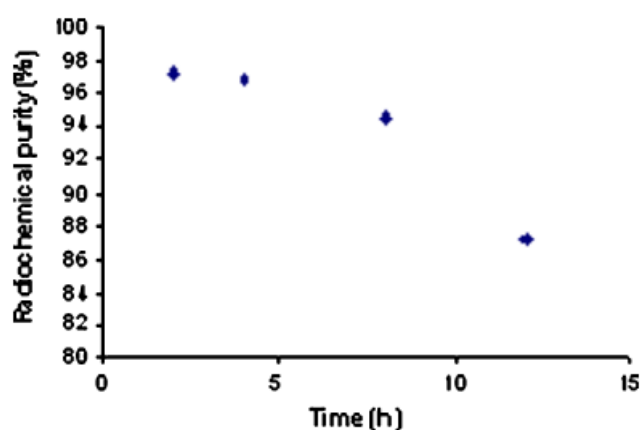


Figure 2. The stability of  $^{177}\text{Lu}$ -DOTA-NT in human serum.

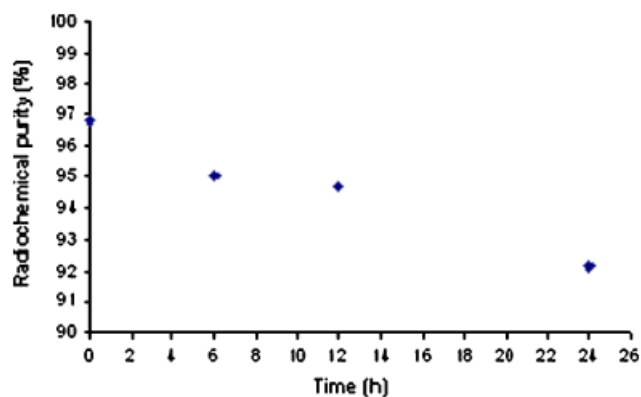


Figure 3. The stability of  $^{177}\text{Lu}$ -DOTA-SR48692 in 0.9% NaCl solution.

**Conclusion:** In this work we report an efficient procedure for the preparation of the radiobioconjugates,  $^{177}\text{Lu}$ -DOTA-NT and  $^{177}\text{Lu}$ -DOTA-SR48692 in weakly acidic solutions suitable for in vivo injection. Physical and chemical properties of  $^{177}\text{Lu}$  make it an excellent radionuclide for the development of therapeutic radiopharmaceuticals. The specific activity and chemical purity of  $^{177}\text{Lu}$  are critical factors which influence stability, labelling yield and receptor mediated uptake. It was possible to develop advanced analytical procedures that were applied to DOTA-NT, but which should be readily extendable to other peptides.

**Acknowledgements:** The authors would like to acknowledge: Ministry of Education and Research for scientific advises and for financial support from Project PNCDI 41-080/2007 from the national budget funds, to SanofiAventis for supplying SR48692, the research workgroup of the National Institute of Oncology (Prof. Dr. Rodica Anghel, Dr. Valentina Negoita, Daniela Glavan, Mirela Dumitru, Cristina Dorobantu, Monica Vasilescu, Cristina Dancus), to collaborators from the BM0607 ESF-COST Project. 'Targeted Radionuclide Therapy'

## References

- [1] J. Mazella, N. Zsuzger, V. Navaro *et al.*, *Journal of Biological Chemistry* **1998**, *273*, 26273–26276.  
[2] Labeled Neurotensin Derivatives US Patent, March 21, **2006**.  
[3] J. C. Reubi, *J. Nucl. Med.*, **1995**, *36*, 1825–1835.

## PHENYL CYCLOPROPYL RING OPENING WITH TRITIUM AND DEUTERIUM IN PALLADIUM CATALYZED HYDROGENATION: EVIDENCE FOR A METALLOCYCLOBUTANE IN EQUILIBRIUM WITH A $\pi$ -ALLYL PALLADIUM COMPLEX

BRUCE W. SURBER, JEFFREY L. CROSS, AND STEVEN M. HANNICK

Abbott Laboratories, 100 Abbott Park Road, Abbott Park, IL 60064

**Summary:** Phenyl cyclopropyl compounds were subjected to catalytic reduction using palladium on carbon and either tritium or deuterium gas. Tritium and deuterium NMR showed the isotopic labeling at the C-1 and C-3 positions of ring opened product, as expected, but also to varying degrees labeling was found at the C-2 methylene, away from the carbon-carbon bond that was broken. This is in contrast to a study of cyclopropyl ring opening reported in 1970 where deuterium and substrate in the gas phase were passed over a silica-supported palladium catalyst at elevated temperatures. In that study, the beta methylene was found to obtain no deuterium while each of the alpha and gamma carbons got about one deuterium. The discrepancy may be due to different mechanisms at work in the gas phase vs. the liquid phase or that the equilibrium is not operative in the gas phase. The present observation can be explained by a 4-membered metallocyclic intermediate in equilibrium with a  $\pi$ -allyl species that is stable enough to undergo tritium/hydrogen exchange with metal hydride.

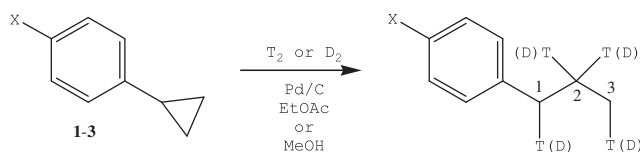
**Introduction:** In the course of a tritium/hydrogen exchange experiment to label a phenyl cyclopropyl group using tritium gas and palladium on carbon, we found that the cyclopropyl ring was opened to give the n-propyl product. Surprisingly, it was found that the beta position, C<sub>2</sub>, held more tritium than either C<sub>1</sub> or C<sub>3</sub>, even though these are the positions that should receive the tritium when the ring is opened. This reaction is known and usually occurs for most substituents (other than alkyl) with bond-breaking at C<sub>1</sub>–C<sub>3</sub>. The mechanism of this ring opening was studied using deuterium gas, palladium on silica, and cyclopropyl compounds in the gas phase at elevated temperature.<sup>1</sup> Contrary to the present results, that study showed no deuterium at C<sub>2</sub> and therefore concluded there was no  $\pi$ -allyl intermediate. Palladium  $\pi$ -allyl species are well-known<sup>2</sup> and have been proposed in heterogeneous catalytic hydrogenation and exchange of alkenes with deuterium or tritium. Indeed, reduction of alkenes is generally accompanied by allylic exchange labeling that can be considered as evidence of a  $\pi$ -allyl intermediate.<sup>3</sup> To gain a better understanding of the cyclopropyl ring opening, we undertook a study of three phenyl cyclopropyl compounds containing various electron-withdrawing or electron-donating groups on the aromatic ring, using both tritium and deuterium, with regard to the relative amounts of isotope incorporation in the three positions of the ring-opened alkyl chain.

**Methods:** Selected cyclopropyl compounds (1–3) were subjected to heterogeneous catalytic reduction using palladium on carbon and either tritium or deuterium gas. A standard reaction time (40h) was chosen and the molar ratios of substrate to catalyst to gas were kept constant. Reactions were run in either methanol or ethyl acetate and the work up consisted of removing unused gas, filtering the catalyst, and analyzing the products by HPLC (with radiodetection) and either deuterium or tritium NMR. In cases where the substrate was not very volatile, the labile tritium was removed by three methanol evaporations prior to NMR analysis. The identities of the products were established by comparison to authentic materials using HPLC retention times.

**Results and Discussion:** Entry 1 of Table 1 shows that deuterium behaves similarly to tritium in that exchange occurs at C<sub>2</sub> as well. Because tritium is easier to quantify and gives a cleaner NMR signal, most of the work was with this isotope. Entry 2 shows that the protic solvent methanol completely washes out any benzylic tritium indicating that benzylic exchange is operative in the product n-propyl compound as would be expected. This result is significant because it points out that exchange does not occur in Positions 2 and 3 after ring opening. The extra isotope found at Position 1 relative to Position 3 in all other entries then is probably due to isotope exchange after ring opening. In this context it is useful to point out that in all tritium experiments recovered cyclopropyl starting material contained no radioactivity. The tritium experiments (Entries 2–5, Table 1) show little change in the amount of tritium at Position 2 regardless of electron donation or withdrawal.

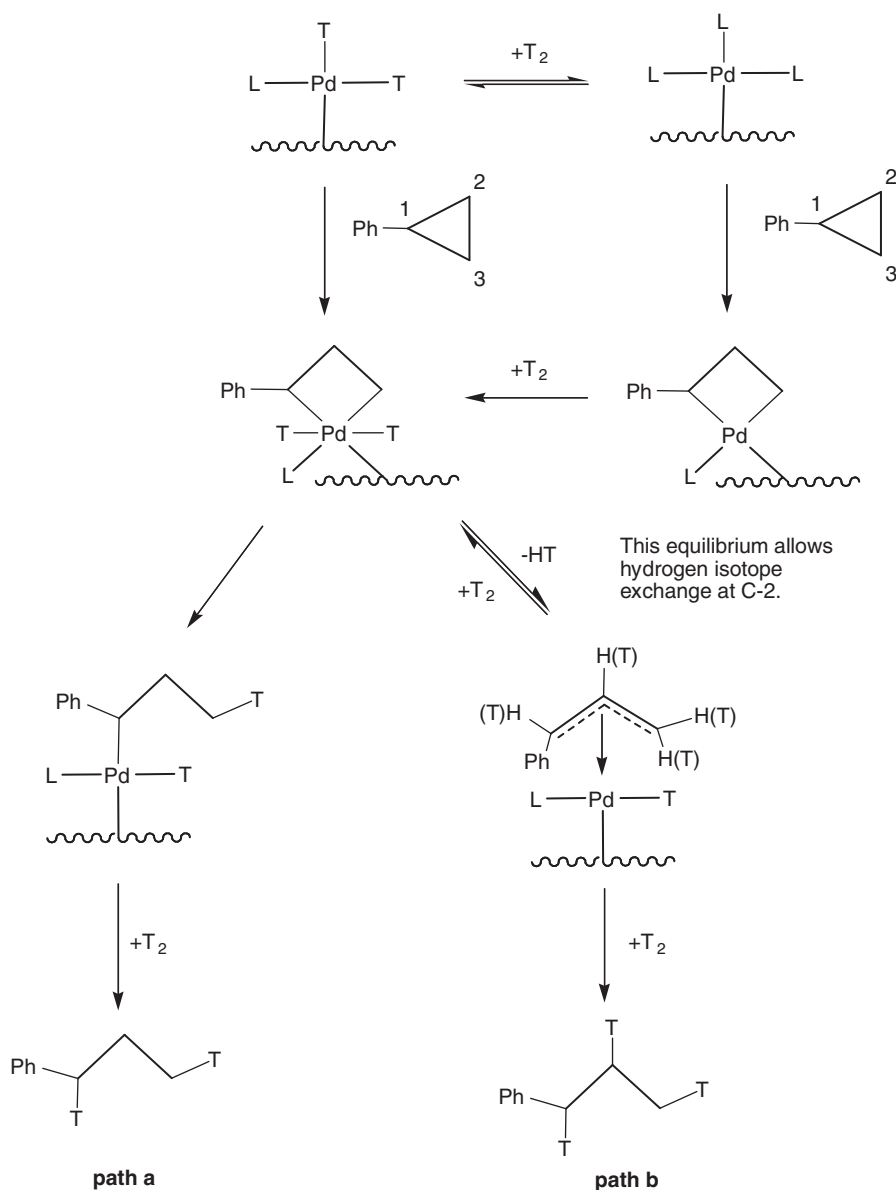
**Table 1.** Relative amounts of label in the propyl chain determined by NMR of the product of cyclopropyl ring opening.

Entry	Compound	X	Solvent	D <sub>2</sub> or T <sub>2</sub>	Relative amounts of D or T in position		
					1	2	3
1	CPB (1)	H	MeOH	D <sub>2</sub>	2.08	0.10	1.00
2	CPB (1)	H	MeOH	T <sub>2</sub>	0.00	0.40	1.00
3	CPB (1)	H	EtOAc	T <sub>2</sub>	1.50	0.42	1.00
4	CPBA (2)	COOH	EtOAc	T <sub>2</sub>	1.81	0.49	1.00
5	CPP (3)	OH	EtOAc	T <sub>2</sub>	1.50	0.50	1.00



In the gas phase studies, Roth concluded that the first step in the catalytic hydrogenolysis of a cyclopropane ring was the irreversible addition of at least one deuterium to give a  $C_1$ -monoabsorbed species (Scheme 1, path a) which would undergo reductive elimination to give a  $C_1, C_3$ -dideuterated species.<sup>4</sup> This mechanism accounts for isotopic labeling at the  $C_1$  and  $C_3$  sites in the molecule but leaves no possibility of labeling at the  $C_2$  site of the propyl chain.

In the present work the mechanism appears to be not so simple. Significant exchange at  $C_2$  suggests a more complicated system that might be initiated via metal insertion into the  $C_1$ - $C_3$  bond forming the metallacyclobutane that then can undergo exchange at  $C_2$  through equilibrium with a palladium  $\pi$ -allyl hydride complex (Scheme 1, path b). Roth's observation of no deuterium incorporation at  $C_2$  in the gas phase reactions may indicate that the gas phase conditions do not allow this equilibrium to operate. Electron withdrawal or donation does not seem to affect the extent of exchange at  $C_2$ .



Scheme 1.

**Conclusion:** In the palladium-catalyzed reductive opening of phenyl cyclopropanes with tritium gas significant labeling of the  $C_2$  site in the propyl chain was observed. This observation can be explained by an equilibrium between a metallacyclobutane intermediate and a  $\pi$ -allyl palladium hydride intermediate.



## References

- [1] J. A. Roth, *J. Am. Chem. Soc.* **1970**, *92*(22), 6658–6660.
- [2] L. S. Hegedus, *Transition Metals in the Synthesis of Complex Organic Molecules*, University Science Books, Sausalito, CA, **1999**, p. 250.
- [3] E. Alexakis, J. R. Jones, W. J. S. Lockley, *J. Label. Compd. Radiopharm.* **2007**, *50*, 507–508.
- [4] J. A. Roth, *J. Catalysis*, **1972**, *26*, 97–105.

## RHENIUM-188 LABELLED ALBUMIN MICROSPHERES FOR THERAPY OF LIVER TUMORS

VIRGINIA N.BORZA,<sup>a</sup> ELENA NEACSU<sup>a</sup>, COSMIN MUSTACIOSU,<sup>a</sup> AURELIAN LUCA<sup>a</sup>, CATALINABARNA,<sup>a</sup> NICOLETA POPESCU,<sup>b</sup> IONEL MERCIONIU,<sup>b</sup> PAL ALBERT,<sup>c</sup> ANCA HURDUC,<sup>c</sup> LUMINITA MOLDOVAN,<sup>c</sup> GHEORGHE P. SAVI,<sup>d</sup> ILEANA SAVI<sup>d</sup>, AND LIDIA MATEI<sup>a</sup>

<sup>a</sup>Horia Hulubei National Institute of R&D for Physics and Nuclear Engineering (IFIN-HH Bucharest), Magurele, Romania

<sup>b</sup>National Institute of Materials Physics, Bucharest, Romania

<sup>c</sup>Institute of Oncology 'Prof. dr. Al. Trestioreanu', Bucharest, Romania

<sup>d</sup>Victor Babes National Institute of R&D in Pathology and Biomedical Sciences, Bucharest, Romania

**Abstract:** Hepatocellular carcinoma is one of the common tumors in the world and response to chemotherapy and external radiotherapy is poor. An alternative treatment option is internal radionuclide therapy using microspheres labelled with radioisotopes with high linear energy transfer. The aim of this study was the preparation of human albumin microspheres, labelling of microspheres with <sup>188</sup>Re and the evaluation of the <sup>188</sup>Re labelled albumin microspheres as a possible new agent for radiotherapy by scintigraphic studies. Albumin microspheres of 10–30 μm were prepared by an emulsion technique. A direct method was used for labelling of albumin microspheres. The radiochemical purity of the radiolabelled albumin microspheres was ≥95%. The scintigraphic studies revealed excellent in vivo stability, over 72 h p.i. Due to its properties, this new compound could be a promising agent for internal radiotherapy of tumors.

**Keywords:** albumin; microspheres; <sup>188</sup>Re; radioactive labelling; scintigraphic studies

**Introduction:** Hepatocellular carcinoma (HCC) is one of the most common tumors in the world and its incidence is increasing in Europe. Despite the advances in radiotherapy, chemotherapy and immunotherapy, the surgical resection of localized tumor is the only mean of improving the survival of these patients but only in a small percent. Therefore, there is a great need for the development of an effective therapy.

Currently studies demonstrate that particles labelled with radioisotopes with high linear energy transfer (LET), such as high energy β emitters could be a promising alternative for endoradiotherapy of tumors. These particles can be based on polymers, resins, albumin, inorganic materials, etc., and the radioisotopes used for labelling are: <sup>90</sup>Y, <sup>188</sup>Re, <sup>186</sup>Re, and <sup>166</sup>Ho<sup>1–5</sup>.

Human serum albumin (HSA) is a natural and very attractive material for the microspheres preparation due to their properties: biodegradability, biocompatibility and nonantigenicity. Due to these advantages of albumin, microspheres obtained from this material and labelled with high-energy beta emitting radioisotopes will become potential agents for radiointernal therapy.

<sup>188</sup>Re due to its nuclear properties is a promising short-lived β-emitter (physical half-life = 17 h, maximum β-energy = 2,11 MeV) for production of radiopharmaceuticals for therapeutic purposes; also, its gama emission of 155 KeV makes biodistribution studies possible with common nuclear medicine techniques.

The aim of this study was the preparation of human albumin microspheres, labelling of microspheres with <sup>188</sup>Re and the evaluation of their potential to become a possible new agent for radiotherapy, by biodistribution studies. Albumin microspheres were prepared by an emulsion technique and the size of particles was, in principal, between 10–30 μm. A direct method was used for labelling of albumin microspheres. Stannous chloride dihydrate was used as a reducing agent of Na<sup>188</sup>ReO<sub>4</sub> and potassium sodium tartrate tetrahydrate was used as a transchelation agent. The scintigraphic studies carried out after intravenous injection of rabbits with radiolabelled microspheres revealed excellent in vivo stability, up to 72 h p.i. Because of the attractive properties of <sup>188</sup>Re and great stability of the microspheres labelled with <sup>188</sup>Re, in vivo, this new compound could be a promising agent for internal radiotherapy of tumors.

**Experimental: Method for the preparation of human serum albumin microspheres:** The emulsion technique was studied for the preparation of HSA (Sigma) microspheres, with dimensions, in principal, between 10–30 μm. 0,5 ml of HSA solution was added in small droplets to a round-bottom flask containing 100 ml of corn oil, under continuous stirring with a glass stirrer attached to an electric motor. The resulting suspension is then stabilized by heating at 130°C. The hardened microspheres were separated from the oil by centrifugation, washed free of oil, four times with diethyl ether and finally dried in air.

Particle size characterization was performed by Scanning Electron Microscopy (SEM) and optic microscopy.

**Method for the preparation of human serum albumin microspheres labelled with <sup>188</sup>Re:** A direct method was used for labelling of albumin microspheres; stannous chloride dihydrate (Sigma) was used as a reducing agent of Na<sup>188</sup>ReO<sub>4</sub> (Polatom, Poland), and potassium sodium tartrate tetrahydrate (Sigma) was used as transchelation agent.

For labeling of albumin microspheres, 1 ml of deoxygenized potassium sodium tartrate tetrahydrate solution and 0.1 ml of deoxygenized stannous chloride dihydrate solution were added to a vial containing 4 mg of HSA microspheres; 0,1–0,2 ml of Na<sup>188</sup>ReO<sub>4</sub> (18.5–37 MBq) eluate was added. The reaction mixture was then heated on a water bath.

The labelling yield and stability of the albumin microspheres labeled with  $^{188}\text{Re}$  was checked by paper chromatography and ITLC using Whatman 1 paper as stationary phase and silicagel respectively, and acetone and saline 0.9% solution as mobile phases.

#### Scintigraphic studies with human serum albumin microspheres labelled with $^{188}\text{Re}$

Scintigraphic studies of the microspheres labelled with  $^{188}\text{Re}$  was carried out after intravenous injection of 2.9 MBq of labelled microspheres in the auricular vein of New Zealand White rabbits using the lung as a model for a well-perfused tumor.<sup>4</sup>

**Results and Discussion:** The HSA microspheres were prepared by an emulsion technique. Several factors for the process that control albumin microspheres size were studied: HSA concentration, the ratio between the dispersed phase volume and the continuous phase volume, dispersion time, stirring rate during albumin dispersion and heat stabilization of microspheres. The optimal method for the preparation of HSA microspheres with dimensions between 10–30  $\mu\text{m}$ , established by these studies, is the following: 0.5 ml of a 25% HSA solution was added in small droplets to a round-bottom flask containing 100 ml of corn oil, under continuous stirring (1000 rpm) with a glass stirrer attached to an electric motor, for 10 minutes. The resulting suspension is then stabilized by heating at 130°C, for 40 minutes, under continuous stirring. Particle size characterization was performed by Scanning Electron Microscopy (SEM) and optic microscopy. The size of microspheres was between 10–30  $\mu\text{m}$ .

The optimal reaction conditions for radiolabelling of HSA microspheres were established by following the effect of the tartrate and stannous chloride concentration, of the temperature and time on the labeling yield.

The optimal method of microspheres radiolabelling, developed in the studies carried out, is the following: 1 ml of deoxygenized 104 mM potassium tartrate tetrahydrate solution, and 0.1 ml of deoxygenized 20 mg/ml stannous chloride dehydrate solution were added to a vial containing 4 mg of HSA microspheres; then,  $\text{Na}^{188}\text{ReO}_4$  (18.5–37 MBq) eluate was added. The reaction mixture was heated on a water bath at 95°C for 1 h. The radiochemical purity of the radiolabelled microspheres is around 90% or even more than 95% depending of the  $^{188}\text{W}/^{188}\text{Re}$  eluate quality.

Scintigraphic studies were carried out after intravenous injection of 2.9 MBq of radiolabelled microspheres in auricular vein of New Zealand White rabbits; images recorded with a gamma camera (Siemens e-cam) revealed an excellent in vivo stability up to 72 h (Figure 1).

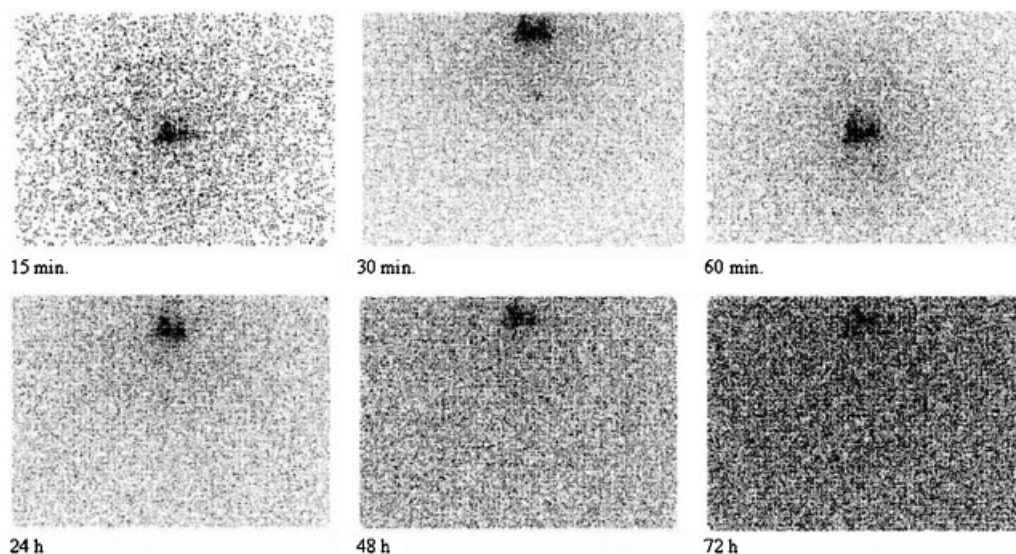


**Figure 1.** Scintigraphic images. Biodistribution of labelled HSA microspheres after intravenous injection in the auricular vein of New Zealand rabbits.

**Conclusion:** The albumin microspheres, prepared and radiolabelled with  $^{188}\text{Re}$  by the methods described in this paper, proved a good localization in the target organ and in the same time a great stability in vivo.

Because of the attractive nuclear properties of  $^{188}\text{Re}$  and great stability in vivo of the HSA microspheres labelled with  $^{188}\text{Re}$ , this new compound could be a promising agent for endoradiotherapy of liver tumors.

#### References

- [1] W. Y. Lau, S. Ho, T. W. Leung, M. Chan, R. Ho, P. J. Johnson, A. K. Li, *Int. Radiat. Oncol. Biol. Phys.* **1998**, *40*, 583–592.
- [2] R. J. Mumper, U. Y. Ryo, M. Jay, *J. Nucl. Med.*, **1991**, *32*, 2139–2143.
- [3] F. Nijssen, D. Rook, C. Brandt, R. Meijer, H. Dullens, B. Zonnenberg, J. de Klerk, *Eur. J. Nucl. Med.* **2001**, *28*, 743–749.
- [4] G. Wunderlich, J. Pinkert, M. Stintz, J. Kotzerke, *Appl. Radiat. Isot.* **2005**, *62*, 745–750.
- [5] G. Wunderlich, A. Drews, J. Kotzerke, *Appl. Radiat. Isot.* **2005**, *62*, 915–918.

## RADIO SYNTHESIS OF CARBON 14 AND TRITIUM LABELED POTENT NEURAMINIDASE INHIBITORS

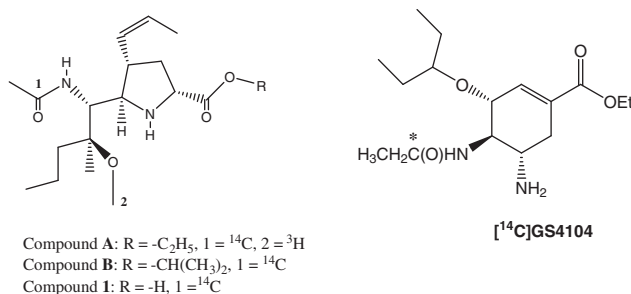
SHIRISH RAJA, KAREN ST. GEORGE, LEIMIN FAN, CLARENCE MARING, KEITH MCDANIEL, AND DAVID DEGOEY

AP9, L171, Abbott Laboratories, 100 Abbott Park, Illinois 60064, USA

**Abstract:** The carbon-14 label Neuraminidase Inhibitor **1**, corresponding ethyl **A** and isopropyl **B** prodrugs, and the benchmark compound [ $^{14}\text{C}$ ]GS4104 were prepared by using [ $^{14}\text{C}$ ]acetic anhydride. The tritium labeled ethyl **A** prodrug was prepared by using [ $^3\text{H}$ ]methyl iodide.

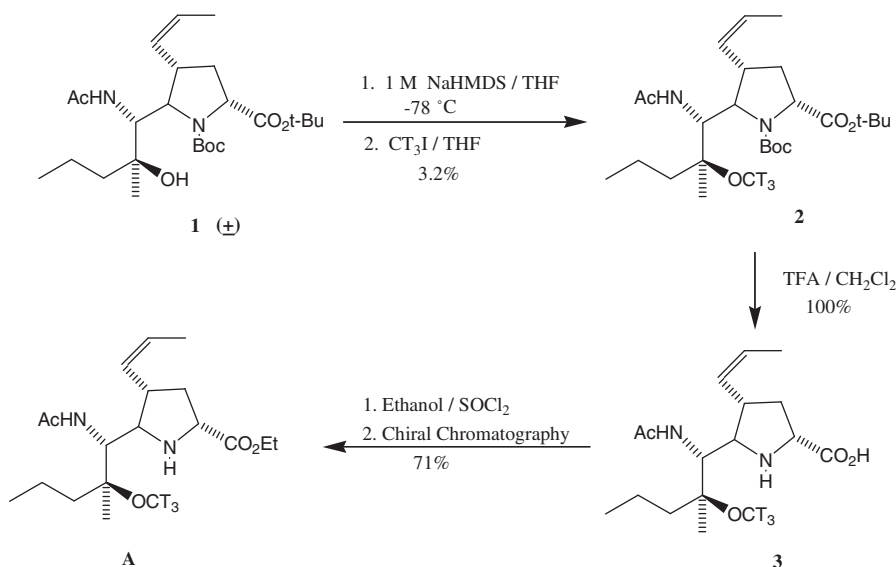
**Keywords:** influenza virus; neuraminidase inhibitors; GS4104

**Introduction:** Influenza virus causes acute respiratory illness with significant morbidity and mortality. The virus replicates in the upper and/or lower respiratory tracts causing fever, headache, cough, chills, myalgia, and weakness.<sup>1</sup> Compound **1** is a potent inhibitor of influenza neuraminidase. The ethyl **A** and isopropyl **B** prodrugs of **1** exhibited good oral bioavailability in rats. Tritium labeled prodrug **A** was synthesized from a racemic tertiary alcohol using tritiated methyl iodide. The active enantiomer **A** was obtained by chiral chromatography. In addition, carbon-14 analogues of **A**, **B** and **GS4104** were synthesized using carbon-14 acetic anhydride. The resulting tritium and carbon-14 labeled analogues were used to understand the pharmacokinetic and pharmacodynamic profiles of these compounds.

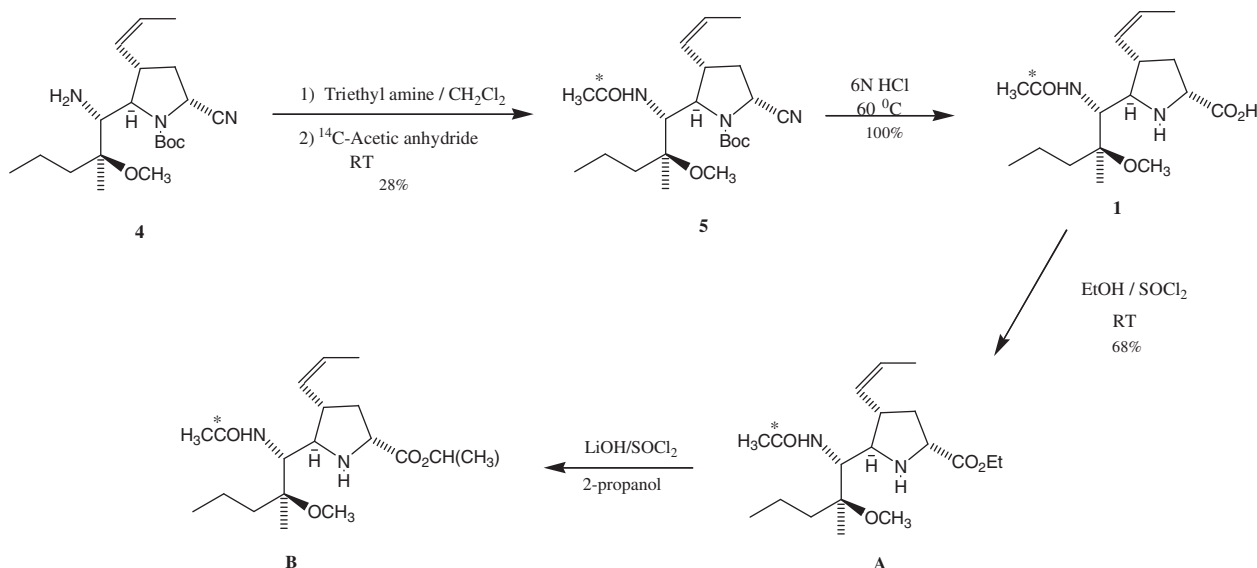


**Results and discussion:** The reaction of racemic alcohol **1** in THF with 1 M sodium dimethyl silazane at  $-78^\circ\text{C}$  for 45 min followed by the addition of [ $^3\text{H}$ ]methyl iodide gave ether **2** as shown in Scheme 1. The hydrolysis of **2** was accomplished by using TFA in CH<sub>2</sub>Cl<sub>2</sub>. The esterification of **3** was achieved by using thionyl chloride and ethanol. The reaction was carried out at room temperature. The ester was resolved using chiral chromatography to yield 1.2 mCi of **A**.

Later the antiviral research group provided the chiral amine **4** that was used to prepare carbon-14 analogue of **A** as shown in Scheme 2. The enantiomerically pure amine **4** in methylene chloride was treated with triethyl amine and [ $^{14}\text{C}$ ]acetic anhydride (50 mCi). After purification, 11 mCi of **5** was obtained. Nitrile **5** was hydrolyzed with 6N hydrochloric acid at  $60^\circ\text{C}$  to give corresponding acid **1** in quantitative yield. Acid **1** was converted to the corresponding ethyl ester at room temperature by using thionyl chloride and ethanol to give after purification 7.5 mCi of **A**. The conversion of **A** to **B** was achieved by using LiOH, SOCl<sub>2</sub> and 2-propanol.



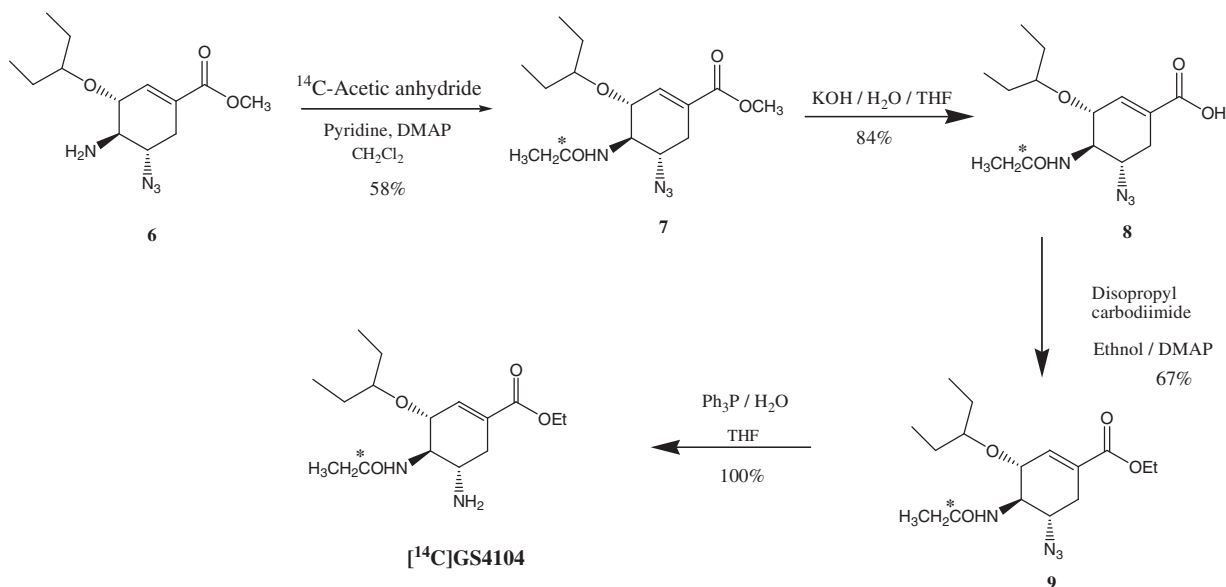
Scheme 1.



Scheme 2.

To obtain comparative Plasma and Lung drug concentration data in animals to determine PK/PD, GS4104 was also labeled with carbon-14. The synthesis of carbon-14 labeled GS4104 is shown Scheme 3. To introduce carbon-14 in the molecule, amine **6** was treated with [ $^{14}\text{C}$ ]acetic anhydride (50 mCi) in methylene chloride in presence of pyridine and DMAP to give after purification amide **7**. Acid **8** was prepared by the hydrolysis of amide **7** by using 1N potassium hydroxide in THF. During work up AG 50W-X8 resins were used.

Acid **8** was converted to corresponding ethyl ester by using diisopropylcarbodiimide, DMAP and ethanol at RT. In the final step, the azide functionality was converted to an amine by using triphenyl phosphine in 10% aqueous THF at an elevated temperature. Purification of the final product was achieved using flash chromatography (silica gel, 10% methanol + 0.1% ammonium hydroxide in methylene chloride) to yield 16 mCi of [ $^{14}\text{C}$ ]GS4104 with RCP > 99%.



Scheme 3.

**Conclusion:** To support the development of the compounds **A** and **B** as highly potent inhibitors of respiratory influenza virus replication, tritium labeled **A** and carbon-14 labeled **A**, **B** and **1** were synthesized. Tritium labeled **A** was synthesized with total activity of 1.2 mCi as shown in Scheme 1. Carbon-14 labeled **A**, **B** and **1** were synthesized with total activity of 7.0 mCi, 1.43 mCi, and 7.5 mCi respectively using the chemistry shown in Scheme 2. As shown in Scheme 3, 16 mCi of the benchmark compound [ $^{14}\text{C}$ ]GS4104 was prepared to compare its broad spectrum activity with **A**.

## Reference

- [1] (a) E. J. Eisenberg, A. Bidgood, K. C. Cundy. *Antimicrobial Agents and Chemotherapy* **1997**, 41, 1949–1952. (b) Kati WM, Montgomery D, Carrick R, Gubareva L, Maring C, McDaniel K, Steffy K, Molla A, Hayden F, Kempf D, Kohlbrenner *Antimicrobial Agents and Chemotherapy* 46, 1014–1021.

EXPLORATORY ROUTES TOWARDS THE SYNTHESIS OF  $^{14}\text{C}$  LABELLED CARBOXYPYRROLOPYRIDINES

DAMIEN SALLABERRY, CATHERINE AUBERT, FRANCK LE STRAT, AND JOHN ALLEN

Isotope Chemistry and Metabolite Synthesis Department, Sanofi-Aventis Recherche et Développement, 1 avenue Pierre Brossollette, 91385 CHILLY-MAZARIN Cédex, France

**Short Abstract:** Several different methods of preparing radiolabelled 2-carboxypyrrolopyridines from polyfunctionalized pyridines using an intramolecular cyclisation method were studied. Of the three methods which succeeded, we chose that due to Cadogan because of time constraints.

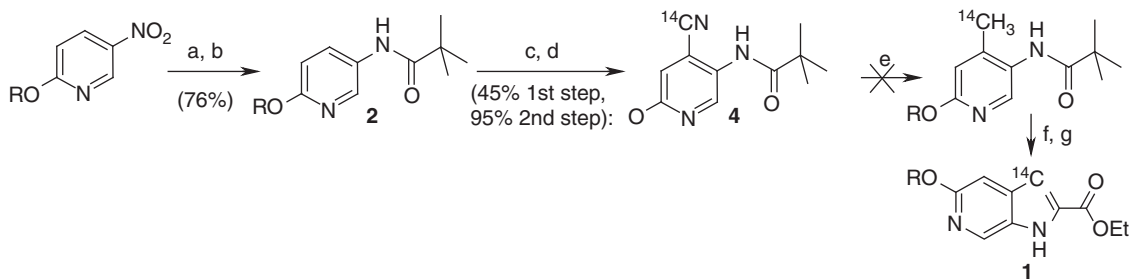
**Keywords:** carboxypyrrolopyridines; Reissert; Leimgruber-Batcho; Cadogan; Nakamura; Hegedus-Mori-Heck and Ullmann cyclizations; polyfunctionalized pyridines

**Introduction:** As part of a drug development programme we needed to prepare a radiolabelled 2-carboxypyrrolopyridine building block (**1**) and then convert it to a radiolabelled development candidate for use in ADME studies. In the scientific literature, many articles describe the synthesis of carboxyindoles, but the preparations of carboxypyrrolopyridines are less common.

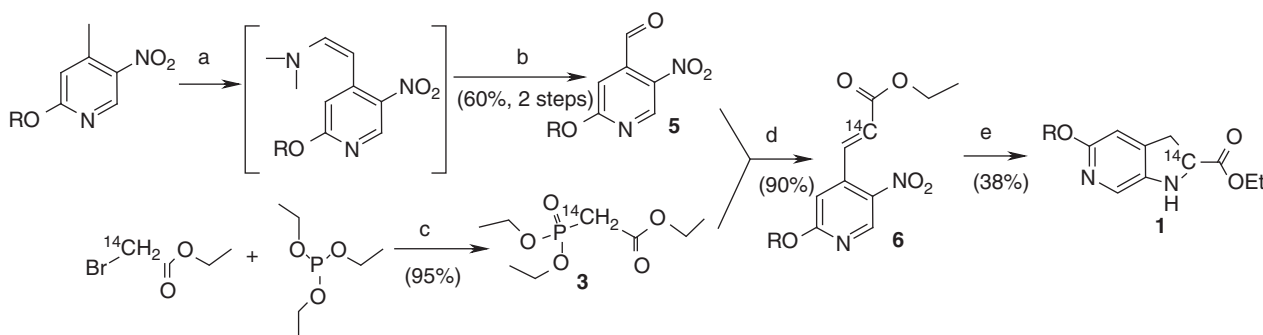
We devised several synthetic pathways for  $^{14}\text{C}$  labelling in the pyrrole core of 2-carboxypyrrolopyridine (**1**). Each of these used a polyfunctionalized pyridine as starting material and an intramolecular cyclisation method.

These syntheses can be classified into two groups. In the first which we call 'reductive cyclization', methods due to Reissert<sup>1,2</sup>, Leimgruber-Batcho<sup>3</sup> and Cadogan<sup>4</sup> were tested. In the second group, called 'organometallic cyclization', methods due to Nakamura<sup>5</sup>, Hegedus-Mori-Heck<sup>6</sup> and Ullmann<sup>7</sup> were studied.

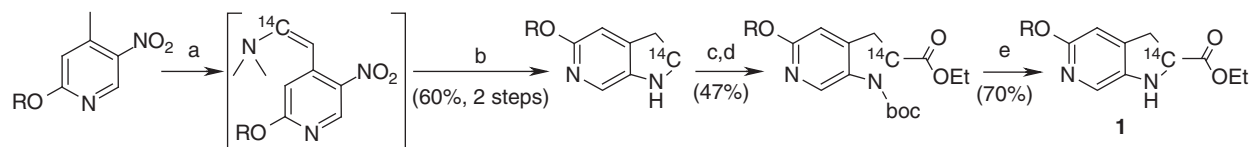
**'Reductive cyclization' methods:** The three syntheses of the first group are outlined (Schemes 1–3). Yields shown are those for unlabelled model reactions. Cadogan's cyclization (Scheme 2) was shown to be the most effective method. Unfortunately, the reduction step of compound **4** in the 'Reissert method' (Scheme 1) failed.



**Scheme 1.** 'Reissert method' Reaction conditions: (a) Ra Ni,  $\text{N}_2\text{H}_4$ , MeOH, r.t., 2h; (b)  $\text{Et}_3\text{N}$  DCM, trimethylacetylchloride,  $0^\circ\text{C}$  to r.t. 2h; (c)  $\text{tBuLi}$ , THF,  $-78^\circ\text{C}$ , 90 mm then  $\text{I}_2$ , THF,  $-78^\circ\text{C}$ , 3h; (d)  $\text{Cu}^{14}\text{C}[\text{CN}]$ ,  $\text{CuI}$ , DMF,  $150^\circ\text{C}$ , 2h; (e) Pd/C 10%  $\text{HCO}_2\text{NH}_4$  MeOH, reflux; (f) diethyl oxalate,  $\text{tBuOK}$ ; (g) 3N HCl.

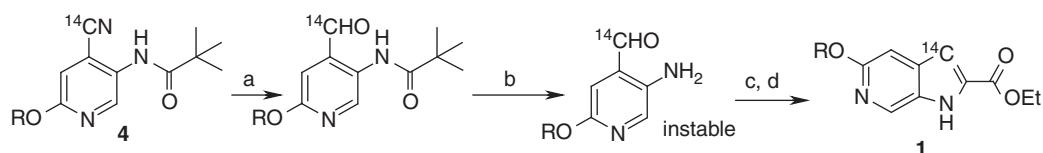


**Scheme 2.** 'Cadogan method' Reaction conditions: (a)  $^{14}\text{C}$ DMF-DMA,  $125^\circ\text{C}$ , 3h; (b)  $\text{NaO}_4$ ,  $\text{THE}/\text{H}_2\text{O}$ , r.t. 2h; (c) toluene,  $120^\circ\text{C}$  3h; (d)  $\text{LiCl}$ , DBU,  $\text{CH}_3\text{CN}$ ,  $-10^\circ\text{C}$  to r.t.; (e)  $\text{P}(\text{O}i\text{Pr})_3$ , xylene,  $170^\circ\text{C}$ , 30 min.

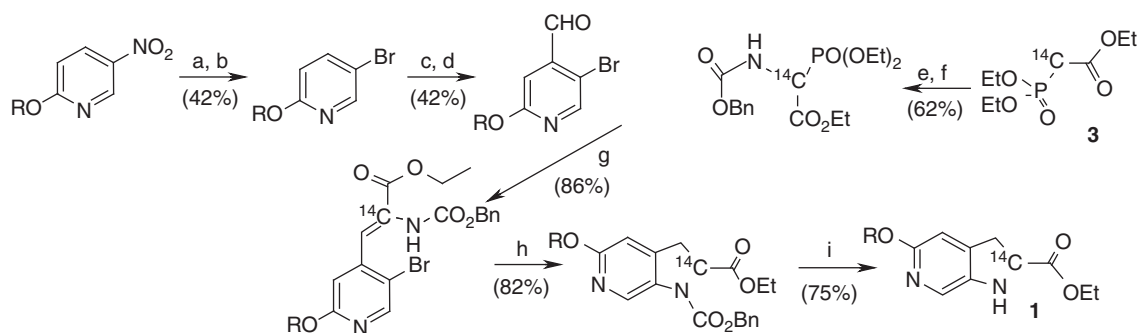


**Scheme 3. 'Leimgruber-Batcho method'** Reaction conditions: (a)  $^{14}\text{C}$  DMF-DMA, 125°C, 3 h; (b) ammonium formate, Pd/C 10%, MeOH, reflux, 3 h; (c) Boc<sub>2</sub>O, DMAP, DCM, r.t. 3 h; (d) nBuLi, -78°C, THF, 60 min then ethyl chloroformate, THF, 90 min; (e) TBAF, THF, reflux, 5 h.

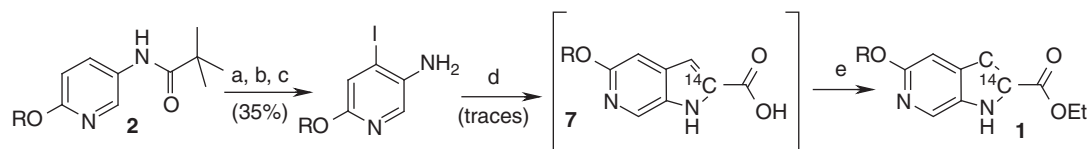
**'Organometallic cyclization' methods:** The Nakamura, Hegedus-Mori-Heck and Ullmann methods are outlined (Schemes 4–6). Yields shown are those for unlabelled model reactions. Ullmann's aromatic amination intramolecular cyclization gave the best result (Scheme 5). Unfortunately, formation of aldehyde from compound **4** in the Nakamura method' (Scheme 4) was difficult because of its instability<sup>8</sup>. Also the difficulty in obtaining the intermediate acid (**7**) in the 'Hegedus-Mori-Heck Synthesis' (Scheme 6) was a limiting factor.



**Scheme 4. 'Nakamura method'** Reaction condition: (a) reduction with PtO<sub>2</sub>, HCO<sub>2</sub>H/H<sub>2</sub>O or with DiBAL; (b) 3N HCl; (c) Rh(OAc)<sub>4</sub>, toluene, N<sub>2</sub>CCO<sub>2</sub> EtPO(OEt)<sub>2</sub>, DBU.



**Scheme 5. 'Copper/L-proline synthesis via intra-amination of Ullmann'** Reaction conditions: (a) Ra Ni, N<sub>2</sub>H<sub>4</sub>, MeOH, r.t. 2 h; (b) CuBr, NaNO<sub>2</sub>, HBr 47%, 5°C, 2 h; (c) LDA, THF, -78°C, 1 h; (d) DMF, THF, -78°C, 2 h; (e) [N(C<sub>2</sub>H<sub>5</sub>)<sub>2</sub>]<sub>3</sub> N<sub>3</sub>P<sup>+</sup> Br<sup>-</sup>, t BuOK, Et<sub>2</sub>O, R.t., 24 h; (f) Rh<sub>2</sub> (OAc)<sub>4</sub> toluene, benzyl carbamate, reflux, 18 h; (g) DBU, DCM, r.t., 2 h; (h) K<sub>2</sub>CO<sub>3</sub>, L-proline, CuI, dioxane, 100°C, 12 h; (i) tBuNH<sub>2</sub>, MeOH, reflux, 2 h.



**Scheme 6. 'Hegedus-Mori-Heck Synthesis'** Reaction conditions: (a) tBuLi, THF, -78°C, 1.5 h; (b) I<sub>2</sub>, THF, -78°C, 3 h; (c) H<sub>2</sub>SO<sub>4</sub>, H<sub>2</sub>O, reflux, 2 h; (d) Pd(OAc)<sub>2</sub>, DABCO, sodium  $^{14}\text{C}$  pyruvate, DMF, 105°C, 3 h; (e) H<sub>2</sub>SO<sub>4</sub>, EtOH, 80°C, 12 h.

**$^{14}\text{C}$ Application:** Carbon-14 labelled 2-carboxypyrolopyridine (**1**) was successfully synthesized by Cadogan's method from labelled 4-ethylacrylate-5-nitropyridine derivative (**6**). This precursor was prepared from  $^{14}\text{C}$ -triethylphosphonoacetate and a 4-formyl-5-nitropyridine (**5**) by a Horner-Wadsworth-Emmons reaction. The radiochemical yield was 36% in three steps from commercially available ethyl  $^{14}\text{C}$ -bromoacetate.

**Conclusion:** Out of the six synthetic pathways chosen from the literature to prepare  $^{14}\text{C}$ -2-carboxypyrolopyridine (**1**), only three were successful – the Leimgruber-Batcho, Cadogan and Ullmann syntheses. For rapidity, we achieved our objective by applying the Cadogan approach for the  $^{14}\text{C}$  synthesis. The copper/L-proline method could be preferable; its less drastic conditions gave a similar yield.

## References

- [1] L. Guandalini, E. Martini, *Archivoc.* **2004**, 286–300.

- [2] F. Popoowycz, J. Y. Mérour, B. Joseph, *Tetrahedron* **2007**, *63*, 8689–8707.  
[3] J. F. Kadow, T. Wang, *Tetrahedron Let.* **2006**, *47*, 5653–5656.  
[4] J. I. G. Cadogan, *Synthesis* **1969**, 11–17.  
[5] Y. Nakamura, *Org. let.* **2002**, *14*, 2317–2320.  
[6] M. Nazaré, C. Schneider, *Angew. Chem. Int. Ed.* **2004**, *43*, 4526–4528.  
[7] C. Barberis, T. D. Gordon, *Tetrahedron Let.* **2005**, *46*, 8877–8880.  
[8] A. Godard, G. Quèguiner, *J. Heterocyclic Chem.* **1980**, *17*, 465.

## SYNTHESIS OF [<sup>14</sup>C-RING-(U)]4-(TRIFLUOROMETHYL)BENZENESULFONYL CHLORIDE

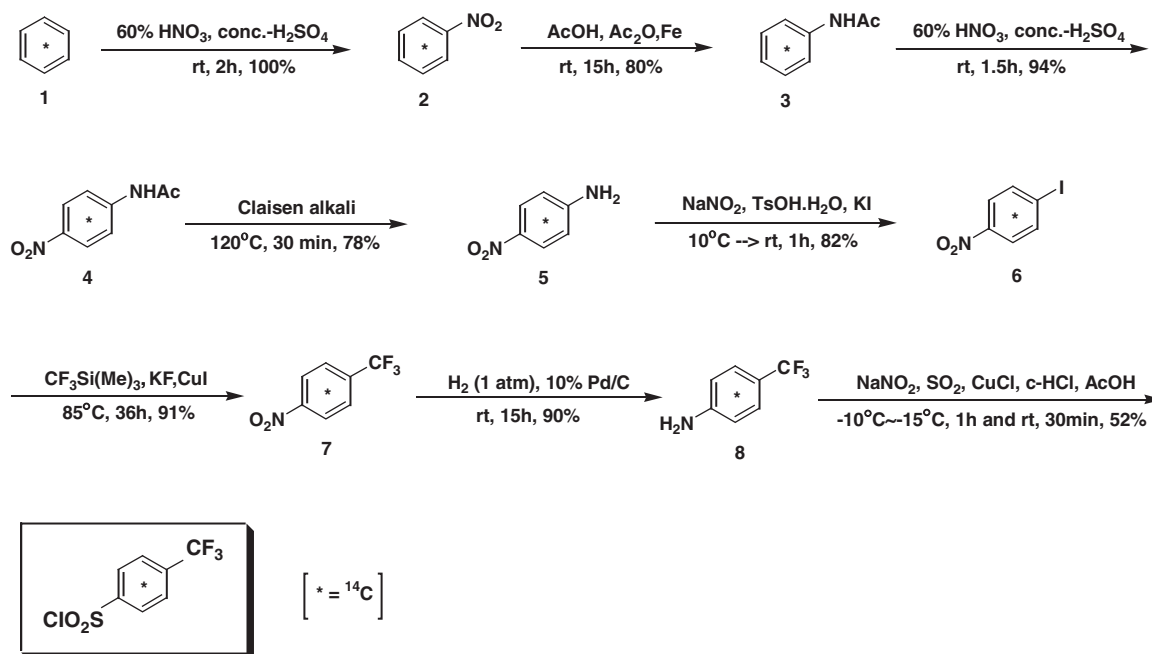
HYUN-IL SHIN AND YOUNG-SEOK KIM

Korea RadioChemicals Center, Suwon, Korea 443–270.

**Abstract:** [<sup>14</sup>C-ring-(U)]4-(trifluoromethyl)benzenesulfonyl chloride (**9**) is a key intermediate in the synthesis of [<sup>14</sup>C]-labeled drugs and can be prepared from [<sup>14</sup>C-ring-(U)]4-(trifluoromethyl)phenylamine (**8**). The key step in the synthesis of **9** is the sulfonation of **8** mediated by a Sandmeyer-type reaction for the introduction of a sulfonyl group. Compound **9** can be synthesized from [<sup>14</sup>C-ring-(U)]benzene via an eight-step process with an overall radiochemical yield of 20%.

**Keywords:** carbon 14; 4-(trifluoromethyl)benzenesulfonyl chloride.

### Results and discussion:



Scheme 1. Synthesis of [<sup>14</sup>C-ring-(U)]4-(trifluoromethyl)benzenesulfonyl chloride.

Benzene **1** was nitrated with 60% HNO<sub>3</sub> and conc.-H<sub>2</sub>SO<sub>4</sub> to afford nitrobenzene **2**, which was reduced to the corresponding acetylated aniline **3** using Fe in acetic acid and acetic anhydride solution. Nitration of **3** was achieved with 60% HNO<sub>3</sub> and conc.-H<sub>2</sub>SO<sub>4</sub> to afford **4**. Subsequent hydrolysis of **4** with Claisen's alkali resulted in the removal of the acetyl group to afford **5**. An iodide group was introduced into **5** through diazonium salt formation with NaNO<sub>2</sub> and subsequent iodation with KI<sup>1)</sup>. The conversion of **6** to **7** (yield: 91%) proceeded upon treatment with CF<sub>3</sub>Si(Me)<sub>3</sub>, KF, and CuI<sup>2)</sup> in a high-pressure glass tube. Among all the reagents used for introducing the trifluoromethyl group into **6** (CF<sub>3</sub>Si(Me)<sub>3</sub>, FSO<sub>2</sub>CF<sub>2</sub>CO<sub>2</sub>CH<sub>3</sub><sup>3)</sup>, CF<sub>3</sub>CO<sub>2</sub>Na<sup>4)</sup>, CF<sub>3</sub>Si(Me)<sub>3</sub> gave the best yield. Reduction of the nitro group in **7** was accomplished by treatment with hydrogen gas and 10% Pd/C to afford **8**. Finally, **8** was converted to [<sup>14</sup>C-ring-(U)]4-(trifluoromethyl)benzenesulfonyl chloride<sup>5)</sup> (**9**) via diazonium salt formation with NaNO<sub>2</sub> and sulfonyl chlorination with SO<sub>2</sub> and CuCl in AcOH and c-HCl solution (Scheme 1).

**Experimental:** [ $^{14}\text{C}$ -ring-(U)]1-Nitro-4-(trifluoromethyl)benzene (**7**): To a solution of compound **6** (1.74 g, 6.99 mmol, 15.5 GBq) in DMF (13 mL) were added CuI (1.33 g, 6.98 mmol), KF (486 mg, 8.38 mmol), and  $\text{CF}_3\text{Si}(\text{Me})_3$  (1.18 g, 8.36 mmol) at room temperature and the mixture was stirred at  $85^\circ\text{C}$  for 36 h in high-pressure glass tube. After diluted with water (50 mL) and diethyl ether (50 mL), the reaction mixture was filtered (celite) and washed with diethyl ether (10 mL  $\times$  5). The organic layer was separated and the aqueous layer was extracted with diethyl ether (50 mL  $\times$  3). The combined organic layers were concentrated and purified (silica, hexane/ethyl acetate = 20/1) to give compound **7** (1.14 g, 5.97 mmol, 14.1 GBq, 91%).

[ $^{14}\text{C}$ -ring-(U)]4-(trifluoromethyl)benzenesulfonyl chloride (**9**): To a suspension of compound **8** (804 mg, 4.99 mmol, 11.3 GBq) in conc. HCl (2.5 mL) and AcOH (0.5 mL) was added  $\text{NaNO}_2$  (373 mg, 5.41 mmol) in water (1 mL) at  $-10^\circ\text{C}$ – $-15^\circ\text{C}$  and the mixture was stirred at  $-10^\circ\text{C}$ – $-15^\circ\text{C}$  for 1 h.  **$\text{SO}_2$  solution manufacture:**  $\text{SO}_2$  was introduced to AcOH (5 mL) for 20 min, CuCl (125 mg, 1.26 mmol) was added to the solution, and the introduction of  $\text{SO}_2$  was continued for 1 h. To the  $\text{SO}_2$  solution was added the diazotization reaction mixture at  $10^\circ\text{C}$  and the mixture was stirred at room temperature for 30 min. After diluting with water (20 mL), the reaction mixture was extracted with diethyl ether (30 mL  $\times$  3). The combined organic layers were concentrated and purified (silica, hexane/ethyl acetate = 30/1) to give compound **9** (611 mg, 2.50 mmol, 5.83 GBq, 52%).

## References

- [1] E. A. Krasnokutskaya, N. I. Semenischeva, V. D. Filimonov, P. Knochel, *Synthesis* **2007**, 81–84.
- [2] H. Urata and T. Fuchikami, *Tetrahedron Letters* **1991**, 32(1), 91–94.
- [3] K. W. Palmer, P. R. Resnick, *US patent: 5,475,165*.
- [4] G. E. Carr, R. D. Chambers, T. F. Holmes, D. G. Parker, *J. Chem. Soc., Perkin Trans. 1*, **1988**, 4, 921–926
- [5] *Organic Syntheses, Coll. Vol. 7*, **1990**, 508.

## THE USE OF TRITIUM RESULTING FROM NUCLEAR ACTIVITIES AS ENVIRONMENTAL TRACER

CORINA ANCA SIMION,<sup>a</sup> ELENA SIMION,<sup>b</sup> NICULINA PĂUNESCU,<sup>a</sup> NICOLAE MOCANU,<sup>a</sup> SALMA EL-SHAMALI,<sup>c,a</sup> STEFAN BURDA,<sup>c</sup> MANTA TANISLAV,<sup>d</sup> and DAN D. IONESCU<sup>e</sup>

<sup>a</sup>Horia Hulubei National Institute for Research and Development in Physics and Nuclear Engineering (IFIN-HH) Magurele-Ilfov, Romania

<sup>b</sup>National Environmental Protection Agency, Bucharest, Romania

<sup>c</sup>University of Agronomic Sciences and Veterinary Medicine, Bucharest, Romania

<sup>d</sup>University of Bucharest, Faculty of Geology and Geophysics, Romania

<sup>e</sup>National Institute for Historical Monuments, Bucharest, Romania

**Abstract:** The study presents some site-specific experimental data related to tritium occurrence in an area subjected to the influence of different nuclear activities implying tritium releases developed at Horia Hulubei National Institute for Physics and Nuclear Engineering. In these specific circumstances, tritium routinely released from IFIN-HH is a permanent presence in the area, thus becoming a convenient environmental tracer. By using tritium as an environmental tracer, investigations into its concentration in vegetation, air, surface water of a semi-natural pond, fish and in soil from the surface to the depth of ground water were measured. Results show the levels of tritium currently released from IFIN-HH are low, however it determined concentrations of the radionuclide higher in the environmental compartments of the investigated area than in reference areas not exposed to tritium. The experimental results regarding tritium distribution in the soil profiles have brought additional information for reconstituting the 'history' of the area, a necessary step in a complex activity dedicated to landscape restoration of the dendrologic park for sustainable development.

**Keywords:** Tritium; environmental tracer; liquid scintillation counting; sustainable development

**Introduction:** A survey regarding environmental tritium was recently performed in an area subjected to the influence of different nuclear activities implying tritium releases at IFIN-HH. Due to the permanent presence of tritium in this area, the results of this work were to be used for geo-hydrological and horticulture studies necessary for landscape restoration of a dendrologic park for sustainable development.

**Experimental: Investigated area description:** The investigated area is in the city of Magurele, about 2 km from IFIN-HH, and 10 km from Bucharest. The site has a quite long history lasting from the mid-nineteenth century, when 6 ha of boggy terrain with a chain of ponds started to be arranged as park of a lordly house Otetelesanu by Carl Friederich Wilhelm Meyer. By subsequent arrangements of the park, nowadays only a semi-natural pond of about 0.08 ha remains, populated with fish and supplied with water by underground springs and rainfall. The park can be considered a real dendrologic reservation, its tree and shrub inventory including some valuable species, both indigenous and exotic. Spontaneous vegetation, especially herbaceous species, completes the vegetation in the area.

**Materials and methods:** Environmental samples of soil (depth profile 0–20 cm), vegetation, surface water, condensed water vapours from air, and fish were collected from the area subjected to the influence of released tritium and from some reference areas not exposed to such



an influence. Samples of surface water and condensed water vapor collected from air with an air dehumidifier (TROTEC TTK 100 S) were subjected to simple distillation in the presence of  $\text{KMnO}_4$ . Soil, vegetation and fish samples were processed by azeotropic distillation with tritium free toluene.<sup>1,2</sup> For completing the site-specific data regarding the terrain lithology and vegetation of the dendrologic park with information about water distribution in the soil profile from surface to ground water level (terrain hydrology), some soil aliquots were collected at different depths from the bore holes performed by manual drilling in three sampling points (F1, F2, F3) inside the perimeter of the park and then processed and measured for their tritium content.

**Results and discussion:** The samples were collected from spring 2008 to the spring 2009, the tritium content is shown in Figure 1.

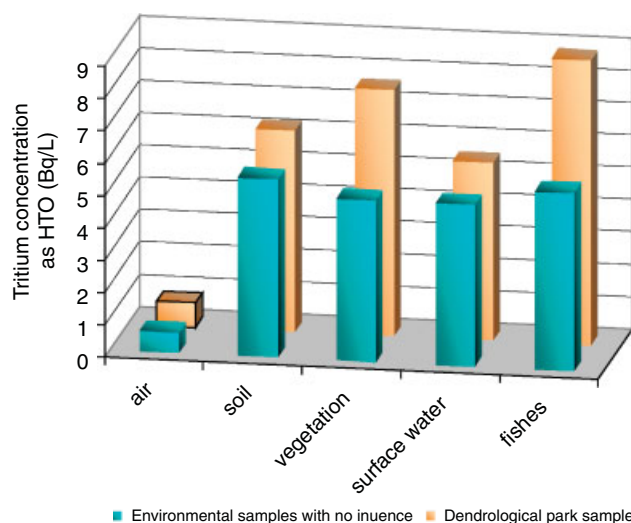


**Figure 1.** Tritium concentration in different environmental compartments of an area subjected to the influence of nuclear activities implying tritium releases (dendrologic park at Magurele) and reference areas.

The results are average values of parallel samples prepared with two scintillation cocktails (Insta-Gel Plus and Ultima Gold) and measured with three liquid scintillation spectrometers (Tri-Carb 1600 TR, Tri-Carb 2770 TR/SL, Quantulus 1220). The measurements on the Quantulus 1220, provided far better results than those performed in other two types of spectrometers.<sup>3–5</sup>

Tritium concentration associated with water filling the soil pores in the soil profile of the sampling points at the dendrologic park shows a water accumulation prevalently in the upper layers (dark gray, muddy clay, medium stiff consistency), at approx. 1.5 m depth, thus demonstrating that a surface water contamination is responsible for  $^3\text{H}$  rather than from ground water (Table 1). The higher level of tritium concentration in the depth range 1.50–1.70 m is due to 'remanent memory' property of muddy clay, associated with the rooting depth of vegetation here, could support the existence of an upper extended water layer placed above the ground water level, thus favouring the development of tree species having an horizontal distribution of roots and the collapse of tree species with revolving roots. The dark grey muddy clay of medium stiff consistency layer placed at different depths in the three sampling sites inside the park demonstrates the boggy origin of the terrain and the existence of an extended chain of ponds in the far past history of this place during the mid-nineteenth century.

**Conclusion:** The methodology applied in assessing tritium concentration in different compartments of the environment proved to be suitable to measure low levels of tritium.

Levels of tritium measurement were situated below maximum levels required by law.

Additionally, tritium analysis was successfully used to reconstruction of 'history' of previous geochemical and hydrological studies to be applied to sustainable development.

**Acknowledgements:** The authors wish to thank to the National Authority for Scientific Research Romania for funding PNCDI-II Nr. 51-053 / 2007 project.

## References

- [1] H. L. Volchok, G. De Planque (eds.), Soil Sampling, EML Procedures Manual, 26-th Edition, Environmental Measurements Laboratory, New York, **1983**, B-05.
- [2] Technical Reports Series No.295, Measurements of Radionuclides in Food and Environment (A Guidebook), IAEA Viena, **1989**, p. 27–28.
- [3] The Tritium Laboratory University of Miami/RSMAS Website, Tritium Laboratory. Environmental Level Measurements of Tritium, Helium and Chlorofluorocarbons (CFC's). Introduction [6 May 2005].
- [4] Ll. Pujol, J. A. Sanchez-Cabeza, *J. Radioanal. and Nucl. Chem.*, **1999**, 242 (2), 391.
- [5] W. Plastino, L. Kaihola, P. Bartolomei, F. Bella, *Radiocarbon* **2001**, 43(2A), 157.

**Table 1.** Experimental results on the site-specific geo-hydrological and horticultural characterization of the dendrologic park at Magurele by using tritium as environmental tracer

Sampling point	Soil profile depth [m]	Lithological properties	Tritium concentration in soil azeotropic distillates [Bq/L]	Absolute humidity [%]	Tritium concentration in soil [Bq/kg]	Rooting depth of vegetation	Ground water level [m]
F1	0.00–0.50	allochton filling soil	9.74 ± 1.30	11.1	1.08	Festuca sp., Poa sp., D. glomerata; Lolium sp., B. sempervirens	2.60
	0.50–0.70	allochton filling soil	4.13 ± 0.62	13.3	0.55		
	0.70–0.90	allochton filling soil	5.35 ± 0.76	16.1	0.86		
	0.90–1.10	allochton filling soil	–	–	–		
	1.10–1.30	allochton filling soil	5.05 ± 0.70	20.3	1.03		
	1.30–1.50	allochton filling soil	2.59 ± 0.38	21.4	0.55		
	1.50–1.70	dark gray, muddy clay, medium stiff consistency	7.18 ± 1.00	17.1	1.23		
	1.70–1.90	dark gray, silty sandy clay, soft–medium stiff consistency	3.39 ± 0.52	27.9	0.95		
	1.90–2.10	dark gray, silty sandy clay, soft–medium stiff consistency	–	–	–		
	2.10–2.40	dark gray, silty sandy clay, soft–medium stiff consistency	2.32 ± 0.37	24.6	0.57		
	2.40–2.60	dark gray, silty sandy clay, soft–medium stiff consistency	–	–	–		
	2.60–3.00	gray, clayey sand	–	–	–		
	0.00–0.30	allochton filling soil	4.96 ± 0.72	9.5	0.47	A. ursinum, R. ficaria, C. majus, A. ranunculoides, H. helix	2.40
F2	0.30–0.50	allochton filling soil	4.98 ± 0.68	11	0.55		
	0.50–0.70	allochton filling soil	3.61 ± 0.53	28.2	1.02		
	0.70–0.90	allochton filling soil	3.30 ± 0.51	10.6	0.35	S. ebulus. C. mas	
	0.90–1.10	allochton filling soil	–	–	–	S. ebulus. C. mas	
	1.10–1.30	dark gray, muddy clay, medium stiff consistency	4.47 ± 0.68	14.9	0.67	S. ebulus. C. mas	
	1.30–1.50	dark gray, muddy clay, medium stiff consistency	6.15 ± 1.04	11.1	0.68		
	1.50–1.70	dark gray, muddy clay, medium stiff consistency	4.66 ± 0.55	15.8	0.74		
	1.70–1.90	dark gray, muddy clay, medium stiff consistency	3.51 ± 0.55	16.1	0.56	A. campestre, A. negundo, Tilia sp.	
	1.90–2.10	dark gray, muddy clay, medium stiff consistency	2.56 ± 0.33	18.5	0.47	U. glabra	

**Table 1.** *Continued*

Sampling point	Soil profile depth [m]	Lithological properties	Tritium concentration in soil azo-tropic distillates [Bq/L]	Absolute humidity [%]	Tritium concentration in soil [Bq/kg]	Rooting depth of vegetation	Ground water level [m]
F3	2.10–2.30	dark gray, muddy clay, medium stiff consistency	3.70 ± 0.55	16.8	0.62	–	
	2.30–2.50	dark gray, muddy clay, medium stiff consistency	3.53 ± 0.53	16.8	0.6	–	
	2.50–2.70	dark gray, muddy clay, medium stiff consistency	2.95 ± 0.45	21.8	0.64	–	
	2.70–2.90	gray, clayey sand, with rare gravel	3.54 ± 0.55	24.5	0.87	–	
	2.90–3.10	gray, clayey sand, with rare gravel	3.02 ± 0.44	23.8	0.72	–	
	0.00–0.30	allochthon filling soil	3.96 ± 0.61	12.6	0.5	A. ursinum, R. ficaria, C. majus, A. ranunculoides, Geranium sp.	
	0.30–0.50	allochthon filling soil	2.84 ± 0.44	18	0.51	H. helix	
	0.50–0.70	allochthon filling soil	–	–	–	S. ebulus, Viburnum sp., C. monogyna, C. mas, Ligustrum sp., S. vulgaris	
	0.70–0.90	dark gray, muddy clay, medium stiff consistency	2.50 ± 0.37	21.5	0.54	S. ebulus, Viburnum sp., C. monogyna, C. mas, Ligustrum sp., S. vulgaris	
	0.90–1.10	dark gray, muddy clay, medium stiff consistency	–	–	–	S. ebulus, Viburnum sp., C. monogyna, C. mas, Ligustrum sp., S. vulgaris	
	1.10–1.30	dark gray, muddy clay, medium stiff consistency	–	–	–	S. ebulus, Viburnum sp., C. monogyna, C. mas, Ligustrum sp., S. vulgaris	
	1.30–1.50	dark gray, muddy clay, medium stiff consistency	4.71 ± 0.68	49.9	2.35	F. excelsior, A. hippocastanum, P. alba, U. Glabra, Q. robur, Platanus sp.	
1.50–1.70	gray, clayey sand, with rare gravel	–	–	–	–		

## 21<sup>ST</sup> CENTURY OPPORTUNITIES TO ENHANCE THE SUPPLY AND APPLICATIONS OF MEDICAL ISOTOPES

G.L. TROYER,<sup>a</sup> R.E. SCHENTER,<sup>b</sup> AND N.R. STEVENSON<sup>b,c</sup>

<sup>a</sup>Citizens for Medical Isotopes, PO Box 802, Richland WA 99352, USA

<sup>b</sup>Advanced Medical Isotope Corp., 6208 W. Okanogan Avenue, Kennewick, WA 99336, USA

<sup>c</sup>Clear Vascular Inc., 717 Fifth Ave., 14<sup>th</sup> Floor, New York, NY 10022, USA

**Abstract:** Research in extending medical isotopes for the diagnosis and treatment of numerous health maladies is hampered by outages and upsets in major supply sources. Investigations in cures for brain cancer (<sup>211</sup>At), HIV/AIDS virus (<sup>213</sup>Bi), and even bacterial vectors are either in reduced progress mode or have been cancelled until isotopes become available. Examples of several key radioactive medical isotopes include <sup>99m</sup>Tc for diagnostics, <sup>131</sup>I for non-Hodgkin's Lymphoma and thyroid cancer, Actinium-225 for acute myelogenous leukemia, and <sup>67</sup>Cu for lymphoma cancer. Possibilities for developing commercially viable sources using compact accelerators and next generation research and production reactors are discussed.

**Keywords:** activation; cancer; diagnosis; fast; isotope; medical; production; reactor; thermal; treatment

**Introduction:** In 1977, Dr. Rosalyn Yalow was awarded the Nobel Prize for pioneering work in and invention of radioisotopic immunoassay of endogenous insulin in man.<sup>1</sup> Since then, numerous examples show successful advancement of her methods for the targeted medical application of isotopes in tens of thousands of daily medical diagnostics.

In addition to diagnostics, medical isotopes have been developed into several direct or in situ therapy methods such as <sup>131</sup>I for non-Hodgkin's Lymphoma<sup>2</sup> and thyroid cancer,<sup>3</sup> <sup>225</sup>Ac for acute myelogenous leukemia,<sup>4</sup> <sup>67</sup>Cu for lymphomas,<sup>5</sup> <sup>211</sup>At for research in brain cancer therapy,<sup>6</sup> <sup>213</sup>Bi for research in HIV/AIDS virus therapy<sup>7</sup> and many others.<sup>8</sup>

**Results and Discussion:** Significant advancement in medical isotope applications is limited by availability and approval of currently rare but attractive isotopes. Traditional sources such as isotope production in research reactors are currently suffering upsets, end-of-life cycle issues and limited activation regimes. The US National Academy of Sciences has identified supply issues due to reduced national funding<sup>9</sup>. A production risk is the 2008 decision by Atomic Energy Canada Ltd.<sup>10</sup> canceling the MAPLE Reactor development targeted for medical isotopes. This decision along with issues regarding highly enriched uranium<sup>10</sup> impacts production of <sup>99</sup>Mo/<sup>99m</sup>Tc affecting over 70,000 medical procedures per day<sup>8</sup> in North America. Major suppliers in Europe<sup>10</sup> South Africa, and Australia have also shown supply interruptions or limitations<sup>10</sup> These world reactor primary suppliers are shown in Table 1. Additional and newer reactors and technologies are needed to fill the gap.

A number of isotopes as shown in Table 2 are technically available for use in medical applications<sup>10</sup> However, due to production challenges, many such as <sup>67</sup>Cu for lymphoma research<sup>5</sup> have limited availability, making research development and clinical trials difficult to the point of cancellation.

**Table 1.** World Nuclear Reactor Medical Isotope Producers

Reactor Facility <sup>[8]</sup>	% World Supply		Startup
	<sup>99m</sup> Tc	<sup>131</sup> I	
NRU at Chalk River in Canada (supplied via MDS Nordion)	40	Small	1957
HFR at Petten in Netherlands (supplied via IRE and Tyco)	30	Small	1962
BR2 at Mol in Belgium (supplied via IRE and Tyco)	12	Small	1964
Osiris & Orphee at Saclay in France (supplied via IRE)	3	75	1967
FRJ-2/FRM-2 at Julich in Germany (supplied via IRE)	Small	Small	1967
LVR-15 at Rez in Czech Republic	Small	Small	1957
HFETR at Chengdu in China	Small	Small	1979
Safari in South Africa (supplied from NTP)	15	25	1965
Opal in Australia (supplied from ANSTO)	Small	Small	2006

**Table 2.** Common medical isotopes sorted by use category and production method<sup>12</sup>

Purpose	Accelerator-produced	Reactor-produced
Diagnostic Isotopes	<sup>11</sup> C, <sup>13</sup> N, <sup>15</sup> O, <sup>18</sup> F, <sup>55</sup> Fe, <sup>57</sup> Co, <sup>61</sup> Cu, <sup>64</sup> Cu, <sup>67</sup> Ga, <sup>74</sup> As, <sup>76</sup> Br, <sup>81m</sup> Kr, <sup>82m</sup> Rb, <sup>94m</sup> Tc, <sup>97</sup> Ru, <sup>111</sup> In, <sup>123</sup> I, <sup>124</sup> I, <sup>179</sup> Ta, <sup>201</sup> Tl	<sup>3</sup> H, <sup>14</sup> C, <sup>51</sup> Cr, <sup>64</sup> Cu, <sup>97</sup> Ru, <sup>99m</sup> Tc, <sup>123</sup> I, <sup>131</sup> I, <sup>133</sup> Xe, <sup>153</sup> Gd, <sup>195m</sup> Pt
Therapeutic Isotopes	<sup>64</sup> Cu, <sup>67</sup> Cu, <sup>77</sup> Br, <sup>88m</sup> Br, <sup>88</sup> Y, <sup>89</sup> Zr, <sup>103</sup> Pd, <sup>111</sup> In, <sup>124</sup> I, <sup>186</sup> Re, <sup>211</sup> At	<sup>32</sup> P, <sup>47</sup> Sc, <sup>60</sup> Co, <sup>64</sup> Cu, <sup>67</sup> Cu, <sup>89</sup> Sr, <sup>90</sup> Sr, <sup>90</sup> Y, <sup>103</sup> Pd, <sup>103</sup> Ru, <sup>106</sup> Ru, <sup>109</sup> Cd, <sup>109</sup> Pd, <sup>117m</sup> Sn, <sup>115</sup> Cd, <sup>125</sup> I, <sup>131</sup> I, <sup>137</sup> Cs, <sup>145</sup> Sm, <sup>153</sup> Sm, <sup>165</sup> Dy, <sup>166</sup> Dy, <sup>166</sup> Ho, <sup>169</sup> Er, <sup>169</sup> Yb, <sup>180</sup> Tm, <sup>175</sup> Yb, <sup>177</sup> Lu, <sup>186</sup> Re, <sup>188</sup> Re, <sup>192</sup> Ir, <sup>195m</sup> Pt, <sup>198</sup> Au, <sup>199</sup> Au, <sup>211</sup> At, <sup>213</sup> Bi, <sup>225</sup> Ac, <sup>241</sup> Am

Emerging isotopes of interest need to have a half-life sufficient for use, but not too long as to continue an unnecessary exposure risk. Depending on source or preparation, attractive half-lives are a few hours to a few days. These short lives require generation within reasonable shipping distances, sometimes requiring generation at the use point either from an isotope generator or an activation method. An example is  $^{18}\text{F}$  For Positron Emission Tomography.<sup>11</sup>

A usefully lived isotope must also have a decay radiation compatible with the application. For diagnostic imaging, a positron or gamma emitter is desired in order for the photon to traverse body tissues to the image sensors. For *in-situ* therapy, a moderate energy beta or high energy alpha emitter is desirable to control collateral effects.

The third and most important feature is the affinity to bind to a chemical transfer compound which will seek the area of interest. Chelating compounds attachable to monoclonal antibodies tailored for target cell affinity are attractive allowing metal element isotopes to be used. In other situations such as thyroid cancer, the natural uptake of iodine by the thyroid makes  $^{131}\text{I}$  the isotope of choice.

Several opportunities exist to use emerging developments in biological and nuclear technologies for production and use of medical isotopes. Conventional approaches use traditional negative ion cyclotrons and thermal reactors. However, certain isotopes are most readily made by tailoring or selecting the reactor neutron energy spectrum. The energies and isotopes identified in Table 3 imply how neutron generators and fast spectrum reactors might be developed or deployed. New fast spectrum neutron reactor designs could include a few production tubes for desired and rare isotopes.

**Table 3.** Major Medical Isotopes Production Neutron Energy Ranges

Neutron Energy	Isotope
Thermal-Epithermal(0.01 eV-10 keV)	$^{75}\text{Se}$ , $^{89}\text{Sr}$ , $^{90}\text{Y}$ , $^{103}\text{Pd}$ , $^{125}\text{I}$ , $^{131}\text{I}$ , $^{127}\text{Xe}$ , $^{131}\text{Cs}$ , $^{153}\text{Gd}$ , $^{153}\text{Sm}$ , $^{165}\text{Dy}$ , $^{166}\text{Ho}$ , $^{177}\text{Lu}$ , $^{186}\text{Re}$ , $^{188}\text{W}$ , $^{192}\text{Ir}$ , $^{198}\text{Au}$ , $^{223}\text{Ra}$ , $^{225}\text{Ac}$
Fast (10 keV-1.0 MeV)	$^{99}\text{Mo}$ , $^{117m}\text{Sn}$
High Energy (1.0 MeV-10 MeV)	$^{32}\text{P}$ , $^{33}\text{P}$ , $^{57}\text{Co}$ , $^{62}\text{Cu}$ , $^{64}\text{Cu}$ , $^{67}\text{Cu}$ , $^{89}\text{Sr}$
14 MeV	$^{99}\text{Mo}$ , $^{225}\text{Ac}$

Emerging methods will use photon, proton, neutron, and electron accelerators for multiple smaller suppliers located near usage centers.<sup>12</sup> In addition, both Lawrence Berkeley National Laboratory<sup>12</sup> and Moscow State Engineering Physics Institute<sup>13</sup> are advancing compact neutron generators with flux densities approaching a research reactor.

Use of  $^{225}\text{Ac}$  and its progeny provide four locally penetrating ( $\sim 50\text{--}100\text{ nm}$ ) high energy alpha particles in chain as shown in Figure 1. However, the decay physics energies can cause the recoiling progeny atoms to separate ( $\sim 100\text{ nm}$ ) from the carrier molecule both physically and chemically allowing these to migrate to healthy tissues. Recent research<sup>14,15</sup> has shown that several  $^{225}\text{Ac}$  atoms can be encased in a liposome structure which localizes the progeny.

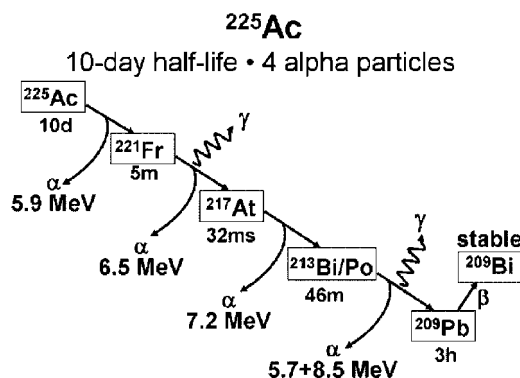


**Figure 1.**  $^{225}\text{Ac}$  decay path. The transitions from  $^{213}\text{Bi}$  to  $^{209}\text{Pb}$  contain branches with two alpha fractions.

The utility of the most widely used imaging isotope,  $^{99m}\text{Tc}$ , stems from good fission yield of  $^{99}\text{Mo}$  as a generator from  $^{235}\text{U}$  fissions. Recent supply interruptions have stimulated consideration and investments in alternate methods and sources such as a liquid fuel reactor, an electron accelerator beam for producing gammas and neutrons, and compact neutron generators.

**Conclusions:** Medical isotopes provide attractive avenues for both medical diagnosis and therapies. Existing and emerging technologies in biology and medical isotope production can be utilized to provide needed supplies for health improvements. The medical profession, medical research institutes, pharmacy businesses, and nuclear technologies must join forces to further encourage the use of and educate people in the advantages of medical isotopes.

## References

- [1] R. S. Yalow, S. A. Berson, *J. Clin. Invest.* **1960**, 391157, PMID 13846364.
- [2] Glaxosmithkline, *Tositumomab/I-131 tositumomab*, U.S. FDA Lic. 1727, Dec 22 2004.

- [3] Draximage, Inc., *Kit for the Preparation of Sodium Iodide I-131 Capsules and Solution USP Therapeutic–Oral*, NDA 21–305, U. S. CDER, Dec 2, 2002.
- [4] S. Satz and S. Schenter, *Method of Producing Actinium 225 and Daughters*, U. S. Patent 6,680,993, Jan 20 2000.
- [5] S. J. DeNardo, G. L. DeNardo, D. L. Kukis, S. Shen, L. A. Kroger, D. A. DeNardo, D. S. G., G. R. Mirick, Q. Salako, L. F. Mausner, S. C. Srivastava and C. F. Meares, *J. Nuc. Med.* **1999**, *40*, 302.
- [6] M. R. Zalutsky, *J. Nuc. Med.* **2005**, *46*, (Suppl) 151S.
- [7] E. Dadachova, M. C. Patel, S. Toussi, C. Apostolidis, A. Morgenstern, M. W. Brechbiel, M. K. Gorny, S. Zolla-Pazner, A. Casadevall, and H. Goldstein, *PLoS Medicine*, **2006**, *3*(11): e427 DOI: 10.1371/journal.pmed.0030427.
- [8] World Nuclear Association, *Radioisotopes in Medicine*, March 2009. Retrieved Mar 27, 2009 from <http://www.world-nuclear.org/info/inf55.html>.
- [9] National Academy of Science, Nat. Acad. Press, ISBN: 978-0-309-11067-9, 2007.
- [10] G. L. Troyer and R. E. Schenter, MARC VIII, Kailua-Kona HI, 2009.
- [11] J. Katzaroff, Adv Med Iso Corp, Press Release, March 4, 2008. Retrieved Mar 27, 2009 from <http://www.isotopeworld.com/newsmedia/amicinthenews/297/>.
- [12] K. Leung; US Pat. 6,907,097, University of California, June 14, 2005.
- [13] A. S. Tsybin, *App. Rad. and Iso.* **1997**, *48*, 1577.
- [14] G. Sgouros, S. Sofou, J. L. Thomas, M. R. McDevitt and D. A. Scheinberg, 4th Alpha-Immunotherapy Symposium, 28–29 June 2004, Düsseldorf, Germany. Retrieved Mar 27 2009 from [http://itu.jrc.ec.europa.eu/fileadmin/Documents/Alpha-Immunotherapy/pdf/23\\_sgour.pdf](http://itu.jrc.ec.europa.eu/fileadmin/Documents/Alpha-Immunotherapy/pdf/23_sgour.pdf).
- [15] S. Sofou, J. L. Thomas, H. Lin, M. R. McDevitt, D. A. Scheinberg, and G. Sgouros, *J. Nucl. Med.* **2004**, *45*, 253.

## SYNTHESIS OF [2-<sup>14</sup>C] 2-METHOXYPYRIMIDINE-5-CARBOXYLIC ACID

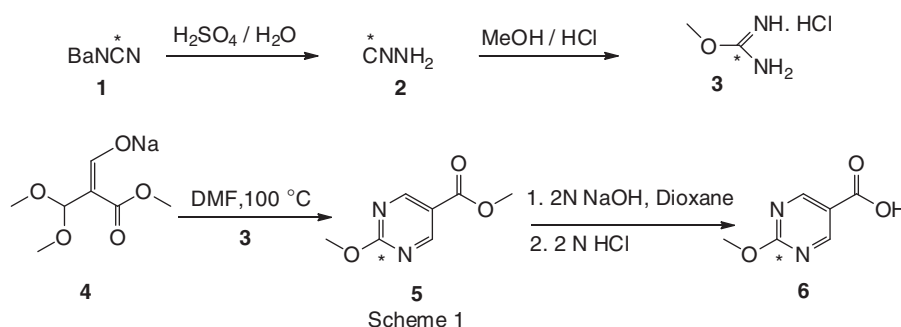
GILIYAR ULLAS,<sup>a</sup> AND AKULA MURTHY<sup>b</sup>

<sup>a</sup>PerkinElmer Health Sciences Inc., 549 Albany Street, Boston, MA 02118, USA

<sup>b</sup>Department of Radiology, The University of Tennessee Medical Center, Knoxville, TN 37920, USA

**Keywords:** [<sup>14</sup>C] 2-methoxypyrimidine-5-carboxylic acid; [<sup>14</sup>C] O-methylisourea hydrochloride.

**Introduction, Results and Discussion:** A versatile method for <sup>14</sup>C ring labeling at the 2- position of 2- methoxypyrimidine-5-carboxylic acid **6** has been developed after unsuccessful attempts to label the title compound at the carboxyl function using traditional approaches. The title compound has been prepared from [<sup>14</sup>C] barium cyanamide **1** in about 14 % yield via the intermediate [<sup>14</sup>C] O-methylisourea hydrochloride **3** as depicted in the Scheme 1.



Scheme 1.

The approach can also be applied to other pyrimidine carboxylic acids with <sup>14</sup>C label at the 4-, 5- and/or 6-position using appropriately labeled precursor **4**. The results and the full experimental details of this investigation has been the subject of a research article published earlier<sup>1</sup>.

## Reference

- [1] Akula Murthy and Giliyar Ullas *J. Label. Compd. Radiopharm* **2009**, *52*, 114–116.

SYNTHESIS OF (+/–)-[<sup>3</sup>H] LEVOSIMENDAN AND ITS METABOLITES

SRIRAJAN VAIDYANATHAN and BRUCE W SURBER

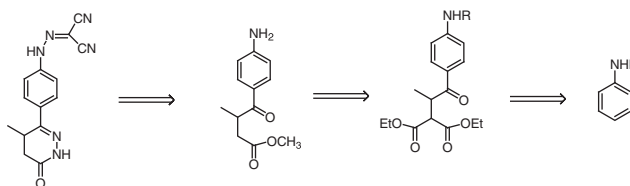
Abbott Laboratories, Process R &amp; D, AP9, 100 Abbott Park Road, IL 60064, USA

**Abstract:** [<sup>3</sup>H] Levosimendan was synthesized via (+/–) OR-1855-3H starting from acetanilide. An intermediate phenyl ketone was tritiated by tritium/hydrogen isotope exchange chemistry using Crabtree's catalyst.

**Keywords:** Levosimendan; Crabtree's catalyst; tritium/hydrogen isotope exchange

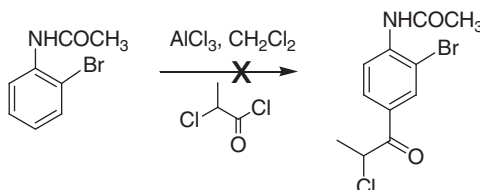
**Introduction:** Levosimendan is a calcium sensitizer that can be administered intravenously (IV) to patients with acute decompensated congestive heart failure (CHF).<sup>1</sup> At therapeutic dosages levosimendan enhances myocardial contractility without increasing oxygen requirements, and causes coronary and systemic vasodilation. In clinical trials levosimendan has been shown to reduce the risk of worsening CHF or death compared with dobutamine and placebo in patients with decompensated CHF. The drug is well tolerated, has minimal potential for interactions with other drugs, and does not reduce short- or long-term (30-day) survival.<sup>2</sup>

**Results and Discussion:** Radioactive levosimendan was required for drug metabolism in vivo studies. This initiated the task of exploring tritium-labeled synthesis of levosimendan. The initial approach was to try catalytic hydrogen isotope exchange to get tritium in the molecule in a short time. The common exchange reaction methods using Crabtree's, platinum black or rhodium trichloride catalysts did not provide any appreciable quantity of [<sup>3</sup>H] levosimendan. So the alternative approach was to incorporate tritium by reaction of a suitable precursor. The retro-synthetic analysis is shown in Scheme 1. The aniline derivative can be acylated to provide keto bis-carboxylate. This keto bis-carboxylate in turn can be converted into keto ester. The ring closing of keto ester with hydrazine and subsequent addition of malononitrile should provide the final product.



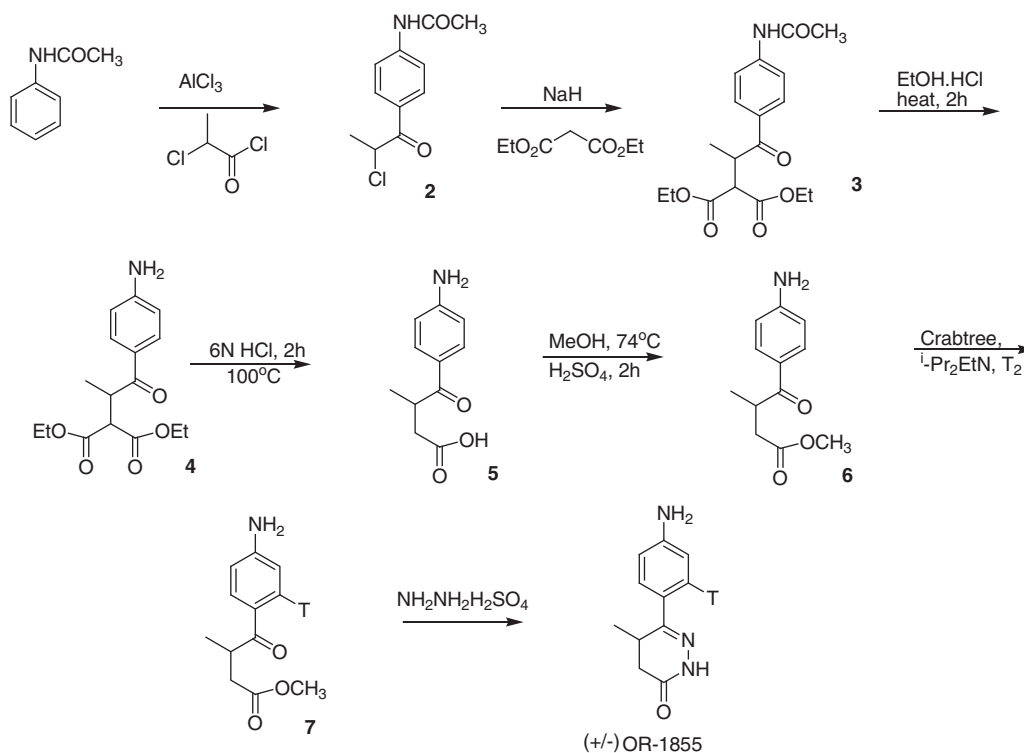
**Scheme 1.** Retrosynthetic analysis for the synthesis of levosimendan.

The introduction of tritium was envisioned by starting from a halogen aniline precursor, which can be reduced at an appropriate stage. Friedel-Crafts acylation of 2-bromoacetanilide using 2-methylchloroacetyl chloride in the presence of AlCl<sub>3</sub> did not provide any appreciable product (Scheme 2).



**Scheme 2.**

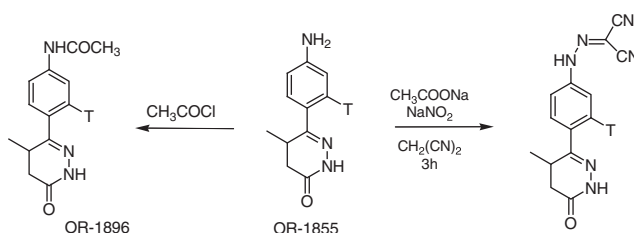
Crabtree-catalyzed hydrogen-tritium isotope exchange with T<sub>2</sub> was then revisited on the more appropriate keto ester intermediate 6.<sup>3</sup> Indeed, Crabtree's catalytic exchange can be envisioned to give tritiated product at other stages of the synthesis, being well known for labeling acetanilides. However, to minimize the number of labeled steps, ketone 6 became the focus of the labeling step. Thus, acylation of acetamide using 2-methylchloroacetyl chloride in the presence of aluminum chloride provided 2 in 77% yield. Compound 2 on treatment diethyl malonate in presence of sodium hydride afforded 3, which was purified by flash column chromatography.



Scheme 3.

Compound **3** was reacted with ethanolic hydrogen chloride to provide **4** in 95% yield. Compound **4** was converted into **5** by treating with 6N HCl and **5** was esterified using methanol/sulfuric acid to provide **6** in 50% yield.<sup>4</sup> Compound **6** was reacted with Crabtree's catalyst in the presence of tritium gas in dichloromethane to provide 27 mCi of **7** after preparative thin layer chromatography. The position of the tritium was determined by tritium NMR spectroscopy. Crabtree's catalyst is known to direct tritium to sites ortho to the carbonyl directing group so this regioselectivity is not surprising. However, we are not aware of any other examples in the literature that have a free amine para to the directing group. Actually, where one does see this combination of functionality in the exchange literature, the regioselectivity is reversed owing to the directing force of the amine on the iridium catalyst containing an acetylacetonate ligand and tritium exchange occurs ortho to the amine in 4-aminoacetophenone.<sup>5</sup> Ring closing of the keto ester **7** was achieved using hydrazine sulfate to afford 15 mCi of [<sup>3</sup>H]OR-1855 (Scheme 3).

Acetylation of [<sup>3</sup>H]OR-1855 with acetyl chloride provided 3 mCi of crude [<sup>3</sup>H]OR-1896. [<sup>3</sup>H]OR-1855, reacted with malonitrile in the presence of sodium acetate and sodium nitrite, provided 6 mCi of 97% pure (+/-)[<sup>3</sup>H] levosimendan after purification by preparative HPLC (Scheme 4).<sup>6</sup> The specific activity of (+/-)[<sup>3</sup>H] OR-1855 was measured as ~0.1 Ci/mmol by mass spectrometry.



Scheme 4.

## References

- [1] H. M. Hona, K. P. Weiss, *Ann. N Y Acad. Sci.* **2005**, 1047, 248–258.
- [2] D. M. Kopustinskiene, P. Pollesello, N. E. Saris, *Eur. J. Pharmacol.* **2001**, 428, 311–314.
- [3] D. Hesk, P. R. Das, B. Evans, *J. Label. Comp. Radiopharm.* **1995**, 36(5), 497–502.
- [4] (a) F. F. Owings, M. Fox, C. J. Kowalski, N. H. Baine, *J. Org. Chem.* **1991**, 56, 1963; (b) F. J. McEvoy, G. R. Allen, *J. Org. Chem.* 1973, 38, 4044; (c) A. M. Armitage, A. M. Crowe, D. A. Lawrie, R. D. Saunders, S. Singh, *J. Label. Comp. Radiopharm.* 1988, 27, 331; (d) B. E. Burpitt, L. P. Crawford, B. J. Davies, J. Mistry, M. B. Mitchell, K. D. J. Pancholi, *Heterocyclic Chem.* 1988, 25, 1689.



- [5] M. J. Hickey, J. J. Jones, L. P. Kingston, W. J. S. Lockley, A. N. Mather, B. M. McAuley, D. J. Wilkinson, *Tet. Lett.* 2003, 44, 3959–3961.
- [6] (a) L. Zhang, H. Song, Y. Wang, A. Song, *Shenyang Yaoke Daxue Xuebao* 2004, 21, 22–23; (b) H. O. Haikala, E. J. Honkanen, K. K. Lonnberg, P. T. Nore, J. J. Pystynen, A. M. Luiro, A. K. Pippuri, *Brit. UK Pat. Appl.* 1990, 35 pp. CODEN: BAXXDU GB 2228004 A 19900815 Application: GB 90–1853 19900126. Priority: GB 89–3130 19890128.

## SYNTHESIS OF $^2\text{H}$ -, AND $^3\text{H}$ -LABELED INDOLE AND L-TRYPTOPHAN

ELZBIETA WINNICKA AND MARIANNA KANSKA

Department of Chemistry, University of Warsaw, Pasteur Str. 1, 02-093 Warsaw, Poland

**Abstract:** The isotopomers of indole and L-tryptophan (L-Trp) labeled with deuterium and tritium have been obtained using chemical and enzymatic methods. The heavy and tritiated water have been used as a sources of stable and radioactive label.

**Keywords:** deuterium; indole; labeling; tritium; L-tryptophan

**Introduction:** L-Tryptophan, L-Trp, is a primary intermediate in the biosynthesis of some hormones such as tryptamine and serotonin. Some of their derivatives also exhibit pharmaceutical activity.<sup>1,2</sup> In order to investigate the metabolic pathways involving L-Trp and its derivatives, a synthesis of specifically labeled isotopomers of L-Trp was required.

In the literature, there are several synthetic routes described leading to the preparation of different isotopomers of L-Trp labeled specifically or not specifically.<sup>3–5</sup> For these purposes we have also made numerous attempts to develop the methods of synthesis of isotopomers of L-Trp labeled with deuterium and tritium. Some of them were published by us earlier<sup>6,7</sup> and other are presented in this report.

**Results and discussion: Synthesis of isotopomers of L-Trp labeled in the 5', 6' and 7' positions of the indole moiety.** The precursors for the deuterium labeled isotopomers were the appropriate halogenated regioisomers. All deuteration procedures were monitored by means of deuterium incorporation by  $^1\text{H}$  NMR. TLC and column chromatography were used to purify the products. Radioactivity was measured using liquid scintillation counting (LSC).

**Isotopomers of indole labeled with deuterium.** The following isotopomers: [5- $^2\text{H}$ ], **1**, [6- $^2\text{H}$ ]-, **2**, and [7- $^2\text{H}$ ]-indole, **3**, were prepared by reduction of 5-bromoindole, 6- and 7-chloroindole, respectively, with sodium borodeuteride dissolved in  $\text{CH}_3\text{OD}$  as shown in Figure 1.

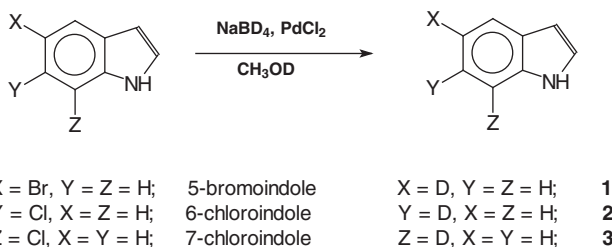


Figure 1. Synthesis of isotopomers of indole.

The reaction was catalyzed by  $\text{PdCl}_2$  and carried out at  $-10^\circ\text{C}$  and produced products in about 30% yield. The extent of incorporation of deuterium into the given positions of the indole ring was about 90% based on integration of the 500 MHz  $^1\text{H}$  NMR spectrum.

**Synthesis of isotopomers of L-Trp.** The isotopomers of [5'- $^2\text{H}$ ]-, **4** [2], [6'- $^2\text{H}$ ]-, **5**, and [7'- $^2\text{H}$ ]-L-Trp, **6**, were synthesized by coupling of **1**, **2** and **3** indoles, respectively, with *S*-methyl-L-cysteine using the specific activity of enzyme L-Tryptophan Indole-Lyase (TPase, EC 4.1.99.1) as shown in Figure 2. The products were prepared in about 30% yield.

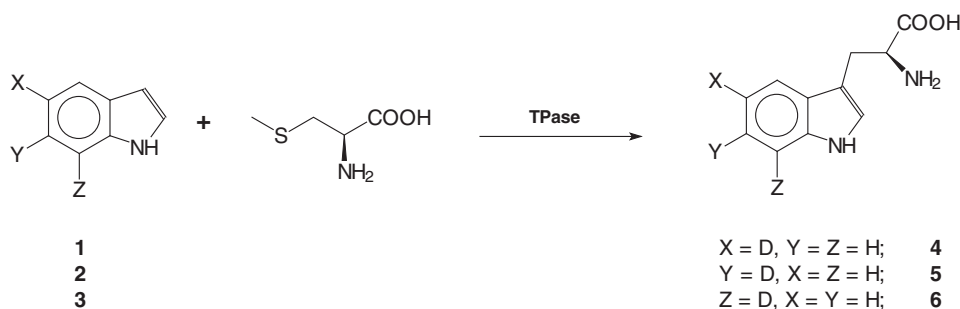


Figure 2. Enzymatic synthesis of isotopomers of L-Trp.

**Synthesis of multiply labeled isotomers of L-Trp by isotope exchange.** Isotope exchange catalyzed by Adams catalyst ( $\text{Pt}^0$ ) was carried out at  $100^\circ\text{C}$  between isotopic water and L-Trp. 40% NaOH was added to permit complete dissolution of the amino acid.

- a) deuterium labeled  $[2',5',6',7'\text{-}^2\text{H}_4]$ -L-Trp, **7**, using 40% NaOD and  $\text{D}_2\text{O}$  as exchanging medium;  
b) tritium labeled  $[2',5',6',7'\text{-}^3\text{H}_4]$ -L-Trp, **8**, using 40% NaOH and HTO as exchanging medium;  
c) doubly labeled with deuterium and tritium  $[2',5',6',7'\text{-}^2\text{H}/^3\text{H}_4]$ -L-Trp, **9**, using 40% NaOD and DTO as exchanging medium.

Labeled **7**, **8** and **9** were synthesized in 80% chemical yield. The level of deuteration was found to exceed 85% based on integration of the 500 MHz  $^1\text{H}$  NMR spectrum.

**Acknowledgements:** This work was sponsored by grant 120000-501/68-BW-179221.

## References

- [1] A. Ek, B. Witkop, *J. Am. Chem. Soc.* **1953**, *75*, 500–501.
- [2] S. Udenfriend, W. W. Clark, E. Titus, *J. Am. Chem. Soc.* **1953**, *75*, 501–502.
- [3] B. Bak, J. J. Led, E. J. Pedersen, *Acta Chem Scand* **1969**, *23*, 3051–3054.
- [4] P. Roepe, D. Gray, J. Lugtenburg, E. M. M. Van der Berg, J. Herzfeld, K. J. Rothschild, *J. Am. Chem. Soc.* **1988**, *110*, 7223–7224.
- [5] D. M. Kiick, R. S. Phillips, *Biochemistry* **1988**, *27*, 7339–7344.
- [6] T. R. Bosin, M. G. Raymond, A. R. Buckpitt, *Tetrahedron Letters* **1973**, *47*, 4699–4700.
- [7] D. S. Wishart, B. D. Sykes, F. M. Richards, *Biochim. Biophys. Acta* **1993**, *1164*, 36–46.

## AN EFFICIENT SYNTHESIS OF RADIOLABELLED SANT-1

YINSHENG ZHANG AND WAYNE T. STOLLE

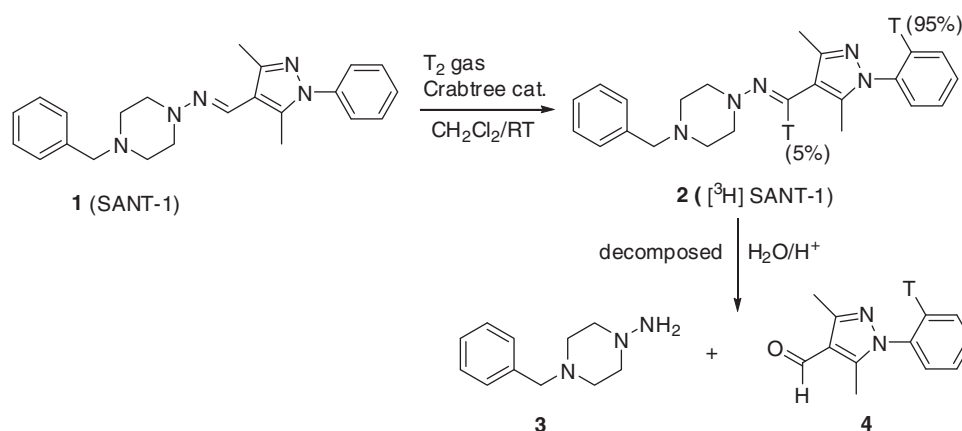
Radiochemistry Group, Research API, Pfizer Global Research and Development, Groton, CT 06340, USA

**Abstract:** SANT-1, (4-benzyl-N-[(3,5-dimethyl-1-phenyl-1H-pyrazol-4-yl)methylene]-1-piperazinamine), is a reference compound and used for establishing a biological assay for the smoothed receptor (SMO). Preparation of radiolabelled material was needed for establishing radioligand protein/receptor binding studies.  $[^3\text{H}]$ SANT-1 was prepared with a radiochemical purity of  $>95\%$  (25 Ci/mmol) using direct Crabtree catalyzed T/H exchange method, while  $[^{14}\text{C}]$ SANT-1 was synthesized at 98.2% radiochemical purity (54 mCi/mmol) using  $[^{14}\text{C}]$ dimethylformamide. The details of the syntheses of radioactive labelled SANT-1 were presented.

**Keywords:**  $^{14}\text{C}$ -labelled;  $^3\text{H}$ -labelled;  $[^{14}\text{C}]$ DMF; selective formylation

**Introduction:** SANT-1, 4-benzyl-N-[(3,5-dimethyl-1-phenyl-1H-pyrazol-4-yl)methylene]-1-piperazinamine, is a potent inhibitor of aberrant growth states resulting from hedgehog mediated patched (ptc) loss-of-function or smoothed (SMO) gain-of-function. This compound may also inhibit the hedgehog pathway in normal cells, where normal levels of hedgehog signaling are unwanted.<sup>1</sup> The radiolabelled SANT-1 was needed to establish a radioligand assay for various SMO receptor antagonists.<sup>1,2</sup> A new synthetic approach needed to be developed. A tritium labelled analog was prepared by direct T/H exchange with help of the Crabtree catalyst, while carbon-14 labelled analog was synthesized in a few steps using  $[^{14}\text{C}]$ dimethylformamide.

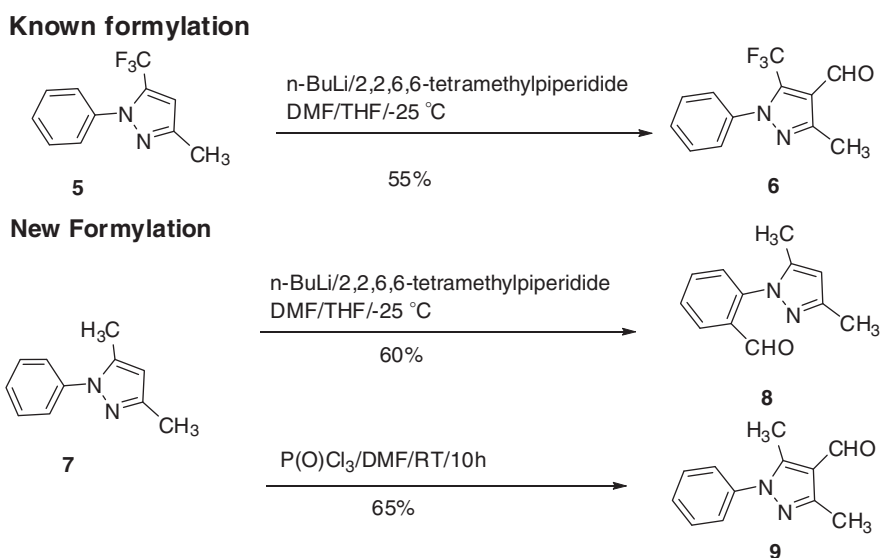
### Results and Discussion:



**Scheme 1.** Crabtree catalyzed tritiation of SANT-1.

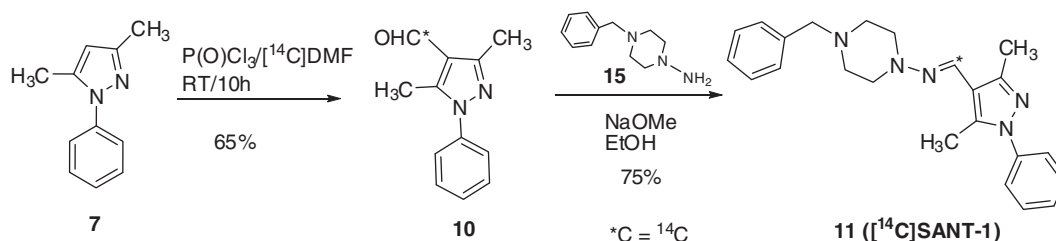
The tritiation of SANT-1 was first performed using a Crabtree catalyzed T/H exchange method as shown in Scheme 1. Based on our previous experience, the nitrogen of the pyrazole ring would direct the location of the tritiation via a 5-membered iridium metalocycle intermediate.  $^3\text{H-NMR}$  indicated tritium incorporation in the aromatic ring (95%) as expected and at the imine carbon (5 %). However, the purification of the tritium labelled compound turned out to be very difficult. We attempted the purification by using 3 different reverse and normal phase HPLC columns with or without adding acids (formic acid or TFA) or a base ( $\text{Et}_3\text{N}$ ). We were able to isolate a batch of 95% pure  $[\text{}^3\text{H}]$  SANT-1 using a Phenomenex silica column (normal phase,  $\text{Et}_3\text{N}/\text{MeOH}/\text{CH}_2\text{Cl}_2$ ). However, the purity of tritium labelled material in MeOH decreased from 95% to 75% after 15 h at  $0^\circ\text{C}$ . One of the decomposition products was  $[\text{}^3\text{H}]$ 3,5-dimethyl-1-phenyl-1H-pyrazole-4-carbaldehyde (**4**), as identified by LC-MS analysis. Since the  $[\text{}^3\text{H}]$  SANT-1 was unstable, it was necessary to consider a carbon-14 label synthesis.

In order to predict the stability of carbon-14 labelled SANT-1 due to radiation effects,  $[\text{}^{14}\text{C}]\text{CuCN}$  (5 mg) and unlabelled SANT-1 (5 mg) were mixed well and stored at room temperature for 5 days. The HPLC analysis showed no decomposition product. Therefore, the synthesis of  $[\text{}^{14}\text{C}]$ SANT (**1**) was designed and carried out. The shortest way to introduce carbon-14 label in  $[\text{}^{14}\text{C}]$  SANT-1 was to label the carbonyl group of 3,5-dimethyl-1-phenyl-1H-pyrazole-4-carbaldehyde (**9**) by the selective formylation of the heteroaromatic ring of 3,5-dimethyl-1-phenyl-1H-pyrazole (**7**, Scheme 2).



**Scheme 2.** The formylation of compound **7**.

Using published reaction conditions<sup>3</sup> for a similar compound, 3-methyl-1-phenyl-5-(trifluoromethyl)-1H-pyrazole (**5**), interestingly, starting with 3,5-dimethyl-1-phenyl-1H-pyrazole (**7**) we only obtained 2-(3,5-dimethyl-1H-pyrazol-1-yl)benzaldehyde (**8**) with the formyl group in the phenyl ring. Our result indicated that the trifluoromethyl substituent favorably lowers the electron density of the pyrazole ring, allowing regioselective proton abstraction with the formation of 3-methyl-1-phenyl-5-(trifluoromethyl)-1H-pyrazole-4-carbaldehyde (**6**). However, the increased electron density of the pyrazole ring of 3,5-dimethyl-1-phenyl-1H-pyrazole (**7**) might favor a Vilsmeier-Haack reaction. Indeed, the Vilsmeier-Haack reaction of compound **7** provided desired 3,5-dimethyl-1-phenyl-1H-pyrazole-4-carbaldehyde (**9**) in 65% yield without solvent (Scheme 3).



**Scheme 3.** The synthesis of  $[\text{}^{14}\text{C}]$ SANT-1.

In our radiosynthesis,  $[\text{}^{14}\text{C}]$ dimethylformamide was the limiting reagent, and 2 equiv of **7** was used in the reaction. Since all the reactants and reagents were liquid, no additional solvent was necessary. Unreacted **7** was easily removed by recrystallization or flash chromatography.  $[\text{}^{14}\text{C}]$ Aldehyde (**10**) was treated with N-amino-N-benzylpiperazine (**15**) in presence of NaOMe and EtOH to provide crude  $[\text{}^{14}\text{C}]$ SANT-1. The purification was achieved by using flash chromatography (silica gel, 30% EtOAc in hexane) to give 14.2 mCi (75% yield) of  $[\text{}^{14}\text{C}]$ SANT-1 with a specific activity of 54.1 mCi/mmol and radiochemical purity of 98.2%. The overall yield for the

